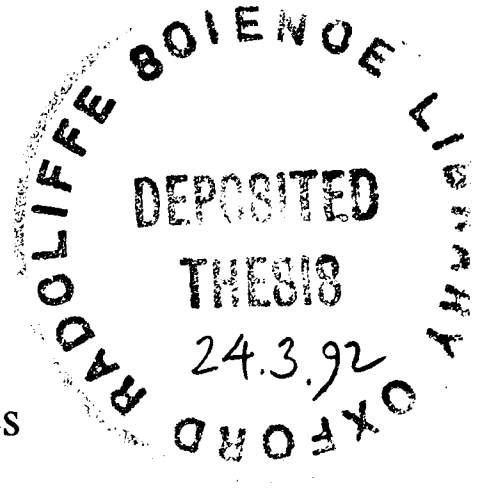
Thesis submitted for the degree of
Doctor of Philosophy

Palaeoceanography and Sedimentology of a Mid-Cretaceous Greensand

Volume 1 - Text

by

Stephen Francis Hart



Department of Earth Sciences
& Wolfson College
University of Oxford

Trinity, 1991

TABLE OF CONTENTS

Page

Short Abstract. i
Long Abstract. ii
Acknowledgements. v

CHAPTER 1 - INTRODUCTION AND HISTORY OF PREVIOUS RESEARCH 1

CHAPTER 2 - SEDIMENTARY CONDENSATION PHENOMENA AND FACIES CONTROLS IN THE UPPER ALBIAN (CRETACEOUS) OF THE ANGLO-PARIS BASIN. 4

2.1 The Upper Greensand of south-east Devon. 5
2.1.1 The Foxmould Member. 6
2.1.2 Sedimentary condensation in the uppermost Foxmould. 6
2.1.3 The Chert Beds Member. 7
2.1.3.1 The lower Chert Beds hardground. 8
2.1.3.2 Intraformational pebble-shell beds. 9
2.1.3.3 The Brecciated Limestone hardground. 10
2.1.4 The Top Sandstones Member. 11
2.1.4.1 The Coarse Band. 11
2.1.4.2 The top Upper Greensand hardground. 12

2.2 The Upper Greensand of south Dorset. 13
2.2.1 The Gault clay and the Foxmould Member of the Upper Greensand. 13
2.2.1.1 Minor hiatus in the Foxmould Member. 15
2.2.2 The Exogyra Rock. 15
2.2.3 The Dispar Zone Ammonite Bed. 16
2.2.4 The Chert Beds. 18
2.2.5 The Eggardon Grit. 18

2.3 Correlation of Upper Albian condensation horizons around the Anglo-Paris Basin. 19
2.3.1 The *cristatum* subzone nodule bed. 19
2.3.2 The *varicosum* subzone nodule bed. 19
2.3.3 Condensation in the ?middle *auritus* subzone. 21
2.3.4 The high *auritus* subzone phosphoritic greensands. 21
2.3.5 The *rostratum* and *perinflatum* subzone nodular hardgrounds and greensands. . .25

2.4 Tectonic influences on sedimentation in the Albian of the Anglo-Paris Basin. 25
2.4.1 Evidence for synsedimentary faulting in the Upper Greensand of south-east Devon. 26
2.4.2 Early Cenomanian faulting at Worbarrow Bay, south Dorset. 27
2.4.3 Influence of positive structures on facies and condensation. 29
2.4.3.1 Complex condensation horizon at Swanage Bay, south Dorset. 29
2.4.3.2 Le Croquet, Normandy coast. 31
2.4.3.3 The Isle of Wight. 32

2.5 Mechanisms controlling late Albian condensation in the Anglo-Paris Basin. 33
2.5.1 *Cristatum* and *varicosum* subzone phosphate beds. 33
2.5.2 Glauconitic facies of high *auritus* subzone age. 35
2.5.2.1 Erosion vs non-deposition. 37
2.5.3 Nodular hardgrounds and greensands of *rostratum* and *perinflatum* subzone age.39
2.5.3.1 Cyclicity in the Upper Greensand of south-east Devon. 41

2.5.3.2 Stable-isotopic data and relative sea-level change. 46
2.5.4 Shallow-water facies in the latest Upper Albian. 46
2.5.5 Sequence stratigraphic analysis of the Upper Albian of the Anglo-Paris Basin. .48
2.5.6 Comparison with the Exxon "eustatic" cycle chart. 50

2.6 Summary and Conclusions. 51

CHAPTER 3 - STORM SEDIMENTATION IN THE UPPER GREENSAND FORMATION (CRETACEOUS) OF SOUTH-WEST ENGLAND. 53

3.1 Storm laminites in the Foxmould Member. 54
3.1.1 Typical features of an individual laminite bed. 55
3.1.2 Description and proximal-distal trends. 56
3.1.3 Reworking of phosphate. 58
3.1.4 Analysis and interpretation. 59
3.1.5 Storm frequency and laminite preservation potential. 62
3.1.6 Glauconitic storm laminites in the uppermost Foxmould. 64
3.1.7 Faunal implications. 65

3.2 Intraformational pebble and shell beds in the uppermost Foxmould. 66

3.3 Storm sedimentation in the Chert Beds Member. 67
3.3.1 Pebble-shell beds. 68
3.3.2 Complex, amalgamated, proximal coquina beds. 69
3.3.3 Interpretation of pebble-shell bed fabrics and storm versus fair weather processes. 70
3.3.3.1 Basal scours and gutters. 76
3.3.4 Storm frequency and preservation. 78

3.4 Storm scouring of nodular hardgrounds. 78

3.5 Palaeogeographic setting. 79

3.6 Conclusions. 80

CHAPTER 4 - STABLE ISOTOPE STRATIGRAPHY OF THE UPPER ALBIAN *DISPAR* ZONE (MID-CRETACEOUS) OF SOUTHERN ENGLAND. 81

4.1 Methodology. 82

4.2 Isotopic data from the Upper Greensand at Beer, south-east Devon. 83
4.2.1 The uppermost Foxmould. 83
4.2.2 The lower Chert Beds. 84
4.2.3 The upper Chert Beds. 84
4.2.4 The Top Sandstones. 84
4.2.5 The Pounds Pool Member, Beer Head Limestone Formation. 85

4.3 Evaluation of the validity and completeness of the secular $\delta^{13}C$ changes. 85
4.3.1 Carbonate mineralogy and isotopic fractionation. 85
4.3.2 Carbonate diagenesis and non-carbonate impurities. 87
4.3.3 Silica diagenesis and modification of the isotopic signatures. 90
4.3.3.1 Silicification control sampling. 91
4.3.3.2 Normalisation of the data. 91
4.3.3.3 $\delta^{13}C$ - $\delta^{18}O$ plot. 92
4.3.4 Time-averaging due to storm reworking and bioturbation. 93
4.3.5 Completeness of the isotope stratigraphy. 94

4.4 Comparison of whole rock data with oyster data. 95

4.5 Interpretation and significance of the isotopic data. 97

4.6 Conclusions. 100

CHAPTER 5 - GEOCHEMICAL ANALYSIS OF GLAUCONITIZATION PROCESSES IN THE UPPER GREENSAND FORMATION. 101

5.1 Mineralogical Classification. 102

5.2 The mechanism of glauconitization. 103

5.3 Morphology of glauconitic minerals in the Upper Greensand Formation. 107

5.4 Chemical analyses of glauconitic grains from the Upper Greensand of southern England.109
- 5.4.1 General chemical characteristics. 111
- 5.4.2 Potassium contents. 111
- 5.4.3 Aluminium contents and depth relationships. 114

5.5 Sulphur-Carbon data from the Upper Greensand and Gault of southern England. 117
- 5.5.1 Methodology. 117
- 5.5.2 Discussion. 118

5.6 Conclusions. 119

CHAPTER 6 - CONTROLS ON THE WORLD-WIDE DEVELOPMENT OF THE CRETACEOUS GLAUCONITIC FACIES. 121

6.1 Review of the World-wide distribution of Cretaceous glauconitic sediments. 122
- 6.1.1 Introduction and methodology. 122
- 6.1.2 Listings of glauconitic facies for each Cretaceous stage. 123

6.2 Cretaceous Greensand Provinces. 131
- 6.2.1 Eastern England. 131
- 6.2.2 Wessex Basin, southern England. 131
- 6.2.3 Celtic Sea and Porcupine Basins. 133
- 6.2.4 Northern Ireland and north-west Scotland. 133
- 6.2.5 Paris Basin. 135
- 6.2.6 West Netherlands Basin. 137
- 6.2.7 Germany. 137
- 6.2.8 Denmark and southern Sweden. 140
- 6.2.9 Polish Lowlands. 142
- 6.2.10 Russian Platform. 143
- 6.2.11 Bohemian Massif. 144
- 6.2.12 Hungary. 146
- 6.2.13 North Tethyan margin. 146
- 6.2.14 India and Pakistan. 149
- 6.2.15 Southeastern Africa. 150
- 6.2.16 Northwestern Australia. 153
- 6.2.17 Western Australia. 154
- 6.2.18 Southern Australia. 155
- 6.2.19 Northern and northeastern Australia. 158
- 6.2.20 New Zealand. 159
- 6.2.21 Venezuela. 161

6.2.22 Eastern coastal plain, U.S.A.. 162
6.2.23 Western Interior Seaway of North America, Canada. 163

6.3 Interpretation of temporal and spatial patterns of Cretaceous glauconite enrichment. 164
6.3.1 Palaeogeographic reconstructions. 164
6.3.2 Depositional settings of Cretaceous glauconitic sediments. 166
6.3.3 Role of smectitic clays. 169
6.3.4 Calculation of Cretaceous glauconite-production rates. 170
6.3.5 Links with sea-level change and anoxia. 171

6.4 Conclusions. 172

REFERENCES. 173

SHORT ABSTRACT

STEPHEN FRANCIS HART
WOLFSON COLLEGE, UNIVERSITY OF OXFORD

D.Phil THESIS
TRINITY, 1991

The Upper Albian (mid-Cretaceous) sediments of the Anglo-Paris Basin display a range of condensation phenomena, including glauconitic and phosphoritic sands, glauconitic intraformational pebble beds, and mineralised nodular hardgrounds. These are interpreted as the result of sedimentation rate fluctuations controlled by small-scale relative sea-level changes of at least regional nature. The regional signal was modified by local tectonics, including occasional synsedimentary faulting and the development of thinned successions and complex condensation horizons over broad submarine highs. Candidate sequence boundaries, marine flooding surfaces and systems tracts are proposed. Episodic, high-energy storm events record a spectrum of storm intensities and periodicities in the Upper Greensand Formation. Storm processes interacted with early submarine lithification to produce a suite of pebble-shell beds, simple and amalgamated coquinas, and storm-scoured hardgrounds. Analysis of shell bed fabrics and taphonomy indicates the important role of high-energy storms in generating a distinct event stratigraphy. Stable isotope analysis has detected a positive secular change in carbon-isotopic ratios within carbonates of *dispar* zone age, resolved as two smaller positive shifts across nodular hardgrounds. This correlates with the development of organic-rich sediments in a range of settings world-wide. Analytical problems, including silica diagenesis, have been addressed by a series of parallel control studies. Geochemical and petrographic analysis has confirmed the widespread development of glauconitic minerals throughout the Upper Greensand, and has been used to investigate grain evolution in a range of lithologies. A review of the global development of the Cretaceous glauconitic facies has been used to compile depositional models for a range of settings. Volumetric calculations of Cretaceous glauconite production rates have shown secular changes, with peak Aptian to Santonian values linked to transgressions across the broad shelf seas which developed globally during this time of rising sea-levels and sea-level highstand.

LONG ABSTRACT

STEPHEN FRANCIS HART
WOLFSON COLLEGE, UNIVERSITY OF OXFORD

D.Phil THESIS
TRINITY, 1991

The Upper Albian (mid-Cretaceous) sediments of southern England and northern France display a range of condensation phenomena, developed at discrete stratigraphic intervals within a predominantly fine-grained siliciclastic and carbonate succession. These include glauconitic and phosphoritic sands (greensands or "glauconitites"), glauconitic pebble-shell beds, and mineralised nodular hardgrounds. Certain of these horizons are laterally very continuous, developed over areas from kilometres across to basin-wide in extent. Such beds are more prominent on the basin margins, and show systematic lateral variations in the degree of early diagenetic (synsedimentary) cementation, in the concentration of glauconite, and in the degree of secondary reworking processes. The Upper Albian lithostratigraphy of southern England is described in detail, with reference to the type sections of south-east Devon and south Dorset, and a correlation of condensed beds across the basin is given, based on lithological and biostratigraphic data. Evaluation of the nature and areal distribution of the beds suggests that they are the result of gross sedimentation rate fluctuations controlled by small-scale relative sea-level changes of at least regional nature. The regional (possibly eustatic) signal was subject to modification by local tectonics, including occasional synsedimentary faulting, and the development of broad submarine highs over which stratigraphically-thinned successions and amalgamated complex condensation horizons developed. Candidate sequence boundaries, marine flooding surfaces and systems tracts are proposed, based on the analysis of outcrop data from around the basin; these provide a detailed framework with which to compare apparent relative sea-level changes in the Upper Albian strata of other sedimentary basins. Candidate sequence boundaries have been identified within the lower *cristatum* and lower *varicosum* subzones, represented by winnowed phosphatic concentrations, and within the high *dispar* zone, expressed in certain areas as a winnowed quartz-rich lag. The glauconite-rich interval of the high *auritus* subzone is considered to represent a condensed section, caused by rapid relative sea-level rise, and nodular hardgrounds and greensands higher up in the succession appear to mark the position of transgressive surfaces. A thin wedge of higher-energy facies of uppermost late Albian age is developed at the top of the succession.

Episodic, high-energy storm events are an important component of the stratification style of the Upper Greensand (Albian, Cretaceous) of south-west England. These storm events are preserved in the sedimentary record of a broad epeiric shelf margin setting. In the lower fine-grained glauconitic siliciclastic member, graded laminite beds of varying thickness and degree of amalgamation record a spectrum of storm intensities and periodicities; they show diagnostic

structures and characteristic proximal-distal trends. Storm processes involved shelf-wide sediment entrainment followed by settling from sediment-laden suspension clouds, rather than unidirectional current transport. Pervasive storm reworking is also recorded at the overlying siliciclastic-carbonate transition, and in the carbonate packstone and grainstone members above. This interacted with very early submarine lithification processes to produce a suite of intraformational pebble-shell beds, simple and amalgamated coquina beds, and storm-scoured hardgrounds. Analysis of bed fabrics shows that the most proximal coquinas have nested, predominantly convex-down shell orientations; these pass offshore into beds with predominantly convex-up shell material. Storm processes identified include both sediment winnowing and transportation of bioclasts. Evaluation of the taphonomy of the shell beds indicates that they were generated by rare, very high-energy storm events, in which skeletal material was buried and preferentially protected from lower energy shell abrasion. The background calcarenites record this lower energy but prolonged weak storm and fair weather reworking, in which physically less-resistant skeletal elements were rapidly broken down into carbonate sand. Evidence for storm-influenced sedimentation can be detected throughout most of the succession, but typically only the highest energy storms were preserved as discrete (sometimes amalgamated) units, resulting in a distinct "event stratigraphy".

Secular changes in δ13C values have been detected in a series of mid-Cretaceous carbonates from south-west England. Increasing carbon-isotope values (a positive shift of around 1.0-1.3‰) are found through the Chert Beds and Top Sandstones Members of the Upper Greensand Formation. This succession encompasses the *dispar* ammonite zone of the Upper Albian. In detail, the increase appears to be resolved as two smaller positive shifts across nodular hardground horizons, separated by carbonates which exhibit uniform isotopic compositions after corrections for diagenetic alteration. The problems associated with the investigation of secular isotopic changes in the subtidal carbonate facies are complex; these include potential isotopic fractionation by the basic carbonate mineralogy, isotopic modification due to silica diagenesis, time-averaging due to storm reworking and bioturbation, and identification of small-scale hiatuses and possible stratigraphic gaps. Whole-rock and oyster analyses coupled with a series of control studies have, however, built up a carbon-isotope stratigraphy which has implications for the palaeoceanographic reconstruction of Upper Albian organic-matter burial rates. Organic-rich sediments of this age are developed in a variety of depositional settings world-wide; the increase in $\delta^{13}C$ values detected in the Upper Greensand carbonates appears to confirm the existence of increased organic-carbon burial rates in the late part of the Upper Albian.

Geochemical analysis has confirmed the widespread development of glauconitic minerals throughout the Upper Greensand of southern England. The potassium contents of grains from different lithologies have been used to indicate the degree of evolution of the glauconitic

minerals. Mid-shelf muddy sands and limestones have moderate concentrations of "evolved" glauconite; laterally-equivalent deeper-water silts (and clays), and the higher-energy facies at the top of the sequence contain lower glauconite concentrations and a higher proportion of less-evolved grains. High glauconite concentrations and "evolved" to "highly-evolved" glauconite characterise thin condensed greensand beds; these relate to basin-wide starvation surfaces, interpreted as controlled by rapid relative sea-level change. Glauconitic grains have a wide range of morphologies, showing evidence for glauconitization of a variety of initial substrates. Correlation between grain morphologies and the potassium contents indicates that morphology cannot be used to give a reliable estimate of the degree of evolution of a given grain. In multiple complex grains, there is no correlation between the accretion stage and the degree of glauconite evolution. Previous workers have suggested that the aluminium contents of glauconitic grains may be linked to the water depth of glauconite formation. The aluminium contents of Upper Greensand glauconites, however, are not depth-specific, but relate largely to aluminium-rich micaceous precursors. Simple sulphur-carbon analyses of Upper Greensand lithologies show that these data are of only limited use in the reconstruction of organic matter influxes during sedimentation.

A thorough review of published data on middle and Upper Cretaceous glauconitic facies has indicated a wide range of depositional settings and facies associations. Reconstructions of the palaeogeographic distribution of world-wide Cretaceous greensands have shown that the facies type was associated with a number of distinct provinces; these are briefly reviewed. Cretaceous greensand depositional settings include development: directly overlying unconformities, over wide epicontinental shelf areas, on submarine highs within broad shelf areas, on stable passive continental margins, on starved continental margins with geostrophic currents, in restricted sedimentary basins, as transgressive deposits within a complex active fold belt, and in zones of upwelling of nutrient-rich waters. Many greensands appear to be associated with smectitic clays of probable volcanogenic origin. Volumetric calculations of Cretaceous glauconite production rates (GPR) have shown that a major increase in production occurred during the middle and late Cretaceous; this commenced in the Aptian, with a four- to five-fold increase. Three GPR peaks have been identified: the Lower Aptian-Lower Albian, the Upper Albian-Upper Cenomanian and the Lower Coniacian-Upper Santonian. These appear to be linked to widespread transgressions and episodes of sediment starvation across the extensive broad shelf seas which developed globally during this time of rising sea-levels and sea-level highstand.

ACKNOWLEDGEMENTS

I wish to acknowledge the award of research studentship GT4/87/GS/86 from the Natural Environmental Research Council, and to offer thanks to all who have been of assistance during the period of the research, notably to **Hugh Jenkyns** and **Jim Kennedy** for their supervision, and to **Steve Hesselbo** and **Angela Coe** for encouragement and discussion especially in the early months. I am also indebted to **Marjorie Woodhouse**, my benevolent aunt, who stepped in to solve my transport problems. Thanks are due to **Julie Cartlidge** and **Richard Corfield** for their aid with the isotopic analyses, to **Steve Wyatt** and **Norman Charnley** for their assistance with the geochemical work, to **Richard McAvoy** for help in the preparation of photographic material and to **Phil Jackson** and **Jeremy Hyde** for preparation of thin sections. Thanks also to **John O'Sullivan** for smoothing out various problems, and to **Dr. Hugh Owen** of the British Museum (Natural History) for the identification of ammonites.

I wish to acknowledge the award of a scholarship from the Centre National de la Recherche Scientifique, which gave me the opportunity to spend three months at the University of Caen, Normandy; I thank **Pierre Juignet** and **Jean-Louis Morgenthaler** for helping to make my stay so enjoyable.

Numerous other friends and colleagues have provided both stimulation and relaxation. Thanks are due to **Ed Thorogood** and **Dave Prescott** for tolerating my domestic eccentricities, to **Sean Hodges**, for his creative input, and to **Martin Shepley,** for many hard-fought squash battles. I wish to thank **Maria Mange**, for creating such a charming work environment, for providing numerous coffee boosts, and for tending our office garden so remarkably well. Many thanks to **Clare Mandeville** and the folk of South Parade, **Pamela**

Sansom, Malcolm Dransfield and **Simon Davey**, for being ever friendly and always welcoming. I also wish to thank my Summertown house-mates, **Elaine Scott** and **Jon Bass**, for their solidarity, **Karen Ogden**, for helping me out with accommodation troubles, and **Grant Wach**, for being a much appreciated friend. Thanks also to **Lidia Lonergan**, for tuition in the art of aerobics and physical exercise, and to **Sanjeev Gupta** and **Sarah Crampton**, for taking the time to read some of this work.

Finally, to all my **family**, for their faith, help and support, a big thank-you.

CHAPTER 1

INTRODUCTION AND HISTORY OF PREVIOUS RESEARCH

Glauconitic sediments of Upper Albian (mid-Cretaceous) age are developed throughout the Anglo-Paris Basin of southern England and northern France. In the Wessex Basin of southern England, these are represented by the Upper Greensand Formation, a thin (typically up to 50m), commonly glauconitic succession which is developed stratigraphically between marine clays of the (Lower) Gault and the deeper-water nannofossil Chalk (Fig.1). Sediments of Upper Albian age comprise both siliciclastic and carbonate lithofacies, deposited in a marine epeiric shelf setting. These have been the subject of sedimentological studies in order to determine the detailed stratigraphy of the interval, the depositional processes during Upper Albian sedimentation, and the controls on spatial and temporal patterns of glauconite enrichment in the Upper Albian, and in the Cretaceous period as a whole. The research has concentrated on the areas of south-east Devon, south Dorset and the Isle of Wight in southern England, and on sections in Normandy, northern France (Fig.2).

The earliest studies of the Upper Greensand and Gault of southern England were undertaken by Meyer (1874), Jukes-Browne (1877; 1879) and Downes (1882). Jukes-Browne & Hill (1900), published a memoir on the succession. Further notes on the stratigraphy and lithologies of these formations were added by Jukes-Browne & Scanes (1901) and Lang (1914). Regional memoirs by Arkell (1947) and Wilson *et al.* (1958) dealt more thoroughly with the detailed stratigraphy of the Upper Greensand and Gault, in southeastern Dorset and in western Dorset respectively.

More recent sedimentological work was undertaken by Tresise (1960; 1961), who described Upper Greensand sediments in Dorset and Devon, and investigated the nature and origin of chert in the Upper Greensand. Silicification processes have been the subject of a series of further studies by Williams (1986), Jeans (1978) and Maliva & Siever (1989). Smith (1961) published a synthesis of heavy mineral data from the Upper Greensand and overlying beds in

Devon, and the work of Drummond (1970) emphasised the role of a major positive swell area in mid-Dorset, which had an important influence on Albian and Cenomanian sedimentation patterns. Hamblin & Wood (1976) produced a new stratigraphic study of the Albian-Cenomanian of the Haldon Hills in south Devon. The uppermost bed of the Upper Greensand in south-east Devon was described by Smith (1957) and Ali (1974; 1976), who misinterpreted it as a beach deposit; it was later recognised as a nodular hardground by Jarvis & Woodroof (1984). Detailed studies of uppermost Albian and Cenomanian sections in south-west England were undertaken by Kennedy (1970), and the nodular beds developed in this interval have been studied by Garrison *et al.* (1987). Sections in the Weald have been described by Owen (1976), and sections in Normandy by Juignet (1974; 1980). The clay mineral assemblages of a wide range of Cretaceous sediments from southern England and Northern Ireland have been documented by Jeans *et al.* (1982), who linked the glauconitization process to clays of inferred volcanic origin.

The ammonite biostratigraphy and lithologies of the Lower and Upper Gault and of the Upper Greensand of the Weald have been studied in considerable detail, and published in a series of papers by Owen (1971a; 1971b; 1972; 1976; 1984). These works erected the standard biozonation scheme for the Middle and Upper Albian, and have been the source of detailed information concerning correlation of beds from southwestern England and France into the Weald. Although a comparative foraminiferal biostratigraphy has been proposed for the Gault clay of southeastern England (M. B. Hart 1973a), attempts to extend the scheme to the Upper Greensand have met with little success and were initially the source of a considerable amount of confusion (M. B. Hart 1971; 1973c; Carter & M. B. Hart 1977). These errors were later rectified by ammonite dating (Hamblin & Wood 1976; M. B. Hart *et al.* 1979b). Further micropalaeontological work (M. B. Hart *et al.* 1979a; Schroeder *et al.* 1986; Williams *et al.* 1988; M. B. Hart & Williams 1990) has described the presence of orbitolinids in the Upper Greensand, but has provided little further stratigraphic or sedimentological information. In contrast, the very detailed foraminiferal studies by Price (1976; 1977a; 1977b), although not examining the Upper Greensand, have given much useful information on benthonic : planktonic

foraminiferal ratios throughout the Upper Albian of north-west Europe. The methodology of Price was more rigorous than that of the other workers mentioned above, with study of total picked foraminiferal populations, rather than those sieved with a specific mesh size. Little detailed palaeoecological work has been published on the Upper Greensand faunas, an exception being the study of predatory gastropods from the Blackdown Hills (Taylor *et al.* 1983).

A detailed Upper Greensand stratigraphic synthesis and correlation, with sedimentary logs covering the full succession, has not been published. This research has established the stratigraphy and correlation of the Devon and Dorset Upper Albian sediments, describing the condensed beds, correlating condensation surfaces around the Anglo-Paris Basin, and interpreting the fundamental controls on their development. In addition, further work has concentrated on the important role of storm sedimentation processes in the Upper Greensand of south Devon, and a detailed study has been undertaken on the stable isotopic signatures of Upper Albian carbonates from south-east Devon. Geochemical studies have been conducted on the glauconitic mineral phases and combined with petrographic work on glauconite grain morphologies and evolution. Finally, a detailed review has been undertaken of the world-wide development of the poorly-understood Cretaceous glauconitic facies association. This is used to interpret the controls on the temporal and spatial patterns of glauconite enrichment and to construct models which classify the depositional settings of a wide range of Cretaceous examples.

CHAPTER 2

SEDIMENTARY CONDENSATION PHENOMENA AND FACIES CONTROLS IN THE UPPER ALBIAN (CRETACEOUS) OF THE ANGLO-PARIS BASIN

Abstract : The Upper Albian (mid-Cretaceous) sediments of southern England and northern France display a range of condensation phenomena, developed at discrete stratigraphic intervals within a predominantly fine-grained siliciclastic and carbonate succession. These include glauconitic and phosphoritic sands (greensands or "glauconitites"), glauconitic pebble-shell beds, and mineralised nodular hardgrounds. Certain horizons are laterally very continuous, developed over areas from kilometres across to basin-wide in extent. Such beds are more prominent on the basin margins, and show systematic lateral variations in the degree of early diagenetic (synsedimentary) cementation, in the concentration of glauconite, and in the degree of secondary reworking processes. The Upper Albian lithostratigraphy of southern England is described in detail, with reference to the type sections of south-east Devon and south Dorset, and a correlation of condensed beds across the basin is given, based on lithological and biostratigraphic data. Evaluation of the nature and areal distribution of the beds suggests that they are the result of gross sedimentation rate fluctuations controlled by small-scale relative sea-level changes of at least regional nature. The regional (possibly eustatic) signal was subject to modification by local tectonics, including occasional synsedimentary faulting, and the development of broad submarine highs over which stratigraphically-thinned successions and amalgamated complex condensation horizons developed. Candidate sequence boundaries, marine flooding surfaces and systems tracts are proposed, based on the analysis of outcrop data from around the basin; these provide a detailed framework with which to compare apparent relative sea-level changes in the Upper Albian strata of other sedimentary basins. Candidate sequence boundaries have been identified within the lower *cristatum* and lower *varicosum* ammonite subzones, represented by winnowed phosphatic concentrations, and within the high *dispar* zone, expressed in certain areas as a winnowed quartz-rich lag. The glauconite-rich interval of the

high *auritus* subzone is considered to represent a condensed section, caused by rapid relative sea-level rise, and nodular hardgrounds and greensands higher up in the succession appear to mark the position of transgressive surfaces. A thin wedge of higher-energy facies of uppermost late Albian age is developed at the top of the succession.

Upper Albian (mid-Cretaceous) sediments outcrop across the Anglo-Paris Basin (Wessex and Paris Basins) of southern England and northern France. They comprise a relatively thin (typically up to 50m) package of both clastic (gravels, sands, silts and clays) and carbonate (bioclastic packstones and grainstones, coquinas, marls) lithofacies. These represent sedimentation in a predominantly open marine, subtidal, epeiric shelf environment. The Middle and Upper Albian sediments of southern England can be considered to be broadly transgressive, stratigraphically overlying the tidal and estuarine facies of the Lower Greensand, and overlain over much of the basin by deeper-water nannofossil Chalk. A prominent unconformity marks the base of the succession (Hancock 1969), with stratigraphic onlap onto the basin margins. In south-west England, Albian sediments sequentially overstep the underlying Lower Cretaceous, Jurassic and Permo-Triassic, to rest on Upper Palaeozoic strata. For the purposes of this study, type sections of the Upper Greensand in south-east Devon and south Dorset are described in detail, with emphasis on the condensed horizons which punctuate the succession. Correlations are made with other parts of the Anglo-Paris Basin, and genetic models are proposed to explain the formation of such beds. A detailed stratigraphic subdivision of the Upper Albian sediments of the Anglo-Paris Basin is given in Figure 3.

2.1 The Upper Greensand of south-east Devon

The Upper Greensand Formation of south Devon is subdivided into three members (Jukes-Browne & Hill 1900; Smith 1961): the Foxmould, Chert Beds and Top Sandstones (Fig.3). In the Beer district, these rest unconformably on Triassic red marls of the Mercia Mudstones. A

graphic summary of the Upper Greensand succession between Hooken Cliffs and Beer Head (SY 220 879 to SY 227 879) is given in Figure 4.

2.1.1 The Foxmould Member

The Foxmould consists of around 25 metres of glauconitic, muddy silts to fine sands, with calcareous concretions and scattered pyrite nodules. The greater part of the succession is strongly bioturbated without preserved sedimentary structures, but traces of depositional lamination and occasionally-preserved beds of laminated sand indicate storm reworking throughout much of the member (Chapter 3). The sediment is glauconitic throughout, concentrations are typically around 5-10%. Ammonites are rare, but the *varicosum* and *auritus* subzones are proven (Hancock 1969); the exact age of the muddy basal beds directly overlying the unconformity is, however, uncertain. The Foxmould sands display a rather uniform sequence, but a minor depositional break is indicated by a thin phosphate bed of *varicosum* age, recognised (for the first time) in the sections around Beer and between Axemouth and Lyme Regis. The phosphate is developed as a low concentration of black nodules of sand-size to small granule-size, with occasional fragments reaching up to 5cm in diameter. These rest in a shelly, muddy fine sand matrix. Most of the phosphatic grains are amorphous, but scattered internal moulds of bivalves, serpulids, gastropods and rare ammonites, completely phosphatised serpulids, small burrows and shell fragments, and shark and fish teeth have been recorded. The bed is only 5cm in thickness, the phosphate having been incorporated into the basal shelly lag of a storm laminite bed, and then subjected to strong post-depositional bioturbation. The *varicosum* subzonal age is indicated by a specimen of *Epihoplites cf. gibbosus* (Spath) (identification by H. G. Owen), collected from the Hooken Cliffs section (SY 220 879) (3.5m above datum, Fig. 4).

2.1.2 Sedimentary condensation in the uppermost Foxmould

In south-west England, the uppermost Foxmould is marked by glauconite-rich sediments and a facies change from siliciclastics to carbonates (Chert Beds Member). This interval is identified in the western sections at Dunscombe Cliff (SY 153 877) by up to six variably-amalgamated

glauconite-rich storm laminite beds (Fig.5), and passes eastwards (basinwards) into glauconitic sediments which display very early diagenetic (synsedimentary) cementation features and show evidence for small-scale cyclicity. Around Beer (Little Beach SY 224 879; Whitecliff SY 234 894), two to three glauconitic intraformational pebble-shell beds are developed, showing varying degrees of storm reworking, and are associated with storm-concentrated coquina lenses (Fig.6; Fig.7). The pebbles represent reworked early concretions; they are commonly bored and marginally glauconitised. Prominent *Thalassinoides* firmground burrowing is developed at the bases of the beds, the burrows being passively filled with glauconite-rich sand (Figs.8-11). Between Axemouth and Lyme Regis, pebble beds are also developed in the uppermost Foxmould, varying somewhat in thickness, but with two successive cycles being well-developed in most sections (Fig.12). Three nodular horizons are developed in the section 0.5km to the east of Corbin Rocks (SY 293 896) (Fig.13), but the lowermost is weak and the associated shelly component is of low concentration. The condensed beds of the uppermost Foxmould of south Devon are of upper *auritus* subzone age, proven by a specimen of a probable macroconch of *Mortoniceras (Mortoniceras) pachys* (Seely) (identification by H. G. Owen), collected from the uppermost of the two nodular beds at Culverhole Point (SY 278 893) (Fig.19). The ammonite is preserved as an unphosphatised mould within a calcareous concretion. The suggestion of Williams *et al.* (1988), that the upper part of the Foxmould may be of *dispar* age, appears to be incorrect.

2.1.3 The Chert Beds Member

The Chert Beds Member of the Upper Greensand Formation comprises a unit of impure siliceous carbonates up to around 17 metres in thickness. These variably quartzose and glauconitic packstones and grainstones are rich in diagenetic silica, with abundant chert nodules (Tresise 1961; Jeans 1978; Williams 1986; Maliva & Siever 1989). At certain horizons, there is evidence for an early diagenetic lithification process, which resulted in cemented limestone nodules (Garrison *et al.* 1987). These formed nodular hardgrounds and intraformational shelly pebble beds, depending on the thickness and degree of reworking of the nodular horizon.

Commonly, storm reworking affected the nodules, exposing them to boring and encrusting agents and to mineralisation processes, and redepositing them with a variable amount of coarse shelly material. Much of the succession shows evidence of storm influence, though only the highest energy events were preserved as discrete beds. Two nodular hardgrounds are developed in the Chert Beds of south-east Devon, and a large number of intraformational pebble and shell beds.

2.1.3.1 The lower Chert Beds hardground. The horizon is well-exposed around Little Beach-Beer Head, near Beer (SY 226 879). It consists of a nodular limestone, 0.9m in thickness, in which calcareous nodules (4-50cm across) rest in a very shelly, glauconite-rich, coarse carbonate-sand matrix which represents the infill of a well-developed *Thalassinoides* burrow system developed between the nodules (Fig.14; Fig.15). In the upper 0.2m, vertical chert nodules follow some of the burrow fills. Certain burrow walls (i.e. nodule margins) in the upper part have been glauconitized, but there is little sign of actual concretion reworking. The nodules become less well-defined in the basal part of the bed; a very slightly concretionary *Thalassinoides*-burrowed calcarenite is present below. Encrusting bivalves and bryozoans are associated with the nodules in the uppermost 10cm of the bed. The calcarenites directly overlying the hardground (0.15m) are shell-rich, with some horizontal alignment of the valve fragments.

The correlative at Whitecliff, Beer is a rather thinner nodular horizon (0.20-0.35m), composed of nodules and pebbles (reworked nodules); the margins of these are often glauconitized (weathering to iron oxides) (Fig.16). The carbonate-sand matrix hosting the nodules is only slightly shelly, and more muddy and glauconitic than the sediments below; muddy carbonate is present for an additional 0.35m above the top of the bed, then passing up into better-sorted packstones and grainstones. Weathering of the matrix highlights *Thalassinoides* burrows, some of which are preferentially silicified. Burrowing is well-developed at the base of the bed (Fig.17). The upper bed boundary is well-defined, with the overlying sediment filling in depressions between the nodules. The small pebbles show borings and marginal

glauconitization; there is a vertical mixture of reworked pebbles and un-reworked nodules, with pebbles often found below the nodules. It is probable that many of the larger nodules post-date the reworking.

Tracing this horizon eastwards, in the sections between Axemouth and Lyme Regis, the lower Chert Beds below the hardground are reduced in thickness, and the hardground itself is absent. This is interpreted as the result of late Albian synsedimentary faulting, probably along the line of a fault which downthrows the Upper Greensand against Triassic marls at Seaton Hole (see later).

2.1.3.2 Intraformational pebble-shell beds. Certain horizons in the Chert Beds display evidence for minor discontinuities in the form of intraformational pebble-shell beds. These consist of storm-reworked concentrations of early diagenetic nodules with associated shells and shell fragments. Although such storm activity had a considerable influence on the depositional fabric of the beds, it does not appear to have exerted a fundamental control on the development of the very early diagenetic (effectively synsedimentary) nodularity. The beds differ from the "background" bioclastic grainstones in that they are more glauconitic, and in the basal parts (where storm reworking is incomplete) firmground *Thalassinoides* burrowing is developed, piping the glauconitic calcarenite into the underlying bed.

Pebble beds range from isolated thin stringers one or two nodules thick, to thicker horizons containing many nodules, some of which show evidence to indicate that they are the amalgamated product of two such beds (Chapter 3). Thicker, little-reworked beds (e.g. the top pebble bed in the Beer Head section) are similar to the nodular hardgrounds in that there is an association of coarser grade (than "background") quartz grains in the matrix around the nodules (Fig.18); this may be the result of sediment winnowing. The beds appear to represent minor hiatuses within the sequence. Their lateral correlation potential (bed by bed) is complicated by differing amounts of storm erosion i.e amalgamation and reworking. They do, however, define an interval between the lower Chert Beds and the Brecciated Limestone hardgrounds where the sequence is dominated by a succession of minor non-sequences (Fig.19). Up to six thin pebble

beds are developed (Beer Stone Adit SY 220 881), though in sections to the east, amalgamation has probably reduced their number (to three at Beer Head). Certain beds are lensoid in geometry and pinch out laterally. Correlation may be further complicated if the nodular hardgrounds are used as "time lines". Clearly, the Brecciated Limestone hardground correlates across the region, and developed at the same time in all sections, but if the bed developed below an erosion surface (present at the top of the bed), it is possible that nodularity may have formed in calcarenite substrates of slightly differing stratigraphic position (?up to a few metres).

2.1.3.3 The Brecciated Limestone hardground. This is a well-developed, thick nodular limestone which can be correlated throughout the coastal sections of south-east Devon (Fig.20). The bed name is proposed following the introduction of the term "brecciated bed" by Tresise (1960). The type exposures are around Beer, at Beer Head (SY 227 879) and Whitecliff (SY 234 893). At these localities, the hardground is 0.85-1.00m in thickness, consisting of a mass of nodules (2-30cm across), ranging from separate to intergrown. Where the nodules are separate, they rest in a thoroughly *Thalassinoides*-reworked, glauconite-rich, shelly, coarse calcarenaceous sand matrix; much appears to be passive burrow fill, filtered down into the bed from above. The burrow system extends for up to 0.5m below the nodular bed, where a system of tunnels and galleries is developed in the underlying calcarenites. In exposures around and to the north of Beer Head, bedding is occasionally preserved in the matrix between the nodules, showing that burrow reworking was not always complete. The top of the bed is sharp and approximately planar; nodules on the upper surface show marginal borings and oyster encrustation. Glauconitization is only weakly-developed and no phosphatisation was recorded. The nodules preserve traces of an original sedimentary horizontal and cross-stratification. The sediment directly overlying the hardground consists of calcarenite containing coarse quartz grains and is very rich in bivalve shells and shell fragments, with occasional stick-like and net-like bryozoans.

Numerous sections between Seaton and Lyme Regis and to the west of Beer (Kempstone Rocks SY 161 881; Fig.21) indicate that the hardground is developed across this area of south Devon. It maintains similar thicknesses and sedimentological features at these

localities. In a small section at Corbin Rocks, however, the upper 0.25m of the bed is reworked, and is composed of smaller glauconitised, and occasionally bored, pebbles. The most easterly exposure, at the inland section of Shapwick Grange quarry (SY 312 918), records a well-developed metre-thick nodular bed at this level. There is a well-developed *Thalassinoides* burrow system between the nodules, extending into the calcarenites below; this is filled with a green, glauconite-rich, quartzose sand.

2.1.4 The Top Sandstones Member

The Top Sandstones Member consists of a unit of well-sorted carbonate grainstones, around 5-6 metres in thickness, with a coarse quartz-rich bed at the base, the Coarse Band, and capped by a nodular hardground which forms the top of the Upper Greensand. A facies change is indicated by the preserved depositional structures of the Top Sandstones which differ from the underlying Chert Beds. The Chert Beds are characterised by low-angle planar to undulose cross-lamination, whereas the Top Sandstones, especially the upper part, show abundant planar and trough cross-bedding, with preserved cross-sets and toe-sets, typically around 0.25m in thickness. Palaeocurrent data indicate a predominant north-west - south-east sediment transport direction. The cross-bedding indicates higher-energy conditions than in the underlying beds, and is interpreted as being generated by fairweather shoaling waves. Around Beer, the lower part of the Top Sandstones is marked by very well-developed, rather compressed *Thalassinoides* burrow systems, dominated by horizontal tunnels and filled with green, glauconite-rich calcarenite (Fig.22). Ammonites collected from the Top Sandstones just below the top Upper Greensand hardground at Shapwick Grange Quarry near Lyme Regis (SY 312 918) represent a level high in the dispar zone (Hamblin + Wood 1976; M.B. Hart et al. 1979b) (see Fig. 19).

2.1.4.1 The Coarse Band. A thin bed of calcarenaceous sand (typically 40-50% quartz; 45-55% carbonate grains) defines the base of the Top Sandstones. It represents a narrow interval (0.3-0.6m) within the limestones, which is rich in coarse quartz grains (abundant grains 2mm across) (Fig.18; Fig.23); these are typically well-rounded and many are polycrystalline. In some sections, the bed rests on the Brecciated Limestone hardground; elsewhere, it is separated from it by up to 2 metres of very pure calcarenites (Fig.21) (3% quartz content at Beer Head). The

base of the bed is planar, but some burrowing is generally developed, with *Thalassinoides* burrows passively filled with glauconitic sand extending down (for 8cm) into the sediments below. Rare small glauconitised limestone pebbles (2-8cm across) and some coarse shelly material (up to 2cm across) are often associated with the basal part of the bed. The sand is soft and only weakly-cemented, typically weathering back preferentially in the coastal sections. The sediment is generally structureless, giving little indication of the original depositional processes, though there are occasional traces of low-angle cross-stratification in sets up to 8cm in thickness. Differential silicification has also produced a weak, bedding-parallel colour banding. The upper bed boundary is gradational, with a progressive fining-upwards and decrease in the quartz content, passing up into the trough cross-bedded calcarenites above. It marks the base of a change from essentially storm-dominated subtidal carbonates below to a fairweather shoaling wave-dominated carbonate facies above.

2.1.4.2 The top Upper Greensand hardground (Small Cove Hardground). A well-developed thick nodular bed is developed at the top of the Upper Greensand Formation and can be correlated across much of south-west England. Around Beer, it consists of a nodular limestone 1.0-1.9m in thickness (Fig.24), containing occasional bivalve shells and shell fragments, and scattered angular medium-to-coarse quartz grains (typically around 0.5mm across), rarely small granules (up to 5mm across). The calcite spar-cemented nodules range in size from a couple of centimetres to over a metre across; there is considerable variability in the degree of nodularity (over just a few metres laterally), from isolated nodules to a compact mass of fully-cemented limestone. Uncemented sediment between the nodules was reworked by the burrowing activity of *Thalassinoides* trace-makers; occasional burrows have been preferentially silicified. Cross-stratification is developed in the calcarenites below the bed and traces of trough cross-bedding are commonly preserved in the hardground itself (Fig.25), in some cases traceable from nodule to nodule. In the upper part of the bed, however, structures preserved in adjacent nodules are often not parallel, showing that the nodules have undergone rotation (as is the case for the Brecciated Limestone; Garrison *et al.* 1987). *Planolites* burrows are also preserved in some

hardground nodules (and in the sediments below); they clearly pre-date the cementation phase. Hardground features include clear evidence of nodule avoidance by the *Thalassinoides* burrowers, glauconitization of many of the burrow walls / nodule margins, and glauconitization and phosphatisation of the nodules on the upper bedding-plane surface. The phosphatisation typically occurs as thin, discontinuous sheets and patches over the hardground surface. There are often multiple phases (up to five), with thin phosphatic crusts (1mm thick), sandwiching layers of sandy limestone (2-5mm thick). The upper surface of the hardground is sharp but not planar; the overlying sediments commonly fill small crevices, pockets and fissures between the nodules (Fig.26) (Ali 1974). The unit was originally interpreted as a bed redeposited from a low ridge (Smith 1957), or as a beach deposit (Ali 1974; 1976). It was correctly interpreted as a hardground by Jarvis & Woodroof (1984), who identified a complex history of sedimentation, bioturbation and erosion, and named the bed the Small Cove hardground.

2.2 The Upper Greensand of south Dorset

2.2.1 The Gault clay and the Foxmould Member of the Upper Greensand

The exact relationship between the Gault clay and the Upper Greensand in south Dorset remains uncertain due to the lack of exposure of this interval (a result of landslipping and vegetation of sections, and faulting out of the clay-rich parts of the sequence). Previous confusion is also the result of uncertainty regarding the classification of muddy silts and fine-grained sands as either Gault or Greensand. The combined thickness of Gault and Upper Greensand in south Dorset is around 60-65 metres (estimate based on the unfaulted but not fully-exposed Worbarrow Bay section).

In certain sections (Durdle Cove SY 805 806, Lulworth Cove SY 825 800, Worbarrow Bay SY 866 804), up to 25-30 metres of the Foxmould are well-exposed below the Exogyra Rock; these consist of muddy coarse silts to fine sands, with scattered pyrite nodules and rare small dark phosphate nodules, many the internal moulds of bivalves. The sediments display a

subtle rhythmic bedding, typically on a 0.5-1.0 metre scale, defined by fluctuating clay contents between adjacent beds (Fig.27; Fig.28). The beds are fully bioturbated, with no relict depositional structures; the mud is redistributed in a series of burrows, of which sub-horizontal, black mud-lined *Palaeophycus* burrows are the most common (Fig.29). The rhythmic bedding dies out in the uppermost 10 metres of the Foxmould, passing up into homogeneous muddy fine sands. Rhythmic bedding is also particularly well-developed in the Passage Beds of the Isle of Wight, again defined by variable amounts of mud within a fine-grained siltstone unit around 18m in thickness (Fig.30). These were accurately measured, and for each bed, a visual estimate of the mud content was made, on an arbitary scale from 1 to 7 (where 1 = very weak mud content; 7 = very strong mud content). Forty such beds are developed, and a simple histogram representation of the mud content data indicates that these beds group into 4 cycles, each of which consists of about ten beds, and defines a more-muddy to less-muddy cycle (Fig.31). The sediments are probably of upper *varicosum* to lower-middle *auritus* age, though the dating is uncertain. The only known ammonite record for this part of the succession consists of a pyritised specimen cf. transitional between *Epihoplites gibbosus* and early *Callihoplites auritus* (collected by this author; identified by H. G. Owen) from the middle part of the Passage Beds at the western end of Gore Cliff (SZ 491 763). This indicates a lower *auritus* age. The succession thus occupies about 2/3 of an ammonite subzone i.e. very approximately 2/3 Ma. The cyclicity may represent Milankovitch rhythms; a rough estimate using the numbers above gives a primary cyclicity at around 16,000yrs and a second order cyclicity at 166,000 yrs; these could feasibly represent precession and eccentricity cycles (cf. Berger 1988).

In south Dorset, a thin bed of black clay is present around 6 metres below the base of the Exogyra Rock, and can be correlated throughout the coastal sections, from just west of White Nothe (SY 768 809) to Swanage Bay (SZ 044 811). The uppermost 4 metres of the Foxmould become marly, reflected in the change in *Palaeophycus* burrow linings, from black mud to buff marl.

2.2.1.1 Minor hiatus in the Foxmould Member. The Foxmould represents a rather uniform sequence throughout the south Dorset sections. At Worbarrow Bay, however, a minor, glauconite- and serpulid-rich bed is developed 2.4m below the Exogyra Rock. This bed consists of a quartzose, richly glauconitic sandy serpulid limestone (Fig.32; Fig.33); the shelly material consists principally of the calcareous serpulid tubes of *Rotularia concava* (J. Sowerby), with associated bivalve shells - *Amphidonte obliquatum* (Pulteney), *Neithea* sp., and occasional bryozoan fragments. The base of the bed is a burrowed contact, marked by small *Thalassinoides* burrows, up to 2cm in diameter, penetrating (up to 0.85m) the underlying fine-grained glauconitic (5-10%) sands. The burrows are passively-filled with glauconite-rich sediment from above. The glauconitic limestone bed is 0.4m in thickness; it passes gradationally up into weakly shelly fine sands. The shell concentration within the bed is rather patchy in distribution, with shell-rich patches passing laterally into occasional patches of sediment with low shell contents. Calcareous concretions are developed along this horizon, centred on the shell concentration. The bed represents a closely-spaced mass of unoriented shelly material; it has undergone strong bioturbation, though in a single example, faint traces of a bedding-parallel lamination were observed. The bed bears little resemblance to the weak shelly lags of storm laminite beds in the south Devon Foxmould. The high glauconite concentration and burrowed basal contact infer a period of reduced sedimentation. The glauconitic serpulid limestone bed is most prominent at Worbarrow Bay; it can be correlated only to Lulworth Cove, 1.7m below the base of the Exogyra Rock. At this locality, it is much less glauconitic, consisting of a patchy concentration of *Rotularia* and *Amphidonte* material (0.25m in thickness), with occasional associated calcareous concretions. This minor condensed bed dies out beyond this point, and has not been recognised in the sections further to the west.

2.2.2 The Exogyra Rock

In south Dorset, the Exogyra Rock (Exogyra Sandstone) is developed at the top of the Foxmould Member (Drummond 1970; Garrison *et al.* 1987). The Exogyra Rock consists of a thick bed of nodular, glauconitic (10-15%) sandstone, rich in shelly material, including

Amphidonte obliquatum (Pultney), *Neithea* sp., *Entolium orbiculare* (J. Sowerby), serpulids including *Rotularia concava* (J. Sowerby), and echinoids. It is typically around 1.0-1.5m in thickness, though occasionally up to 2.75m. The bed is an intergrown mass of calcareous nodules, some of which have formed around patches of calcareous serpulid tubes. The fauna is within the nodules and not piped in from above. The shells are generally large and little-broken; there appears to have been little physical reworking other than intense bioturbation. The upper half of the bed is often the most shell-rich. Nodularity appears progressively, passing upwards from the underlying uncemented sands. The bed top is generally irregular and not planar; its upper surface shows no boring, encrustation or mineralisation (except at one locality, where it was truncated by early Cenomanian faulting; see later), even though an ammonite subzone (*rostratum*) is apparently absent at the top of the bed. At Lulworth Cove, however, it is overlain by up to 3 thin, coalescing seams of glauconitic clay up to 6mm in thickness. At Swanage Bay the interval is represented by a shelly, glauconitic (approximately 12%) sandy calcarenite with calcareous nodules and a little phosphate. The shelly fauna of bivalves, serpulids and occasional bryozoans is mostly whole and unfragmented.

The Exogyra Rock also outcrops in inland sections of southern and central Dorset (Wilson *et al.* 1958). It is dated as within the *auritus* subzone by a specimen of *Mortoniceras aff. commune* Spath (H. G. Owen) from a sand pit at Higher Wraxall, north-west of Maiden Newton (the original *Ammonites rostratus* of Jukes-Browne & Hill 1900, p. 172). In central Dorset (Eggardon Hill, SY 939 948; Stander's Mill Plantation near Maiden Newton, SY 588 975), the Exogyra Rock is developed as two amalgamated glauconitic nodular sandstones, the tops of which (at Eggardon Hill) have been reworked into intraformational pebble beds. The nodularity has developed as a secondary feature within an original strongly-bioturbated, glauconitic, shelly host sediment.

2.2.3 The Dispar Zone Ammonite Bed

In the south Dorset sections, the sediments stratigraphically overlying the Exogyra Rock consist of around 0.5-2.0 metres of glauconite-rich (up to 30%), fine-grained marly sands with scattered

phosphate nodules. These are overlain by a thin phosphatic greensand horizon, the Dispar Zone Ammonite Bed (DZAB) (Fig.34), developed at the base of the thin unit of Chert Beds. The bed contains abundant dark brown phosphate nodules, up to 5cm across; many represent the phosphatised internal moulds of ammonites, bivalves (*Entolium*, *Trigonia*, *Neithea*; moulds of articulated bivalves are common), gastropods and sponges (*Siphonia tulipa*). Scattered unphosphatised *Amphidonte* oysters are also present. The host sediment consists of a dark green, silty, marly greensand; the glauconite concentration typically reaches 50-70%. It is fully-bioturbated, with sub-horizontal buff marl-lined burrows common. The base of the bed is marked by a zone of burrowing into the underlying sediments. The *Thalassinoides* burrows, 2-3cm in diameter, are passively filled with the more glauconitic sediment of the DZAB. They typically penetrate down up to 0.95m, though most of the burrowing is concentrated in the top 0.2m of the underlying bed. The numerous ammonites indicate a *perinflatum* subzonal age (Wright, in Arkell 1947; Owen 1976).

In the south Dorset sections of Lulworth Cove, St. Oswald's Bay (SY 815 800), Durdle Cove and White Nothe, an additional thin greensand bed is developed above the DZAB. The top of the DZAB is defined by an abrupt decrease in the glauconite concentration and at Lulworth, passes into 0.33m of glauconite-poor (about 3%), cream-coloured sandy limestone. This is then overlain by the second bed of calcareous greensand (0.15m), with a glauconite concentration of 50% and a basal burrowed contact, greensand-filled burrows extending down (0.3m) into the underlying bed. The Chert Beds are directly above. In the eastern sections around Worbarrow Bay (below Flower's Barrow), the thin Chert Beds sequence disappears, and the two greensand beds are amalgamated into a single 0.75m-thick bed of slightly quartzose, marly, phosphatic greensand, again with a basal burrowed zone (Fig.35).

At Swanage Bay (Punfield Cove), the upper part of the Upper Greensand is very thin, consisting of a complex condensation horizon with several different generations of nodules (see below). The DZAB is represented by calcareous nodules of a glauconitic sandy limestone with small pale brown phosphatic nodules. The glauconite enrichment at this level dies out eastwards into the basin, but a horizon of very scattered phosphate nodules is developed in the upper part

of the Upper Greensand at Compton Bay, in the Isle of Wight. These are developed in a fine-grained marly silt, only weakly glauconitic, and have been dated as *dispar* age (Wright & Wright 1942).

2.2.4 The Chert Beds

A thin succession (up to around 2.5 metres) of fine-grained, slightly sandy, glauconitic (5-10%) limestones is developed between the Dispar Zone Ammonite Bed and the Eggardon Grit (Fig.36). The limestones are very rich in diagenetic silica, with up to about half the sediment having been replaced by siliceous nodules and chert. A weak horizontal lamination is occasionally developed, deflected by chert nodule growth. Silicified *Thalassinoides* burrows, with originally sandy fills, are common in the upper part, penetrating down from the bed above. The limestones contain scattered small bivalves and bivalve shell fragments, including *Entolium* sp.. Echinoid fragments occur throughout; occasional small complete echinoids a few millimetres across are also present.

2.2.5 The Eggardon Grit

Across Dorset, the top of the Upper Greensand is marked by a bed of nodular, sandy limestone, the Eggardon Grit (Calcareous Grit) (Wilson *et al.* 1958) (Fig.37). This typically reaches up to 1.5m in thickness; at the base, scattered large nodules (up to 25cm in diameter) grade up into fully nodular limestone (nodules typically up to 10cm in diameter). The nodules consist of a greyish brown sandy limestone; the glauconite content is low (around 2%) and the quartz grains are of medium to coarse grade (up to 2mm in diameter). Scattered bivalves and large echinoid plates are often present. The contact with the overlying Chalk Basement Bed is sharp but not planar, with the overlying sediment penetrating down for up to 10 centimetres into the bed. Small phosphate nodules are sometimes loosely concentrated in pockets between the nodules. In the main part of the bed, the uncemented sediment between the nodules consists of a medium-grained calcarenaceous sand; it is pervasively *Thalassinoides*-reworked and the burrows penetrate down into the underlying limestones for 1.95m below the top of the bed.

Some of these burrows have been preferentially silicified, forming chert nodules. The nodules in the uppermost part of the bed and on the upper surface are phosphatised and glauconitized. However, no evidence of nodule boring and only a single example of serpulid encrustation was recorded. The glauconitization has affected burrow walls i.e. nodule margins within the top 0.5m of the bed, rarely for up to 0.85m below the contact. At St. Oswald's Bay, the upper surface preserves phosphatic nodules, quartz grains and small patches of Chalk Basement Bed which have been cemented onto the nodules by thin discontinuous sheets of phosphate. Such phosphatic crusts do not appear to be developed to the west, however, where mineralisation is reduced to weak burrow wall glauconitisation (around White Nothe). The correlation of the Exogyra Rock, Dispar Zone Ammonite Bed and Eggardon Grit across south Dorset is shown in Figure 35. The Eggardon Grit is of Upper Albian perinflatum age, apparently extending into the Lower Cenomanian (see discussion of Kennedy 1970)

2.3 Correlation of Upper Albian condensation horizons around the Anglo-Paris Basin

2.3.1 The cristatum subzone nodule bed

Across much of southern England, the base of the Upper Albian is marked by a prominent bed of phosphate nodules. The detailed work of Owen (1971a; 1976) has shown that the bed contains phosphatic debris derived from the erosion of underlying lower *cristatum* subzone age and older Gault clays, in a middle *cristatum* subzone clay matrix. Up to five subzones of the underlying clays have been eroded; in the western Weald, Upper Gault rests directly on sediments of the *intermedius* subzone. Sediments of the underlying *daviesi* subzone are very restricted in occurrence, known only from the eastern Weald and Transcaspia (U.S.S.R.) (Owen 1976). The continuation of this erosion surface into south-west England is undocumented, however, due to poor exposure and poor biostratigraphic resolution.

2.3.2 The varicosum subzone nodule bed

The lowest depositional hiatus recognised in the succession is the thin, weak phosphate

concentration of *varicosum* subzone age developed in the south-east Devon Foxmould. No phosphatic bed has been identified at this level in the south Dorset Foxmould, but nodule beds, of which the most prominent generally forms the basal part of the subzone, are developed within the Upper Gault of the Weald, in Bedfordshire, in Buckinghamshire and in east Anglia. Owen (1976) describes thin seams of phosphatic nodules at the base and at the top of *varicosum* clays at Folkestone. In the northern Weald, at Paddlesworth, he records phosphatic nodule horizons at the base of, and within the sediments of the *varicosum* subzone. Milbourne (1963) also records several phosphatic nodule seams within the *varicosum* subzonal clays at Ford Place, Wrotham, Kent, with a prominent bed defining the base of the subzone. A *varicosum*-age phosphate bed has been recorded at Alice Holt in the western Weald (Owen 1976) and in the Virginia Water borehole at Egham, north of the Gault outcrop of the northern Weald (Owen 1971a). In the Leighton Buzzard area of Bedfordshire, Owen (1972) has documented a phosphate nodule bed of lower *varicosum* subzone age in which the black phosphate nodules are concentrated into "current-swirled pockets". The base of this appears to be erosional, and in the Aylesbury-Ford area of Buckinghamshire the bed also contains faunal elements from the underlying *orbignyi* subzone. In the Gault of East Anglia, Gallois & Morter (1982) describe a phosphate nodule bed with a burrowed basal erosion surface at the base of the *varicosum* subzonal sediments. A flood of belemnites occurs at this level, continuing throughout the overlying subzone.

In the coastal sections of Normandy, *varicosum*-age glauconitic sandy clays of the Gault overlie a major erosion surface, resting on the Poudingue Ferrugineux of the Middle Albian (Fig.38) (*niobe* subzone, *loricatus* zone at Cauville; Destombes *et al.* 1977). The erosion surface is marked by an increase in glauconite (up to about 20-25% in the basal sediments), nodules of partly-phosphatised gravelly clay, and strongly-phosphatised and bored wood fragments. In addition, a thin seam of phosphate nodules is often developed between 1.25 and 2.00 metres above the base of the Gault.

2.3.3 Condensation in the ?middle auritus subzone

The thin glauconitic limestone of ?middle *auritus* subzonal age, developed in the upper Foxmould at Worbarrow Bay and Lulworth Cove has not been identified in any other sections. This minor hiatus appears to be a purely local phenomenon, perhaps related to synsedimentary faulting preceding the prominent early Cenomanian faulting in this area (see below).

2.3.4 The high auritus subzone phosphoritic greensands

The high *auritus* ammonite subzone is represented throughout much of the Anglo-Paris Basin by an interval of glauconite-rich and locally phosphatic sediments. Early diagenetic (effectively synsedimentary) nodule growth occurred within a mid-shelf setting in the north-western part of the basin, where storm reworking resulted in glauconitic pebble-shell beds and glauconitic storm laminites. Uppermost Foxmould glauconitic storm laminites and glauconitic intraformational pebble beds are exposed in south-east Devon, and the glauconitic, nodular sandstone, the Exogyra Rock, is widely exposed across Dorset.

Tracing this interval eastwards from south Dorset to the Isle of Wight, the condensation becomes less pronounced and the sediment is less shelly. At Compton Bay (SZ 367 853), it is represented by a rather weakly-defined increase in glauconite, with a basal zone of sediment mixing, in which burrows penetrating the underlying silt are passively filled with glauconitic marly silt from the bed above (Fig.39; Fig.40). At Gore Cliff (SY 492 763), a marked concentration of glauconite is absent, but there is a rather gradual facies change from marly fine sands and silts with small phosphatic nodules, into glauconitic, silty, siliceous marls (the Chert Beds equivalent) (Fig.41).

In Wiltshire, near Edington, a horizon of phosphatised ammonites of *auritus* subzone age is developed within a unit of glauconitic sands (Kelly 1971). Both phosphatised and non-phosphatised fossils are present; the non-phosphatised forms indicate a slightly younger age than the phosphatised fauna. *Auritus*-subzone sediments are probably preserved below this horizon - the bed lies stratigraphically above the *auritus*-age Potterne Rock, a prominent concretionary horizon (though apparently not developed in the immediate area).

At Folkestone, the high *auritus* subzone is represented by Bed 12/XII of Jukes-Browne & Hill (1900) and Owen (1976), consisting of a prominent firmground-based erosion surface cut into the underlying pale grey clay (also *auritus* subzone), overlain by a highly glauconitic clay. Phosphate nodules are present, both concentrated in the basal part of the bed, where they sometimes form a lag to small scours, and also scattered throughout the bed itself. Jukes-Browne & Hill noted the two generations of phosphate (dark and pale) present. The bed is overlain by marly clay.

The detailed biostratigraphic work of Owen (1976) has indicated that Bed XII is represented in the northern Weald by one, or a series of phosphatic nodule seams in glauconitic clay and that, in these localities, it rests on clays of the *varicosum* subzone. Casey (1959) documented the Bed XII equivalent around Maidstone, where it consists of a bed of glauconitic marl, resting on an irregular surface of Gault clay. The bed contains numerous phosphate nodules, including phosphatised ammonites, reptilian (including pterodactyl) bones, and crab carapaces. In the Upper Gault below the Thames estuary, a bed of clay with small black phosphatic nodules has been recognised at this level (Owen 1971b) and in the East Anglian Gault, Gallois & Morter (1982) have correlated a bed of clay rich in *Aucellina coquiandiana* (d'Orbigny) with Bed XII at Folkestone; a flood of the planktonic foraminifera *Globigerinelloides bentonensis* (Morrow) occurs in the East Anglian bed, a feature which has been identified across north-west Europe by Price (1977a). *Callihoplites auritus* subzone clays below the interval have only been identified in the northern Weald at Folkestone, and below Canvey Island in the Thames estuary. Owen infers that the phosphate represents an erosion residual derived from previously-deposited clays of the *auritus* subzone, which are only preserved at these two localities. In the southern Weald, at Eastbourne, a corresponding glauconite-rich bed has been recognised in the Gault clay just below the Upper Greensand (A. S. Gale, pers. comm.).

A possible shallow water correlative of this interval, developed in the Haldon Hills of south Devon, is the Haldon Coral Bed in the Haldon Sands Formation (Hamblin & Wood 1976; Selwood and others 1984). This bed marks a facies change from glauconitic, well-sorted, clay-free sands (Telegraph Hill Sands Member) to glauconitic, clayey sands (Woodlands Sands

Member) which may represent a decalcified product of a "chert-free" Chert Beds lithology (Hamblin & Wood 1976). In the Grammarcombe Wood section, Great Haldon, the bed consists of a patchily-silicified, shell-rich, weakly glauconitic sand. The sand grade varies from predominantly fine-grained to occasional coarse, well-rounded grains. The shell concentration is principally composed of thin-shelled *Amphidonte* oysters, with occasional small corals. The shells show a range of fragmentation, from whole to comminuted; they show no preferred orientation of shell axes or of convexity.

In northern France, sections are exposed in the Boulonnais and in Normandy. The Boulonnais sections have been documented by Robaszynski *et al.* (1980). At Wissant, the equivalent of Bed XII at Folkestone is absent, with a large biostratigraphic gap encompassing the *dispar* and upper part of the *inflatum* ammonite zones. At Lottinghen, in the southern Boulonnais, clays of this age are preserved, and Robaszynski *et al.* (1980) document an interval of 1.5 metres of glauconitic clay with phosphatic nodules overlying a marked level of burrowing into the underlying clay. (N.B. This is within the authors' *Pervinquiera inflata* zone, equivalent to the *Callihoplites auritus* subzone of Owen 1976). The bed marks the base of the Formation de Lottinghen, and is equivalent to Bed XII at Folkestone.

On the Normandy coast, sections of this interval outcrop between Le Havre and St. Jouin-Bruneval; the horizon has been named the surface perforeé "Cauville" (Juignet 1974; Destombes *et al.* 1977; Juignet 1980), separating the Gaize Inférieure and the Gaize Supérieure (Fig.38). At St. Jouin, the interval is represented by four small cycles in an interval 4 metres in thickness (Fig.42; Fig.43). Each cycle consists of a sharp-based greensand bed (glauconite-rich muddy to marly, pyritic silts), passing up gradationally into glauconite-poor silts and marls. The base of each glauconitic bed is marked by an interval of burrowing; the burrowing extends downwards for as much as 20cm into the underlying sediment and the burrows are passively filled with greensand. Sediment mixing has taken place along the basal contacts, with isolated patches and shreds of sediment seen at the bases of the upper two cycles. At the bases of the lower two cycles, silty mud-lined burrows have been weakly phosphatised. The greensand beds become more pronounced upwards i.e. becoming thicker, more glauconite-rich, and with more

pronounced basal burrowing. The basal two beds are weakly developed, but the upper two have high glauconite concentrations and also weak basal lags of coarse quartz grains and small granules. The third greensand bed has granules up to 3mm across, and in the fourth, granules up to 6mm across are present. The quartz has been mixed into the basal parts of the greensand beds due to burrowing activity; in the fourth cycle, coarse grains are found up to 0.45m above the basal contact. Two phosphate generations are present in the upper two greensand beds. The first generation was derived from the underlying muddy silts, a result of either winnowing or burrow-exhumation, and was then redistributed due to bioturbation. The nodules are pale buff-coloured and tend to be larger than the second generation nodules, typically around 2-5cm across. The buff-coloured nodules can be seen *in situ*, scattered at low concentrations throughout the underlying muddy silt lithology. The second nodule generation developed within the greensand lithology. These nodules are small, typically a few millimetres across and are dark brown to black in colour; they occasionally show oyster sprat encrustation.

In the sections to the south, the cyclic nature of the interval is not developed. At Le Croquet and St. Adresse, the interval is represented by a single greensand bed 0.25-0.50m in thickness (Fig.38).

In the inland Normandy sections, a corresponding condensed glauconitic horizon has been documented by Ragot (1989) from sections in the area between Lillebonne and Villequier (along a major fault line). This is again represented by a metre-thick greensand bed, with a burrowed basal contact.

On the eastern side of the Armorican Massif, a very thin Albian sequence exposed in the Carrière le Livet, Cordebugle displays well-developed greensand beds (Fig.44); the lowest of these has a coarse quartzose basal lag overlying an burrowed erosion surface (Fig.45; Fig.46). The age of this bed is not certain; a phosphatised ammonite fragment from the base (first recorded specimen) was identified as *Hysteroceras orbignyi* Spath (identification by H. G. Owen). This is a typical *varicosum* subzone form (with a keel and slight chevron ribs), but could conceivably be of *auritus* subzone age. The greensand bed is probably of high *auritus* subzone age, based on this evidence and on the lithology; the ammonite specimen is remanié, derived

from winnowing of the underlying sediments.

Little detailed information exists concerning sections in the southern part of the Anglo-Paris Basin, where the outcrop is limited and the biostratigraphic resolution is poor. This interval has not been identified.

2.3.5 The rostratum and perinflatum subzone nodular hardgrounds and greensands

The lower Chert Beds hardground of south-east Devon has only been recognised around Beer, being absent in sections to the east due to erosion associated with synsedimentary faulting (see below). The Brecciated Limestone hardground has been recognised across south-east Devon, and apparently correlates with the Dispar Zone Ammonite Bed of south Dorset. To the east of Compton Bay, Isle of Wight, it is not present, and has not been recognised in the Weald. An erosion surface across south-east Devon marked by the Coarse Band is represented by a prominent greensand bed at the base of the Upper Greensand sequence around Eastbourne. The significance of this will be discussed below. The hardground at the top of the Upper Greensand is laterally very extensive, extending across hundreds of square kilometres of south-west England. A corresponding hiatus marked by the phosphatic greensand at the base of the Chalk, is present across much of southern England and northern France. The correlation of hardgrounds and greensands requires explanation and is addressed later.

2.4 Tectonic influences on sedimentation in the Albian of the Anglo-Paris Basin

Across much of southern England and northern France, the role of late Albian syn-depositional faulting appears to have been minor. However, a phase of folding and faulting accompanied Haldon Greensand deposition on Great Haldon, Devon (Durrance & Hamblin 1969), indicated by the thickness changes revealed by a seismic survey, and the Fecamp-Lillebonne-Villequier Fault in Normandy continued to have a important influence on sedimentation (Ragot 1989). Owen (1971b) has also invoked late Albian faulting along the southern margin of the London

Platform to explain the absence of the Lower Gault in this area.

2.4.1 Evidence for synsedimentary faulting in the Upper Greensand of south-east Devon

Detailed correlation of the Chert Beds and Top Sandstones has demonstrated the persistence of many of the marker horizons over the 10-20km of coastal sections. Evidence of synsedimentary faulting has been detected only at one locality - between the Whitecliff and Culverhole-to-Corbin Rocks sections. This is shown by the abrupt thinning of the lower Chert Beds, from 6.5m at Whitecliff, to 1.25m at Culverhole, to 1.0m around Corbin Rocks (Fig.19). To the east of Whitecliff, the lower Chert Beds hardground is absent, and the lower Chert Beds are capped by a marked erosion surface. A thin, glauconitic, variably clayey, pebble bed overlies the erosion surface (Fig.47; Fig.48). The pebbles are composed of glauconite-poor limestone; they range from 1-10cm across and display well-developed marginal borings (up to 2-3mm across) and marginal glauconitisation. Some of the glauconite grains are of coarse grade, up to 1-2mm across. Thin developments of the bed are shell-poor, but where the bed is thicker, it is often shelly, containing large pectinid bivalves and serpulids. Over short distances (tens of metres), the bed is laterally very variable in both thickness and clay content, ranging from 0.04m to 0.40m thick, and from clay-rich to clay-poor. The bed is at its thinnest overlying calcareous nodules in the underlying beds, indicating that these are probably of early diagenetic origin. The lower contact is irregular, with *Thalassinoides* burrows penetrating up to 1.1m into the pale brown calcarenites below (passively filled with the glauconitic clay). The lateral changes are interpreted as the result of late Albian synsedimentary faulting, probably along the line of a north-north-west - south-south-east -trending fault, which at Seaton Hole downthrows the Upper Greensand against Triassic red marls. The fault has an estimated throw of about twenty metres. The upthrown side of the fault was to the east, and the individual fault block to the east of Seaton Hole (as indicated by correlation of the erosion surface) was a minimum of 6km across.

2.4.2 Early Cenomanian faulting at Worbarrow Bay, south Dorset

In south Dorset, the Eggardon Grit at the top of the Upper Greensand consists of a 2 metre-thick bed of hard, grey nodular limestone. It is overlain by the Chalk Basement Bed, a pale, glauconitic, sandy limestone with scattered phosphate nodules, which grades up into pale grey chalk. A series of *Thalassinoides* burrows between the Eggardon Grit nodules pipe down the Chalk Basement Bed lithology for up to 30cm into the bed, and burrow wall (i.e. nodule margin) glauconitization is well-developed. A concentration of small phosphatised and glauconitized fragments is present at the contact between the two beds. At Lulworth Cove, phosphatisation and glauconitization of the hardground nodules is developed, and at Worbarrow Bay, thin chert lenses are present in the sediment just above the contact.

At Worbarrow Bay, below Flower's Barrow, there is good evidence for erosion at the top of the Upper Greensand, with truncation of the uppermost hardground nodules (Fig.49; Fig.50) and occasional erosional scours into the top of the Eggardon Grit, which are filled with disinterred calcareous nodules in a sandy limestone matrix. A section just 100m to the west of this locality shows the Eggardon Grit thinning rapidly, from 1.8m to only 0.2m of scattered calcareous nodules. Also, slipped blocks on the foreshore show isolated nodules of the Eggardon Grit, resting in a glauconitic marly matrix, and occasionally mixed with nodules of Exogyra Rock lithology (Fig.51). At Cow Corner, 250m to the west of the Flower's Barrow section, the Eggardon Grit and underlying Dispar Zone Ammonite Bed are absent; the Chalk Basement Bed rests on the Exogyra Rock (Fig.52). *Thalassinoides* burrowing penetrates between the nodules at the top of the Exogyra Rock; such burrowing is not present in other Exogyra Rock outcrops in south Dorset (except at Swanage Bay; see section 2.4.3.1), and infers that erosion has removed originally closely intergrown nodules in the uppermost part of the bed. There is also some glauconitization and weak phosphatisation of the uppermost nodules, a feature not seen in other sections.

At Mupe Bay, approximately 2km west of Flower's Barrow, the Chalk Basement Bed rests on silty clays and muddy fine sands of the Gault. At the contact, small concentrations of dark brown phosphate nodules are developed, some of which are serpulid-encrusted; pale brown

phosphates are present above. The glauconitic limestone rests on sandy glauconitic clay and the contact shows gentle undulations of a few centimetres in height. Only around 13m of Gault is present at Mupe Bay, though it is probable that some of the section has been cut out by a fault running up the gulley in which the beds are exposed. The exact position of the fault is not exposed, but its presence is inferred by an increase in the dip of the beds. From the phosphatic nodule bed at the contact, a specimen of *Anahoplites* sp. has been recorded (identification by H. G. Owen), which suggests a *varicosum* subzonal age. Thus at this locality, sediments of the *perinflatum*, *rostratum* and *auritus* subzones are missing (and possibly more of the underlying subzones also).

Thickness and facies changes in the Chalk Basement Bed also accompany the thickness changes in the Upper Greensand. Below Flower's Barrow, the Chalk Basement Bed consists of a pale, glauconitic (around 10%), sandy (around 3%) limestone with scattered phosphate nodules; this is 1.2m in thickness, and grades up into pale grey chalk. Just 100m west of this, the bed is 2.2m in thickness, and consists of a more glauconitic (20-25%) sandy limestone with scattered phosphate nodules. At Cow Corner, at least 1.75m are visible; it is strongly glauconitic, and phosphate nodules are common. At Mupe Bay, it is anomalously thick, consisting of around 6m of strongly bioturbated, glauconitic (15-20%), sandy (around 10%), marly limestone with scattered small phosphate nodules. At Lulworth Cove to the west, a "normal" thickness and facies is again exposed - 0.7m of a pale cream-coloured, glauconitic (around 5-7%), sandy (around 10%) limestone with scattered small phosphate nodules, grading up into pale grey chalk.

The lateral facies and thickness changes are interpreted as due to early Cenomanian synsedimentary faulting (Drummond 1970; Garrison *et al.* 1987). Unambiguous erosion of previously deposited Upper Albian beds is demonstrated by the thinning of the Eggardon Grit and the presence of eroded Eggardon Grit nodules, in some sections mixed with Exogyra Rock nodules. The erosion appears to be controlled in part by the lithologies of the underlying Upper Greensand. The Eggardon Grit, a hard nodular bed, proved resistant to erosion (below Flower's Barrow); where penetrated, the underlying soft, unlithified glauconitic marls and silts were easily

eroded. The erosion then cut down to the next resistant layer, the hard nodular Exogyra Rock. Where this has been penetrated, erosion has rapidly cut down to a much lower stratigraphic level (Mupe Bay). The Chalk Basement Bed is at its thickest, most glauconitic and most phosphatic at the locality of maximum erosion of the Upper Greensand and Gault - from 1.2m thick, 10% glauconite, weakly phosphatic (below Flower's Barrow), to 6m thick, 20% glauconite, strongly phosphatic (Mupe Bay). This is interpreted as reflecting a longer period of sediment starvation on the upthrown side of the early Cenomanian fault block, as sedimentation continued in the area.

2.4.3 Influence of positive structures on facies and condensation

In certain areas, pre-existing positive structures with low subsidence rates, but which were not undergoing active syndepositional faulting, had a strong influence on sedimentation, accentuating the effects of regional depositional hiatuses or erosion.

2.4.3.1 Complex condensation horizon at Swanage Bay, south Dorset. In central Dorset and in the Isle of Purbeck, Drummond (1970) recognised a north-west to south-east -trending belt of thinning in the Upper Albian and Cenomanian sequences. The structural feature responsible for this was named the Mid-Dorset Swell; the Chert Beds developed in south-east Devon (24m) thin eastwards over this broad positive area. At Swanage Bay (SY 044 811), the Chert Beds and Top Sandstones are represented by just 1.2m of sediment. Garrison *et al.* (1987) suggested that the Glauconitic Marl rests on the Dispar Zone Ammonite Bed at this locality (which is itself developed immediately above the Exogyra Rock). The interval is, however, more complex, comprising four generations of concretionary growth, two of which, as scattered isolated nodules, preserve lithologies which are developed further to the west. This is termed a complex condensation horizon.

The lowest beds of this part of the sequence consist of well-sorted, fine-grained, glauconitic (about 20%) sands. These contain scattered calcareous concretions up to 0.3m across. Such concretions are of the simplest kind, with no evidence for a complex history; they

preserve a lithology and bioturbated fabric identical to that of the host sediment. The sediments above this form the complex condensation horizon (Fig.53):

Generation 4: Eggardon Grit equivalent. At the same level as the type 3 concretions, and in a bed (0.27m thick) above it, a generation of glauconite-rich sandy limestone nodules is developed. These rest in a matrix which is actually Glauconitic Marl, containing small scattered phosphate nodules; this has been piped down into the Upper Greensand for up to 0.6m. Thus it also forms the matrix to the types 2 and 3 concretions; in some instances, Cenomanian phosphate nodules rest **below** the concretions which contain the Upper Albian phosphates (generation 3). The type 4 nodules differ from the matrix and overlying sediment in that they do not contain phosphate. There is a weak concentration of small phosphatic nodules at the top of the uppermost Upper Greensand nodule bed, but no nodule boring or encrustation was noted and only weak suggestions of marginal glauconitisation (brown, weathered, iron oxide coatings). The overlying bed of Glauconitic Marl is a greenish-grey, glauconite-rich (40%), quartzose (5%) marl, containing scattered small (typically 0.5cm across), pale brown phosphatic nodules and phosphatised fossils. It is structureless and strongly bioturbated, with abundant glauconite-free marl-lined sub-horizontal burrows. It reaches 0.75m in thickness, then grading over 0.35m into soft grey, only slightly glauconitic, non-phosphatic chalk.

Generation 3: Dispar Zone Ammonite Bed equivalent (0.20m) (Fig.55). A third nodule generation consists of glauconitic sandy limestone incorporating pale brown phosphate nodules and phosphatised fossil fragments. These rest in a sandy, glauconitic calcarenite matrix; they are not common, and occur scattered throughout the sediment just above the type 2 concretions. The phosphatic fossils are of Upper Albian *dispar* subzone age (A. S. Gale, pers. comm.). Type 4 concretions occur at the same stratigraphic level as these nodules and in the sediment just above.

Generation 2: Chert Beds equivalent (scattered nodules only) (Fig.54). The second nodule generation consists of isolated large nodules (typically 0.2m across), preserving a pale brown, only weakly glauconitic (3-4%) limestone lithology. These concretions preserve burrows filled with glauconite-rich sand in their outer parts, as a result of concretion growth in a burrow-mixed soft host sediment. The concretions rest in a sandy glauconitic calcarenite matrix.

Generation 1: Exogyra Rock equivalent (0.67m). Glauconitic fine sands pass gradationally up into a medium-grained, shell-rich, glauconitic (about 12%) slightly sandy calcarenite with abundant bivalves (*Amphidonte obliquatum* (Pulteney), *Neithea* sp.), serpulids (*Rotularia concava* (J. Sowerby)), and occasional bryozoans. The shells are mostly whole and unfragmented. Rare tiny (3-4mm across) dark brown phosphate nodules are present. Simple concretions of variably shelly glauconitic limestone are associated with this bed (generation 1); they have a relatively simple history. The shell concentration dies out at the top of the bed.

Thus in 1.2m of sediment, the complex condensation horizon contains four concretion generations. Nodular beds equivalent in age to both the Exogyra Rock and the Eggardon Grit are present. Two intervening nodule generations (2 and 3) representing different lithologies occur as isolated examples within a Glauconitic Marl matrix piped in from above by burrowing activity. Clearly, there has been a complex cycle of non-deposition and erosion over the crest of the "swell" area. The generation 2 concretions (Fig.54) attest to the deposition of pale brown, glauconite-poor limestones, which were then succeeded by greensand deposition (greensand-filled burrows preserved in their outer parts). This limestone lithology is characteristic of the Chert Beds Member. Generation 3 concretions indicate deposition of a phosphate bed of *dispar* subzone age, equivalent to the Dispar Zone Ammonite Bed, developed further to the west. These essentially represent "remanié type" concretions (though they are not bored or encrusted), remnants of original beds which experienced erosion during the late Albian / early Cenomanian, leaving only scattered nodules of already lithified sediment. This is shown by the fact that although the generation 2 concretions indicate deposition of Chert Beds limestones before deposition of the Dispar Zone Ammonite Bed, such limestones are not actually preserved in other south Dorset sections, where a variety of glauconitic, weakly phosphatic marls are developed at the same stratigraphic level. Such pale cream-coloured, glauconite-free sediments were only preserved further to the west, in south-east Devon. Thus, in summary, condensation and bed preservation over the crest of the Mid-Dorset Swell represent a combination of both non-depositional (slow sedimentation, glauconite enrichment) and erosive (removal of successive sediment generations) processes. These produced the complex condensation horizon.

2.4.3.2 Le Croquet, Normandy coast. In the southern part of the Normandy coast, the Gaize Supérieure (3.5m thick at St. Jouin) thins over a swell area, developed around Le Croquet (Fig.38). Amalgamation of condensed beds of different ages occurs, to produce a complex greensand horizon. These beds correlate with the surface perforée "Cauville" (high *auritus* subzone, Upper Albian) and the surface de ravinement "Octeville" (Lower Cenomanian); the swell is named the "Seuil d'Octeville" (Juignet 1980). Single greensand beds mark these two

intervals to the north and the south, the bases of which are marked by burrowing into the underlying sediment. Where the Gaize Supérieure is absent, however, they form a single bed 0.8m in thickness. The fabric of the strongly-bioturbated greensands is such that no distinct zone of burrowing is detectable between the two. They are distinguished by the fact that the Cenomanian bed is richer in phosphates compared with the underlying phosphate-poor Albian greensand, also by a decrease in the glauconite concentration, passing up into the Cenomanian bed.

Careful examination of other greensand beds (e.g. at St. Jouin, Normandy; Carrière le Livet, Cordebugle; south Dorset (Dispar Zone Ammonite Bed)) has also revealed minor discontinuities which are recorded by small fluctuations in the glauconite concentration and in the size grade of associated quartz grains.

2.4.3.3 The Isle of Wight. Strong thinning of the Chert Beds at the top of the Upper Greensand is shown in the northern half of the Isle of Wight. At Gore Cliff (SZ 492 763) and in the sections along the south coast of the island, the Chert Beds comprise around 11 metres of silty marl, rich in diagenetic silica which takes the form of massive, bedding-parallel bands of chertified sediment (Fig.41). These sediments are reduced to just 4 metres of silica-poor sediment at Compton Bay in the north-west of the island (SZ 367 853) (Fig.56), and are also markedly reduced in thickness at Culver Cliff in the north-east (SZ 265 855). The thinning of the Chert Beds coincides with the northern side of a prominent east-west trending fault zone running across the Isle of Wight, and the thickness changes appear to reflect "passive" thinning due to lowered subsidence rates over the northern upthrown side of the fault block. No evidence has been found which would indicate that the fault was active during the late Albian, but Owen (1971a) noted thickness changes in the Lower Gault at Rookley (SZ 510 840), which are attributable to sediment slumping. The lithological changes in the Upper Greensand indicate a deeper water more silica-rich facies to the south.

2.5 Mechanisms controlling late Albian condensation in the Anglo-Paris Basin

2.5.1 Cristatum and varicosum subzone phosphate beds

The *cristatum* subzone nodule bed marks the base of Upper Albian sedimentation and is the designated boundary between the Lower and Upper Gault. It represents a prominent erosion surface developed across much of southern England and apparently across northern Europe also (see earlier). Owen (1971a; 1971b; 1976) related the erosion surface to a tectonic cause, documenting the absence of the Lower Gault over the southern part of the London platform. In places, Upper Gault *orbignyi* subzone clays rest directly on Palaeozoic strata, and Owen suggested that Lower Gault deposition across the area was followed by Upper Albian erosion due to east-west -trending normal faulting. Recently, however, Hancock (1989) and Hesselbo *et al.* (1990) have suggested that erosion at this level represents a good candidate for interpretation as the result of relative sea-level fall. Similarly, the *varicosum* subzone phosphate bed marks a surface of non-deposition, which appears to be marked by erosion in some localities, though this is very minor in comparison to the *cristatum* subzone erosion.

Micropalaeontological evidence provides an excellent additional data set with which to compare the sedimentological evidence. The *cristatum* subzone nodule bed marks a major change in the foraminiferal populations (M. B. Hart 1973a). The Lower Gault population is dominated by the Robertinacea, whereas the Upper Gault contains a large percentage of Lituolacea, a dominantly agglutinated fauna, the development of which was related to an increase in the fine-grained clastic component of the sediments. In addition, the detailed methodology of Price (1976; 1977a, 1977b) has shown variations in the benthonic : planktonic foraminiferal ratios throughout the Albian of north-west Europe. Price showed that planktonic "lows" often correlate with phosphatic nodule horizons, suggesting reduced basinal circulation (inferred erosion), although a taphonomic contribution to the foraminiferal distribution remains a possibility. Planktonic "highs" normally follow such horizons, interpreted as a return to more open-marine conditions. Abundant planktonic foraminifera are found in the sediments just below the *cristatum* subzone nodule bed, but decrease rapidly in abundance in the nodule bed itself.

A rapid diversification and evolution of species is found in the sediments immediately above. An increase in planktonics throughout the *orbignyi* subzone is followed by a drop associated with the basal *varicosum* subzone phosphate bed. Increasing planktonics are found throughout the *varicosum* and *auritus* subzones, reaching greater than 65% of the total population.

Dinoflagellates are intimately associated with many of the thin phosphatic beds developed within the Albian clays of the Anglo-Paris Basin, and appear to be involved in phosphate neoformation (Fauconnier & Slansky 1979). Periodic single species domination suggests the development of planktonic blooms similar to "red tides". It is possible that many of the very thin single-nodule phosphate beds, in which the phosphate is not remanié and with no basal erosion surfaces, record such planktonic blooms.

The combination of sedimentological and micropalaeontological data strongly suggest that the formation of the *cristatum* subzone and *varicosum* subzone phosphate nodule horizons are the result of minor high-frequency relative sea-level falls. In the model proposed here, rapid relative falls resulted in basin-wide sediment erosion due to a lowering of storm wave base across the area. A larger relative fall is indicated by the *cristatum* subzone erosion surface, and a minor relative fall by the *varicosum* subzone erosion surface. Such erosion resulted in the winnowing of phosphate nodules from the underlying clays, concentrating them into a phosphate bed. The relative falls were of high frequency, and no evidence has been found for the introduction of coarser clastics at the basin margins. An erosive regime changed to one of sediment starvation as relative sea-level began to rise, until mean storm wave base had been raised to a level where clay sedimentation re-commenced; the influxes of planktonic foraminifera in these sediments testify to increased basinal circulation. The tectonic regime had an important role in governing the pattern of erosion across the basin; increased winnowing occurred over structural highs, resulting in the removal of greater thicknesses of underlying clays.

2.5.2 Glauconitic facies of high auritus subzone age

The salient features of the interval can be summarised thus:

1) An enrichment in the concentration of glauconite, a green K-Fe-Mg-rich clay mineral family which typically forms at or close to the sediment-seawater interface under low sedimentation rates (Odin & Matter 1981). Glauconite is often present in the "background" sediments, though at low concentrations (up to a maximum of 5-10%, compared with values typically in excess of 15-20% for the greensands). This reflects an absence of clastic dilutants and increased substrate glauconitization during the period of condensation.

2) Apparently normal water oxygenation/salinity in the Devon and Dorset sections, as evidenced by the presence of a fairly diverse fauna of bivalves (*Amphidonte*, *Neithea*, *Merklinia*), echinoids, bryozoans and serpulids.

3) The development of mid-shelf, very early diagenetic / synsedimentary cementation, producing glauconitic nodular calcareous sandstones (e.g. the Exogyra Rock and intraformational pebble beds).

4) a marked facies change across the interval in south-west England, from glauconitic, fine-grained siliciclastics (Foxmould Member) to fine-grained carbonate packstones and grainstones (Chert Beds Member) (rather muddy and quartzose in the basal part).

5) A change in the heavy mineral assemblages across the interval has been documented from south-west England (Smith 1961). The Foxmould Member contains abundant zircon, also kyanite, sillimanite, garnet and anatase, interpreted as an assemblage containing a high proportion of grains derived from pre-Cretaceous sediments; much could have been derived from the New Red Sandstone (Permo-Triassic). The kyanite and garnet appear to reflect some first-cycle metamorphic detritus. In contrast, the overlying carbonates (Chert Beds and Top Sandstones Members) have much lower sand contents and yield abundant tourmaline and zircon, also some topaz and pleochroic andalusite. This assemblage is interpreted as reflecting derivation from granitic source rocks to the west. Smith notes that the glauconite-rich sediments at or near the Foxmould-Chert Beds contact contain heavy minerals similar to those of the underlying member.

6) In certain sections, the condensation shows cyclicity, expressed by up to four small cycles. Each cycle consists of a thin, more glauconitic bed, with basal firmground burrowing which pipes the greensand into the underlying "background" sediment. Phosphate is associated with some greensand horizons; in the Folkestone section, it forms a lag to small scours at the base of the bed. Phosphate is also typically present throughout the bed; much appears to have been derived from the underlying sediments and dispersed due to the strong bioturbation. A second generation of phosphate which developed within the greensand may also be present. The greensand cycles increase in both thickness and glauconite concentration upwards, with the last two being particularly well-expressed, and the uppermost being the thickest and most prominent. Each cycle may be followed by a return to the "background" sedimentation (marls, silts) e.g. in the Whitecliff (Beer) and St. Jouin sections. In many sections, however, the cyclicity is not developed and only a single glauconitic bed is present. This could be the result of: deposition of the final most prominent cycle only, a selective preservation process by which previous cycles were eroded before deposition of the uppermost greensand bed, or amalgamation of successive cycles. The amalgamation of cycles is recorded in certain outcrops e.g. in central Dorset, where two successive beds of nodular greensand are developed; these pass into a single thick unit when traced into south Dorset. It is often the case that only the uppermost two cycles appear to be developed e.g. in sections between Axemouth and Lyme Regis, south-east Devon.

7) Ammonite biostratigraphic evidence dates the interval and also gives an order of magnitude for the time period represented in such sections. The condensation is dated to the upper part of the *Callihoplites auritus* ammonite subzone (*Mortoniceras (Mortoniceras) inflatum* zone of Owen 1976), though in some sections there is a possibility that it continued just into the lowermost *rostratum* subzone. Owen (pers. comm. in Gallois & Morter 1982, p.362) has suggested that the matrix sediment of Bed XII at Folkstone is of *rostratum* subzone age, based on the rare occurrence of *in situ* ammonites. Given a broad estimate of 0.30-0.45Ma for the length of the ammonite subzone (based on the numerical dating of the limits of the Upper Albian; Kennedy & Odin 1982), approximately one third of that subzone represented by the interval, and four cycles in the interval, a periodicity of around 25,000-40,000 years per cycle

can be inferred. i.e. the controlling mechanism for sedimentary condensation was of high frequency. Mean (compacted) sedimentation rates within this interval were extremely low, of the order of 7mm/1000years. This compares with background sedimentation rates calculated for the Devon Foxmould which are also very slow, of the order of around 10mm/1000years.

The glauconitic interval of the high *auritus* subzone is interpreted as a condensed deposit of a period of lowered sedimentation rate which affected much of the basin. This period can be resolved into four cycles, each of which consists of a greensand bed, followed by a return to background sediments. This infers four successive fluctuations in sedimentation rate, each of which produced a condensed bed. The interval appears to be present over much of the basin, being particularly well-developed on the basin margin of south-west England. When traced eastwards into the central part of the basin, however, the characteristic lithology dies out and is replaced by a more gradual facies change.

2.5.2.1 Erosion vs non-deposition. Evaluation of the relative importance of erosive and non-depositional processes is important to the interpretation of the interval. The presence of derived phosphate from the underlying beds and in certain sections, a weak concentration of coarse quartz grains in the basal parts of the greensand beds infers some erosion of the sediments below. This is also supported by the abrupt basal contacts of the beds, with their associated firmground burrowing. Erosion is also inferred from sections in the Weald described by Owen (1976), who notes that in the northern Weald, *auritus* subzone clays are only present below the condensed bed at Folkstone and below Canvey Island (in the Thames estuary). He suggests that the phosphate represents an erosion residual derived from previously-deposited clays of the *auritus* subzone. (N.B. At Folkstone, these clays are 10.67m in thickness.) The Upper Greensand is poorly-dated in the southern and western Weald, but at Eastbourne, the silty Upper Gault around 6m below the Upper Greensand belongs to the *inflatum* zone, based on a specimen of *Mortoniceras (M.) inflatum orbignyi* (Spath) (Kennedy 1967), and is probably of *auritus* subzone age. Owen (1976) records *auritus* subzone "malmstone" facies at the base of the Upper Greensand in the western Weald. In Wiltshire, the Potterne Rock, a prominent

concretionary horizon in the Upper Greensand, contains an unphosphatised *auritus* subzone fauna (Spath 1923-43). Sediments of the *auritus* subzone have been proven directly below the condensation horizon in the Isle of Wight (Gore Cliff), where the middle part of the Passage Beds is dated as within the lower *auritus* subzone (see earlier). The *auritus* subzone sediments are thus very thick in this area. In southern Dorset, *Callihoplites auritus* has been recorded from sands about 5m below the base of the Exogyra Rock by Wright (in Arkell 1947). In western Dorset, *Callihoplites auritus* has been recorded from sands near the base of the Upper Greensand at Picket Farm, between Mosterton and Cheddington, north of Beaminster (Wilson *et al.* 1958). In south-east Devon, *Callihoplites aff. auritus* has been recorded from the Foxmould by Hancock (1969). Thus, the erosion at the base of the interval is variable, reaching a maximum in the clay facies of the more central parts of the basin, where no underlying *auritus* subzone clays are preserved.

The stratigraphically-thin but geographically-widespread nature of the interval makes it an excellent candidate for interpretation as the result of low-magnitude, but high-frequency relative sea-level change. It appears to be of a transgressive nature overall, given the facies change in south-west England (from siliciclastics to impure carbonates), and the change in heavy mineral suites, which points to a shift in sediment source regions. This interpretation is in disagreement with the suggestion of Hesselbo *et al.* (1990) that the interval represents a candidate sequence boundary. In south-west England, the condensed interval is developed above storm-reworked sands and silts, and is itself affected by storm reworking; this constrains the magnitude of the inferred relative sea-level change. Independent evidence which points to a water depth increase across the interval comes from the micropalaeontological results of Price (1976; 1977a, 1977b). Planktonic : benthonic ratios reached a high in the high *auritus* subzone, and a widespread incursion and abundance of *Globigerinelloides bentonensis* occurs at this interval throughout north-west Europe. M. B. Hart (1973a) also found high planktonic percentages at this interval in the Folkstone section. Price (1976) notes that maximum foraminiferal diversity during the upper part of the Albian is related to increased mixing of

elements from both boreal and tethyan provinces, leading to a "diversity pump", with temperature and depth increase accompanied by increased current circulation. In the later Albian, increased benthonic diversity has been found to occur in association with every case of planktonic influx. The foraminiferal evidence thus supports the model of sediment starvation due to relative sea-level change, rather than, for example, climatic change (cf. Wignall & Ruffell 1990).

Given the interpretation of this interval as the condensed deposits of a rapid relative sea-level rise (resolved as four smaller rapid relative rises), it appears that a certain amount of erosion can occur due to non-deposition and sediment winnowing during such a rise, possibly of a similar magnitude to that occurring during a low magnitude sea-level fall.

2.5.3 Nodular hardgrounds and greensands of rostratum and perinflatum subzone age

The three nodular hardgrounds in the Upper Greensand of south-east Devon represent periods of low sedimentation rates across the carbonate shelf. The beds have certain fundamental features in common, implying that they may be genetically similar. Each hardground is characterised by the development of nodularity below a well-defined non-depositional surface, within a commonly cross-stratified and burrowed calcarenite substrate (cross-stratification seen in the Brecciated Limestone and top Upper Greensand hardgrounds). It thus represents a secondary modification of the original sediment fabric, which may be preserved as relict traces in the nodules. Evidence of storm activity is detectable throughout much of the Upper Greensand and represents the most likely agent for erosion of unconsolidated sediment above the nodules, and the maintenance of nodule exposure at the sea floor. Exposure resulted in boring, encrustation and mineralisation, and *Thalassinoides* burrowing excavated a complex gallery of shafts and tunnels between the nodules. The burrow-fills are generally coarser and much more quartz-rich than the original nodule lithology, and the open burrows appear to have acted as a trap for a coarser detrital fraction, probably concentrated by sediment winnowing.

The upper two hardgrounds pass laterally in a basinward direction into glauconite-rich, phosphatic greensands. The marked depositional hiatus recorded by the Brecciated Limestone

hardground in south-east Devon correlates with the development of the Dispar Zone Ammonite Bed in south Dorset. The marked hiatus recorded by the top Upper Greensand hardground in south-east Devon and the Eggardon Grit of south Dorset correlates with the development of a phosphatic greensand across much of the rest of the basin: the Glauconitic Marl of southern England (Kennedy 1969), the Formation de Strouanne of the Boulonnais (Robaszynski *et al.* 1980), and the Craie glauconieuse of Normandy (Juignet 1980). The greensands are interpreted as representing time periods during which the hardground nodularity developed and nodule mineralisation, boring and encrustation occurred. A summary of the sequential development of hardground and greensand beds is given in Figure 57. Within the marly clays of the Upper Gault of the Weald, phosphate beds equivalent to the lower Chert Beds hardground and the Brecciated Limestone hardground / Dispar Zone Ammonite Bed are not developed. This may be due in part to the disappearance of phosphate-forming dinoflagellates in the biogenic opaline facies of late Albian age in the Anglo-Paris Basin (Fauconnier & Slansky 1979).

The hardgrounds vary considerably in thickness and lateral correlation potential: the lower Chert Beds hardground (0.2-0.9m in the type sections around Beer) is proven laterally over just 1km (of coastal sections), the Brecciated Limestone hardground (0.85-1.00m) is traceable over an area about 15km across, and the top Upper Greensand hardground (1.0-1.9m) is present across south-west England, over an area about 85km across. Greater thickness, increased lateral continuity, and a greater degree of mineralisation reflect a greater length of the depositional hiatus which resulted in hardground development. The time gap associated with the lower Chert Beds hardground is the most minor; that associated with the Brecciated Limestone hardground is greater, and that represented by the top Upper Greensand hardground and Eggardon Grit is the longest. Only the hardground at this level is phosphatised, and the hiatus which it reflects has the most complex history, with several cycles of lithification, exposure, phosphatisation, boring and encrustation having been recorded (Garrison *et al.* 1987; Kennedy & Garrison 1975b).

2.5.3.1 Cyclicity in the Upper Greensand of south-east Devon. In south-east Devon, the facies associations suggest that the hardgrounds form the uppermost beds of shallowing-up cycles, though each cycle has slightly different characteristics. In the section at Little Beach to Beer Head, the following subdivisions are made (Fig.58):

D) The Top Sandstones. The uppermost cycle comprises a unit of well-sorted grainstones, 5.3m in thickness. At the base of the cycle is the Coarse Band, a coarse calcarenaceous sand which appears to represent a winnowed quartz-rich lag deposit; it grades up into quartz-poor carbonate grainstones above. The cycle is capped by the thick, laterally-extensive top Upper Greensand hardground. There is also a suggestion of shallowing-upwards within the cycle; the lower grainstones show occasional faint traces of low-angle tabular cross-lamination and of trough cross-bedding, whereas the structures of the uppermost grainstones and the hardground nodules themselves consist of well-developed trough cross-bedding.

C) The upper Chert Beds. Above the Brecciated Limestone hardground is a unit of well-sorted, pure grainstones. Rather than being capped by a hardground, however, the upper part has been removed by erosion, and the preserved beds only reach a maximum of 2 metres in thickness. This erosion resulted in the formation of the Coarse Band. In places, erosion has cut down to the top of the underlying Brecciated Limestone hardground, and the cycle is thus absent.

B) The upper Chert Beds. The second cycle begins with muddy packstones overlying the lower Chert Beds hardground; these pass up into fine-grained packstones with abundant chert nodules and traces of horizontal and low-angle to gently undulose cross-lamination. The calcarenites in the upper part of the cycle are well-sorted grainstones, and there is abundant evidence for higher-energy storm reworking, in the form of several intraformational pebble-shell concentrations. The sediments in the upper part of the cycle are less silica-rich than those in the lower part; the disappearance of chert is particularly well-defined in the Beer Head and Culverhole Point sections. The uppermost part of the cycle, which is capped by the Brecciated

Limestone hardground, also shows a different suite of sedimentary structures to the lower part, sets of trough cross-bedding being common.

A) The lower Chert Beds. The lowermost cycle begins with a facies change from the muddy silts of the uppermost Foxmould to fine-grained, silty carbonate packstones with abundant chert nodules. The lower beds show occasional vague traces of horizontal stratification; increasing storm activity in the upper part of the cycle is inferred by the development of a thick coquina shell bed representing two or more high-energy events. The cycle is capped by a nodular hardground.

Possible mechanisms to explain hardground formation include a tectonic control, with hardgrounds representing surfaces of non-deposition on the upthrown sides of fault blocks. Analogous nodular hardground beds are widely developed in the overlying Upper Cretaceous Chalk of the Anglo-Paris Basin (Bromley 1967; 1975; Hancock 1975; Kennedy & Garrison 1975a; Juignet 1980) and their temporal distribution has recently been summarised by Hancock (1989). Mortimore & Pomerol (1991) documented the spatial association between syndepositional faulting and hardgrounds in the Chalk. This occurs on a small scale in southern England, associated with small fault blocks and along fault lines controlling the development of periclinal folds, and on a larger scale in the Pays de Caux of northern France, where Middle Turonian hardgrounds extend across hundreds of square kilometres, but isolated between two well-known fault systems. Although Chalk hardgrounds correlate spatially with the upthrown sides of fault blocks, it is less clear whether their formation need have involved eustatic change. The cessation of sedimentation which resulted in hardground development was associated with a shallower depositional regime of increased sediment winnowing, but it is unclear whether fault movement alone could have produced these bathymetric effects. Models have been proposed which invoke eustatic mechanisms in order to generate hardgrounds; these have typically associated hardgrounds with regression (Juignet 1980; Hancock 1989).

The relative importance of synsedimentary faulting during Upper Greensand deposition

is demonstrated by correlation of the lower Chert Beds hardground (see earlier). The lower Chert Beds are markedly thinned, and are capped by an erosion surface to the east of the Seaton Hole fault (suggesting the upthrown side); the lower Chert Beds hardground is developed on the downthrown westerly side only. This is the opposite relationship to that predicted if faulting had generated the hardground (analogous to the Chalk examples listed above). This relationship strongly suggests that hardground initiation was essentially independent of faulting, though minor changes in hardground thickness across south-east Devon may relate to small-scale sea-floor topographic variation. The development of the hardground at the top of the Upper Greensand which extends across most of south-west England, within a variety of structural settings, also supports the hypothesis that hardground formation is independent of faulting.

Within this carbonate system, sediment production was essentially *in situ*, though widespread reworking is recorded. Although the sediments are impure, containing detrital quartz, this is a volumetrically minor component within the greater part of both members (Fig.18). Nodular hardgrounds appear at the tops of small shallowing-up cycles in the Chert Beds and Top Sandstones. Although this indicates formation during **relative** regression, followed by **relative** transgression and renewed sedimentation, this need not necessarily have been due to eustatic sea-level change, and an autocyclic mechanism may have been involved. Carbonate systems tracts, particularly during relative highstands in sea level, may be characterised by aggradational geometries (Sarg 1988); it is conceivable that with a slow subsidence rate across the area, the cycles could be formed by simple aggradation to a level at which sediment accumulation ceased. Continued slow subsidence across the area could then have resulted in resumed carbonate sedimentation. Average sedimentation rates for the Chert Beds and Top Sandstones Members taken as a whole (considering the length of the *dispar* zone to be around 2Ma) are very low: of the order of about 10mm/1000yrs. However, this does not account for the non-sequences and a few metres of missing stratigraphy at the base of the Coarse Band. Assuming that the time represented by each hardground may have been around five to ten times

that represented by an equivalent thickness of "background" sediments, that represented by each pebble bed to be around five times an equivalent thickness, and a total of five metres of eroded carbonates below the Coarse Band, a closer estimate of sedimentation rates for the background carbonates would be more than double this, of the order of 25-35mm/1000yrs. Given these considerations, the autocyclic mechanism of shallowing-up by simple aggradation during a sea-level still stand appears plausible. (Note that rates of Holocene glacio-eustatic sea-level rises are one to two orders of magnitude greater than these values; Schlager 1981.)

In summary, a shallowing-up cycle could feasibly represent local autocyclic sediment aggradation during a eustatic still-stand, or shallowing due to basin-wide relative sea-level fall (? of eustatic origin).

A hardground surface could represent non-deposition due to simple local aggradation to a level where carbonate production had shifted basinwards of the area, or non-deposition due to a basin-wide lowering of mean wave base (mean fairweather and mean storm wave base), preventing sedimentation.

Resumption of sedimentation above the hardground could represent local relative sea-level rise due to continued subsidence only, allowing carbonate production to resume in the area, or due to relative sea-level rise on a basin-wide scale, raising the mean wave base across the whole region.

Evaluation of the nature of the relative sea-level changes requires consideration of the facies on a basin-wide scale. Both the Brecciated Limestone hardground and the hardground at the top of the Upper Greensand correlate with phosphatic greensands when traced from the basin margin into the deeper basin. In southern England, the facies change at the top of the Upper Greensand and Upper Gault is from limestones and marls into nannofossil chalks, with the Glauconitic Marl developed at the contact; this represents an obvious change to a deeper-water facies. The facies change across the Dispar Zone Ammonite Bed of south Dorset is complicated by the presence of a stratigraphic gap of *rostratum* subzone age across the area;

glauconitic marls pass upwards into cherty limestones. The gap in the succession between the Exogyra Rock and the Dispar Zone Ammonite Bed (over the Mid-Dorset Swell) is in itself suggestive of an erosive episode preceding the sediment starvation which resulted in the development of the phosphatic greensand. The phosphates in the DZAB are not remanié nodules, derived from erosion of the underlying sediments (as is the phosphate in the Cambridge Greensand; M. B. Hart 1973b; Cooper & Kennedy 1977); nodules which appear to be developing *in situ* are seen, and are pale brown in colour, unlike reworked phosphate which tends to have a black coating (e.g. phosphate in the *cristatum* subzone and *varicosum* subzone nodule beds, and reworked *dispar* zone phosphate in the Cambridge Greensand).

Widespread sediment starvation (notably that at the top of the Upper Greensand) supports the model of rapid **basin-wide** relative sea-level rise following hardground formation i.e. the top of each hardground is a transgressive surface. This is also reflected in hardground nodule mineralisation. However, the nature of the preceding relative regression is less obvious. A high-frequency sea-level fall in such a carbonate facies appears not to produce a hardground but an erosion surface marked by a quartz-rich lag (the Coarse Band; see below). Thus the relative regression seen could be due to either a slower basin-wide relative sea-level fall, or simple aggradation during a still stand. Micropalaeontological evidence (Price 1977a) shows that within the Anglo-Paris Basin, a peak in the ratios of planktonic : benthonic foraminifera in the highest *auritus* ammonite subzone is followed by a very gradual fall in the planktonic percentage throughout the succeeding *rostratum* and *perinflatum* subzones (lower and upper Chert Beds). This suggests that a very slow low-magnitude relative sea-level fall may have occurred across the whole basin during these subzones, not just in the carbonates of south-west England. Thus for each shallowing-up cycle of the Chert Beds, the most feasible mechanism given these lines of evidence is that of **slow** low-magnitude relative sea-level **fall on a basin-wide scale**, followed by a relatively **rapid** relative sea-level **rise on a basin-wide scale**.

The presence of several glauconitic intraformational pebble beds in the upper Chert Beds also relates to small depositional hiatuses punctuating this part of the succession. They

are hiatuses of shorter duration than those represented by the thicker nodular hardgrounds, and successive minor relative sea-level rises may have occured across the intervals, though these appear too small to be reflected in shifts in facies.

2.5.3.2 Stable-isotopic data and relative sea-level change. Stable-isotopic signatures indicate rising δ13C values throughout the Chert Beds and Top Sandstones, reflecting increasing amounts of global organic-carbon burial (Chapter 4). This, however, may not provide a good indication of eustatic change. Certain positive carbon-isotope excursions may have been linked to transgressions (Jenkyns 1980), promoting large-scale burial of plant material during the drowning of deltas and coastal plains, and/or promoting high plankton productivity e.g. the Cenomanian-Turonian Oceanic Anoxic Event (Arthur *et al.* 1987). For the mid-Cretaceous, however, models have been advanced which invoke carbon burial in low-productivity oceans with slow deep-water circulation (Bralower & Thierstein 1984), though these models are disputed (Pedersen & Calvert 1990). If increased global carbon burial during the mid-Cretaceous was promoted by preferential preservation in a regime of sluggish basinal circulation, it is conceivable that the positive δ13C change across the Chert Beds and Top Sandstones may have occurred during a sea-level still stand or even slight regression. However, the conincidence between small positive carbon-isotope shifts across the nodular hardgrounds and water-depth increases (as proven by the lithologies and associated sedimentary structures) does suggest that transgression across the hardgrounds was on a scale large enough to affect the oceanic isotopic balance.

2.5.4 Shallow-water facies in the latest Upper Albian

In south-west England, a thin unit of shallower-water, higher-energy facies is developed at the top of the Upper Albian succession. In the most proximal sections, tidally-influenced sands with interbedded thick gravels are developed within the Bovey Basin (Babcombe Copse SX 312 918), just to the east of the Dartmoor Granite, which was supplying large volumes of sediment. Further east, in the Haldon Hills, the development of the Ashcombe Gravels of the Haldon

Sands Formation marks a change from glauconitic clayey sands with shell concentrations and siliceous nodules (the Woodlands Sands, probably the decalcified Chert Beds equivalent; Hamblin & Wood 1976) to interbedded sandy gravels and coarse gravelly quartz sands. Three prominent gravel beds are developed on Great Haldon. In south-east Devon, the Top Sandstones are developed at this interval, and represent sedimentation in an environment dominated by fair weather shoaling waves, in contrast to the storm-dominated Chert Beds below. A prominent erosion surface, with overlying quartzose lag, the Coarse Band, marks the base of the unit. In south Dorset, the stratigraphic interval correlates with the appearance of coarse quartz sand in the uppermost part of the section, at the level of the Eggardon Grit. This thin package of shallower-water facies dies out to the east of this area, and is not developed in the Isle of Wight.

An additional thin package of Upper Greensand sediments has been recognised above the Gault in the southern Weald and English Channel area, and has been documented by Young (1978) and Mortimore (1986). To the south of Eastbourne (TV 610 977), 5.75m of Upper Greensand are developed above the Gault sequence. The base is marked by a prominent, marly, sandy, greensand (around 65% glauconite) with phosphatised burrows (Fig.59), and a burrowed basal contact with the underlying Gault clay. This passes up into glauconite-poor, muddy, compact calcareous siltstones. In this area, the Upper Greensand thins northwards from Cow Cap, to die out below Eastbourne. Between Eastbourne and Hassocks (about 35km to the west-north-west), the Upper Greensand is not developed, the Lower Chalk resting directly on Gault clay (Young 1978). To the west of Hassocks, the Upper Greensand is again developed, consisting of fine-grained calcareous siltstone or "malmstone". Isopachyte maps within the Chalk show that the structural style of the area is dominated by a series of shallow *en echelon* anticlines and synclines (Mortimore 1986; Mortimore & Pomerol 1991). The Upper Greensand of this area occupies a narrow WNW-ESE-trending zone, north of which it is absent. A 15° angular unconformity was recognised at the contact between the Gault and Glauconitic Marl in a pit at Asham (Mortimore 1986). The Upper Greensand appears to represent selective deposition and/or preservation in a NNW-ESE-trending basin within this structural zone.

A very thin Upper Greensand sequence of latest Upper Albian age has also been recognised at a number of other localities (M. B. Hart 1973a; Owen 1976; Carter & M. B. Hart 1977). A facies lithologically similar to the Eastbourne Upper Greensand is developed in the English Channel between Dover and Folkstone; also the highest part of the Upper Greensand in the northern Weald (Godstone-Dorking-Leatherhead) and in boreholes to the north at Fletcham Mill and Canvey Island is probably of this age. Elsewhere, the thin sequence is absent (not deposited or eroded) or not identified. Price (1977a) has recognised three foraminiferal subzones within the unit, which is of uppermost Albian age, and which has been assigned to a stratigraphic level higher than the *perinflatum* ammonite subzone. Clearly, the ammonite biostratigraphy of the highest Albian/lowest Cenomanian is in need of clarification, the stratigraphic gap over much of the basin at this level has resulted in some confusion. Within the Albian sediments across north-west Europe, a minor low in planktonic : benthonic foraminiferal ratios has been identified at the top of the *perinflatum* subzone (Price 1977a), coinciding with the development of this erosion surface across southern England. Ratios increase gradually through the uppermost post-*perinflatum dispar* zone.

2.5.5 Sequence stratigraphic analysis of the Upper Albian of the Anglo-Paris Basin

As discussed above, prominent erosion surfaces and intervals of sedimentary condensation extending across the Anglo-Paris Basin represent good candidates for interpretation as the result of high-frequency relative sea-level change. Using the sequence stratigraphic models and terminology developed by Haq *et al.* (1988), Posamentier *et al.* (1988), Posamentier & Vail (1988) and Loutit *et al.* (1988), the Upper Albian sediments can be subdivided into three candidate depositional sequences (Sequences 1-3; Table 1); within each of these, candidate systems tracts are proposed, separated by marine flooding surfaces across which there is evidence for an increase in water depth (Table 1; Fig.60).

The three surfaces which show evidence for erosion on a widespread scale are: 1) the *cristatum* subzone nodule bed (discussed in sections 2.3.1 and 2.5.1), 2) the *varicosum* subzone nodule bed (discussed in sections 2.3.2 and 2.5.1), and 3) the base of the thin unit of shallow-

water facies in the latest Albian (discussed in sections 2.1.4.1 and 2.5.4). The phosphatic beds consist of nodules which have been concentrated by winnowing of the underlying sediments (section 2.5.1). Erosion in the highest *dispar* zone (Fig.60) resulted in the development of a winnowed quartzose lag across south-east Devon. The three erosion surfaces are considered to represent good candidates for sequence boundaries.

There is no evidence for the development of shallower-water, higher-energy facies (other than low planktonic : benthonic foraminiferal ratios) at the levels of the *cristatum* subzone and *varicosum* subzone nodule beds. The sequence boundary is placed at the base of each phosphate bed, and a transgressive surface, with renewed deposition of clays (designated as the transgressive systems tract) is identified directly above the bed. On a small scale, however, considerable sediment mixing due to bioturbation has occurred, and the sequence boundary and transgressive surface can be considered to be amalgamated.

However, across the highest *dispar* zone erosion surface, there is no such evidence for immediate deepening, and a thin unit of shallower-water facies is developed above. This thin higher-energy unit is termed a shelf margin systems tract. It appears to have a weak progradational geometry when traced from west-to-east across south-west England, and thins and fines in this direction. Evidence for deepening occurs at the top of the thin wedge, marked by greensand and hardground development at the top of the Upper Greensand (sections 2.1.4.2, 2.2.5 and 2.5.3); this is considered to mark a transgressive surface.

Thus, for the lower two candidate sequence boundaries (bases of Sequences 1 and 2), a transgressive surface is considered to directly overlie the sequence boundary, whereas in the upper example (base of Sequence 3), the transgressive surface is separated from it by a thin shelf margin wedge.

The high *auritus* subzone interval of sedimentary condensation (as discussed in section 2.5.2) is considered to be the result of a rapid relative sea-level rise. It is interpreted as a condensed section, developed at the junction between the transgressive systems tract of the Foxmould Member and lower Upper Gault (glauconitic sands, silts and clays) and the highstand systems tract of the Chert Beds and upper Upper Gault (glauconitic limestones and marls).

Within the highstand carbonates, shallowing-upward cycles are developed; these are capped by nodular hardground/greensand development (discussed in section 2.5.3). Across the surfaces, there is evidence for minor depth increases; interpretation is consistent with generation by minor rapid relative sea-level rises, superimposed on a longer-term still-stand or slow relative sea-level fall. In the analysis below, they have been termed transgressive surfaces. The surfaces subdivide the highstand deposits into early, middle and late parts. The middle highstand deposits contain a number of additional minor non-sequences.

2.5.6 Comparison with the Exxon "eustatic" cycle chart

The present interpretation allows comparison with the sea-level cycle chart of Haq *et al.* (1988), to determine whether the surfaces recorded therein are reflected in the Upper Albian sediments of the Anglo-Paris Basin. (Note, however, that some of the data used to compile that chart may feasibly have been taken from the British area.)

Identification of the lower *cristatum* subzone surface of the Wessex Basin as a candidate sequence boundary within the Wessex Basin was made by Hesselbo *et al.* (1990). This work confirms the interpretation; it corresponds to the 99Ma medium-sized type II sequence boundary on the cycle chart.

In the sediments above there is, however, less agreement with the cycle chart. The minor candidate sequence boundary proposed here for the basal *varicosum* subzone is not recorded by Haq *et al.* (1988). The major condensed section marked at 98.25Ma on the chart may be represented by the upper *auritus* subzone condensed sediments of the Anglo-Paris Basin. However, the following major 98Ma type I sequence boundary on the chart, of the high *inflatum* zone, does not correlate with the development of such a major erosion surface in the Anglo-Paris Basin at this time.

The sediments above this level in south-west England are complex, and an interpretation has been advanced which postulates that the tops of hardgrounds represent transgressive surfaces. The cycle chart infers increasing coastal onlap with development of a medium-sized condensed section during this interval (97Ma); however, a relative still stand or slow relative

regression is inferred from the southern England sections, with superimposed minor relative transgressions.

The 96.5Ma minor sequence boundary on the cycle chart agrees well with the sequence boundary recognised in the highest *dispar* zone across southern England.

Thus, in summary, there is some agreement between the interpreted relative sea-level changes identified in the Anglo-Paris Basin, and the global cycle chart of Haq *et al.* (1988), but also a measure of disagreement. This comparison is summarised in Figure 61. A major discrepancy concerns the 98Ma major type I sequence boundary given on the chart; no equivalent has been found in sediments of this age in southern England and northern France. The significance of this will not be discussed further here, but must await similar detailed studies in the Upper Albian sequences of other sedimentary basins.

2.6 Summary and Conclusions

The Upper Albian sediments of the southern England have been described with reference to type sections of the Upper Greensand in south-east Devon and south Dorset. These sediments have been shown to display a range of condensation phenomena, ranging from phosphatic nodule beds, to glauconite-rich greensands, to intraformational pebble beds and nodular hardgrounds. These intervals and associated erosion surfaces are correlated across the basin, using data from outcrop study and published biostratigraphic information. Certain of these beds are very widespread in outcrop; coupled with their narrow stratigraphic ranges, this argues that their development was controlled by sedimentation rate changes relating to rapid relative sea-level change of at least regional nature. Each surface identified is discussed in detail, relating to its sedimentological expression, its age and correlation potential, and possible controlling mechanisms to explain its development. The role of tectonic influences is also discussed for a variety of localities, including synsedimentary faulting and thinning and amalgamation over

broad submarine highs. A sequence stratigraphic analysis is proposed, subdividing the Upper Albian succession, and a comparison is made with the Exxon cycle chart.

Candidate sequence boundaries have been identified within the lower *cristatum* and lower *varicosum* subzones; these are represented by winnowed phosphatic lag deposits. An additional candidate sequence boundary is developed within the upper *dispar* zone, at the base of a thin wedge of higher-energy facies of latest Upper Albian age. The glauconite-rich interval of the high *auritus* subzone is considered to represent a condensed section, caused by rapid relative sea-level rise, and nodular hardgrounds and greensands higher up in the succession appear to mark the position of transgressive surfaces.

CHAPTER 3

STORM SEDIMENTATION IN THE UPPER GREENSAND FORMATION (CRETACEOUS) OF SOUTH-WEST ENGLAND

Abstract: Episodic, high-energy storm beds are an important component of the stratification style of the Upper Greensand (Albian, Cretaceous) of south-west England. These storm events are preserved in the sedimentary record of a broad epeiric shelf-margin setting. In the lower fine-grained glauconitic siliciclastic member, graded laminite beds of varying thickness and degree of amalgamation record a spectrum of storm intensities and periodicities; they show diagnostic structures and characteristic proximal-distal trends. Storm processes involved shelf-wide sediment entrainment followed by settling from sediment-laden suspension clouds, rather than unidirectional current transport. Pervasive storm reworking is also recorded at the overlying siliciclastic-carbonate transition, and in the carbonate packstone and grainstone members above. This interacted with very early submarine lithification processes to produce a suite of intraformational pebble-shell beds, simple and amalgamated coquina beds, and storm-scoured hardgrounds. Analysis of bed fabrics shows that the most proximal coquinas have nested, predominantly convex-down shell orientations; these pass offshore into beds with predominantly convex-up shell material. Storm processes identified include both sediment winnowing and transportation of bioclasts. Evaluation of the taphonomy of the shell beds indicates that they were generated by rare, very high-energy storm events, in which skeletal material was buried and preferentially protected from lower energy shell abrasion. The background calcarenites record this lower energy but prolonged weak storm and fair weather reworking, in which physically less-resistant skeletal elements were rapidly broken down into carbonate sand. Evidence for storm-influenced sedimentation can be detected throughout most of the succession, but typically only the highest energy storms were preserved as discrete (sometimes amalgamated) units, resulting in a distinct "event stratigraphy".

The Upper Greensand Formation of southern England and its stratigraphic equivalents comprise a thin (typically approximately 50 metres), generally glauconitic succession of Upper Albian (Cretaceous) age, developed across the Anglo-Paris Basin (Wessex and Paris Basins) of southern England and northern France. Facies associations broadly comprise basin-margin gravels, sands and limestones, passing into deeper basinal silts, clays and marls (contiguous with the Upper Gault of the Weald; Owen 1976). The formation stratigraphically overlies the tidal and estuarine facies of the Lower Greensand and marine clays of the Lower Gault; it is itself overlain over much of the basin by deeper-water nannofossil Chalk. Taken as a whole, the formation is thus transgressive, reflected in the prominent basal unconformity seen across south-west England (Hancock 1969). On this basin margin, the Albian sediments transgress the eastern part of the Cornubian Massif, sequentially overstepping the underlying Lower Cretaceous, Jurassic, and Permo-Triassic, to rest on Upper Palaeozoic (Carboniferous and Devonian) sediments in the Bovey Basin (Selwood and others 1984).

In south-west England, the Upper Greensand is represented by about 50m of variably glauconitic siliciclastic and carbonate sediments. In south-east Devon (Fig.62), the formation has been subdivided into three members (Jukes-Browne & Hill 1900; Smith 1961), consisting of glauconitic fine-grained sands and coarse silts (Foxmould Member), overlain by bioclastic packstones and grainstones with pebble-shell beds and nodular hardgrounds (Chert Beds and Top Sandstones Members).

The formation rests unconformably on Triassic red beds in south Devon; it is of Upper Albian age (*varicosum* to *perinflatum* ammonite subzones of Owen 1976), though the exact age and nature of the muddy basal beds directly overlying the unconformity are uncertain.

3.1 Storm laminites in the Foxmould Member

The Foxmould consists of approximately 25m of muddy, very fine sands and coarse silts; these are glauconitic (typically 5-10%), weakly pyritic, and occasionally phosphatic. A shelly fauna

of bivalves (*Amphidonte obliquatum* (Pulteney); syn. *Exogyra obliquata*, *Trigonia sp.*, *Merklinia aspera* (Lamarck), *Neithea gibbosa* (Pulteney)), gastropods, rare ammonites, serpulids (*Rotularia concava* (J.Sowerby)), and echinoids is present; the aragonitic fossils are now preserved as moulds. Sedimentary textures consist of an original depositional lamination developed in discrete beds; this alternates with very strongly- to completely-bioturbated sediment often preserving weak traces of lamination (Fig.63). The laminites record discrete, high-energy depositional events, which alternated with periods of lower energy during which burrowing activity exerted the main control on the resulting sediment fabric.

3.1.1 Typical features of an individual laminite bed (Fig.64)

1) A sharp, erosional contact with the underlying sediment. The contact is generally horizontal and planar, but occasionally, in more proximal beds, scouring is developed.

2) A thin (typically 1-7cm), irregular, shelly basal layer. This consists predominantly of calcareous serpulid tubes (*Rotularia concava* (J.Sowerby)) and calcareous bivalve shell fragments; aragonitic bivalve shells were also incorporated, but are now preserved as moulds. Small mud clasts are sometimes found; these represent intraformational rip-up clasts, derived from mud-lined *Palaeophycus* burrows.

3) A laminated fine sand to coarse silt. The sedimentary structures are characterised by dominantly planar horizontal lamination, with subordinate low-angle planar cross-lamination. In more proximal beds, scour and fill structures are present. Small black mud clasts overlie some of the low-angle reactivation surfaces. The lamination is typically on the scale of 1mm-1cm, defined by variations in the concentration of sand, fine sand-sized glauconite grains, silt and clay.

4) A general fining-up, and thinning-up of laminae through the bed can sometimes be discerned, depending on the amount of bioturbation in the upper part.

5) A bioturbated top; the degree of bioturbation increases upwards, laminated non-bioturbated sediment passing transitionally up into fully-bioturbated sediment (Fig.65).

6) High concentrations of concretions (siliceous concretions in proximal beds; calcareous

concretions in more distal beds) are often associated with the thicker laminites. Their presence presumably relates to the increased sediment permeability resulting from segregation of the sandy and muddy components. Both early and late diagenetic nodules are found; the early nodules demonstrate distortion of the surrounding sediment fabric (differential compaction, displacive growth), whereas the late concretions preserve a compacted sedimentary fabric. Such late nodules have often formed around the basal shelly layers of the laminites.

3.1.2 Description and proximal-distal trends

Proximal-distal trends in both the thicknesses, and suites of sedimentary structures of the laminites can be recognised. The laminites show a general west-to-east thinning and fining trend, and the sequence passes into homogenous, followed by rhythmically-bedded silts in the direction of deepening (Fig.66). The offshore-thinning trend is well displayed by correlation of four thick, closely-spaced laminites at Peak Hill, near Sidmouth (SY 109 866), to three thinner units at the Hooken Cliffs, Beer (SY 220 879), and to mere traces of lamination in bioturbated sediment at Seaton Hole, Beer (SY 235 896).

The most proximal beds exposed display a range of thicknesses and degrees of amalgamation, recording different event intensities and frequencies. Measured bed thicknesses range from 4cm (thin amalgamated beds) to >0.8m (thick beds with bioturbated tops, Fig.67). Such beds have sharp bases, generally planar, but rarely scoured (up to 0.2m) into the underlying beds (Fig.68). The shelly, serpulid-rich bases are considerably reduced in the thicker beds, but are better developed in the thinner examples, inferring that the higher-energy events transported this sediment component offshore. Sedimentary structures record predominantly vertical sediment accretion; there is a distinct absence of angle-of-repose cross-lamination. The dominant lamination style is of simple, horizontal structures, with associated low-angle reactivations and low-angle (up to 10°) to gently undulose cross-lamination (Fig.69). Small-scale scours are also developed within laminite beds; these are typically on a scale of 5cm deep, and 10-20cm across. They are generally asymmetrical, with a single steeper side. Such scours are developed throughout individual beds, although they tend to be less common in the

upper part. Laminae filling the scours thicken towards the scour centres, either draping the scour concordantly, or maintaining discordant contacts with the scour margin. The highest dip angle recorded (32°) represented lamination deposited on the margin of a steep-sided basal scour; within the shallower scours, low-angle laminae pass laterally into horizontal laminae. Occasional intraclasts of brown mud are present, overlying reactivation surfaces, and revealing local erosion of mud-lined *Palaeophycus* burrows. Taken as a whole, a thicker laminite bed shows a graded rhythmite sequence, with thicker laminae and a coarser grain size at the base, passing up into pale brown muddy silt (with very weakly-defined horizontal lamination) towards the top of the bed. (Wave ripples are absent.) On a small scale, however, considerable variations in lamina thickness are present within a single bed (between 1mm and 1cm). Hydrodynamically, the glauconite grains are seen to follow the fine sand fraction, and are rare in the upper fine-grained silty bed tops.

Discrete laminite beds have bioturbated tops; laminated muddy silt passes up into almost structureless silt (limited grain size variability preserves only weak structures), and then into progressively more bioturbated, muddy, fine-grained, glauconitic sand (Fig.70). *Thalassinoides* burrows, passively filled with glauconitic sediment, typically penetrate to a maximum of 0.3m below the inferred top of an individual bed, implying that beds thinner than this have the potential to be lost through homogenisation due to burrowing activity.

Amalgamated units comprise two or more vertically-stacked laminites. Each individual bed within such a unit consists of a sharp base and shelly serpulid lag, with overlying laminated sediment. A variable proportion of each bed, including the bioturbated top, is not preserved, this sediment having been eroded by a succeeding event.

More distal laminites are characterised by generally thinner individual beds (typically 0.10-0.75m), interpreted as the result of a combination of lower original sedimentary thickness (deeper water, lower energy), and increased biogenic reworking (less-frequent events). The lamination style is again dominated by simple planar horizontal structures, with rare low-angle reactivations, and low-angle to very slightly undulose planar cross-lamination (up to 10°).

Occasional small mud intraclasts, 1-2cm across are present. The scour and fill structures are very rare to absent in these more distal beds (only a single small scour, 2cm deep, was found in the upper laminite bed at the Hooken Cliffs). Bases of the beds are overlain by shelly, serpulid-rich debris; this material does not form a well-sorted shell lag, occurring at fairly low concentrations irregularly dispersed throughout the basal few centimetres. Such material appears to be a winnowed fraction of the underlying sediment, probably then subjected to minor transportation. No evidence of infiltration textures (eg shelter-porosity below convex-up shells) has been detected, the aragonitic shells now being represented by composite moulds. Discrete beds again have bioturbated tops, with small *Thalassinoides* being common. Occasional amalgamated thin beds are present (Fig.71). Graded rhythmite sequences (thinning and fining up of the laminae) are less easy to recognise, due to the fact that the upper parts of the beds are strongly-burrowed. However, in some examples, a distinct increase in the mud content of the sediment can be recognised above the laminite, despite the bioturbation, attesting to the original fine-grained bed tops.

A similar Foxmould succession is developed in the Blackdown Hills, about 20km to the north, and was described by Downes (1882) from a series of small quarries, now no longer exposed. The middle part of the Foxmould consists of sands, interbedded with thin bivalve-rich layers. Some of the shell material is broken and abraded, and certain layers are lenticular and impersistent. Siliceous concretionary horizons are common. These beds contain a rich and diverse molluscan fauna (Taylor *et al.* 1983).

3.1.3 Reworking of phosphate

A thin, weak concentration of black phosphate nodules is present in the Foxmould at Beer, and in the Axemouth-Lyme Regis sections (SY 274 893 to SY 307 899) (Fig.72). This is of *varicosum* subzone age, shown by a specimen of *Epihoplites cf. gibbosus* (Spath) collected from the Hooken Cliffs section (identification by H. G. Owen). The phosphate occurs as small black nodules, typically of sand- to small granule-grade, with occasional larger fragments up to 5cm across. The phosphate occurs as amorphous grains, internal moulds of bivalves and gastropods,

phosphatised serpulids, burrows and shell fragments, rare ammonite steinkerns, and small shark and fish teeth. Reworking of the phosphate is evident from its incorporation into a shelly horizon, with *Amphidonte* (both whole and broken; often rich in the smaller lid-like upper valves), *Entolium*, and the serpulid *Rotularia*. The shelly horizon is itself only 5cm thick, and is overlain by 0.2m of muddy, fully bioturbated fine sand, into which some of the phosphate is admixed. The bed represents event reworking of a thin, immature phosphate horizon, followed by incorporation of the phosphate into the shelly basal layer of a laminite, and subsequent bioturbation down to this level. Reworking was essentially *in situ*, with only minor lateral sediment transport of the phosphate implied by the incorporation of rare larger nodules up to 5cm across.

3.1.4 Analysis and interpretation

The vertical sequence of sharp-based laminites with bioturbated tops, developed at particular horizons within an otherwise strongly-bioturbated, fully marine siliciclastic sequence, record discrete higher-energy events alternating with longer periods of lower energy; they are typical of storm-influenced deposition. The vertical sequences preserved within individual laminite beds are particularly diagnostic of storm events, while maintaining dissimilarities with those of certain other interpreted tempestites. Sedimentary structures indicate predominantly vertical suspension settling of sediment, without showing waning flow (Bouma) features typically associated with turbidites and graded sand layers interpreted as of storm surge origin (see below). Similar sequences of structures and vertical successions have been described and reviewed by various authors (e.g. Reineck & Singh 1972; Kumar & Sanders 1976; Kreisa 1981; Aigner 1982; 1985).

The thicknesses and successions of sedimentary structures of the Foxmould laminites have important implications for the morphology and hydrodynamic regime of the late Albian epeiric shelf. The gradual lateral facies change from bioturbated muddy sands with laminite beds, into fully-bioturbated, rhythmically-bedded muddy silts (over a distance of about 100km) shows an eastward-deepening direction. The sequence of sedimentary structures within a laminite bed records principally vertical sediment accretion; even when apparently almost-complete beds

are preserved, horizontally-laminated fine sand passes up into horizontally-laminated muddy silt. No ripple cross-lamination has been recorded from the bed tops. The laminites thus differ from many documented ancient and modern storm beds, in which wave or current-generated structures in the upper parts of the laminite sequence result from waning-storm activity (oscillatory flow or storm-generated unidirectional current).

Basic models which have been advanced to account for offshore sediment transport in a storm-influenced depositional regime include the storm surge ebb model, involving onshore build-up of coastal waters due to storm activity, followed by a waning-storm seaward return flow (which may be geostrophic and thus shoreline-parallel). A 6m build-up was quoted for Hurricane Carla (Hayes 1967); up to 5m was quoted for the modern Bering shelf (Nelson 1982). Morton (1981), however, re-examined the Carla and other data (Gulf of Mexico and the North Sea), and invoked a process of wind-forced currents to explain the offshore transport of sediment, in which the upper water column is envisaged to move onshore under the influence of wind activity, accompanied by simultaneous offshore bottom currents; these may constructively or destructively interfere with existing (e.g. tidal) currents. (See also German Bay, North Sea summary by Aigner 1985). Nelson (1982) recognised both processes on the modern Bering shelf, but suggested that ebb-flow currents are the dominant sand transport agent.

No evidence for dominant unidirectional current processes has been detected in the Foxmould laminites studied. Only a single, isolated lens of tabular cross-lamination (set height 13cm, 4m across, enclosed within bioturbated sediment) has been recorded (at Whitecliff, Beer, SY 234 893, Fig.73). This indicated a current direction towards 244° i.e. approximately westwards, in the inferred onshore direction; its origin remains unclear. Storm wave entrainment of large quantities of fine-grained sediment across the low-angle shelf appears to have been an important process, followed by vertical deposition from suspension. Such a process of suspension cloud formation due to the rather irregular turbulence caused by storm wave interference has been postulated by Reineck & Singh (1972) to explain similar recent laminated beds. The horizontal lamination does not pass up into cross-lamination as a waning-flow sequence, as would be expected if it had been generated by an upper plane bed phase regime.

Beds up to a maximum of approximately 1m in thickness recorded from the Foxmould appear to record suspension settling on a particularly large scale. Sediment entrainment during the storm is indicated by the erosive bases of the laminites (rare scouring), and small scours within a laminite bed, becoming less frequent as the beds are traced offshore, record evidence for minor current activity (interpreted as turbidity generated by storm wave interference). Estimates of the depth of storm scouring within two other siliciclastic systems (German coast, New Jersey; Kumar & Sanders 1976), based on direct measurements and on the disinterment of burrowing organisms, suggest erosion of around 20-30cm of sediment. Late waning-storm deposition produced fine-grained (mud and silt-rich), horizontally-laminated bed tops. The relative importance of offshore sediment transport is difficult to evaluate for the Foxmould shelf, given the lack of evidence for current or combined wave-current systems operating in this mid-shelf setting; possibly these processes were operative in a more proximal, shallower water environment, whose sediments are not exposed or eroded. It is probable that the whole of the Foxmould laminites observed were actually deposited during waning storm conditions, when most wave-generated currents no longer reached the sea-floor. Kreisa (1981) described very similar laminated structures from the Martinsburg Formation (Ordovician), and suggested that the gentle undulations of the laminae may be the result of weak wave oscillations, or partly transitional to climbing wave ripple cross-lamination. The lack of ripples even in preserved bed tops in the Foxmould does, however, indicate an absence of strong oscillatory flows. The model proposed here is consistent with the measured grain sizes (median Foxmould grain sizes between 0.052 and 0.075mm i.e. coarse silt to very fine sand), easily transported in suspension (McCave 1971).

The thicknesses of the Foxmould laminites range from a few centimetres to >0.8m, analogous to many other inner shelf to lower shoreface storm beds (e.g. Kumar & Sanders 1976; Kreisa 1981). Within the relatively poor three-dimensional control given by the available sections, it appears probable that the beds are sheet-like in geometry. The general setting inferred is that of a lower shoreface or offshore-transition zone (Elliott 1986), with "proximal" storm layers (in the sense of Aigner 1985) in the most westerly sections. Thick (several dm)

beds associated with a shallower shoreface setting generally have different internal structures such as hummocky or swaley cross-stratification (e.g. Harms *et al.* 1975; Walker 1984; Duke 1985; 1987; Swift *et al.* 1983; 1987), although such structures are not environmentally diagnostic (e.g. Allen & Underhill 1989). Storm wave sediment entrainment followed by suspension cloud settling was an important sedimentological process across the broad, low-gradient epeiric shelf setting of south-west England. Morton (1981) suggested that steeper shelves are more conducive to the development of strong currents than those with low gradients, though Nelson (1982) identified storm-associated bottom currents as an important sand transport agent across the flat, shallow (<20m) epicontinental shelf of the northern Bering Sea, and Brenchley *et al.* (1979) infer storm-induced offshore currents as a sand transport mechanism (>40km) across the broad Upper Ordovician epicontinental platform of southern Norway.

3.1.5 Storm frequency and laminite preservation potential

The greater part of the Foxmould consists of strongly- to completely-bioturbated muddy fine sand; laminites are present as discrete interbeds. For example, the bioturbated Foxmould comprises about 78% of the succession at Peak Hill, Sidmouth, increasing in the postulated deepening direction to 93% at the Hooken Cliffs section, Beer. Further east still, a completely homogenous muddy fine sand unit is developed (e.g. at Golden Cap, SY 406 921), and this passes offshore into rhythmically-bedded, muddy glauconitic silt (e.g. at Lulworth Cove, SY 825 800). However, despite the general offshore trend from thicker, more numerous laminites to thinner and rarer laminites, there are smaller-scale irregularities in the degree of bioturbation of a specific part of the sequence. Over a scale of 1-3km, the degree of bioturbation appears variable, for example laminite beds preserved in the upper Foxmould at Culverhole are seen only as mere traces of lamination in a slightly more proximal section (Seaton Hole).

The Foxmould often shows scattered weak traces of horizontal lamination, preserved in small patches of moderately-bioturbated sediment. In addition, at certain levels, bedding-parallel, very weak concentrations of shell fragments are preserved. These observations have important implications for the evaluation of the relative frequencies and magnitudes of the

Foxmould storm events. It appears likely that a large part of the Devon Foxmould was originally deposited as discrete laminites, which were then subjected to burrowing activity. Such bioturbation, which in some cases can penetrate 0.3m into the bed, then proceeded to homogenise the laminite. Preservation of a given laminite is therefore a function of (a) the magnitude of the storm i.e. higher energy storms would generate thicker beds, and (b) the relative frequency of the storms. Infrequent storms would tend to lead to the destruction of the laminites under burrowing activity. More frequent storms would have the dual effect of erosion of the underlying beds (perhaps removing a previously-deposited laminite either completely or partially), but also burying and preserving (from bioturbation) previous laminites. Only thin, amalgamated beds, and parts of thicker, discrete beds (original thicknesses >0.25m) were preserved in the sedimentary record. The middle part of the Foxmould is notable in that several very thick laminite beds are developed and can be correlated laterally. The bioturbated lithofacies thus consists of a mixture of storm-deposited fine sand, silt and clay, and some fair-weather finer fraction contribution.

The average frequency of storm event preservation in the Foxmould can be estimated from the total period of deposition of the member. The thickness of 25m spans about two ammonite subzones (*varicosum* and *auritus* subzones, upper *inflatum* zone), probably representing about 0.6-0.9Ma, based on the numerical dating of the limits of the Upper Albian (Kennedy and Odin 1982). In the Beer sections, only three to eight discrete laminite beds are typically preserved (though there are weak traces of lamination throughout much of the bioturbated sequence). This gives a bed preservation frequency of one per 75,000-100,000 years. Such a figure is obviously affected by the relative position on the shelf (i.e. fewer laminites preserved in more distal sections), but is considerably less, often an order of magnitude lower, than periodicities calculated by other authors from different sedimentary systems - e.g. one per 1,200-3,100 years for the Martinsburg Formation (Middle and Upper Ordovician) (Kreisa 1981); one per 2,500-10,000 years for the Muschelkalk (Middle Triassic) (Aigner 1985), and one per 10,000-20,000 years for the Ashgill (Upper Ordovician) of southern Norway (Brenchley *et al.* 1979). However, relevant comparisons are also complicated by the fact that analogies between

Palaeozoic and Mesozoic storm bed preservation rates may be misleading, for it is possible that the depth of burrowing in open shelf sediments has increased through the Phanerozoic (Kreisa & Bambach 1982; Sepkoski 1982). Most Palaeozoic shelf sediments apparently show intense downward bioturbation of only 3-8cm, compared with about 20cm for the Upper Greensand facies studied. Brandt (1986) noted that a Jurassic increase in minimum event bed preservation thickness (relative to the Palaeozoic) coincided with an increase in the mean reworking depth of infaunal organisms.

3.1.6 Glauconitic storm laminites in the uppermost Foxmould

In south Devon, the contact between the Foxmould and Chert Beds Members is marked by an interval of sedimentary condensation, recording low sedimentation rates, and a coincident facies change from siliciclastics to carbonates. The boundary beds consist of glauconite-enriched sediments, which have undergone a very early submarine lithification process (cf. Garrison et al. 1987). Storm events occurring during this period of reduced sedimentation were responsible for the reworking of the condensed facies, to produce glauconitic sand laminites, and glauconitic intraformational pebble-shell beds (see below).

The more proximal beds consist of glauconite-rich muddy fine sands and silts; diagenetic nodules are not developed. These laminites are very similar to those described from the main part of the Foxmould, and provide an important control on the evaluation of the number and magnitude of the storm events which might be represented in a particular pebble bed. In the Dunscombe Cliff section (SY 153 877), the contact between the Foxmould and the Chert Beds is marked by six variably-amalgamated thin laminites, the bases of which are rich in serpulid debris (Fig.74). Sedimentary structures consist of a predominantly horizontal lamination, often passing into low-angle (5°) cross-lamination, or weakly undulose lamination. Rare, small erosive scours cut into the underlying sediments (up to a depth of 10cm) are draped and filled by vertically-accreted, variably glauconitic silt.

The green glauconite grains accentuate a small-scale cyclicity, in which several rhythms are typically present within a single, shelly-based laminite bed (i.e. within a single depositional

storm event). Each rhythm, comprising several laminae, and typically 1-4cm thick, comprises an attenuated fining-up sequence. This is highlighted by the greatest concentration of fine sand-sized glauconite grains in the basal laminae, decreasing in concentration through the laminae above. Such rhythmicity accords with the proposed mechanism of deposition from irregular, sediment-laden suspension clouds; each rhythm would represent suspension settling from a single such cloud. Within the overall fining-up sequence (recorded in complete laminite beds from lower in the Foxmould; see earlier), these small rhythms show rather irregular thickness variations, each bearing little relation to the thickness of the rhythm immediately preceding. This reflects an irregularity in the size and amount of sediment in the suspension clouds.

3.1.7 Faunal implications

Despite containing a moderately-diverse benthic fauna (bivalves, gastropods, serpulids and echinoids), only extremely rare escape traces have been observed in the Foxmould laminite beds. Taking into account the reworked tops of the beds, estimates of original sedimentary thicknesses reveal abundant beds over 0.2m, reaching >0.8m. It is likely that major storms, winnowing the soft sediment seafloor, and then depositing a thick, fine-grained sediment blanket from suspension, proved fatal to the fauna. Their remains are concentrated in the shelly basal parts of such laminites, thus constituting a death assemblage. It is likely that such a fauna was able to survive minor storms, escaping upwards through a thin laminated bed, but the relative interplay between original sedimentary thickness, and depth below the sediment surface to which strong bioturbation operated, has resulted in the biogenic destruction of the escape traces predicted for thin beds. Modern experiments (Nichols *et al.* 1978) have shown that faunal escape is not even attempted if the covering sediment exceeds approximately 0.3m. This has been interpreted as a result of "overburden stress", where bulk density and burial depth reach a critical point. Since Upper Greensand laminites of about this thickness and less were unlikely to escape thorough bioturbation, this would explain the absence of such escape traces in the sediment record, despite the presence of a benthic in- and epifauna.

Within the Foxmould, the epifaunal elements, mainly *Amphidonte* (free-living oysters),

tend to occur as single, scattered individuals. Clustering was only observed in one example, as a group of eighteen oysters preserved in a concretion. This may represent an actual life assemblage, with storm reworking having, in many cases, disaggregated faunal clusters.

A moderately diverse trace fossil assemblage is present in the Foxmould, dominated by *Palaeophycus* (Hall), *Thalassinoides* (Eherenberg), *Chondrites* sp., and *Cylindrichnus* (Howard) (Fig.75, Fig.76). These are preserved in weakly-cemented, compact muddy sand, and can be classified as a Cruziana ichnofacies, typical of poorly-consolidated substrates, and often characteristic of subtidal zones between mean fair weather- and mean storm-wave base (Frey & Seilacher 1980; Ekdale *et al.* 1984). The structure of endobenthic interaction reveals complex cross-cutting inter-relationships between *Palaeophycus* and *Thalassinoides*. No different ichnospecies were found associated with the tops of laminite beds, suggesting a general absence of opportunistic infaunal trace makers. These beds therefore differ from classic storm-associated opportunism, typically more prominent in systems which show strong grain-size variations between storm beds and "background" sediments (e.g. discrete storm sands interbedded with fine-grained muds); a different ichnocoenosis may be associated with such differing lithologies, reflecting opportunistic colonisation of a newly available substrate (Pemberton & Frey 1984). The bioturbated tops of thicker laminite beds in the Foxmould record *Thalassinoides* burrows (0.5-5cm diameters, penetrating downwards for up to 25-30cm), passively filled with glauconitic sand, passing up into the *Palaeophycus-Thalassinoides-Chondrites* association; such a change is interpreted as a tiering effect, rather than as opportunism, the *Thalassinoides* burrowing to deeper levels.

3.2 Intraformational pebble and shell beds in the uppermost Foxmould

In the Little Beach and Whitecliff sections, near Beer, the junction beds between the Foxmould and Chert Beds Members consist of a variety of glauconite-rich, shelly intraformational pebble beds (Fig.77, Fig.78). The autochthonous pebbles are reworked very early diagenetic nodules,

which grew within the sediment at shallow depths. The beds range from a coquina lens (2.25m across), isolated within muddy, bioturbated silt (Fig.79), to thicker (0.37m, 0.40m, 0.67m), laterally more persistent pebble-shell beds. They contain large numbers of glauconitic sandstone pebbles, averaging 2-3cm, occasionally up to 20cm in diameter. Evidence for reworking consists of marginal boring and glauconitization (shown by a green rim) of the pebbles. The pebbles are typically mixed with a substantial component of muddy, glauconite-rich, greensand matrix, containing both whole and fragmentary shelly material; textures vary from matrix-supported to clast-supported. Long axes of the pebbles generally show a tendency for horizontal to sub-horizontal orientations in relation to bedding (Fig.80), though orientations up to sub-vertical and vertical are not uncommon. The nodularity at this horizon dies out westwards, and the interval passes laterally into (more proximal) glauconitic, amalgamated storm laminites (described above; Fig.74). Storm processes are the likely agent for exposing and reworking the early diagenetic nodules of the pebble beds. Similar beds are also developed in the Chert Beds Member, and their origin is addressed below.

3.3 Storm sedimentation in the Chert Beds Member

The Chert Beds display a range of interacting storm and condensation phenomena. They consist of weakly-cemented grainstones and packstones, variably quartzose and glauconitic, and commonly rich in diagenetic silica, with abundant chert nodules (Tresise 1961; Williams 1986; Maliva & Siever 1989). The principal bioclasts are echinoid plates and spines, strongly micritised amorphous peloidal grains, calcitic bivalve fragments, and occasional foraminifera and bryozoans; they form a carbonate sand of fine to medium grade. Discrete horizons in the Chert Beds show evidence for an early diagenetic lithification process in the form of cemented limestone nodules. Certain nodular beds were "reworked", the nodules being exhumed and sometimes bored, encrusted, and mineralised. This led to the development of nodular hardgrounds and intraformational conglomerates (Garrison *et al.* 1987). The intraformational

pebble beds are generally richer in coarser and less-fragmented shell material than the "background" grainstones; a spectrum of pebble-shell beds, simple coquina beds, and complex amalgamated coquinas can be identified. Storm processes of *in situ* winnowing and a degree of sediment transportation are envisaged to be the principal reworking agents, responsible for the nodule exhumation and the pebble and shell concentrations.

3.3.1 Pebble-shell beds

A variety of pebble-shell beds are developed in the Chert Beds Member in the sections around Weston Ebb (SY 175 878), around Beer (SY 175 878), and between Axemouth and Lyme Regis (Fig.19, Fig.81, Fig.82). Such beds (0.3-0.7m thick) typically consist of a mixture of intraformational pebbles and shelly material (predominantly *Amphidonte obliquatum* (Pulteney), with *Merklinia aspera* (Lamarck) and *Neithea gibbosa* (Pulteney). The pebbles are small (0.5-12cm) early nodules, reworked from the sediment below; they often show marginal glauconitization and borings, and are occasionally encrusted by oysters (*Nanogyra*) and serpulids. A variable proportion of shelly material ranges from whole or little-broken shells several centimetres across, to finely-comminuted sand-sized grains. Basal bed contacts vary from abrupt to gradational over 10-20cm; occasionally, pebbles and shells fill poorly-defined shallow depressions (?scours; up to 15cm deep) in the underlying bed (Fig.83). Gradational lower contacts show basal *in situ* calcareous concretions, with *Thalassinoides* firmground burrowing between the nodules; these pass up into reworked pebbles (glauconitized, bored, encrusted) and shells.

Pebbles are often ellipsoidal, and their long axes show a tendency for alignment within about 25° of the bedding direction; pebbles in sub-vertical and vertical orientations are, however, not uncommon (Fig.84). Shell material also shows predominantly bedding-parallel to sub-parallel orientations, though a whole range of orientations are always present; where shells are sufficiently whole so as to show convexity, convex-up orientations predominate. Convex-up:convex-down ratios range from 2:1 to 8:1 for the pebble-shell beds, reaching 14:1 in interbedded weak shelly concentrations. The beds are typically inhomogeneous, with lenses and

patches of more pebbly, more shelly, or more sandy sediment (Fig.84); fabrics vary from matrix-supported (isolated pebbles) to pebble-supported (pebbles in contact; infrequent). Occasional patches of pebble-rich sediment at the tops of certain beds suggest infilling of small scours (Fig.83). Bed tops are more usually gradational into pebble-free sediment, where the shell fragments are of sand-size. Different beds show variable amounts of pebble and shell material: from shell-rich, pebble-poor coquinas to pebble-rich, shell-poor horizons. There is a complete gradation from thin, laterally impersistent lenses (persistent over a few metres or less) of pebble or shell material only one or two pebbles thick, into thicker, more laterally-persistent pebble-shell beds.

Cross-stratified coquina beds are occasionally developed, clearly indicating lateral transport of shell fragments (Fig.85). For example, a coquina in the lower Chert Beds at Little Beach, Beer (correlatable over >1km) is composed predominantly of coarse sand-sized and small granule-sized shell fragments, slightly more glauconitic at the base, with only very rare small limestone pebbles. The base is sharp and planar, and the top is gently mounded (thickness from 0.30-0.75m). Current ripple cross-lamination and low-angle planar cross-lamination, typically in sets 5-15cm thick, are developed throughout; the unit also displays several carbonate sand lenses, suggesting amalgamation of at least two discrete events.

3.3.2 Complex, amalgamated, proximal coquina beds

In the most proximal sections exposed (landslipped blocks at Weston Ebb), amalgamated, coarse-grained coquina beds are developed just below the Brecciated Limestone hardground (Fig.86, Fig.87). There is a whole continuum from calcarenites with thin, shell-rich stringers and lenses (typically only 5cm thick and 1-2m across), to thicker, more laterally-extensive wedges and beds, with rather gradational bases, and bored limestone pebbles scattered throughout (Fig.87, Fig.88, Fig.89). The coquinas are almost monospecific, being composed principally of *Amphidonte* oysters (smaller *Amphidonte obliquatum* (Pulteney) and larger *Exogyra columba*). Shell beds are also developed in the overlying Beer Head Limestone Formation (Lower Cenomanian); these, however, have a different assemblage, composed mainly of *Merklinia*

aspera (Lamarck) and *Neithea gibbosa* (Pulteney), with *Amphidonte* being subordinate (Fig.90).

The shell material is variably-fragmented : from sand-sized fragments to large, little-abraded shells up to 5cm across; there is, however, a very high proportion of the larger elements. The amalgamated coquinas show internal sandy lenses within the coarse shelly sediment, and display lensoid geometries over short distances. Such beds are thus built up from a series of vertically-stacked and sometimes laterally-overlapping coquinas. Shell orientations are again predominantly horizontally-aligned, but differ from more distal beds in that shell stacking with convex-down alignments is predominant (Fig.91). e.g. the horizon just below the Brecciated Limestone hardground (after Tresise 1960) at Weston Ebb (Fig.86) shows 65% of oysters (>2.5cm across, n=100), whose long axes are at 0°-30° to the bedding; the convex-up:convex-down ratio is around 1:4 (compared with typical ratios of around 3:1 for more distal beds - Fig.81). However, the thin, 1-2 shell-thick *Amphidonte* stringers and lenses within the calcarenites, and in certain cases, the tops of the amalgamated coquinas, show the reverse - a tendency for higher proportions of convex-up shells, with ratios of between 1:1 and 3:1 convex-up:convex-down (Fig.88). Occasional scours, infilled with shelly sediment, are present at the bases of the beds (Fig.92).

3.3.3 Interpretation of pebble-shell bed fabrics and storm versus fair weather processes

The concentration and horizontal alignment of pebbles and shells in discrete beds within finer-grained bioclastic packstones and grainstones is interpreted as the result of periodic high-energy storm events, within an overall lower-energy sequence. The pebbles represent very early diagenetic nodules, which grew within the sediments (glauconitic silts and variably glauconitic bioclastic grainstones), presumably at shallow depths (a few tens of centimetres). These were then subjected to higher-energy processes which disinterred and concentrated the nodules, re-depositing them with variable amounts of coarser shell material. (Siliceous nodules and chert are not reworked in the Upper Greensand pebble beds, despite the fact that the silicification process occurred at a shallow burial depth; Maliva & Siever 1989). The matrix to the pebble beds is often more glauconitic than the "background" sediments, and the pebble beds appear

to represent depositional hiatuses within the succession.

Pebbles generally tend to show approximately bedding-parallel fabrics. The fabric also varies from matrix-supported to pebble-supported. A winnowing process is necessary to disinter the early nodules from their host sediment, and align them in roughly horizontal orientations. Occasional weak indications of pebble imbrication are seen, though lateral transport of these pebbles was distinctly limited, because of their size and weight. Limited bedding plane data on the orientation of pebble axes in one of the uppermost Foxmould pebble-shell beds (Fig.78) indicates an essentially random pattern, but characteristic wave or current alignment (cf. Nagle 1967) would probably not be expected because of the pebble size.

The processes which are envisaged to have produced an individual pebble-shell bed in this stratigraphic interval are :

1) a reduction in the sedimentation rate from the "normal" background rate, with resulting sediment starvation and relative enrichment in the green, authigenic clay mineral glauconite,

2) firmground burrowing at the base of the bed, generally by *Thalassinoides*, piping down the glauconitic carbonate sand into the underlying sediment in passive burrow fills,

3) concomitant nodule development within the calcarenites.

It is envisaged that storm processes operating on the sediments then produced :

4) an initial erosive phase (storm peak), winnowing the nodules and shells from the underlying sediment, and concentrating them at the sediment-seawater interface. The pebbles and shells tended to be redeposited with their long axes aligned parallel to bedding.

5) Low amounts of fine-grained sediment are preserved in the carbonate storm beds, compared to the siliciclastic system. The fairly high concentration of fine muddy matrix within the pebble-shell beds in the uppermost Foxmould suggests either incomplete winnowing of pebbles from the host sediment, and/or some deposition of waning-storm, fine-grained sediment, which became incorporated due to infiltration, and was followed by bioturbation.

Beds may show *in situ* nodules at the base overlain by reworked pebbles, or be reworked throughout. Both types, however, contain considerable thicknesses of reworked

(glauconitized, bored, encrusted), horizontally-oriented pebbles (e.g. 0.25m out of 0.4m, and 0.45m out of 0.67m for two such beds in the uppermost Foxmould at Beer). It would be expected that only pebbles at, or very close to the surface following a storm, would be bored/glauconitized, and it appears likely that such beds were subjected to more than one storm event, which mixed the pebble concentrate, exposing different nodules at the surface after different events. Evidence for this is shown by a horizon within the upper Chert Beds at Beer Head, which has evidence for at least three amalgamated shell and pebble concentrations (Fig.93). The two to four pebble-shell beds exposed in the uppermost Foxmould at Beer correlate with one to six amalgamated glauconitic storm laminites in the sections further to the west. Individual pebble-shell beds, depending on the degree of completeness of the matrix-winnowing and nodule-disinterment process, rest on either (Fig.94) :

a) *in situ* nodules, and firmground burrowing (overlain by reworked pebbles and shells) (incomplete *in situ* reworking)

b) on traces of firmground burrowing (almost complete *in situ* reworking)

c) on more irregular basal contacts, but with all reworked nodules, and no firmground burrowing (complete *in situ* reworking; probably minor lateral transport of pebbles and shells)

or, more rarely :

d) have sharp bases, overlain by a lensoid or cross-stratified bed, shell-rich, but pebble-poor (component of lateral transport inferred).

The pebble-shell beds in the uppermost Foxmould contain a more diverse faunal assemblage than the background sediments, being fairly rich in bivalves, serpulids, bryozoans, and echinoid debris. Both whole and fragmentary fossils are preserved. Epifaunal elements are mostly free-living genera, and there is not a noticeable increase in cemented forms. It is not immediately clear whether the greater fossil content in such beds is due to a real increase in palaeodiversity, or is a preservational effect. A period of slow sedimentation accompanied by sediment winnowing appear to be the most likely processes for producing the fossil-rich beds.

In the Chert Beds, the shelly fauna associated with the pebble and shell beds is

dominated by the oyster *Amphidonte*, with occasional *Merklinia*, *Neithea*, and *Lopha*. *Amphidonte* represents a free-living, reclining epifaunal genus (Seilacher 1984; Seilacher *et al.* 1985), and although a hardground fauna of occasional nodule-encrusting *Nanogyra* (?juvenile *Amphidonte*) and serpulids is generally present, this represents only a small part of the faunal assemblage. The bulk of the fauna preserved in a typical pebble-shell bed is not specifically adapted to the hardground (or a firmground) environment, and is also found in the background bioclastic grainstone facies. The shell beds thus do not appear to reflect specific colonisation events which might occur associated with, for example, substrate changes. These differ from firmground-based shell beds which reflect storm reworking followed by biological responses to specific substrates (e.g. those associated with mud deposition, described by Aigner (1982) from the Eocene of Egypt). Distinctive taphonomic feedback processes (Kidwell & Jablonski 1983) have not been recognised, with the hardground encrustation and boring being the principal ecophenotypic response. The only distinct faunal change observed is the association of large Orbitolinid (benthic) foraminifera with the sediment just above the top of one of the thick proximal coquina beds (Fig.86), but the significance of this is uncertain.

Sedimentary structures are only weakly preserved in the well-sorted and often pervasively-silicified calcarenites. The growth of siliceous nodules accompanied by differential compaction has often resulted in deflection of any preserved lamination. In certain wave-polished blocks, however, the structures can be seen to consist of horizontal lamination, passing into undulose and low-angle cross-lamination (dips of 10° or less); low-angle to gently curving reactivation surfaces are fairly common (Fig.95). The stratification is defined by grain-size variations, and variations in the proportions of quartz and glauconite. Angle-of-repose cross-stratification is rare, but occasional sets of trough cross-stratification (up to 20cm in height) are preserved in the calcarenites. The structures record predominantly vertical sedimentation, with a lesser component of horizontal sediment transport. (Trough cross-bedding is, however, well-developed in the Top Sandstones Member, in a slightly coarser grainstone facies, and is interpreted as shoaling wave-generated.) Such a suite of structures is consistent with an interpretation as the result of pervasive storm reworking of the Chert Beds calcarenites (but

lower energy storms than those which produced the pebble-shell beds), and may be analogous to hummocky cross-stratification (Harms *et al.* 1975); the weakness of the preserved structures, however, precludes any more rigorous treatment.

The packstones and grainstones contain abundant sand-sized bivalve shell fragments; this material is usually aligned parallel/sub-parallel to the bedding. In contrast, whole or even partly-fragmented echinoids are extremely rare in the Chert Beds and Top Sandstones of south-east Devon (despite comprising a very substantial proportion of the bioclasts), and unfragmented stick-like bryozoans are also uncommon. (Whole echinoids are found in the Chert Beds of south Dorset, however, in deeper-water carbonates deposited at a depth not influenced by strong storm reworking.) Studies of fossil skeletal durability (Chave 1964) have shown that the skeletons of echinoderms and bryozoans (with much openwork and organic matrix) are particularly susceptible to destruction by physical processes, whereas oyster shells (coarsely-crystalline) will survive longer periods of reworking. The presence of large, less-fragmented shell material in the shell-pebble beds is interpreted to be primarily a preservational effect, where shell material was buried and thus preferentially protected from the fair weather and weak storm processes of prolonged abrading and biogenic attack. Only the more major storms would produce the thicker beds and lenses; weak shell concentrations produced by the minor storms would tend not to be preserved, the shell material being winnowed and abraded by successive weak storm events and fair weather processes, or incorporated into the next pebble-shell bed. Driscoll (1970) noted that in higher-energy environments, physical abrasion of shells will be the principal destructive agent, rather than biogenic processes (e.g. boring), and Kreisa (1981) suggested that storms, to a large extent, probably preserve rather than destroy loose skeletal material, by burying and thus protecting it from the destructive fair weather processes. The presence of large oysters in certain coquinas may, however, indicate long periods of fair weather and low-energy storm processes, during which the individuals could grow to full maturity.

Bivalve shell orientations and convexity positions have been discussed by various authors (Emery 1968; Brenchley & Newall 1970; Clifton 1971; Futterer 1978; Allen 1984),

indicating that in the absence of waves and currents, concavo-convex particles generally lie in concave-up positions due to the action of predators or scavengers and/or due to bioturbational shell rotation. Under the influence of waves and currents, shells will be predominantly convex-up, in hydraulically-stable positions, provided that the currents exceed an "overturning threshold". However, concave-up orientations in small shells can be produced by small migrating asymmetric wave ripples (Clifton & Boggs 1970). Vertically-oriented valves, tightly-packed and concentrically-imbricated, typically result from turbulence and wave swash in the intertidal zone (Salazar-Jiménez *et al.* 1982) and may also form on intertidal flats resulting from alternating ebb and flood currents (Reineck & Singh 1973); thin shell beds may even concentrate in intertidal flat sediments as a result of burrowing activity (Reineck & Singh 1973). Nagle (1967), on the basis of shell orientation experiments, noted differing wave and current patterns in shell axis data taken along bedding planes. Broadly, current-oriented shells tend to show one strong maximum either into or away from the current, and shell axes tend to align parallel to shoaling wave crests, though perpendicular to the ripple marks in low-angle surf zones. Heavy shells may show non-diagnostic orientations, as may shells on grain-rough substrates (such as gravel- and shell-rich sediment), where the shells tend to pivot around the small irregularities. Futterer (1978) noted that on sandy and silty flume beds, shell orientation is hindered by the formation of ripples, with scouring followed by shell tilting into the scour depression.

Shells in the more distal beds of the Upper Greensand Chert Beds Member show a tendency for horizontal to sub-horizontal alignment, and a dominance of convex-up orientations, which are thus in current-stable (either uni- or bi-directional) positions. Actual lateral transport of the shell material is unambiguously recorded in a single finer-grained coquina, in which cross-stratification is well-developed, with vertical centimetre-scale variations in grain size and shell orientations (Fig.96). As well as showing changes in both thickness and grain-size, shell beds also occasionally display sorting of the two *Amphidonte* valves. Each pair of valves typically consists of a large thick and sturdy lower valve, and a smaller and thinner lid-like upper valve. In the complex proximal coquinas, the large lower valves are notably predominant,

though this may be a preservational effect, with the smaller and thinner upper valves being prone to breakage into smaller fragments. However, rare pebble-shell beds seen further east, between Axemouth and Lyme Regis show a predominance of the smaller upper valves, with only rare larger valves. This suggests offshore transportation of the smaller valves by unidirectional currents which were not strong enough to move the larger valves.

3.3.3.1 Basal scours and gutters. Occasional gutters are present at the bases of the more proximal coquina beds. The oyster-rich fill in the example shown in Figure 92 comprises shells and shell fragments with a similar fabric to the main part of the bed - in stacked, predominantly horizontally-oriented and convex-down orientations, though with examples ranging up to vertical to bedding. Analogous gutter casts have been documented by Whitaker (1973), who invoked a scouring process, involving helicoidal current flow along a horizontal axis, to explain their formation (based on side-wall striations and plan-view sinuosity). The Upper Greensand gutters may have been cut by storm-generated currents (their orientations are uncertain, as the features were observed in slipped blocks). The scouring which excavated the gutters may have been caused by unidirectional flows, though might feasibly have resulted from irregular storm wave turbulence. Gutter-filling processes must be explained by a certain amount of shell transport, though by currents not strong enough to flip shells into convex-up orientations. Note that oysters of this size are not too heavy to invert into such positions, as shown by convex-down examples at the tops of the beds and in thin lenses and stringers.

Thus, both current transportation of shells (and to a certain extent pebbles also), and sediment winnowing are recorded in the coquina beds. The winnowing process appears to have been most effective in the shallower-water settings, removing most of the fine- and medium-sized bioclasts to leave a coarse, shell-rich sediment. Bivalve skeletal debris is essentially parautochthonous i.e. reworked, but not transported out of the original life habitat (Kidwell *et al.* 1986). This may reflect both bidirectional and unidirectional currents (perhaps also combined flows). The fact that thick proximal coquinas often show predominantly convex-down shell

alignments, compared with convex-up (current-stable) alignments in thinner beds and in more distal beds, is the reverse of what might be predicted from a simple evaluation of the relative energy of different event intensities and at different water depths. It appears to result from the fact that shallower-water oysters are thicker and heavier than their deeper-water equivalents, and can be transported by currents in convex-down positions, only inverting into convex-up positions at higher current velocities.

A whole spectrum of storm intensities (and degrees of winnowing) is represented in these sections. "Background" sedimentation records lower-intensity storms and fair weather processes. Only the very major storms winnowed early nodules (pebbles) and buried significant amounts of whole and partly-broken shell material, thus protecting it from lower-energy, but more prolonged and more destructive abrasion processes.

Reported descriptions of analogous shell and pebble beds from modern and ancient subtidal carbonate systems are uncommon, though many authors have reported shell concentrations associated with storm-influenced, muddy siliciclastic environments (e.g. Brenner & Davies 1973; Specht & Brenner 1979; Miller *et al.* 1988), and modern beaches and shallow estuarine facies (e.g. Salazar-Jiménez *et al.* 1982; Fürsich & Flessa 1987). Modern analogues of firmground-based, glauconitic shell concentrations may be those described from the basin offshore the Mississippi delta (Coleman & Gagliano 1965), whereas in the geological record, similar storm-reworked oyster shell beds have been documented from the Kimmeridgian of France by Fürsich & Oschmann (1986). Examples of intraformational conglomerates of Jurassic age from the Wessex Basin of southern England, which have undergone a complex history of sea-floor exposure and bioerosion, possibly including storm reworking, include the Eype Nodule Bed, Eype Clay (Middle Lias) (Wilson *et al.* 1958; Ensom 1985) and the Margaritatus Stone, Down Cliff Sands (Middle Lias) (Wilson *et al.* 1958). Analagous intraformational (sometimes glauconitic) flat pebble conglomerates of Cambrian and Lower Ordovician age are developed in many parts of North America (Sepkoski 1982; Brett *et al.* 1983). These have been interpreted as due to episodic sea-floor scouring during intense storms, and are associated with thin storm laminite beds.

3.3.4 Storm frequency and preservation

The preservation frequency of the storm events can be calculated by the same method used previously. In the uppermost Foxmould, the condensed glauconitic sequence preserves one to six storm beds within the upper *auritus* ammonite subzone. This gives a bed preservation rate of around one bed per 20,000 years. For the Chert Beds Member, up to eight discrete beds have been recognised, representing the *rostratum* and probably part of the *perinflatum* ammonite subzones. An estimated bed preservation rate is thus around one bed per 180,000 years. Such figures are of only limited use, given the fact that individual pebble-shell beds often appear to preserve the reworking effects of several storms. This nevertheless illustrates how infrequently an individual storm event was translated into a discrete stratigraphic bed.

3.4 Storm scouring of nodular hardgrounds

Nodular hardgrounds are present in the Upper Greensand Chert Beds and Top Sandstones Members, reflecting a process of early submarine lithification, described by Garrison *et al.* (1987). Three such horizons are present in the south-east Devon sections (Fig.19): the lower Chert Beds hardground, the Brecciated Limestone hardground (after Tresise 1960), and the top Upper Greensand hardground (the Small Cove hardground of Jarvis & Woodroof 1984). The hardgrounds consist of beds of nodular limestone (typically 0.5-1.5m in thickness); they represent depositional hiatuses of longer duration than those reflected by the thinner pebble beds. The calcareous nodules developed within a cross-stratified bioclastic grainstone facies. The top surfaces of the hardgrounds are sharp and planar, and the uppermost nodules are bored, encrusted, glauconitized, and sometimes truncated. The nodular horizon at the top of the Upper Greensand around Beer was originally interpreted as a bed redeposited from a low ridge (Smith 1957) or as a beach deposit (Ali 1974; 1976). It was correctly interpreted as a hardground by Jarvis & Woodroof (1984), who identified a complex history of sedimentation, bioturbation and erosion. The hardground is present throughout the coastal sections of south-east Devon.

It is envisaged that the nodularity developed below the sediment-seawater interface, and given the direct evidence for storm activity throughout the succession, storm erosive processes represent the likely agent for exposing, and maintaining exposure of the nodular bed at the sea-floor. For the most part, the nodules were large enough to be unaffected by storm transport, though in occasional examples, angular discordances between the cross-stratification preserved in adjacent nodules indicate a certain amount of nodule rotation (Garrison *et al.* 1987). In one locality, however, (Stockham's Hill Quarry, north of Branscombe Mouth; SY 206 889), the top 0.25m of the 0.90m-thick hardground at the top of the Upper Greensand has been reworked into an intraformational pebble bed, consisting of abundant small limestone pebbles (1-5cm across). This is interpreted as storm reworking at a fairly early stage of nodule growth, halting the growth of the nodules, and concentrating them into a single bed. Such hardgrounds can thus be considered to be tempestitic condensation horizons (Seilacher 1982), with storm events emphasising and highlighting the sedimentological expression of non-deposition (which is itself not fundamentally controlled by storm influence). Analogous, but more complex condensation in Albian glauconitic sediments from Clars, south-east France, has also been explained by processes of storm winnowing and resedimentation (Gebhard 1982).

3.5 Palaeogeographic setting

Palaeocontinental and palaeogeographic reconstructions for the Albian (mid-Cretaceous) (Funnel 1990; Tyson & Funnel 1990) show that the southern part of the British region occupied an area around 50°N, in a similar position to the present-day, on the northwestern side of the European area. Palaeoclimatic reconstructions for the mid-Cretaceous (Lloyd 1982) indicate a tendency for winter westerly to north-westerly winds across the British area. The region is outside the hurricane-dominated areas predicted for the late Cretaceous by Marsaglia & Klein (1983), within a region defined by these authors as winter storm-dominated shallow seas.

3.6 Conclusions

The Upper Greensand of south-west England shows evidence for storm-influenced sedimentation throughout a large part of the formation. The lower Foxmould Member (glauconitic, muddy fine sands and silts) displays a range of storm laminite beds with characteristic internal sequences. These were formed by deposition from storm-produced, sediment-laden suspension clouds, not by unidirectional or combined-flow sediment transport processes. A thinning and fining trend in such beds indicates the direction of offshore-deepening. Fair-weather bioturbation proved capable of homogenising all but the thickest beds and thinner but amalgamated examples. In the Chert Beds Member above (carbonate packstones and grainstones), a range of intraformational pebble and shell beds and nodular hardgrounds, of varying thickness and geometry, show interaction between early diagenetic nodule growth and storm reworking processes. Both sediment winnowing and current transportation can be detected from an evaluation of shell bed taphonomy. Shell fabric analysis shows that beds with predominantly convex-up (current-stable) shell orientations pass into more proximal beds with predominantly nested, convex-down orientations. This is opposite to predictions based on simple energy considerations, and is the result of winnowing of large heavy oysters in proximal settings, with a greater component of sediment transport (finer-grained bioclaststs) in more distal settings. Whole to little-fragmented shell material in such beds reflects early burial and preservation from lower energy, but more prolonged weak storm and fair-weather skeletal abrasion. Evaluation of storm frequency indicates that only very rare, very high-energy events are preserved as discrete beds; lower energy storms can, however, be detected throughout much of the formation. This has resulted in a distinct event stratigraphy.

CHAPTER 4

STABLE ISOTOPE STRATIGRAPHY OF THE UPPER ALBIAN *DISPAR* ZONE (MID-CRETACEOUS) OF SOUTHERN ENGLAND

Abstract : Secular changes in δ13C values have been detected in a series of mid-Cretaceous carbonates from south-west England. Increasing carbon-isotope values (a positive shift of around 1.0-1.3‰) are found through the Chert Beds and Top Sandstones Members of the Upper Greensand Formation. This succession encompasses the *dispar* ammonite zone of the Upper Albian. In detail, the increase appears to be resolved as two smaller positive shifts across nodular hardground horizons, separated by carbonates which exhibit uniform isotopic compositions after corrections for diagenetic alteration. The problems associated with the investigation of secular isotopic changes in the subtidal carbonate facies are complex; these include potential isotopic fractionation by the basic carbonate mineralogy, isotopic modification due to silica diagenesis, time-averaging due to storm reworking and bioturbation, and identification of small-scale hiatuses and possible stratigraphic gaps. Whole-rock and oyster analyses coupled with a series of control studies have, however, built up a carbon-isotope stratigraphy which has implications for the palaeoceanographic reconstruction of Upper Albian organic-matter burial rates. Organic-rich sediments of this age are developed in a variety of depositional settings world-wide; the increase in $\delta^{13}C$ values detected in the Upper Greensand carbonates appears to confirm the existence of increased organic-carbon burial rates in the late part of the Upper Albian.

The Upper Greensand Formation of south-west England comprises a sequence of glauconitic siliciclastics and carbonates of mid-Cretaceous (Albian) age; in Devon, it has been subdivided into the Foxmould (muddy fine sands), Chert Beds (siliceous carbonate packstones and grainstones) and Top Sandstones (carbonate grainstones) Members (Jukes-Browne & Hill 1900) (Fig.97). In the Beer area of south-east Devon, the formation rests unconformably on Triassic

red marls. The Chert Beds represent deposition in a subtidal, storm-dominated environment; the member displays a distinct event stratigraphy, with interbedded shelly coquinas and intraformational pebble-shell beds, representing storm reworking at a range of intensities and periodicities. At certain horizons, there is evidence for an early diagenetic lithification process which resulted in cemented limestone nodules; these were subjected to later reworking processes including exhumation, boring, encrustation and mineralisation (Garrison *et al.* 1987). Three nodular hardgrounds are developed in the sequence around Beer: the lower Chert Beds hardground, the Brecciated Limestone hardground and the top Upper Greensand hardground. The sequence is rich in diagenetic silica (Maliva & Siever 1989), reflecting large concentrations of sponge spicules in the original host sediment. The Chert Beds and Top Sandstones are of *dispar* ammonite zone age; in the uppermost Foxmould glauconitic pebble-shell beds at Culverhole Point (around 5km to the east) (SY 275 893), a specimen of a probable macromorph of *Mortoniceras* (*Mortoniceras*) *pachys* (Seeley) (identification by H. G. Owen), preserved as an unphosphatised mould within a calcareous concretion, confirms a high *auritus* subzonal age. Ammonites collected from just below the top Upper Greensand hardground at Shapwick Grange Quarry near Lyme Regis (SY 312 918) represent a level high in the *dispar* zone (Hamblin & Wood 1976; M. B. Hart *et al.* 1979b).

4.1 Methodology

Forty seven whole-rock and thirty oyster samples were collected from the Chert Beds and Top Sandstones Members of the Upper Greensand Formation at the Little Beach - Beer Head section in south-east Devon (SY 226 879) (Fig.98). The aim of the sediment sampling programme was to collect the most unlithified material possible at a particular horizon; this ranged from uncemented packstones and grainstones to moderately well-cemented (silicified) limestones. A qualitative estimate of the degree of lithification was made for each sample, expressed as a cementation index; this ranges from 1 (uncemented) to 5 (strongly-cemented). Each sample was

broken into small chips, and any weathered material discarded. Samples of between about 30g and 100g (averaging about 60g) were ground into fine powder using a planetary boremill with agate grinding balls and mortars. Crushing such a large sample ensured that a powder representative of the bulk sediment was withdrawn for analysis, thus eliminating any small-scale variations within a single hand specimen. The powder samples were analysed for stable isotopes of carbon and oxygen; liberation of CO_2 for isotopic analysis was accomplished by reacting the sample with H_3PO_4 at 90°, following cleaning with acetone and peroxide to remove organic-matter. The resulting gas was analysed on a VG isotech prism mass spectrometer at the Department of Earth Sciences, University of Oxford. In addition, analyses were performed on powders generated by drilling fresh surfaces of hand specimens, and powders generated by drilling oysters collected throughout the succession. The results are expressed as per mil (‰) deviations from the PDB international standard (Tables 2-5). Five samples were re-run in order to test the precision of the measuring technique; these showed mean deviations of 0.07‰ $\delta^{13}C$ and 0.07‰ $\delta^{18}O$ from previously-measured values.

4.2 Isotopic data from the Upper Greensand at Beer, south-east Devon

The secular changes in $\delta^{13}C$ and $\delta^{18}O$ values throughout the Chert Beds and Top Sandstones (at Little Beach - Beer Head) are shown in Figure 99. There is evidence for positive shifts in the $\delta^{13}C$ values across both the lower Chert Beds and the Brecciated Limestone hardgrounds; this is, however, complicated by superimposed high-frequency noise resulting from diagenetic modification of the isotopic signature.

4.2.1 The uppermost Foxmould

The lowest three samples in the sequence are from the glauconitic shell-pebble beds at the top of the Foxmould Member. These represent a different lithology to the overlying carbonates and the $\delta^{13}C$ values show a high degree of variability (1.45-2.33‰).

4.2.2 The lower Chert Beds

The lowest 1.75m of the Chert Beds are muddier than the overlying cleaner packstones and grainstones. The three samples taken within this interval display $\delta^{13}C$ values between 1.66 and 1.79‰, little different to the overlying beds, though they do have slightly higher $\delta^{18}O$ values. $\delta^{13}C$ values in the lower Chert Beds stratigraphically above range from about 1.15 to 1.95‰, averaging around 1.65‰.

4.2.3 The upper Chert Beds

A pronounced carbon-isotope shift occurs across the lower Chert Beds hardground, with the mean $\delta^{13}C$ values increasing from 1.65‰ to 2.45‰, a positive shift of around 0.8‰. If maximum carbon-isotopic ratios are used, which may record the values closest to the original unlithified sediments (see below), the change amounts to 0.85‰. An apparent minor carbon-isotope shift occurs across the lowest glauconitic pebble-shell bed in the upper Chert Beds, from mean $\delta^{13}C$ values of 2.46‰ below to 2.66‰ above (a positive shift of around 0.20‰). This shift does not appear to be primary, however, and appears to be a result of silica diagenesis (see below).

4.2.4 The Top Sandstones

There appears to be a minor carbon-isotope shift across the Brecciated Limestone hardground, from $\delta^{13}C$ values around 2.65‰ below, to values around 2.93‰ above, a positive shift of around 0.28‰. However, it should be noted that the lithostratigraphy indicates the presence of a gap in the succession at this bed boundary. At this locality, the bed immediately overlying the hardground is the Coarse Band, a quartz-rich bed up to 0.6m in thickness, interpreted as a lag derived from winnowing of underlying carbonates. Thus, although the shift may be a real primary phenomenon, its timing is less well constrained than the shift identified lower in the section.

The $\delta^{13}C$ isotopic values of the Top Sandstones (actually a fairly pure carbonate grainstone facies) show a spread of data ranging from 2.72 to 3.05‰, and averaging 2.93‰.

The data are little smoothed by normalisation (see below); the reason for the variations is uncertain. The uppermost data point represents a quartz-rich horizon in the bottom part of the top Upper Greensand hardground (comprising a passive *Thalassinoides* burrow fill, piped in from above).

4.2.5 The Pounds Pool Member, Beer Head Limestone Formation

At the top of the Upper Greensand there is a well-defined hiatus, which encompasses part of the *carcitanense* ammonite subzone of the Lower Cenomanian *Mantelliceras mantelli* zone (Kennedy 1970; Juignet & Kennedy 1976; Wright & Kennedy 1984). Only a single sample was analysed from the overlying Pounds Pool Member of the Beer Head Limestone Formation. This gave a value of 3.19‰, about 0.26‰ higher than the average value for the Top Sandstones, and 0.14‰ higher than the maximum value. This is, however, within the scatter recorded by these samples, and in the absence of more data, it is not clear whether or not an isotopic shift occurs across the top Upper Greensand hardground.

4.3 Evaluation of the validity and completeness of the secular $\delta^{13}C$ changes

The ultimate aim of the investigation of the Upper Greensand carbonates was to gain information on any Upper Albian secular variations in the $\delta^{13}C$ oceanic reservoir. For the curves to be correctly interpreted, however, it is necessary to examine certain factors which might affect whether or not the data are a valid indicator of the palaeoceanographic isotopic ratios, and whether the stratigraphy represents the complete *dispar* zone time period.

4.3.1 Carbonate mineralogy and isotopic fractionation

The Chert Beds and Top Sandstones Members consist of bioclastic packstones and grainstones, composed predominantly of echinoid and oyster bioclasts, with contributions from foraminifera, occasional bryozoans, and rare serpulids. A fundamental assumption which must be tested is

whether the whole rock samples give a valid representation of the original seawater isotopic signatures. Only certain groups of marine organisms secrete calcium carbonate in isotopic equilibrium with the ambient seawater; disequilibrium fractionation may be caused by varying precipitation rates and / or physiological controls (Arthur *et al.* 1983). Organisms with efficient respiratory systems do not incorporate metabolic CO_2 into their calcite skeletons; these include bivalves and foraminifera (Weber & Raup 1966b) and it appears that the calcite skeletons of these organisms undergo equilibrium fractionation with seawater. In contrast, echinoderm families appear to fractionate both carbon- and oxygen-isotopes. Studies on the isotopic composition of modern echinoids (Weber & Raup 1966a) have detected large systematic variations in the $\delta^{13}C$ and $\delta^{18}O$ values within a single skeleton, in most orders the tests being enriched in ^{12}C and ^{16}O relative to the spines. The spines preserve isotopic values similar to those of marine mollusca and foraminifera, whereas the test may be enriched in ^{12}C. This is interpreted as due to the incorporation of a variable amount of metabolic CO_2 into the skeletal calcite. The fractionation is largely genetically-controlled rather than environmentally-controlled, although temperature effects can be detected. Limited data on variations within single fossil specimens suggests that these may also show ^{12}C enrichment in the tests, relative to the spines (Weber & Raup 1968). Data from present-day echinoids shows that the different orders also fractionate carbon-isotopes differently. The Upper Greensand contains echinoids from the following orders; $\delta^{13}C_{test}$ - $\delta^{13}C_{spine}$ data from present-day orders (Weber & Raup 1966a) are given in parentheses: Holectypoida (+0.21‰), Cassiduloida (-0.02‰), Cidaroida (-4.92‰), Holasteroida (no data), Salenoida (no data) (Smith *et al.* 1988; Jukes-Browne & Hill 1900; Meyer 1874).

If the Upper Albian echinoids also fractionated carbon- and oxygen-isotopes, this has implications for the interpretation of the whole rock isotopic values. The validity of such an extrapolation to the Upper Greensand is uncertain; there are not enough data on the relative proportions of the different echinoid orders (and echinoderm families) in the Chert Beds and Top Sandstones, and too much uncertainty regarding the applicability of limited data from present-day echinoids to mixed whole rock samples of the Cretaceous echinoids, to draw firm

conclusions. Assuming, however, that some non-equilibrium fractionation did occur, whole rock samples would contain a mixture of echinoid spines with isotopic values close to that of the ambient seawater, and skeletal plates, many of which would record anomalously low $\delta^{13}C$ values. Assuming that plates made up the greater part of an original echinoid skeleton (petrography confirms the dominance of plates over spines), it can be postulated that the absolute values recorded from whole rock samples might also be anomalously low. A positive carbon-isotope shift could thus be theoretically caused by: 1) a change in the contribution made by echinoids to the bulk sediment composition, from an echinoid-richer to an echinoid-poorer lithology. 2) a change in the relative proportions of the different echinoid skeletal elements, from a more plate-rich to a more spine-rich lithology. 3) a change in echinoid orders (or echinoderm families), from an order (or family) with lower skeletal plate $\delta^{13}C$ values, to an order (or family) with higher values.

Petrographic analysis has not detected any such secular changes in the overall composition of the bioclasts; echinoid plates followed by oyster shell fragments are the dominant components throughout the lower Chert Beds, the upper Chert Beds and the Top Sandstones. The proportion of echinoid plates is much greater than that of the spines, and there is no evidence for secular plate : spine variations. The magnitudes of the Upper Greensand whole rock $\delta^{13}C$ values (with a range of 1.15-3.05‰ measured values; 1.83-3.27‰ normalised values) suggest that large scale fractionation (of the order of several parts per mil) did not occur. These values compare with values from typical Cenomanian chalks of around 3.0-3.3‰ (south Humberside, England) and 1.5-3.0‰ (Cap d'Antifer, France) (Schlanger *et al.* 1987). In Upper Cenomanian sandy biomicritic limestones with associated hardgrounds, from south-east Devon (a marginal facies to the Chalk), $\delta^{13}C$ values range from 2.21-2.65‰ (Jarvis *et al.* 1988). Thus although large scale fractionation in the Upper Greensand samples can be ruled out, smaller-scale fractionation, altering the whole rock values by up to 1.0-2.0‰, may be possible.

4.3.2 Carbonate diagenesis and non-carbonate impurities

Analogous previous research into Upper Cretaceous carbon-isotope stratigraphy has been

conducted predominantly on whole rock samples of nannofossil chalks (e.g. Schlanger *et al.* 1987). This lithology is ideal for the measurement of whole rock $\delta^{13}C$ ratios because of its predominantly low-Mg calcite mineralogy, making it less susceptible to later diagenetic changes which might modify the isotopic values, and its purity, composed principally of coccolith platelets contaminated with only relatively small quantities of clay minerals and clay-grade material, mostly quartz (typically 96-99% $CaCO_3$) (Hancock 1975). The Upper Greensand carbonates differ from such chalks in that they consist primarily of echinoid and bivalve bioclasts (with contributions from foraminifera, occasional bryozoans, and rare serpulids). There are considerable admixed non-carbonate contaminants of quartz, glauconite and minor muscovite.

The effect of non-carbonate contaminants on the isotopic measurements must be evaluated. Quartz will not affect the values, as it does not react to the phosphoric acid treatment. The role of clay minerals, including glauconite, is less certain. As previously noted, the lowest three samples of the Chert Beds Member, a muddy packstone lithology, have carbon-isotopic ratios little different to the overlying cleaner beds, though the oxygen-isotopic ratios are slightly higher. The highest concentrations of glauconite are associated with the interval of glauconitic pebble-shell beds in the upper Chert Beds (up to around 10%), and glauconite occurs at lower concentrations in the lower Chert Beds (around 3%) and the Top Sandstones (around 1-2%) (Fig.18). The carbon-isotopic ratios of these parts of the succession do not appear to have any positive correlation with the glauconite contents.

The primary calcite mineralogy of the Chert Beds and Top Sandstones differs from that of most chalks in that there was a significant initial concentration of high-Mg calcite echinoid bioclasts. High Mg-calcite typically recrystallises to low-Mg calcite quite early in diagenesis (Weber & Raup 1968), and is often accompanied by the precipitation of secondary calcite within the porous skeleton. It is uncertain whether or not this process would have affected the whole rock isotopic values, but given that echinoid grains are abundant throughout the succession, may not be responsible for any apparently secular changes.

The Upper Greensand carbonates typically contain two reported principal carbonate cement generations: syntaxial overgrowths on echinoderm grains, and bladed calcite overgrowths

on other bioclasts (Maliva & Siever 1989). Up to five cement generations can be recognised in carbonates which have undergone early lithification processes (Garrison *et al.* 1987); whole rock samples from these have $\delta^{13}C$ values around 0.45‰ more positive than the "background" weakly-lithified sediment, and higher $\delta^{18}O$ values (nodule from the Brecciated Limestone hardground: $\delta^{13}C$ = 3.11‰; $\delta^{18}O$ = -1.75‰ ; nodule from the top Upper Greensand hardground: $\delta^{13}C$ = 3.37‰; $\delta^{18}O$ = -1.37‰). Such values were not included in the final plots.

Petrographic analysis of the samples analysed has confirmed that syntaxial overgrowths of calcite spar around echinoid grains are the dominant cement type. Such overgrowths are commonly a relatively early phase in carbonate diagenesis, and are generally thought to originate from aragonite dissolution (Harwood 1988). No aragonitic fossils were recorded from the Chert Beds and Top Sandstones. The bladed calcite cement is volumetrically very minor, and where present, tends to be restricted to the edges of oyster shell fragments. Rare scattered spar crystals may also be present, infilling the intergranular porosity between the overgrown echinoid grains.

In the lower Chert Beds, the degree of cementation is very variable (between 0 and 10% cement in all except one sample, at 30.15m (in the log, Fig.99), which has 30% cement); the echinoid overgrowth cement is not present in all samples, and its relative importance appears to be controlled at least partly by the original degree of sorting of the sediment. It is less well-developed in samples with a higher proportion of fine-grained carbonate and is absent in the lowermost four muddy samples of the lower Chert Beds. Certain samples also show a millimetre-scale lamination, with the individual laminae showing variable sorting, and correspondingly higher amounts of overgrowth cement in the slightly coarser, better-sorted layers. However, certain better-sorted packstones have no cement (e.g. the sample from 31.71m), and may reflect an original paucity of aragonitic material. The lithologies thus range from packstones with a moderate amount of matrix and almost no cement, to better-sorted packstones with a variable amount of cement, to occasional well-sorted grainstones with larger amounts of overgrowth cement. In the grainstones at 30.01m and 30.15m, the isotopic values are lower than in other samples, but this appears to be the result of later silica diagenesis (Fig.100).

The upper Chert Beds are compositionally similar to the beds below, except that there are more abundant grainstones. Certain well-sorted grainstones (37.05, 37.95, 39.20, 41.62m) have well-developed overgrowth cements (10-15% cement, reaching 20% in the sample from 41.62m). A single well-sorted grainstone has almost no cement (38.45m); this, however, has carbon-isotopic values little different from adjacent samples with higher amounts of overgrowth (only around 0.1‰ difference). This infers that the overgrowth cement has little effect on the whole rock isotopic values, though it may be that the thin sections taken are not fully representative of the large whole rock samples homogenised for analysis. If this is the case, the homogenisation has the advantage of removing small-scale variations in cementation and matrix content within single hand specimens.

The Top Sandstones consist of well-sorted slightly quartzose grainstones. Many of the echinoid grains have thin calcite overgrowths, but the amount of this cement is not volumetrically large (around 2-3% cement); in addition, there is a small amount of bladed calcite cement (<1%). The carbonate phases of the grainstones differ little from those of grainstones in the upper Chert Beds, and their higher $\delta^{13}C$ values do not appear to reflect control by carbonate diagenesis.

In summary, the precipitation of relatively small amounts of calcite cement, predominantly overgrowths on echinoid grains, appears not to have had any observable effect on the $\delta^{13}C$ values.

4.3.3 Silica diagenesis and modification of the isotopic signatures

The Chert Beds are rich in diagenetic silica, which takes the form of nodules of partly-silicified limestone and chert (Tresise 1961; Williams 1986). Chertification occurred at a shallow burial depth, preceding significant intergranular compaction; the silica source appears to have been siliceous sponge spicules (Maliva & Siever 1989). The silicification process represents a candidate for alteration of the isotopic values, and was investigated.

4.3.3.1 Silicification control sampling. The very detailed sampling over the interval 29.68 to 31.31m was intended to establish whether the original isotopic signatures could be modified by silica diagenesis processes. The detailed sample set across 1.63m of sediment thickness shows a range of $\delta^{13}C$ values between 1.15 and 1.95‰, and $\delta^{18}O$ values between -1.85 and -3.90‰ (Fig.100A). The carbon- and oxygen-isotopic ratios show a good positive correlation (correlation coefficient r = 0.90), with lower $\delta^{13}C$ values accompanied by lower (more negative) $\delta^{18}O$ values (Fig.100B). Over this thin part of the sequence, it would be expected that the $\delta^{13}C$ values remain approximately constant; there is no evidence which would indicate either gaps or condensation in the sediment record. It can therefore be postulated that the fluctuations in the $\delta^{13}C$ values across this interval are caused entirely by diagenesis (silicification); from the slope of the best fit line, a function can be calculated which indicates the change in $\delta^{13}C$ for a given change in $\delta^{18}O$. A change of -1.000‰ $\delta^{18}O$ is thus accompanied by a change of approximately -0.345‰ $\delta^{13}C$. A study of the variations recorded within a single hand specimen showing varying degrees of silicification indicates that silicified areas show lower isotopic values than the surrounding matrix, and suggests that the silicification process involves a reduction in both the $\delta^{13}C$ and $\delta^{18}O$ values (Fig.101). A similar study by Clayton (1986) has shown that silicification in Upper Cretaceous chalks leads to a reduction of both carbon- and oxygen-isotopic ratios, with a $\delta^{13}C$ decrease of up to 2.0‰ in the centre of a chert nodule. This is compatible with the introduction of an isotopically light cement, such as would be expected from a sulphate reduction source.

4.3.3.2 Normalisation of the data. Given this information, the highest $\delta^{13}C$/highest $\delta^{18}O$ values appear to represent the least diagenetic modification of the original signature. Isotopic values across the detailed sampling interval were then normalised to the lowest value of $\delta^{18}O$, recalculating the $\delta^{13}C$ values accordingly (positive adjustments). This led to a plot with higher isotopic values, interpreted as closer to the original sediment signatures, and with less scatter of the $\delta^{13}C$ values (Fig.100C) (mean measured $\delta^{13}C$ = 1.66‰, standard deviation = 0.20; mean normalised $\delta^{13}C$ = 1.97‰, standard deviation = 0.10). Given that silicified limestone nodules

are developed throughout most of the sequence, the whole Chert Beds and Top Sandstones data set was then normalised to the lowest absolute $\delta^{18}O$ value (-1.484‰) of the packstone/grainstone lithology (i.e. disregarding analyses from the uppermost Foxmould shell-pebble beds) and compared with the original plot (Fig.102). This makes the assumption that all high-frequency changes in the section reflect the silicification process, but can only, however, be a simplification. This is shown by consideration of the correlation coefficients for the whole lower Chert Beds sample set (r = 0.51), the upper Chert Beds sample set (r = 0.65), and the Top Sandstones sample set (r = 0.21). In the normalised plot, there is still an obvious positive shift across the lower Chert Beds hardground, from values averaging 2.12‰ below, to values averaging 2.83‰ above, a change of 0.71‰. Across the Brecciated Limestone hardground, $\delta^{13}C$ values change from average values of 2.83‰ below, to an average of 3.21‰ above, a positive shift of 0.38‰. Thus, normalisation of the values, removing high-frequency variations assumed to represent isotopic modification due to silicification, indicates that the isotopic shifts are not controlled simply by silica diagenesis. Silica diagenesis also explains the apparent small positive carbon-isotope shift (0.20‰) coinciding with the lowest glauconitic pebble-shell bed in the upper Chert Beds. This change is caused by a greater degree of silicification in the sediments below, and coincides with the disappearance of chert nodules in the section (see the log). Normalisation of the data removes the apparent shift.

4.3.3.3 $\delta^{13}C$ - $\delta^{18}O$ plot. The possibility that the apparent shifts observed are controlled by silica diagenesis can also be ruled out by consideration of a $\delta^{13}C$ vs $\delta^{18}O$ plot for the whole data set (Fig.103). Data for the lower Chert Beds, the upper Chert Beds and the Top Sandstones form three distinct groups, as indicated. For the lower Chert Beds, the silicification trend defined by the detailed sampling programme is shown. The values for the upper Chert Beds and Top Sandstones also show scatter which is consistent with varying degrees of silicification (i.e. falling around lines of similar gradient), but in each set, the range of $\delta^{13}C$ values for the silicification trend is different. There is no overlap between the $\delta^{13}C$ values of the lower and upper Chert Beds, and little overlap between the $\delta^{13}C$ values of the upper Chert Beds and Top

Sandstones.

Diagenetic modification is recorded by the scatter of the isotopic data for each part of the sequence, particularly the $\delta^{18}O$ isotope values. There is more scatter in the isotopic values of the lower Chert Beds (-1.85 to -4.40‰), and much less in the values of the Upper Chert Beds and Top Sandstones (-1.48 to -2.81‰). Rather than reflecting an actual shift in oxygen-isotopic signatures coinciding with the $\delta^{13}C$ shift across the lower Chert Beds hardground, the $\delta^{18}O$ values simply reflect a general tendency towards less diagenetic modification in the upper beds. This scatter reflects a broadly lower volume of diagenetic silica in the upper part of the sequence, compared to the lower part. This led to the collection of samples of upper Chert Beds and Top Sandstones which were mostly only weakly-cemented; in comparison, the lower Chert Beds sample set included more samples showing a slightly higher degree of silicification, as reflected in the higher cementation indexes.

4.3.4 Time-averaging due to storm reworking and bioturbation

The Upper Greensand carbonates are a shallower-water facies than the Upper Cretaceous chalks of southern England, the Chert Beds and Top Sandstones Members of south-east Devon representing deposition in storm-dominated and fairweather shoaling wave-dominated environments respectively. Such environments were characterised by the reworking of the carbonate bioclasts; in the Chert Beds, this involved repeated sediment entrainment and redeposition, resulting in frequent bed amalgamation. Rare very high energy events produced a distinct event stratigraphy. Thus, depending on the frequency and magnitude of storm events, there will be an element of time-averaging in the isotopic data. The presence of exposed and reworked nodules in intraformational pebble-shell beds infers that winnowing processes were capable of the removal of up to a few tens of centimetres of sediment. The bedform style in the carbonates reflects the degree of reworking, comprising predominantly horizontal and undulose to low-angle cross-stratification in the Chert Beds, and trough cross-bedding in the Top Sandstones. Time-averaging will occur on a scale less than that of the individual bedform, with greater significance in the case of the more major storm events, which resulted in

amalgamated pebble and shell beds. These factors, coupled with the need to collect only the most unlithified sediment possible at a particular horizon governed the sampling programme. There is a resultant lesser degree of confidence in the validity of a specific data point, but since time-averaging will presumably only occur at a scale less than about 0.5m, the observed secular changes up the section appear to be valid.

Time-averaging on a smaller scale also resulted from sediment mixing due to bioturbation. Both *Planolites* and *Thalassinoides* burrows are present in the Chert Beds and Top Sandstones Members. The smaller *Planolites* burrows mixed sediment over a vertical thickness of only a few centimetres, but the *Thalassinoides* burrows tend to reach larger dimensions (several tens of centimetres). They are commonly developed as complex galleries of shafts and tunnels around the nodules of the hardgrounds. The burrows are passively filled with coarser, quartzose, and often glauconitic carbonate sand piped in from above, and penetrate below the hardground into the grainstones below. Large *Thalassinoides* tunnels, filled with glauconite-rich calcarenites are also developed in the cross-bedded grainstone facies of the Top Sandstones (Fig.22). Despite this sediment mixing, because of the generally large burrow size, it proved relatively simple to avoid burrow fills when sampling. The nature of the hardgrounds resulted in an absence of secular data for the three beds on the isotope plots. The nodules are diagenetically more complex than the background lithology, and give anomalous values (see above), whereas the matrix is piped in from above as passive burrow fills.

4.3.5 Completeness of the isotope stratigraphy

While encompassing the whole of the *dispar* ammonite zone, the Chert Beds and Top Sandstones Members contain certain beds which represent intervals of non-deposition, and at one horizon, unambiguous evidence for erosion. The three nodular hardgrounds represent periods of anomalously low sedimentation rates across the carbonate shelf. The nodularity was imposed upon a previously-deposited calcarenite substrate (as indicated by the presence of relict depositional structures and burrows). Intraformational pebble beds appear to represent relatively minor hiatuses, during which lowered sedimentation rates resulted in the development of early

diagenetic nodules and an increase in glauconite concentration. The sedimentary record is thus complicated in that the nodular beds represent greater time periods than the background packstones and grainstones. Part of the record has been obscured by the development of the nodularity within such a host sediment and there are thus time gaps in the secular plots, representing the period between deposition of the carbonates immediately below the nodular hardground and those immediately above. e.g. part of the *carcitanense* subzone is absent above the top of the Upper Greensand (see above). In the three intraformational pebble beds of the upper Chert Beds, which record shorter hiatuses, matrix carbonate was sampled, and the isotopic values are little different from the associated grainstones.

In addition, a single bed displays evidence for actual erosion of the underlying carbonates - the Coarse Band at the base of the Top Sandstones Member. This is a thin bed of calcarenaceous sand (typically 40-50% quartz; 45-55% carbonate grains), with an abrupt basal contact and gradational upper contact. The base of the bed is demonstrably erosive across the south-east Devon sections; in certain sections, up to 2 metres of carbonates are present above the Brecciated Limestone hardground, whereas in other sections, the Coarse Band cuts down to rest directly on the hardground (as at Little Beach - Beer Head). The bed is interpreted as a lag deposit, concentrating quartz due to winnowing of the underlying sediments. Thus, the time equivalent of greater than 2 metres of sediment are absent from the upper *dispar* zone carbon-isotope stratigraphy, probably within the *perinflatum* subzone of Owen (1976).

4.4 Comparison of whole rock data with oyster data

Oysters were collected throughout the succession, so that measured isotopic values of the shell calcite could provide an independent comparison with the whole rock values. The isotopic data show wide scatter, with the $\delta^{13}C$ values ranging from 0.81 to 4.05‰ and the $\delta^{18}O$ values from -2.54 to -4.32‰ (Fig.104). The $\delta^{13}C$ values in the upper part of the succession show rather less scatter than those in the lower part and a tendency towards correspondingly higher $\delta^{18}O$ values.

The rapid fluctuations in the carbon-isotope ratios are interpreted as reflecting diagenetic modification of the shell calcite; many of the oysters are silicified, as indicated by the beekite rings on the surface of the shell (cf. Holdaway & Clayton 1982). A plot of $\delta^{13}C$ vs $\delta^{18}O$ establishes some degree of positive correlation (r = 0.52) (Fig.105), and the data were normalised (as for the whole rock samples), in an attempt to remove the isotopic modifications of the silica diagenesis. For the oysters, a change of 1.000‰ $\delta^{18}O$ is accompanied by a change of approximately 0.736‰ $\delta^{13}C$ (compared with 0.345‰ for the whole rock samples). Two oyster samples from the uppermost Foxmould glauconitic pebble-shell beds fall well outside the silicification trend and were not normalised or plotted. These appear to have undergone considerable diagenetic modification which cannot be explained by silicification. Two further samples from the upper Chert Beds plot off the silicification trend, and appear not to reflect silicification.

Normalisation results in a plot with reduced scatter (Fig.106), again with the upper part of the succession showing much less $\delta^{13}C$ variability than the lower part. This change occurs at the level at which chert nodules disappear from the succession, around the level of the first pebble-shell bed in the upper Chert Beds. The oysters (composed originally of low Mg-calcite) appear to be very susceptible to silicification, much more so than the whole rock (matrix) samples. The abundant echinoid grains in the matrix consisted originally of high Mg-calcite, now recrystallised to low Mg-calcite; this stabilisation process appears to have reduced the silicification potential of the grains. Maliva & Siever (1988) propose that organic-matter may provide an important role in the silicification of fossils in limestones, by providing nucleation sites for initial silica precipitation; they note the potential importance of matrix stabilisation processes.

In summary, the resulting plots are very strongly influenced by diagenetic processes, reflecting only the gross amount of diagenetic silica in the host sediment. Because of their high susceptibility to silicification, oyster samples within this siliceous carbonate facies are thus unsuitable for the investigation of secular variations in the $\delta^{13}C$ oceanic reservoir.

4.5 Interpretation and significance of the isotopic data

The Cretaceous period is characterised by the widespread distribution of the black shale facies (typically black, laminated, organic-carbon-rich, pyritic sediments). Previous research has confirmed that deposition of the facies tended to be more prevalent at specific time intervals - in the Aptian-Albian, at the Cenomanian-Turonian boundary, and in the Coniacian-Santonian; these time intervals have been termed oceanic anoxic events (OAEs) (Schlanger & Jenkyns 1976; Jenkyns 1980). Carbon-isotope stratigraphy has been used to provide an independent control on the rates and magnitude of global burial of organic-carbon. A positive anomaly in $\delta^{13}C$ values has been documented from the Cenomanian-Turonian boundary at many localities, reflecting widespread burial of ^{12}C-rich organic-material in a world-wide oceanic anoxic event (comprehensively described and interpreted by Schlanger *et al.* 1987 and Arthur *et al.* 1987). In contrast to the relatively short-lived Cenomanian-Turonian OAE (not >1Ma), the Aptian-Albian OAE appears to be a more complex phase of black shale deposition, over a longer time period (17Ma for both stages, using the time scale complied by Haq *et al.* 1988). Patterns of black shale deposition, however, suggest that this may be resolved into subevents of early Aptian, early Albian and late Albian age (Arthur *et al.* 1990). Data from previous workers (Scholle & Arthur 1980) has suggested that $\delta^{13}C$ values fall throughout the Albian, to a low at the Albian-Cenomanian boundary, and in European sections, appear to be followed by rising $\delta^{13}C$ values (note that in contrast, the Mexican sections studied show decreasing $\delta^{13}C$ values until the Middle Cenomanian).

This study, however, provides isotopic evidence showing a positive secular increase in $\delta^{13}C$, inferring increasing organic-carbon burial during the Upper Albian *dispar* ammonite zone. Evaluation of spatial and temporal patterns of black shale deposition reveals that Upper Albian organic-rich sediments of confirmed and possible *dispar* zone age are known from a variety of locations world-wide (Fig.107), and are thus consistent with such an interpretation.

From the Vocontian Trough, south-east France, Bréhéret (1988) records a phase of organic-rich sedimentation of lower *dispar* (*buxtorfi* foraminiferal zone) age. The organic-

matter is of marine origin, and reaches concentrations of 1-2%. In the Pieniny Klippen Belt of the Polish Carpathians, the Brynczkowa Marl Member of the Jaworkli Formation, Klippen Successions, comprises an Upper Albian to Lower Cenomanian sequence of marls and marly limestones, with interbedded black, anoxic radiolarian shales (Birkenmajer & Jednorowska 1987). A discrete anoxic event in the late Albian characterises sequences developed in Italy (Scisti a Fucoidi and equivalents), and was reflected in rhythmic black shale deposition; this has been related to restricted circulation during a period of relatively low organic productivity (Arthur & Premoli Silva 1982; Erba *et al.* 1991).

In the Atlantic, Albian black shales are widespread (see the comprehensive review by Stein *et al.* 1989). Along the Celtic Sea margin of the northern North Atlantic, the Cenozoic sediments are dominated by terrestrially-derived organic-matter. Uppermost Albian (Vraconian, *dispar* zone) to Turonian sediments at DSDP sites 549-551 record enrichment in organic-material (up to around 2% TOC) of mixed marine and terrestrial origin (Cunningham & Gilbert 1985). Facies types consist of rhythmically-bedded, dark, laminated organic-rich chalks and light, bioturbated, organic-poor chalks. A peak TOC_{marine} occurs in the *dispar*-age strata and the beds have been interpreted as the result of alternating oxidising and reducing bottom waters; the covariance of TOC and $CaCO_3$ in many of the bands suggests that their development was controlled by marine productivity variations. In addition, mid-Cretaceous upwelling, coupled with increased organic-matter preservation, appears to have contributed to global carbon burial e.g. the Upper Albian black shales off north-west Africa (DSDP Site 367; Stein *et al.* 1989); this is a region of upwelling predicted by Parrish & Curtis (1982). In the western North Atlantic, an enrichment in organic-material has been recorded from mid-Cretaceous black shales (DSDP sites 105, 386, 534, 391), and is of mixed marine-terrestrial origin (Summerhayes 1981; Stein *et al.* 1989). In the Angola Basin of the South Atlantic, Tissot *et al.* (1980) record a succession of black shales and marls rich in planktonic material, of late Albian to Coniacian or Santonian age.

In North America, late Albian siliceous dark grey to black laminated mudstones, the Mowry Shale, were deposited across the Western Interior Seaway (Byers & Larson 1979). This

facies is rich in organic-matter, averaging 2% TOC (Nixon 1973). The high silica contents resulted from proliferations of radiolaria (Davis 1970). Deposition was within a restricted Mowry seaway which had developed by the late late Albian, following a middle late Albian peak Lower Cretaceous transgression (Kauffman 1984).

Late Albian to early Cenomanian (*R.appenennica* - *P.buxtorfi* foraminiferal zones) organic-carbon-rich laminated limestones (up to a maximum of around 8% TOC) have been drilled on the Hess Rise of the central North Pacific Ocean (DSDP sites 310, 465, 466; Dean *et al.* 1978; 1984; Thiede *et al.* 1982). These organic-rich strata are confined to such elevated plateaux and rises, and the interpreted depositional environment is within an expanded oxygen-minimum zone, the result of high equatorial surface-water productivity.

In the Venezuelan Andes of South America, deposition of alternating dark-grey laminated limestones and shales of the La Aguada Member, La Luna Formation, commenced in the late Albian (Tribovillard *et al.* 1991). TOC values reach 5% in these sediments, deposition of which continued during the Upper Cretaceous; they have been related to sedimentation within a shallow stratified water column, perhaps with coastal upwelling. In northeastern Venezuela, deposition of bituminous micritic limestones of the Querecual Formation also commenced in the late Albian (Renz 1981).

In Australia, the Toolebuc Formation comprises a thin (10-20m) but widespread sequence of bituminous calcareous shales and limestones of Albian age which occur throughout much of the Erromanga Basin and the southern Carpenteria Basin of north-west Queensland (Ramsden *et al.* 1982; Ramsden 1983). The limestones are similar to European chalks, composed principally of coccoliths and foraminifera; the organic-rich beds were deposited under anoxic conditions in an epeiric seaway which covered this part of central Australia during the Albian.

A Cretaceous black shale facies, including laminated, organic-rich sediments of Albian age, has been also recorded from the Cauvery Basin, on the east coast of south India (Govindan 1982).

4.6 Conclusions

Whole rock samples from the Chert Beds and Top Sandstones Members of the Upper Greensand Formation reveal secular changes in $\delta^{13}C$ and $\delta^{18}O$ values. Carbon-isotopic values indicate increasingly positive values through the *dispar* zone. In detail, the increase appears to be resolved as two smaller positive shifts across nodular hardground horizons, separated by carbonates which exhibit uniform isotopic compositions after corrections for diagenetic alteration. The apparent change across the zone is in the range of +1.0-1.3‰ $\delta^{13}C$ PDB. Silicification proved capable of reducing the whole rock $\delta^{13}C$ values by as much as 0.8‰ in the samples collected (presumably greater still for greater degrees of silicification, as occurs in chert nodules). Oxygen-isotopic values reflect strong modification due to silica diagenesis. Normalisation, however, removed a certain amount of the high-frequency $\delta^{13}C$ changes interpreted as due to silicification. Precipitation of minor amounts of carbonate cement, predominantly calcite overgrowths on echinoid grains, have had no observable effect on the $\delta^{13}C$ values. The carbonate mineralogy is dominated by echinoid and oyster bioclasts. Evidence from modern echinoids suggests that the test plates of this echinoderm family undergo disequilibrium fractionation with ambient seawater (often anomalously light $\delta^{13}C$ values), in comparison with the spines, which undergo equilibrium fractionation. The relevance of this to the Upper Greensand whole rock values is difficult to evaluate; certainly the magnitudes of the whole rock values tend to suggest that large magnitude fractionation (of the order of several parts per mil) did not occur. In the section studied, the $\delta^{13}C$ values do not peak and decay to more negative values, inferring increasing amounts of organic-carbon burial through the *dispar* zone. Oyster shells proved to be very prone to silicification, and were unsuitable for the detection of secular $\delta^{13}C$ isotopic changes. The positive increase of around 1.0-1.3‰ $\delta^{13}C$ through the *dispar* zone correlates with an apparent increase in the deposition of organic-carbon-rich facies in many parts of the world.

CHAPTER 5

GEOCHEMICAL ANALYSIS OF GLAUCONITIZATION PROCESSES IN THE UPPER GREENSAND FORMATION

Abstract: Geochemical analysis has confirmed the widespread development of glauconitic minerals throughout the Upper Greensand of southern England. The potassium contents of grains from different lithologies have been used to indicate the degree of evolution of the glauconitic minerals. Mid-shelf muddy sands and limestones have moderate concentrations of "evolved" glauconite; laterally-equivalent deeper-water silts (and clays), and the higher-energy facies at the top of the sequence contain lower glauconite concentrations and a higher proportion of less-evolved grains. High glauconite concentrations and "evolved" to "highly-evolved" glauconite characterise thin condensed greensand beds; these relate to basin-wide starvation surfaces, interpreted as controlled by rapid relative sea-level change. Glauconitic grains have a wide range of morphologies, showing evidence for glauconitization of a variety of initial substrates. Correlation between grain morphologies and the potassium contents indicates that morphology cannot be used to give a reliable estimate of the degree of evolution of a given grain. In multiple complex grains, there is no correlation between the accretion stage and the degree of glauconite evolution. Previous workers have suggested that the aluminium contents of glauconitic grains may be linked to the water depth of glauconite formation. The aluminium contents of Upper Greensand glauconites, however, are not depth-specific, but relate largely to aluminium-rich micaceous precursors. Simple sulphur-carbon analyses of Upper Greensand lithologies shows that these data are of only limited use in the reconstruction of organic matter influxes during sedimentation.

5.1 Mineralogical Classification

The term "glauconite" has acquired a dual connotation, being applied firstly in a morphological sense to sand-sized greenish grains in sedimentary rocks, and secondly in a mineralogical sense to a mineral species (McRae 1972). Such a double meaning has resulted in some confusion, as "glauconite" used in a purely morphological context may not equate with its use in a mineralogical sense. For example, berthierine also forms green granules, visually indistinguishable from glauconite; and the so-called Chloritic Marl of southern England (e.g. Jukes-Browne 1877; Meyer 1878) was later correctly renamed the Glauconitic Marl. There is also further complexity regarding the use of the term "glauconite" in a mineralogical sense; as a phyllosilicate and a clay mineral there is considerable and structural variability.

Following review of the current literature, the classification scheme used here is closely based on those of Odin & Matter (1981) and Van Houten & Purucker (1984). The term "glauconite" is retained, and used throughout in a morphological sense to represent grains which range mineralogically from glauconitic smectite to glauconitic mica.

Glauconitic Minerals

Glauconitic mica

This a hydrous iron-potassium-magnesium aluminosilicate. It is a phyllosilicate clay mineral, with a 10A dioctahedral (illite-type) structure, and has a substantial amount of K in the interlayer positions and a high content of Fe in the octahedral sheet. The A.I.P.E.A. Nomenclature Committee defined glauconite as "an iron-rich dioctahedral mica with tetrahedral Al (or Fe^{3+}) usually >0.2 atoms per formula unit and octahedral R^{3+} correspondingly >1.2 atoms." A generalised formula is: $K\ (R^{3+}_{1.33}\ R^{2+}_{0.67})\ (Si_{3.67}\ Al_{0.33})\ O_{10}\ (OH)_2$

(with Fe^{3+} >> Al and Mg > Fe^{2+}) (Odom 1985).

Glauconitic smectite

This is a mixed layer (interstratified) glauconite and smectite with >20% (to as much as 60%) expandable smectite layers. There is some degraded illite among the expandable layers (McConchie & Lewis 1980). It is low in K and usually extremely disordered, though in a few cases, there may be some ordering (Thompson & Hower 1978).

Mixed Mineral Glauconites

This further class includes glauconites with two or more clay minerals. For example, frequent combinations are glauconite with: illite and montmorillonite, and illite plus chlorite or kaolinite; also mixtures including clay and non-clay minerals occur (see Burst 1958a, 1958b; Bentnor & Kastner 1965).

5.2 The mechanism of glauconitization

Early theories proposed such mechanisms as co-precipitation of Mg, Fe, Al and Si gels to which K was attracted, alteration of "mud", and conversion of biotite. These were superceded by the Layer Lattice Theory (Burst 1958a; 1958b), which required a degraded layer silicate lattice, a plentiful supply of Fe and K, and a suitable redox potential, typically provided by decaying organic matter (which would produce micro-reducing conditions, even in what might be a generally oxidising macro-environment). This degraded 2:1 clay mineral lattice would transform into a glauconitic mica by substitution of Fe for Al and fixation of K (by ionic exchange).

These early theories were superceded by the current established glauconitization mechanism proposed by Odin & Matter (1981), that of authigenic growth of glauconitic minerals (comprehensively described and reviewed by Odin & Fullagar 1988). The Layer Lattice Theory was inadequate because it allowed simultaneous replacement of Al^{3+} by Fe^{3+}; these ions are in fact geochemically very similar and occur in similar concentrations in seawater. Also, it

became evident that glauconitic minerals are associated with more than just clay mineral precursors, indeed with widely-varying substrates: these include internal moulds or casts (mainly of carbonate microfossil tests e.g. foraminifera), faecal pellets formed by various sediment feeders (these may initially have contained such components as clay minerals, carbonate, organic matter), biogenic carbonate material, and mineral grains and rock fragments of widely varying compositions (e.g. quartz, chert, feldspar, biotite, muscovite, calcite, dolomite, phosphates, volcanic glass shards and fragments, and plutonic rock fragments).

The theory of authigenic growth of glauconitic minerals (Odin & Matter 1981) is at present the most widely accepted mechanism to explain glauconitization. It appears that glauconitic minerals form by "de novo authigenic growth of automorphous crystallites in the pores of a substrate, accompanied by progressive alteration and replacement of the substrate." Initial crystal growth is of a nascent glauconitic smectite (or of a ferruginous gel which transforms diagenetically to a glauconitic smectite, and as glauconitization proceeds, there is a progression towards a more evolved glauconitic mica composition. This process involves incorporation of potassium, producing decreasingly-expandable minerals as glauconitization proceeds.

Morphologically, on increasing glauconitization, there is increasing loss of the primary substrate texture, growth of larger and better shaped crystallites, deformation of the grain by displacive crystal growth, so that it takes on a bulbous and cracked form, and finally, in its last stage of evolution, the grain may be embedded beneath an outer crust of little-evolved glauconitic minerals. At the end of this process, a smooth crust is formed over the initially irregular surface, increasing the roundness of the grain.

The prerequisite for glauconitization is of a micro-environment with partial isolation of pore fluids within the substrate from seawater. The neccessity for a certain confinement before glauconitization will proceed is indicated by the association of glauconitic minerals with microfossil tests, with pores and fissures in particles, and with burrows and borings in hardgrounds. This has been supported by the observations made in several case studies (see references in Odin & Matter 1981), that statistically, glauconitic grains are found in the 0.1-

1.0 mm size-range. With larger grains (2-3mm) and pebbles, glauconitization only occurs at the grain surface (and along cracks), with the interiors remaining unaltered because ionic exchange did not reach deeply enough.

The inherent substrate porosity will also affect the degree of glauconitization. e.g. thallophyte borings in bioclasts will enhance glauconitization; similarly, quartz grains and pebbles will only develop thin films of glauconitic minerals, whereas a chalk substrate will often have a much thicker glauconitized outer zone.

Laboratory syntheses of glauconitic minerals (Harder 1978; 1980) have demonstrated that "glauconite may form by the precipitation of Fe-hydroxides and adsorbtion of silica and potassium from dilute solutions." In such a process, Fe and Al in detrital minerals are dissolved in very early-diagenetic reducing micro-environments, and precipitated in more oxidising ones in various sediment substrates.

Kohler & Köster (1976) and Valeton *et al.* (1982) have, however, proposed that the peloidal substrate origin of glauconite cannot adequately account for Cretaceous and Cenozoic deposits in Germany. They have attributed variations in peloidal chemistry, mineralogy, shape, size and cracking to specific environments that prevailed during periodic precipitation of coagulated gel-like lenses. These periodically broke up into soft peloids (by dehydration cracking) which were reworked and redeposited locally, though without significant distortion or compaction.

Ireland *et al.* (1983) support the model of Odin & Matter (1981), qualifying more precisely the mechanisms and geochemical conditions of glauconitization: glauconite forms at or near the sediment-seawater interface, in the transition zone between oxidising conditions above and reducing conditions below. Fe^{2+}, mobilized at depth in the sediments under reducing conditions, migrates upwards resulting in porewaters supersaturated in Fe^{3+} in the transition zone near the sediment-seawater interface. Significant levels of Fe^{3+} in solution cannot be equilibrium concentrations because high Eh and extreme acidity would be required. It appears that Fe^{3+} in solution is found at the interface between oxidising and reducing environments, where spontaneous diffusive migration or mixing cause transient, metastable concentrations. Where

supersaturation conditions are high, nontronite is formed; when iron supersaturation is lower, glauconitic minerals are precipitated.

These ideas are also supported by Bornhold & Giresse (1985), but these authors suggest that a more oxidising microenvironment for glauconite formation is more attractive than other models. Evidence given to support this theory is the more common association of glauconitic minerals with Pleistocene sediments which typically contain <0.4% organic-carbon, compared with similar Recent shelf sediments containing >1.52% organic-carbon. Fundamentally, Bornhold & Giresse support the theory that the principal requirements for glauconitization are: a suitable substrate, slow rates of sedimentation, and an abundant supply of available iron. They note that glauconitic grains are particularly common on the Vancouver Island active continental margin compared with many other high latitude shelf areas (e.g. eastern Canada, western Europe). To explain this, they suggest that this is because the former area has sediments rich in labile, iron-rich silicate minerals (lithic sands and muddy sands), while the latter areas tend to display more mature orthoquartzitic to arkosic sand and muddy sand facies with much less available iron.

In summary, a consensus of opinion has emerged that glauconitic minerals form by a process of authigenic growth of crystallites within the pores of a substrate, accompanied by the progressive alteration and replacement of the substrate. As glauconitization continues, the glauconitic minerals evolve from a glauconitic smectite to a glauconitic mica composition. This occurs within a semi-confined micro-environment. Opinion is somewhat varied about whether the micro-environment is slightly oxidising or slightly reducing. Odin & Matter (1981) favour slightly reducing conditions, and Bornhold & Giresse (1985) favour a more oxidising micro-environment. Ireland *et al.* (1983) suggest that glauconitization occurs in the transition zone between oxidising and reducing conditions. It is of fundamental importance in the understanding of the micro-environment of glauconitization that the mobilisation and migration of Fe^{3+} is involved. The theory of Ireland *et al.* (1983) appears to offer the most likely explanation for the broad Eh conditions prevalent during the glauconitization process.

5.3 Morphology of glauconitic minerals in the Upper Greensand Formation

Odin & Matter (1981) subdivided glauconite morphologies into: the granular facies, consisting of sand-sized, greenish grains from tens of microns to several millimetres across, and the film facies, consisting of finely-divided glauconitic minerals coating and penetrating a substrate to depths of several hundred microns to a few centimetres. This facies typically occurs associated with hardgrounds. Although the facies are separated for convenience, they are in fact part of a continuous morphological sequence, from fully glauconitized grains, to small pebbles with only a glauconitic surface film.

Various morphological varieties of these grains or peloids can be recognised. These were classified by Triplehorn (1966). (Note the term "peloid" is used as a term for a granular particle of inorganic or unknown origin; syn. with "glaucolith" of Berg-Madsen (1983); "pellet" is restricted for application to a grain whose faecal origin has been established.)

Morphological varieties of glauconitic grains (after Triplehorn 1966)

a) Spherical or ovoidal, b) Tabular or discoidal, c) Mammilated or lobate (rounded protuberances separated by cracks), d) Capsule-shaped, e) Composite (small grains of glauconitic and detrital minerals), f) Vermicular (book-like or accordion/concertina-like), g) Fossil casts and moulds (e.g. of foraminifera tests; sponge spicules etc.), h) Moulds of internal pore space (may be marked by imprints of crystal faces of calcite cement, Berg-Madsen 1983)

The morphologies of glauconitic grains were studied petrographically in order to gain information about the glauconite precursors / substrates in Upper Greensand sediments. Previous workers have stressed a volcanogenic origin for the clay mineral assemblages and associated glauconitization in the Albian sediments of southern England (Jeans *et al.* 1982). Smectite-mica clays have been found at the base of the Gault and in the Upper Gault and Upper Greensand; these have been interpreted as bentonitic clays which developed from volcanic ash introduced into a marine environment, with additional input of detrital sands and clays. The

presence of a smectitic clay mineral substrate appears to be an important factor in the development of glauconitic minerals, and glauconite has been recorded replacing volcanic grains. Glauconitic sediments are not developed in the mica-kaolinite clay assemblages of the middle part of the Gault (*subdelaurei* to middle-upper *auritus* subzonal clays at Folkstone).

In this study, the external morphologies of glauconitic grains in a range of Upper Greensand facies not studied by Jeans *et al.* (1982), were investigated in order to provide further evidence about the mode of origin of the glauconitic minerals. Units studied included: the Foxmould Member of south Devon and south Dorset; the uppermost Foxmould Member around Beer, south-east Devon; the Chert Beds Member of south Devon; and the Blue Rag, a siliceous bed in the Upper Greensand at Selbourne in the western Weald.

The majority of Upper Greensand glauconitic grains are of spheroidal or lobate morphologies, and yield little information on the glauconite precursor. However, certain grains show evidence for glauconitization of a variety of initial substrates, including:

1) glauconitic moulds and porosity-infills of calcareous fossils e.g. the porosity infill of bryozoan bioclasts (Fig.108), chambers of foraminifera (Fig.109), and the axial canals of sponge spicules (Fig.110, Fig.111).

2) glauconitic rims to, and development along cracks in quartz grains (Fig.112, Fig.113).

3) glauconitized mica flakes (Fig.114, Fig.115).

4) vermicular, book-like grains (Fig.112).

5) glauconitized carbonate grains, such as echinoid bioclasts (Fig.116).

6) glauconite replacing aggregates of silt-sized quartz grains and mud, interpreted as representing faecal pellets (Fig.117).

7) glauconite replacing the muddy matrix sediment of fine-grained siliciclastic sediments (Fig.118).

8) rims to earlier glauconitic grains, producing complex grains, with evidence for more than one glauconitization phase (Fig.109).

9) glauconitization of the margins of calcareous nodules (found in intraformational pebble beds and in nodular hardgrounds).

10) films of glauconite coating phosphate nodules (e.g. in the Dispar Zone Ammonite Bed of south Dorset).

Glauconitic grains in the Upper Greensand thus represent a whole range of different substrates. Glauconitization of actual volcanic grains is not a feasible mechanism to account for the high glauconite concentrations, though the presence of a smectitic clay assemblage was probably an important prerequisite. Of particular interest is the development of complex rimmed grains, which typically occur associated with depositional hiatuses (as compared with just slow sedimentation rates). Complex multiple grains are well-developed in the uppermost Foxmould glauconitic pebble beds developed around Beer (see Fig.119.1 - 119.8 for sketches of grains with up to four glauconitization phases). These grains record a complex history of glauconitization, burial and winnowing/erosion. Glauconitic grains with distinct internal rims have also been recorded from the Lower Cenomanian Glauconitic Marl of the Isle of Wight (Zumpe 1971).

5.4 Chemical analyses of glauconitic grains from the Upper Greensand of southern England

A total of 114 green grains from 8 different Upper Greensand samples were analysed for 10 major element compositions, using an electron microprobe. Si, K, Fe, Al, Mg, Ca, Na, Mg, Ti and P contents were measured; the results are expressed in the following tables (Tables 6-13).

The high potassium contents of the green grains from the Upper Greensand samples (average values from 5.16-8.02 wt% K_2O) confirm that the grains are glauconitic, rather than berthierine (around 1.0-1.4% K_2O; Odin & Matter 1981) or chamosite (around 0-0.16% for Jurassic chamosites from Switzerland; Delaloye & Odin 1988).

Chemical analyses of glauconitic grains reported by Odin & Matter (1981) have shown

that such grains have a number of common, and even specific chemical characteristics. SiO_2 contents are fairly constant, around 47.5%-50%. K_2O contents are the most variable of all the cations; the lower limit is vague but Odin & Matter suggest that pure glauconitic smectite contains at least 3% K_2O; the upper limit is around 8.5-9%. Al_2O_3 contents in general vary between 5% and 8% (but see later discussion of high-Al glauconite). MgO contents are very constant between 2.6% and 4.6%.

Upper Greensand samples were analysed from:

1) the Foxmould Member of the Upper Greensand, Beer, which consists of a fine-grained muddy, silty glauconitic sand.

2) the uppermost part of the Foxmould Member, Beer, which consists of condensed glauconite-rich intraformational pebble-shell beds, developed at the contact with the overlying Chert Beds Member.

3) The lower part of the upper Chert Beds Member of the Upper Greensand, Beer, which consists of carbonate packstones and grainstones with around 5% glauconite.

4) The upper part of the upper Chert Beds Member of the Upper Greensand around Beer, which consists of carbonate grainstones and packstones with around 5% glauconite.

5) The top Upper Greensand hardground, Top Sandstones Member, of the Upper Greensand, Beer, which consists of a thick bed of nodular limestone with relict trough cross-bedding; glauconitic grains analysed are those incorporated in a calcareous nodule.

6) The Dispar Zone Ammonite Bed, Durdle Cove, south Dorset, which consists of a thin bed of glauconite-rich (around 75% glauconite) marly, phosphoritic greensand.

7) The Upper Greensand, Gore Cliff, the Isle of Wight, which consists of fine-grained, weakly-glauconitic and phosphatic marly silts.

8) The basal part of the Upper Greensand, Eastbourne, which consists of a fine-grained, glauconite-rich phosphatic greensand.

5.4.1 General chemical characteristics

The silica contents of the glauconitic grains are similar to those reported by Odin & Matter (1981), the average values for the sample sets ranging from 39.98-51.32% SiO_2. Average iron contents range from 12.40-20.07% oxide; iron limitation does not appear to have been a factor in the development of glauconites in the carbonate facies studied. Iron oxides are quoted as Fe_2O_3 in the tables; this actually represents total iron oxide. The magnesium contents are less variable, typically around 2.63-4.08% MgO. Of the remaining elements, Ca, Na, Mn, Ti and P are generally all very low, less than 1% oxide. Occasional analyses, however, have higher Ca, Ti or P contents, due to the presence of calcite, opaque accessory minerals, or phosphate within the glauconitic grain. Samples marked with an asterisk in the tables are anomalously high, and were not included in the mean values at the end of each table. Potassium and aluminium contents are discussed below. In the analyses of the Upper Greensand glauconites, no correction was made for the water contents, which account for the remaining percentages, typically around 10-20%.

5.4.2 Potassium contents

The degree of evolution of the grains in a range of lithologies was determined by the K_2O measurements; Odin & Matter (1981) have shown that as the glauconitization process proceeds towards a more evolved glauconitic mica composition, the K_2O content rises accordingly:

"highly-evolved" glauconitic mica : >8% K_2O

"evolved" glauconite : 6-8% K_2O

"little-evolved" glauconite : 4-6% K_2O

"nascent" glauconite : <4% K_2O

The following potassium contents were recorded:

1) Foxmould: 3.27-8.66% K_2O ("nascent" glauconite to "highly-evolved" glauconitic mica). Mean value of 15 analyses = 7.57% K_2O ("evolved" glauconite).

2) uppermost Foxmould: 6.66-8.20% K_2O ("evolved" glauconite to "highly-evolved" glauconitic

mica).

Mean value of 17 analyses = 7.47% K_2O ("evolved" glauconite).

3) Upper Chert Beds (lower part): 5.92-8.48% K_2O ("little-evolved" glauconite to "highly-evolved" glauconitic mica).

Mean value of 11 analyses = 7.65% K_2O ("evolved" glauconite).

4) Upper Chert Beds (upper part): 5.44-8.24% K_2O ("little-evolved" glauconite to "highly-evolved" glauconitic mica).

Mean value of 11 analyses = 6.74% K_2O ("evolved" glauconite).

5) top Upper Greensand hardground: 3.86-6.77% K_2O ("nascent" to "evolved" glauconite).

Mean value of 5 analyses = 5.52% ("little-evolved" glauconite).

6) Dispar Zone Ammonite Bed: 5.91-8.76% K_2O ("little-evolved" glauconite to "highly-evolved" glauconitic mica)

Mean value of 19 analyses = 7.92% K_2O ("evolved" glauconite).

7) Upper Greensand, Gore Cliff: 2.44-6.84% K_2O ("nascent" to "evolved" glauconite).

Mean value of 11 analyses = 5.16% K_2O ("little-evolved" glauconite).

8) Upper Greensand, Eastbourne: 5.94-7.04% K_2O ("little-evolved" to "evolved" glauconite).

Mean value of 14 analyses = 6.61% K_2O ("evolved" glauconite).

To summarise, within each unit, there is typically a range of degrees of evolution of the glauconitic grains. However, the following generalisations can be made: glauconitic grains from the Foxmould muddy sands, the uppermost Foxmould glauconitic pebble-shell beds, and the storm-influenced carbonate packstones and grainstones of the Chert Beds are characterised by "evolved" glauconite (6-8% K_2O). Surprisingly, the degree of evolution of the glauconitic grains differs little between the strongly condensed uppermost Foxmould greensands and the less condensed beds below. The average potassium values of the glauconitic grains from the Chert Beds tend to be slightly lower than those from the Foxmould (by about 1%), but this is probably within the variability of the measuring technique.

Glauconitic grains from the higher-energy (fairweather shoaling-wave-dominated)

carbonate facies of the Top Sandstones are composed of less evolved glauconite than the lower-energy (storm-dominated) Chert Beds below, characterised by "little-evolved" glauconite (4-6% K_2O).

A deeper-water phosphatic greensand, the Dispar Zone Ammonite Bed, is characterised by very high glauconite concentrations (up to 75%) and an abundance of "evolved" glauconite to "highly-evolved" glauconitic mica. A glauconite-rich phosphatic greensand bed from Eastbourne (developed above a marked erosion surface cut into the Gault clay) yielded predominantly "evolved" glauconite.

"Little-evolved" glauconite characterises the deeper-water, weakly glauconitic sediments of the Isle of Wight Upper Greensand.

The potassium contents of the grains were compared with grain morphologies (Fig.119) in order to determine whether grain morphology could be used to predict the K content, and thus the degree of evolution of a given grain. Grains which have mammilated forms are at advanced stages of glauconitization (see above); these were compared with rounded spherical to ovoid grains. In summary, rounded grains with K_2O contents both higher and lower than those of the mammilated grains were recorded; this is in accord with the glauconitization sequence of Odin & Matter (1981), which records the final stage of evolution as the development of a smooth outer crust of glauconitic minerals. (see above). It is thus impossible to accurately predict the degree of evolution of an individual grain from its morphology alone.

Similarly, there appears to be no correlation between successive glauconite accretion stages, and the degree of glauconite evolution. Analyses were undertaken of multiple grains to investigate the mineralogies of earlier and later accretion stages. Such grains include (from grain centre to grain rim; $\%K_2O$ values are given in parentheses:

TF2(8.20%) - TF3(8.10%)

TF10(7.17%) - TF11(7.19%) - TF12(7.30%) - TF13(7.46%)

CB12(6.26%) - CB14(6.31%) - CB13(6.12%)

CB15(6.61%) - CB16(6.63%)

E3(6.63%) - E4(6.62%)

In these multiple grains, the degree of evolution of the glauconitic minerals varies very little between the centres and rims; there is no relationship between the timing of the glauconite phase within a multiple grain (core or rim) and the degree of evolution of the glauconitic minerals.

In summary, in the Upper Albian of southern England, the mid-shelf sediments of the Foxmould and Chert Beds typically have moderate concentrations of "evolved" glauconite. The laterally-equivalent deeper-water sediments and the higher-energy facies above contain lower overall glauconite concentrations, with a higher component of less evolved grains. High glauconite concentrations and "evolved" to "highly-evolved" glauconites characterise thin, condensed greensand beds (described above); these have been related to basin-wide starvation surfaces, relating to rapid relative sea-level change (discussed fully in Chapter 2). Development of the glauconitic minerals results from low sedimentation rates, typically of the order of 10mm/1000yrs for both the Foxmould and Chert Beds Members of the Upper Greensand, and 7mm/1000years for the uppermost Foxmould pebble-shell beds. Odin & Matter (1981) have estimated that at a hiatus in sedimentation, the time required for the formation of the initial glauconitic smectite is around 1,000-10,000 years, and for "highly-evolved" glauconitic mica, around 100,000yrs-1 Ma.

5.4.3 Aluminium contents and depth relationships

Porrenga (1967) described a zonation of iron minerals from the Niger Delta, where goethite was found at depths from 0-10m, berthierine at depths from 10-50m, and glauconite at 50m and deeper, depending on the water temperature. Low-alumina glauconite was abundant between 125m and 500m, at temperatures between 10^0 and 15^0C. Low-alumina glauconites appear to be typical of these conditions, and Norwegian examples have been recorded from waters with mean annual temperatures as low as 6^0C (at a depth of 250m) (Bjerkli & Östmo-Saeter 1973). A study by Owens & Sohl (1973) inferred a goethite (nearshore gulf) - high-alumina glauconite (inner shelf) - low-alumina glauconite (middle to outer shelf) zonation in Cretaceous sediments

from the New Jersey-Maryland coastal plain of North America. Berg-Madsen (1983) has also identified high-alumina (>10%) glauconite in Early Palaeozoic sediments from Baltoscandia, inferring deposition in shallow (<50m) and cool water. So far, however, modern high-alumina glauconite has not yet been documented.

The following alumina contents were recorded:

1) Foxmould: 6.85-20.37% Al_2O3; mean value of 15 analyses = 9.51%.

2) uppermost Foxmould: 7.23-10.56% Al_2O3; mean value of 17 analyses = 8.13%.

3) upper Chert Beds (lower part): 6.99-11.07% Al_2O_3; mean value of 11 analyses = 8.45%.

4) upper Chert Beds (upper part): 6.90-9.57% Al_2O_3; mean value of 11 analyses = 8.15%.

5) top Upper Greensand hardground: 6.22-8.70% Al_2O_3; mean value of 5 analyses = 7.36%.

6) Dispar Zone Ammonite Bed: 5.75-11.05% Al_2O_3; mean value of 19 analyses = 8.03%.

7) Upper Greensand, Gore Cliff: 5.87-14.54% $Al2O_3$; mean value of 11 analyses = 8.86%.

8) Upper Greensand, Eastbourne: 6.35-9.60% Al_2O_3; mean value of 14 analyses = 7.80%.

The alumina contents of Upper Greensand glauconites thus range from 5.75-20.37% Al_2O_3. Using the classification scheme above, this represents a mixture of low-Al and high-Al glauconite, with grains around 9-10% Al_2O_3 being fairly common. All samples (except the top Upper Greensand hardground) contain a proportion of glauconitic grains with >9% Al_2O_3. No corresponding aluminium zonation has been revealed; the fact that the shallowest-water sediments, represented by the cross-bedded grainstones of the Top Upper Greensand hardground have generally lower values than the storm-dominated siliciclastics and carbonates below is the opposite to what might be expected from the models described above.

The morphologies of the glauconitic grains analysed are shown on the accompanying charts. Grains with >9% Al_2O_3: F 7,11,12,13,15; TF 8,10; CB 9,11,18,20; DZ 1,3,4,6,8,18; GC 6,7,9,11; E 4,7. The grain morphologies of these high-Al glauconites comprise: 11 spherical to ovoidal grains, 8 vermicular grains, 4 mammilated grains and 1 spicule mould.

The majority of vermicular grains analysed have high-alumina contents, and this is

interpreted as reflecting an original high-alumina precursor, typically a mica flake. Sample CB11 represents "little-evolved" glauconite replacing a large muscovite flake, and has 11.07% Al_2O_3. The highest recorded values, 15.27% (F15) and 20.37% Al_2O_3 (F12) were from vermicular grains in the Foxmould. Not all high-Al glauconites have vermicular morphologies, for example F7, F11, which are ovoidal in shape. These, however, have higher K_2O contents (>8%), indicating a "highly-evolved" glauconitic mica composition. It is probable that the Al contents of glauconitic grains within the Upper Greensand samples are not depth-specific, but relate largely to the composition of the grain precursors. "Little-evolved" to "evolved" high-alumina glauconites with vermicular morphologies relate to micaceous substrates (high in Al) and preserve the high Al contents during glauconitization. "Evolved" to "highly-evolved" high-alumina glauconites with spheroidal to ovoidal morphologies are also interpreted as representing glauconitization of micaceous precursors, but due to more complete glauconitization (alteration and replacement of the substrate), the layered structure has been lost. The majority of the high-Al grains with spheroidal to ovoidal morphologies also show "evolved" compositions (>6% K_2O), which is consistent with this hypothesis. There are 2 exceptions, however, which have high-Al and low-K contents: G6 (ovoidal grain, 9.26% Al_2O_3, 5.70%K_2O) and G11 (sponge spicule infill, 9.25% Al_2O_3); the origin of these is uncertain. In addition, the rim of a glauconitic grain (CB18), with high-Al and an "evolved" glauconite composition, probably did not relate to a micaceous precursor. However, it is clear from the grain morphologies that glauconites with very high Al contents ($\geq$ 12% Al_2O_3) are not depth-related, but are substrate-controlled. The glauconites studied by Owen & Sohl (1973) commonly show high-alumina glauconites with "accordion" morphologies, compared with low-alumina glauconites which are botryoidal; this probably represents a zonation in the composition of the original (micaceous and non-micaceous) precursors.

Most previous studies have generally assumed that the substrate has little influence on the glauconitization reactions. However, Hughes & Whitehead (1987), investigating the Barton Formation (Upper Eocene) of southern England, identified two different glauconitic mineral compositions associated with two different forms of silica (quartz and chert). This was

interpreted as due to different surface reaction control mechanisms associated with the two forms of silica.

5.5 Sulphur-carbon data from the Upper Greensand and Gault of southern England

As discussed above, glauconitic minerals have been interpreted as forming at oxidising-reducing interfaces at or very close to the sediment-seawater interface. The presence of organic matter in the sediment (at an optimum concentration) would generate increased surface area of such an interface, and thus could enhance the glauconitization process. The sulphur and carbon contents of a range of Upper Greensand sediments were thus investigated.

5.5.1 Methodology

A total of 54 sediment samples were collected from the Upper Greensand and Gault. Each sample was broken into small chips, and any weathered material discarded. Samples of between about 30g and 100g (averaging about 60g) were ground into fine powder using a planetary boremill with agate grinding balls and mortars. Crushing such large samples ensured that representative powder was withdrawn for analysis. From each powder sample, 100-200g were extracted and analysed for total organic-carbon (TOC) contents, and 100-200g used for analysis of sulphur contents (a measure of disseminated pyrite). The analyses were made by heating the powder to 1200°C, followed by coulometric titration; this was performed on a Coulomat 702 instrument at the Department of Earth Sciences, University of Oxford. The organic-carbon content of a sample was determined by subtracting measured inorganic-carbon from measured total carbon. Total carbon was measured in a first sample; inorganic-carbon was measured in a second sample in which the organic-carbon had been oxidised by heating to 450°C for 10 hours. Each carbon and sulphur analysis was repeated, and the values quoted are the mean of the two analyses (Table 14).

5.5.2 Discussion

The Upper Greensand and Gault samples do not contain anomalously high organic-carbon contents. In the Foxmould, TOC values range from 0.07 to 0.38%. In the Upper Greensand of south Dorset, TOC values range from 0 to 0.38% (Note: the value of 0.72% TOC recorded from the Chert Beds at Durdle Cove, sample RP15, is anomalous, and is due to the high $C_{carbonate}$ content). In the Gault of south Dorset, TOC values range from 0.26 to 1.74%. The Upper Greensand samples of the Isle of Wight have TOC values ranging from 0 to 1.10%, and 3 samples of the Gault at Folkstone show values ranging from 0.43 to 0.80% TOC. The sediments tend not to be pyrite-rich, with the maximum S value recorded being 0.46% (basal Upper Gault, Folkstone). For certain Foxmould samples, the S values will, however, be underestimates, as the sediment contains occasional small pyrite nodules.

Sulphur-carbon plots for each locality studied are given (Figs.120-123); these show that the majority of samples display a positive S-C correlation on a line of positive gradient with close to zero intercept. Such trends are typical of modern normal marine (non-euxinic) sediments (Berner 1984; Raiswell & Berner 1985). Scattered samples, however, plot off these trends, notably a small grouping of samples from south Dorset, with values of around 0.3% S; these samples, however, have low TOC contents (0.16-0.37%). In addition, a single Gault sample showed high TOC (1.74%), with 0.22% S (this is probably an underestimate, however, as the sample was slightly weathered).

The glauconite-rich Dispar Zone Ammonite Bed (DZAB) has a low TOC content (up to 0.18%) and a low S (low pyrite) content. Although the preserved TOC content implies a low initial organic-carbon concentration, the presence of large amounts of diagenetic phosphate in the sediment indicate the burial of a substantial organic matter with the sediment. For sediments with very low depositional rates and with phosphate development, such as the DZAB, the preserved TOC values would not be expected to reflect accurately the amount of organic matter initially contributing to the sediment. This is because much of the organic matter would have been oxidised under the low sedimentation rates, and much of the remainder then lost during phosphate neoformation. Studies of storm sedimentation (Chapter 3) have shown that Foxmould

deposition occurred across south Devon (and probably south Dorset also) in a well-oxygenated depositional environment. In conclusion, for this glauconitic facies type, it appears that simple S-C analyses are only of limited use in the reconstruction of organic matter influxes into the host sediment during deposition.

5.6 Conclusions

Geochemical analysis of selected mineral grains has confirmed the widespread development of glauconitic minerals throughout the Upper Greensand of southern England. The processes of glauconitization have been briefly reviewed, and data from the Upper Greensand compared with published glauconite data. The measured potassium contents of glauconitic grains from different lithologies within the Upper Greensand indicate the degree of evolution of the glauconitic minerals. In the Upper Albian of southern England, the mid-shelf muddy sands and limestones of the Foxmould and Chert Beds typically have moderate concentrations (5-10%) of "evolved" glauconite; laterally-equivalent deeper-water silts (and clays), and the higher-energy facies at the top of the sequence in south-west England contain lower overall glauconite concentrations, with a higher component of less evolved grains. High glauconite concentrations and "evolved" to "highly-evolved" glauconite characterise thin, condensed greensand beds; these relate to basin-wide starvation surfaces, interpreted as relating to rapid relative sea-level change. Glauconitic grains have a wide range of morphologies, showing evidence for glauconitization of a variety of initial substrates. Correlation between grain morphologies and the potassium contents of the glauconitic grains indicates that grain morphology cannot be used to give a reliable estimate of the degree of evolution of a given grain. Similarly, in multiple complex grains recording several glauconitization phases, there is no correlation between accretion stage and the degree of glauconite evolution. Previous workers have suggested that the aluminium contents of glauconitic grains may be linked to the water depth of glauconite formation, with high-alumina glauconite representing deposition in cool, shallow water. The aluminium contents of glauconitic grains in the Upper Greensand, however, are not depth-specific, but relate largely to the

composition of the grain precursors. Many high-alumina glauconites have been shown to relate to aluminium-rich micaceous precursors, the structures of which are often preserved. A preliminary study was undertaken in order to determine the preserved organic-carbon and sulphur (pyrite) contents of a range of lithologies in the Upper Greensand and Gault, but for this glauconitic facies type, simple S-C analyses are of only limited use in the reconstruction of organic matter influxes during sedimentation.

CHAPTER 6

CONTROLS ON THE WORLD-WIDE DEVELOPMENT OF THE CRETACEOUS GLAUCONITIC FACIES

Abstract: A thorough review of published data on middle and Upper Cretaceous glauconitic facies has indicated a wide range of depositional settings and facies associations. Reconstructions of the palaeogeographic distribution of world-wide Cretaceous greensands have shown that the facies type was associated with a number of distinct provinces; these are briefly reviewed. Cretaceous greensand depositional settings include development: directly overlying unconformities, over wide epicontinental shelf areas, on submarine highs within broad shelf areas, on stable passive continental margins, on starved continental margins with geostrophic currents, in restricted sedimentary basins, as transgressive deposits within a complex active fold belt, and in zones of upwelling of nutrient-rich waters. Many greensands appear to be associated with smectitic clays of probable volcanogenic origin. Volumetric calculations of Cretaceous glauconite production rates (GPR) have shown that a major increase in production occurred during the middle and late Cretaceous; this commenced in the Aptian, with a four- to five-fold increase. Three GPR peaks have been identified: the Lower Aptian-Lower Albian, the Upper Albian-Upper Cenomanian and the Lower Coniacian-Upper Santonian. These appear to be linked to widespread transgressions and episodes of sediment starvation across the extensive broad shelf seas which developed globally during this time of rising sea-levels and sea-level highstand.

The oldest record of glauconitic peloids is in Proterozoic sediments of Western Australia (Hall & Goode 1978). Glauconitic sediments continued to accumulate, at least locally, throughout most of the Phanerozoic; however, glauconitic minerals are especially common in rocks of Middle Cambrian-Ordovician age, middle-Upper Cretaceous age, and late Cenozoic age (Van Houten & Purucker 1984). These three episodes of abundant glauconitic facies development

coincide with major high-stands of sea-level. In the light of this, the distribution and facies associations of Cretaceous occurrences have been investigated in order to determine the possible controlling factors on the facies development.

6.1 Review of the world-wide distribution of Cretaceous glauconitic sediments

6.1.1 Introduction and methodology

An extensive review of published literature on the Cretaceous period has established a large data base of information on glauconitic sediments. This yields information on the spatial and temporal distribution of glauconitic facies on a world-wide basis. The data indicate the prevalence of the facies type in a number of "greensand provinces", and can be treated semi-quantitatively in order to determine glauconite production rates for each Cretaceous sub-stage. In the following lists, glauconitic sediments used in the volumetric calculations below are listed by substage; within each substage, they are grouped into areal associations. Where formations span two or more substages, they have repeat listings for each. The data are based on numerous references, many cited in the following review; additional data sources include : Adatte & Rumley 1987; Arnaud-Vanneau *et al.* 1987; Besnosov *et al.* 1978; Birkenmajer & Jednorowska 1987; Bismuth *et al.* 1982; Cavon & Schwizer 1987; Charrier & Lahsen 1969; Dingle & Klinger 1972; El-Sharkawi & Al-Awadi 1982; Flexer 1971; Franks 1975; Hirano *et al.* 1976; Kaddowvi 1982; Kennedy *et al.* 1979; McLachlan *et al.* 1976; Mollan *et al.* 1970; Obata & Futokomi 1976; Powell 1970; Rinaldi 1982; Scrutton & Dingle 1976; Soliman & El Badry 1970; Stapleton & Beer 1977; Toshimitsu 1988; Van Hinte *et al.* 1975; Van Houten & Smith 1984; Webb 1971; Winterer 1973.

6.1.2 Listings of glauconitic facies for each Cretaceous stage

MAASTRICHTIAN

Abbotsford Mudstone, Otago, South Island, New Zealand (uppermost Maastrichtian-Palaeocene)
Claverley Sandstone, Marlborough, South Island, New Zealand (Upper Maastrichtian-Lower Palaeocene)
Raukauroa Formation, Raukumara Peninsula, North Island, New Zealand (Maastrichtian-Palaeocene)
Mead Hill Flint (lower part) Marlborough, South Island, New Zealand (Upper Maastrichtian)
Butt Formation (basal part) Iwitahi Group, Marlborough, South Island, New Zealand (Upper Maastrichtian)
Unnamed greensands, Otago, South Island, New Zealand (Maastrichtian)
Tapuaeroa Formation (part only), Raukumara Peninsula, North Island, New Zealand (Maastrichtian)
Unnamed sediments, south-east Wellington, North Island, New Zealand (Lower Maastrichtian)
Herring Formation (upper part), Iwitahi Group, Marlborough, South Island, New Zealand (Lower Maastrichtian)
Tahora Sandstone, Rakauroa Formation, Raukumara Peninsula, North Island, New Zealand (basal Maastrichtian)
Miria Marl, Carnarvon Basin, Western Australia (Maastrichtian)
Alphard Formation (part only), Outeniqua Basin, southern Cape, South Africa (Maastrichtian)
Grudja Formation, southern Mozambique (Coniacian/Santonian-Palaeocene)
St. Lucia Formation, Zululand Group, Zululand/Natal, South Africa (Lower Coniacian-Maastrichtian)
Tinton Formation, New Jersey coastal plain, U.S.A. (Upper Maastrichtian)
Redbank Formation, New Jersey coastal plain, U.S.A. (Upper Maastrichtian)
Navesink Formation, New Jersey coastal plain, U.S.A. (Lower Maastrichtian)
Nacatoch Formation, Navarro Group, Arkansas and Texas, U.S.A. (Maastrichtian)
Chorillo Chico Formation, Magellanes Province, Chile (Upper Maastrichtian-Lower Palaeocene)
Rocallosa Formation, Magellanes Province, Chile (Upper Maastrichtian)
Carrera Formation, Magellanes Province, Chile (Upper Maastrichtian)
Rio Blanco Formation, Magellanes Province, Chile (middle Maastrichtian)
Santa Ana Beds, Magellanes Province, Chile (middle Maastrichtian)
Sobral Formation, Marambio Group, (previous Snow Hill Island Series), Seymour (Vicecomorodo Marambio) Island, Antarctic Peninsula (Lower Maastrichtian)
Unnamed sediments, northern Israel (uppermost Campanian-basal Maastrichtian)

CAMPANIAN

Paton Formation, Iwitahi Group, Marlborough, South Island, New Zealand (uppermost Santonian-Campanian)
Ess Creek Formation, Iwitahi Group, Marlborough, South Island, New Zealand (Upper Santonian-Campanian)
Poison Hill Greensand, Coolyeana Group, Perth Basin, Western Australia (Campanian)
Mahedo Formation, Assam shelf, India (Campanian)
Upper Haborogawa Formation, Yezo Group, north-west Hokkaido, Japan (Lower Campanian)
Umzamba Formation, St. John's Basin, Pondoland, South Africa (Middle Santonian - Lower Campanian)
St. Lucia Formation, Zululand Group, Zululand/Natal, South Africa (Lower Coniacian-Maastrichtian)
Grudja Formation, southern Mozambique (Coniacian/Santonian-Palaeocene)
Duwi Group (upper member), western and eastern Desert, Egypt (late Campanian)
Unnamed sediments, northern Israel (uppermost Campanian-basal Maastrichtian)
Unnamed sediments, Kamyshin area, north of Volgograd (Campanian)
Lund Sandstone, Malmö area, southern Sweden (Santonian-Campanian)
Merchantville Formation, Atlantic coastal plain, New Jersey-Georgia, U.S.A. (Camapanian)
Marshalltown Formation, Atlantic coastal plain, New Jersey-Georgia, U.S.A. (Campanian)
Pecan Gap Formation, Taylor Group (basal part), Texas, U.S.A. (middle Lower Campanian)
Tres Esquinas Member, Colon Formation, Venezuelan Andes and Maracaibo Basin, Venezuela (Santonian-Campanian)

SANTONIAN

Paton Formation, Iwitahi Group, Marlborough, South Island, New Zealand (uppermost Santonian-Campanian)
Ess Creek Formation, Iwitahi Group, Marlborough, South Island, New Zealand (Upper Santonian-Campanian)
Nidd Formation, Iwitahi Group, Marlborough, South Island, New Zealand (Middle Cenomanian-Upper Santonian)
Madura Formation (Madura Shale), Eucla Basin, southern Australia (Aptian-Santonian)
Belfast Mudstone Member, Paaratte Formation, Sherbrook Group, Otway Basin, southern Australia (Cenomanian-Santonian)
Umzamba Formation, St. John's Basin, Pondoland, South Africa (middle Santonian-Lower Campanian)
St. Lucia Formation, Zululand Group, Zululand/Natal, South Africa (Lower Coniacian-Maastrichtian)
Grudja Formation, southern Mozambique (Coniacian/Santonian-Palaeocene)
Sirte Shale Formation (basal part), Sirte Bain, northern Libya (Santonian-Campanian boundary)
Unnamed sediments, Usa Basin, western slope of Artic Urals, U.S.S.R. (Santonian)
Unnamed sediments, Lar'yak, western Siberian Lowlands (Coniacian-Santonian)
Unnamed sediments, Kristianstad Basin, southern Sweden (Santonian)
Lund Sandstone, Malmö area, southern Sweden (Santonian-Campanian)
Eriksdal Marl, Malmö area, southern Sweden (Coniacian-Lower Santonian)
Bavnødde Greensand, Bornholm, Denmark (Upper Coniacian-Lower/middle Santonian)
Senonian Greensands, Hibernian Greensand Formation, Northern Ireland (Upper Conicaian-Santonian, *testudinarius* and *pilula* echinoid zones)
Dawson Canyon Formation, Nova Scotian shelf, Canada (Turonian-Santonian)
Tres Esquinas Member, Colon Formation, Venezuelan Andes and Maracaibo Basin, Venezuela (Santonian-Campanian)
Sebaruco Member, La Luna Formation, western Venezuela (?Lower Turonian-Upper Santonian)

CONIACIAN

Nidd Formation, Iwitahi Group, Marlborough, South Island, New Zealand (Middle Cenomanian-Upper Santonian)
Molecap Greensand, Coolyeana Group, Perth Basin, Western Australia (?Middle Turonian-?Lower Coniacian)
Madura Formation (Madura Shale), Eucla Basin, southern Australia (Aptian-Santonian)
Belfast Mudstone Member, Paaratte Formation, Sherbrook Group, Otway Basin, southern Australia (Cenomanian-Santonian)
St. Lucia Formation, Zululand Group, Zululand/Natal, South Africa (Lower Coniacian-Maastrichtian)
Grudja Formation, southern Mozambique (Coniacian/Santonian-Palaeocene)
Unnamed sediments, western Madagascar (Coniacian)
Unnamed sediments, Lar'yak, western Siberian Lowlands (Coniacian-Santonian)
Klement Formation, western Carpathians, Czechoslovakia (Upper Turonian-Coniacian)
Palkovice Formation (lower part only; minor), western Carpathians, Czechoslovakia (Conicaian)
Godula Formation s.s., Godula Group (part), western Carpathians, Czechoslovakia (latest Cenomanian-Coniacian)
Eriksdal Marl, Malmö area, southern Sweden (Coniacian-Lower Santonian)
Bavnødde Greensand, Bornholm, Denmark (Upper Coniacian-Lower/middle Santonian)
Craie grise glauconifère, northern France (basal Coniacian)
Senonian Greensands, Hibernian Greensand Formation, Northern Ireland (Upper Coniacian, *cortestudinarium* and *corangium* echinoid zones -Santonian)
Dawson Canyon Formation, Nova Scotian shelf, Canada (Turonian-Santonian)
Sebaruco Member, La Luna Formation, western Venezuela (?Lower Turonian-Upper Santonian)

TURONIAN

Nidd Formation, Iwitahi Group, Marlborough, South Island, New Zealand (Middle Cenomanian-Upper Santonian)
Peepingee Greensand, Winning Group, Carnarvon Basin, Western Australia (?Albian/Cenomanian/Turonian)
Alinga Formation (Alinga Greensand), Winning Group, Carnarvon Basin, Western Australia (?Albian-Turonian)
Molecap Greensand, Coolyeana Group, Perth Basin, Western Australia (?Middle Turonian-?Lower Coniacian)
Osborne Formation (upper part of old South Perth Formation), Coolyeana Group, Perth Basin, Western Australia (?Middle Albian-Turonian)
Madura Formation (Madura Shale), Eucla Basin, southern Australia (Aptian-Santonian)
Belfast Mudstone Member, Paaratte Formation, Sherbrook Group, Otway Basin, southern Australia (Cenomanian-Santonian)
Unnamed sediments, western Desert, Egypt (Cenomanian-Turonian)
Etel Formation (part), Sirte Basin, northern Libya (Turonian)
Unnamed sediments, Bohemian Massif, Czechoslovakia (Upper Cenomanian-basal Upper Turonian)
Zlotno Sandstone, southwestern Table Mountains, southwestern Poland (middle Middle Turonian)
Skalniak Sandstone (basal part), Table Mountains, southwestern Poland (Upper Turonian)
Godula Formation s.s., Godula Group (part), western Carpathians, Czechoslovakia (latest Cenomanian-Coniacian)
Klement Formation, western Carpathians, Czechoslovakia (Upper Turonian-Coniacian)
Bochumer Greensand, Essen area, western Germany (Turonian)
Pilé Marin/Sables glauconieux, Touraine-Poitou, southwestern Paris Basin, France (upper Upper Turonian)
Glauconie de Maubeuge, Hainaut, northern Paris Basin, France (upper Middle Turonian)
Unnamed sediments (minor part), Faroe Basin (Cenomanian-Turonian)
Dawson Canyon Formation, Nova Scotian shelf, Canada (Turonian-Santonian)
Sebaruco Member, Sebaruco Shales, La Luna Formation, western Venezuela (?Lower Turonian-Upper Santonian)
Tigre Formation, Temblador Group, eastern Venezuela (Turonian)

CENOMANIAN

Nidd Formation, Iwitahi Group, Marlborough, South Island, New Zealand (Middle Cenomanian-Upper Santonian)
Peepingee Greensand, Winning Group, Carnarvon Basin, Western Australia (?Albian/Cenomanian/Turonian)
Alinga Formation (Alinga Greensand), Winning Group, Carnarvon Basin, Western Australia (?Albian-Turonian)
Osborne Formation (upper part of old South Perth Formation), Coolyeana Group, Perth Basin, Western Australia (Middle Albian-Turonian)
Madura Formation (Madura Shale), Eucla Basin, southern Australia (Aptian-Santonian)
Belfast Mudstone Member, Paaratte Formation, Sherbrook Group, Otway Basin, southern Australia (Cenomanian-Santonian)
Unnnamed sediments, Oyubari area, western Yubari range, central Hokkaido, Japan (Cenomanian)
Maputo Formation, southern Mozambique (Barremian-Middle Cenomanian)
Mzinine Formation, Zululand Group, Zululand/Natal, South Africa (Lower Albian-Upper Cenomanian)
Unnamed sediments, western Desert, Egypt (Cenomanian-Turonian)
Bahi Formation (upper part), Sirte Basin, northern Libya (Middle-Upper Cenomanian)
Wara Formation, Wasia Group, Great Burgan oil field, Kuwait (Middle Cenomanian)
Mauddud Formation, Wasia Group, Great Burgan oil field, Kuwait (Lower Cenomanian)
Glauconitic Limestone, south-east of Esfahan, Iran (Upper Albian-Cenomanian)
Unnamed sediments, Kopet-Dag range, U.S.S.R. (Aptian-Cenomanian)
Unnamed sediments, Tuar-Kyr range, east of the Caspian Sea, U.S.S.R. (Cenomanian)
Unnamed sediments, Crimea, U.S.S.R. (basal Lower Cenomanian)
Unnamed sediments, Russian Platform (Cenomanian)

Unnamed sediments, Polish-Lithuanian depression, U.S.S.R. (Albian-Cenomanian)
Unnamed sediments, Chelmowa Mountain, central Poland (Upper Albian-Cenomanian)
Unnamed sediments, northeastern Table Mountains, Poland (?Middle-Upper Cenomanian)
Unnamed sediments, Miechów-Pomerania region, Polish Lowlands (Cenomanian)
Unnamed sediments, Bohemian Massif, northern Czechoslovakia (Upper Cenomanian-basal Upper Turonian)
Ostravice Sandstone, Godula Variegated Formation, Godula Group, western Carpathians, Czechoslovakia (Cenomanian)
Godula Formation s.s., Godula Group (part), western Carpathians, Czechoslovakia (latest Cenomanian-Coniacian)
Baška Formation (part), western Carpathians, Czechoslovakia (Middle Albian-Lower Cenomanian)
Unnamed sediments, Malmö area, southern Sweden (Albian-Cenomanian)
Unnamed sediments, Båstad Basin, southern Sweden (Albian-Cenomanian)
Arnager Greensand, Bornholm, Denmark (Middle Cenomanian)
Essen Greensand/Glauconitische Scammergel, Essen area, western Germany (Lower Cenomanian)
Texel Greensand, West Netherlands Basin (Lower Cenomanian)
Ueberturriliten bed, Seewen Limestone, Helvetic Zone, Swiss Alps (Cenomanian)
Unnamed sediments, Angeoumois, central-west France (Lower Cenomanian)
Craie à Terebratella carantonensis, Maine/Touraine, western Paris Basin, France (Upper Cenomanian, *gracile* zone)
Sables de la Hardoye, eastern Paris Basin, Ardennes, Belgium (Middle-Upper Cenomanian)
Sables de Maine/du Perche, western Paris Basin, France (upper Middle-Upper Cenomanian)
Sables/Grès de Vierzon, Cher, southern Paris Basin, France (Middle Cenomanian)
Marnes de Nogent-le-Bernard, Sarthe, western Paris Basin, France (Middle Cenomanian, *costatus* to *jukesbrowni* zones)
Craie de Théligny, Perche, western Paris Basin, France (Middle Cenomanian, *costatus* to *jukesbrowni* zones)
Sables de Varennes, southwestern Paris Basin, France (Middle Cenomanian)
Sables/Grès/Craie de Vendeuvre, southeastern Paris Basin, France (lower Middle Cenomanian)
Craie Glauconieuse/Marnes de Ballon, western Paris Basin, France (Lower Cenomanian, *carcitanense*, *saxbi*, *dixoni* zones)
Argile Glauconieuse à minerai de fer, Maine, Paris Basin, France (Lower Cenomanian)
Gaize de Marlemont, eastern Paris Basin, Ardennes, Belgium (Lower Cenomanian)
Cambridge Greensand, Wessex Basin, southern England (Lower Cenomanian; upper *carcitanense* ammonite subzone)
Glauconitic Marl, Wessex Basin, southern England (Lower Cenomanian)
Glauconie de base, western margin of Paris Basin (middle Albian-Lower Cenomanian)
Meules du Hainaut, Bassin de Mons, Belgium (Middle Albian-Lower Cenomanian)
Glauconitic Sandstone, Hibernian Greensand Formation, Northern Ireland (Cenomanian)
Unnamed sediments, north-west Scotland (Cenomanian)
Glauconite Sands, Hibernian Greensand Formation, Northern Ireland (Cenomanian)
Unnamed sediments (minor), Faroe Basin (Cenomanian-Turonian)
Unnamed sediments, Orphan Knoll, D.S.D.P. Site 111, off the Labrador coast, Canada (Albian-Cenomanian)
Eider Member, Logan Canyon Formation, Nova Scotian shelf, Canada (Cenomanian)

ALBIAN

Alinga Formation (Alinga Greensand), Winning Group, Carnarvon Basin, Western Australia (?Albian-Turonian)
Peepingee Greensand, Winning Group, Carnarvon Basin, Western Australia (?Albian/Cenomanian/Turonian)
Windalia Radiolarite, Winning Group, Carnarvon Basin, Western Australia (Upper Aptian-Lower Albian)
Osborne Formation (upper part of old South Perth Formation), Coolyeana Group, Perth Basin, Western Australia (?Middle Albian-Turonian)
Parda Formation, Canning Basin, northwestern Australia (Neocomian-Aptian/Albian)
Anketell Formation, Canning Basin, northwestern Australia (Neocomian-Aptian/Albian)
Tambo Formation, Great Artesian Basin, eastern central Australia (Upper Albian)

Madura Formation (Madura Shale), Eucla Basin, southern Australia (Aptian-Santonian)
Lower Giumal Sandstone, Garhwal-Kumaun Himalayas, India & Tibet (Hauterivian-Lower Albian)
Belemnites Shale Formation, Parh Group, Lower Indus Basin, Pakistan (Neocomian-Albian)
Maputo Formation, southern Mozambique (Barremian-Middle Cenomanian)
Mzinine Formation, Zululand Group, Zululand/Natal, South Africa (Lower Albian-Upper Cenomanian)
Fahdene-Zebbag Formation, séquence du Selloum (basal part), Djebel Semmama area, Tunisia (basal Upper Albian)
Glauconitic Limestone, south-east of Esfahan, Iran (Upper Albian-Cenomanian)
Burgan Formation, Wasia Group, Great Burgan oil field, Kuwait (Upper Albian)
Qamchuqa Formation, north-west Iraq (Albian)
Unnamed sediments, Kopet-Dag range, U.S.S.R. (Aptian-Cenomanian)
Unnamed sediments, Bol'shoi Balkhan area, Russian Platform, U.S.S.R. (Aptian-Albian)
Unnamed sediments, northern Caucusus, U.S.S.R. (Upper Aptian-Lower Albian)
Unnamed sediments, Polish-Lithuanian depression, U.S.S.R. (Albian-Cenomanian)
Unnamed sediments, Chelmowa Mountain, central Poland (Upper Albian-Cenomanian)
Unnamed sediments, Polish lowlands (?Barremian-Middle Albian)
Unnamed sediments, Malmö area, southern Sweden (Albian-Cenomanian)
Unnamed sediments, Kristianstad Basin, southern Sweden (Aptian-Albian)
Unnamed sediments, Båstad Basin, southern Sweden (Albian-Cenomanian)
Zirc Limestone Formation (upper member), Bakony Unit, north-west Pannonian Basin, Hungary (Upper Albian, *dispar* zone)
Pénzeskút Marl (very basal part), north-west Pannonian Basin, Hungary (upper Upper Albian)
Unnmamed sediments, Manín Unit, western Carpathians, Czechoslovakia (Upper Albian)
Baška Formation (part), western Carpathians, Czechoslovakia (Middle Albian-Lower Cenomanian)
Glauconitic Limestone, Tatra Mountains, western Carpathians, Czechoslovakia (Lower Albian - lower Upper Albian, *mammilatum-inflatum* zones)
Hluk Formation (part; minor), western Carpathians, Czechoslovakia (Barremian-Albian)
Pieninny Limestone (uppermost part), Pienniny Klippen Belt, Carpathians, Poland (?Upper Aptian-Albian)
Altenbecken Greensand, Rhenish Massif, Lower Saxony Basin, western Germany (Upper Albian)
Rüthen Greensand, Rhenish Massif, Lower Saxony Basin, western Germany (Upper Albian)
Mininimum Greensand, Lower Saxony Basin, western Germany (Albian)
Hils Clay, Lower Saxony Basin, western Germany (Albian)
Flammenmergel, Lower Saxony/Münster Basin, western Germany (uppermost Middle Albian-lower Upper Albian, *lautus* and *inflatum* zones)
Osning Greensand, Alstäatte Embayment, southwestern Lower Saxony Basin, western Germany (Middle Albian)
Unnamed sediments, Rhenish Massif, Lower Saxony Basin, western Germany (Middle Albian)
Hils Sandstone, Lower Saxony/Münster Basin, western Germany (Upper Aptian-Lower Albian, *nutfieldiensis-regularis* zones)
Rothenberg Sandstone, Lower Saxony/Münster Basin, western Germany (Upper Aptian-Lower Albian, *nutfieldiensis-regularis* zones)
Dörenther Sandstone, Lower Saxony/Münster Basin, western Germany (Aptian-Lower Albian)
Osning Sandstone, Lower Saxony/Münster Basin, western Germany (Aptian-Lower Albian)
Holland Greensand, West Netherlands Basin (Aptian/Albian, exact age uncertain)
Béton phosphaté, Albian, western Alps, France (Albian)
Unnamed sediments, Clars, Escragnolles, Basse-Provence, southeastern France (Albian)
Garschella Formation/"Gault", Helvetic Zone, Swiss Alps, western Austria (Upper Aptian-Albian)
Grès Verts, northern Pyrenees, Spain (Upper Aptian-Middle Albian)
Upper Greensand, Wessex Basin, southern England (Upper Albian)
Gaize inférieure/supérieure, northern Paris Basin (Upper Albian)
Marnes à Ostrea vesiculosa, southeastern Paris Basin (Upper Albian)
Gault/Argiles du Gault, Anglo-Paris Basin, southern England and northern France (Middle-Upper Albian)
Glauconie de base, western margin of Paris Basin (middle Albian-Lower Cenomanian)
Poudingue Ferrugineux, Normandy, northern France (Middle Albian, *dentatus*, *loricatus* zones)
Sables/Grès des Drillons, southeastern Paris Basin (Midlle Albian, basal *dentatus* zone)
Argiles tegulines, southeastern Paris Basin (Lower-Middle Albian, *mammilatum-dentatus* zones)
Sables grossiers de Liart, eastern Paris Basin, Ardennes, Belgium (Lower-Middle Albian, *mammilatum* zone)
Sables/Grès de la Puisaye, southeastern Paris Basin (Lower-Middle Albian, *mammilatum-dentatus* zones)
Meules du Hainaut (part), Bassin de Mons, Belgium (Middle Albian-Lower Cenomanian)

Sables Verts, Paris Basin (basal Lower Albian, *tardefurcata-mammilatum* ammonite zones)
Green Clays, "Gault and Greensand Equivalents", Celtic Sea Basin (Middle-Upper Albian)
Unnamed sediments, Porcupine Basin (Albian)
Unnamed sediments, Orphan Knoll, D.S.D.P. Site 111, off the Labrador coast, Canada (Albian-Cenomanian)
Kiowa Formation (part, minor), eastern margin of Cretaceous seaway, Kansas, USA (Upper Albian)
Sparky Formation, Mannville Group (minor component), Alberta/Saskatchewan, Canada (lower third of Upper Albian)
Ashville Sand, Ashville Formation, Colorado Group, Saskatchewan-Manitoba, Canada (lower Upper Albian)
Flotten Lake Sand, Colorado Group, west-central Saskatchewan, Canada (lower Upper Albian)
Skull Creek Member (lower part), Ashville Formation, Manitoba Escarpment, western Manitioba/eastern Saskatchewan, Canada (lower Upper Albian)
Swan River Formation (upper part), Greenhorn Cyclothem (Manville Group), western Manitoba-eastern Saskatchewan, Canada (upper Middle-lower Upper Albian)
Scatter Formation, Fort St. John Group, Liard River area, northeastern British Columbia, Canada (late Middle Albian)
Spinney Hill Sandstone, Joli Fou Formation, Colorado Group, western and southwestern Saskatchewan, Canada (upper Middle Albian)
Pense Formation (minor part), Manville Group, Saskatchewan, Canada (?lower/middle Middle Albian)
Bullwell Member, Scatter Formation, Fort St. John Group, Liard River area, northern British Columbia-southern North-West Territories, Canada (upper Lower Albian)
Moosebar Formation (minor, part), Fort St. John Group, northern Alberta-British Columbia, Canada (upper Lower Albian)
Bluesky Formation, Fort St. John Group, Peace River Plains, Alberta, Canada (middle Lower Albian)
Buckinghorse Formation, Fort St. John Group, British Columbia, Canada (?Upper Aptian-lower Upper Albian)
Garbutt Formation, Fort St. John Group, North-West Territories, southern interior plains, Canada (?Upper Aptian-upper Lower Albian)
Arctic Red Formation (basal part), northwestern Peel Trough, McKenzie area, North-West Territories, Canada (Lower Albian)
Aguardiente Formation, Perijá Range and Andes, western Venezuela (Albian)
Chimana Formation, Serranía del Interior, eastern Venezuela (upper Lower-lower Middle Albian, *mammilatum-dentatus* zones)
Lisure Formation, Cogollo Group, Perijá Tange and Andes, western and northwestern Venezuela (Upper Aptian-Lower Albian)

APTIAN

Windalia Radiolarite, Winning Group, Carnarvon Basin, Western Australia (Upper Aptian-Lower Albian)
Muderong Greensand Member, Muderong Shale, Winning Group, Carnarvon Basin, Western Australia (?basal middle Aptian)
Grierson Member, Birdrong Formation, Winning Group, Carnarvon Basin, Western Australia (Lower Aptian)
Parda Formation, Canning Basin, northwestern Australia (Neocomian-Aptian/Albian)
Anketell Formation, Canning Basin, northwestern Australia (Neocomian-Aptian/Albian)
Battle Camp Formation, Laura Basin, northeastern Australia (Neocomian-Aptian)
Roma Formation, Great Artesian Basin, eastern central Australia (Aptian)
Madura Formation (Madura Shale), Eucla Basin, southern Australia (Aptian-Santonian)
Lower Giumal Sandstone, Garhwal-Kumaun Himalayas, India & Tibet (Hauterivian-Lower Albian)
Belemnites Shale Formation, Parh Group, Lower Indus Basin, Pakistan (Neocomian-Albian)
Maputo Formation, southern Mozambique (Barremian-Middle Cenomanian)
Makatini Formation, Zululand Group, Zululand/Natal, South Africa (Upper Barremian-Upper Aptian)
Sundays River Formation (part), Outeniqua Basin, southern Cape, South Africa (Berriasian-Aptian)
Unnamed sediments, Kopet-Dag range, U.S.S.R. (Aptian-Cenomanian)
Unnamed sediments, Bol'shoi Balkhan area, Russian Platform, U.S.S.R. (Aptian-Albian)
Unnamed sediments, northern Caucusus, U.S.S.R. (Upper Aptian-Lower Albian)
Unnamed sediments, Polish lowlands (?Barremian-Middle Albian)

Unnamed sediments, Kristianstad Basin, southern Sweden (Aptian-Albian)
Tata Limestone, Bakony Unit, north-west Pannonian Basin, Hungary (Aptian)
Pieninny Limestone (uppermost part), Pieninny Klippen Belt, Carpathians, Poland (?Upper Aptian-Albian)
Hluk Formation (part; minor), western Carpathians, Czechoslovakia (Barremian-Albian)
Hils Sandstone, Lower Saxony/Münster Basin, western Germany (Upper Aptian-Lower Albian, *nutfieldiensis-regularis* zones)
Rothenberg Sandstone, Lower Saxony/Münster Basin, western Germany (Upper Aptian-Lower Albian, *nutfieldiensis-regularis* zones)
Dörenther Sandstone, Lower Saxony/Münster Basin, western Germany (Aptian-Lower Albian)
Osning Sandstone, Lower Saxony/Münster Basin, western Germany (Aptian-Lower Albian)
Holland Greensand, West Netherlands Basin (Aptian/Albian, exact age uncertain)
Garschella Formation/"Gault", Helvetic Zone, Swiss Alps, western Austria (Upper Aptian-Albian)
Grès Verts, northern Pyrenees, Spain (Upper Aptian-Middle Albian)
Calcaires gréso-glauconieux, Helvetic Zone, Swiss Alps (Aptian)
Bois des Loges, Ardennes, Belgium (Upper Aptian)
Formation de Wissant, Boulonnais, northern France (Upper Aptian, summit of the *jacobi* zone)
Sables Ferrugineux, Normandy, northern France (Upper Aptian, *jacobi* zone)
Argilles Noires à Bucaillela, Normandy, northern France (Upper Aptian, *jacobi* zone)
Formation de Verlincthun, Boulonnais, northern France (and Argiles à Ostrea leymeriei) (Upper Aptian, *nutfieldiensis*-basal *jacobi* zones)
Formation du Cat Cornu, Boulonnais, Paris Basin (Lower Aptian, summit of *deshayesi-bowerbanki* zones)
Folkstone Beds, Lower Greensand Group, Wessex Basin, southern England (Upper Aptian, *jacobi-tardefurcata* zones)
Sandgate Beds, Lower Greensand Group, Wessex Basin, southern England (Upper Aptian, *martinoides-nutfiediensis* zones)
Hythe Beds, Lower Greensand Group, Wessex Basin, southern England (Lower Aptian, *dehayesi-bowerbanki* zones)
Ferruginous Sands, Lower Greensand Group, Isle of Wight, Wessex Basin, southern England (Aptian, *deshayesi-nutfieldiensis* zones)
Buckinghorse Formation, Fort St. John Group, Muskwa-Tetsa River area, British Columbia, Canada (?Upper Aptian-lower Upper Albian)
Garbutt Formation, Fort St. John Group, Liard River area, North-West Territories, Canada (?Upper Aptian-upper Lower Albian)
Martin House Formation, North-West Territories, Canada (Upper Aptian)
Lisure Formation, Cogollo Group, Perijá Tange and Andes, western and northwestern Venezuela (Upper Aptian-Lower Albian)
Valle Grande Formation, eastern Venezuela (Upper Aptian, *martini-subnodosocostatum* zones)

BARREMIAN

Parda Formation, Canning Basin, northwestern Australia (Neocomian-Aptian/Albian)
Anketell Formation, Canning Basin, northwestern Australia (Neocomian-Aptian/Albian)
Battle Camp Formation, Laura Basin, northeastern Australia (Neocomian-Aptian)
Lower Giumal Sandstone, Garhwal-Kumaun Himalayas, India & Tibet (Hauterivian-Lower Albian)
Belemnites Shale Formation, Parh Group, Lower Indus Basin, Pakistan (Neocomian-Albian)
Maputo Formation, southern Mozambique (Barremian-Middle Cenomanian)
Makatini Formation, Zululand Group, Zululand/Natal, South Africa (Upper Barremian-Upper Aptian)
Sundays River Formation (part), Outeniqua Basin, southern Cape, South Africa (Berriasian-Aptian)
Unnamed sediments, Polish lowlands (?Barremian-Middle Albian)
Unnamed sediments, Kristianstad Basin, southern Sweden (Upper Baremian)
Hluk Formation (part; minor), western Carpathians, Czechoslovakia (Barremian-Albian)
Altman Beds, Helvetic Zone, Swiss Alps (Barremian)

HAUTERIVIAN

Jowlaenga Formation, Canning Basin, northwestern Australia (?uppermost Jurassic-Neocomian)
Parda Formation, Canning Basin, northwestern Australia (Neocomian-Aptian/Albian)
Anketell Formation, Canning Basin, northwestern Australia (Neocomian-Aptian/Albian)
Battle Camp Formation, Laura Basin, northeastern Australia (Neocomian-Aptian)
Sundays River Formation (part), Outeniqua Basin, southern Cape, South Africa (Berriasian-Aptian)
Brenton Formation (Brenton Beds, Infanta Formation), Knysna Basin, southern Cape, South Africa (?Upper Valanginian-Hauterivian)
Lower Giumal Sandstone, Garhwal-Kumaun Himalayas, India & Tibet (Hauterivian-Lower Albian)
Belemnites Shale Formation, Parh Group, Lower Indus Basin, Pakistan (Neocomian-Albian)
Unnamed sediments, Polish lowlands (upper Upper Hauterivian)
Gemsmätti Beds, Helvetic Zone, Swiss Alps (Hauterivian)
Lidernen Beds, Kieselkalk Formation, Helvetic Zone, Swiss Alps (Hauterivian)
Pierre jaune de Neuchâtel (low concentration), Swiss Jura (middle Hauterivian)
Marnes bleues d'Hauterive (low concentration), Swiss Jura (Lower Hauterivian)
Pierre de Foucherès (Calcaires à Spatangues), Paris Basin (Hauterivian)

VALANGINIAN

Jowlaenga Formation, Canning Basin, northwestern Australia (?uppermost Jurassic-Neocomian)
Parda Formation, Canning Basin, northwestern Australia (Neocomian-Aptian/Albian)
Anketell Formation, Canning Basin, northwestern Australia (Neocomian-Aptian/Albian)
Battle Camp Formation, Laura Basin, northeastern Australia (Neocomian-Aptian)
Belemnites Shale Formation, Parh Group, Lower Indus Basin, Pakistan (Neocomian-Albian)
Sundays River Formation (part), Outeniqua Basin, southern Cape, South Africa (Berriasian-Aptian)
Brenton Formation (Brenton Beds, Infanta Formation), Knysna Basin, southern Cape, South Africa (?Upper Valanginian-Hauterivian)
Unnamed sediments, Lena-Khatanga depression, northwards of pre-Verthoyansk depression, U.S.S.R. (Rhyazanian-Lower Valanginian)
Unnamed sediments, eastern flanks of the Urals, U.S.S.R. (Berriasian-Valanginian)

RYAZANIAN

Jowlaenga Formation, Canning Basin, northwestern Australia (?uppermost Jurassic-Neocomian)
Parda Formation, Canning Basin, northwestern Australia (Neocomian-Aptian/Albian)
Anketell Formation, Canning Basin, northwestern Australia (Neocomian-Aptian/Albian)
Battle Camp Formation, Laura Basin, northeastern Australia (Neocomian-Aptian)
Belemnites Shale Formation, Parh Group, Lower Indus Basin, Pakistan (Neocomian-Albian)
Sundays River Formation (part), Outeniqua Basin, southern Cape, South Africa (Berriasian-Aptian)
Unnamed sediments, Lena-Khatanga depression, northwards of pre-Verthoyansk depression, U.S.S.R. (Ryazanian-Lower Valanginian)
Unnamed sediments, eastern flanks of the Urals, U.S.S.R. (Berriasian-Valanginian)
Spilsby Sandstone (part), eastern England (Ryazanian)
Sandringham Sands (part), eastern England (Middle Volgian-Ryazanian)

6.2 Cretaceous Greensand Provinces

Evaluation of the spatial and temporal distribution of Cretaceous glauconitic sediments has shown that on a world-wide scale, the facies type tends to be associated with specific regions. A short synthesis of each of these, concentrating on areas outside the Anglo-Paris Basin, is presented in order to show greensand depositional settings and a develop a broad picture of the complete facies associations.

6.2.1 Eastern England

Upper Jurassic to Ryazanian greensands are developed in Norfolk, Lincolnshire, and adjacent offshore areas of the North Sea. The Upper Jurassic Kimmeridge Clay Formation is overlain by thin glauconitic and phosphatic sandstones of the Spilsby Sandstone (in Lincolnshire), and the Sandringham Sands (in Norfolk) (Casey 1972; Anderton *et al.* 1983). The Spilsby Sandstone (Ryazanian) consists of beds of grey sandstone with phosphate nodules, overlain by coarse pebbly, glauconitic sands with calcareous concretions. These are overlain by the Middle Spilsby nodule bed, comprising several generations of phosphate nodules and small chert pebbles; it is overlain by pale fine- to medium-grained sands which are coarser and greener in colour in the basal part. Overlying this is the Ferruginous Grit, a coarse-grained, grey or brown pebbly sandstone, with some ferruginous ooids. The Sandringham Sands are strongly condensed nearshore sands, deposited on the northern margin of the London Platform. They are of latest Jurassic and early Cretaceous age, and contain around 2m of green glauconite-rich, phosphate-bearing clayey sands, the Runcton Beds (Upper Volgian), and up to 15m of glauconitic, clayey sand with ironstone horizons and thin seams of phosphate nodules, the Mintlyn Beds (Ryazanian).

6.2.2 Wessex Basin, southern England

The Lower Greensand of the Wessex Basin of southern England comprises a complex series of shallow marine sediments, various lithofacies of which are glauconitic. In the Isle of Wight,

the Lower Greensand is around 250m in thickness, and is subdivided into the Atherfield Clay, Ferruginous Sands, Sandrock and Carstone Formations (Anderton *et al.* 1983). The Ferruginous Sands (80m) (upper Lower Aptian to middle/upper Upper Aptian) consist of muddy sands with abundant glauconite, commonly altered to limonite. Glauconite is present in smaller quantities in the overlying Sandrock (56m) (upper Upper Aptian to lower Lower Albian) and Carstone (4m) (upper Lower Albian) Formations. To the east, in the Weald, the Lower Greensand consists of a basal marine mudstone; overlying this are glauconitic sands and limestones of the Hythe Beds (20-90m) (upper Lower Aptian). The overlying Sandgate Beds Formation (1-45m) (lower and middle Upper Aptian) is very variable in lithology, containing muddy glauconitic sands and cross-stratified sands.

The Upper Greensand and Gault Formations (Middle-Upper Albian) are a more geographically-widespread facies, representing an overall transgressive sequence across the Wessex Basin. In the deeper parts of the basin, the formations conformably overlie the Lower Greensand; on the basin margins, they transgress across Mesozoic sediments to rest on Palaeozoic strata. The Lower Gault is mainly of Middle Albian age; the Upper Gault and Upper Greensand are Upper Albian. The formations consist principally of grey clays and silty marls with phosphate nodule horizons, glauconitic clays, marls and silts with scattered phosphate nodules, fine-grained glauconitic sands, and variably glauconitic cherty limestones with hardgrounds and intraformational pebble beds. The thickness of the two formations is typically of the order of 50-80m.

The Glauconitic Marl represents the basal bed of the Chalk across much of the Wessex Basin, separating clastic Albian clays and greensands from the pelagic Cenomanian chalks above (Kennedy & Garrison 1975b); it represents a strongly-condensed deposit, formed during late Cretaceous transgression. It typically consists of a thin (0.3-4.8m), strongly condensed glauconitic marl or marly greensand (may be up to 80% glauconite), rich in brown phosphate nodules, and usually strongly-bioturbated and unbedded. The base of the bed may consist of a level of bored, encrusted and phosphatised calcareous concretions (e.g. in the Isle of Wight). The age of the Glauconitic Marl is diachronous, ranging from Lower to Middle Cenomanian

age when traced southwestwards into eastern Dorset; it passes into a diachronous sandy limestone called the Chalk Basement Bed.

6.2.3 Celtic Sea and Porcupine Basins

Glauconitic claystones of Albian age have been reported from the Kinsdale Head Gas field, north Celtic Sea Basin (Colley *et al.* 1981). Overlying the Wealden is a sequence of sands and clays containing three highly glauconitic claystones in a sequence of well-sorted, fine-grained glauconitic claystones, shallow marine sands, fine-grained glauconitic sandstones and bioturbated, fossiliferous claystones. An Albian glauconitic facies (glauconitic siltstones, glauconitic sandstones, and associated limestones) has also been reported from the north Celtic Sea and Fastnet Basins, south of Ireland (Ainsworth *et al.* 1987).

An Albian glauconitic facies has been reported from the Porcupine Basin, to the west of Ireland (MacDonald *et al.* 1987; Croker & Shannon 1987). During the Albian, there was a marked change in sedimentation, with deposition of a blanket deposit of 200m of marine, glauconitic, calcareous sandstones and thin limestones. Croker & Shannon (1987) note the beginning of a marine transgression in Albian times, with a series of offshore-bar glauconitic sandstones rimming the basin during the onset of the transgression.

6.2.4 Northern Ireland and north-west Scotland

In Northern Ireland (south-east and north-east Antrim, and County Derry), Cretaceous glauconitic sediments are preserved below Tertiary basalts. They have been documented by Hancock (1961) and Wilson (1981). The Cretaceous rocks of Antrim range from Cenomanian to Maastrichtian age, but the succession is not uniform, and there are numerous hiatuses. The Cretaceous deposits have been subdivided into the Hibernian Greensand Formation (glauconitic siliciclastics), and the White Limestone Formation (chalk with flint). The Hibernian Greensand Formation consists of a lower unit of Cenomanian-Lower Turonian sediments (the Glauconite Sands, Yellow Sandstones and Grey Marls, Glauconitic Sand and Sandstone, and Quartzose Sands) and an upper unit of Coniacian-Lower Santonian sediments (the Senonian Greensands).

The lower, mainly Cenomanian sediments represent a trangressive sequence, resting unconformably on older rocks; the Glauconite Sands overstep onto pre-Liassic formations. The Glauconite Sands consist of dark green, unbedded glauconitic sands (glauconite never <50%, and usually considerably higher), with a dark grey muddy matrix, including accessory quartz, authigenic pyrite and scattered black phosphatic nodules. The fauna includes *Exogyra obliquata* (common), thin-shelled bivalves, ammonites, belemnites and rare brachiopods. Wood fragments have been recorded, and Cenomanian foraminifera reported. The overlying Yellow Sandstones and Grey Marls consist of a largely calcareous group of argillaceous sandstones and mudstones, with localised calcareous, and occasional cherty concretions. The fauna contains poorly-preserved echinoids and small bivalves. There is a sharp disconformity, followed by the Glauconitic Sand and Sandstones; these consist of quartzose sandstones with abundant glauconite. They contain common *Exogyra columba.* Across the region, the Cenomanian beds are only preserved in restricted areas, reaching a maximum of about 22m in thickness. They are separated from the Senonian Greensands above by a major break in deposition. Renewed transgression occurred in the Coniacian, with the result that the Senonian Greensands and White Limestone onlap across the Cenomanian-Lower Turonian sediments, transgressing onto the Dalradian basement of the Highland Border Ridge. The Senonian Greensands succession (0.75-9.5m) begins with soft, unbedded glauconitic sands containing horizons of *Inoceramus* fragments and some reworked Cenomanian greensand material. Above the greensand is a glauconitic limestone, with abundant hexactinellid sponges, the Cloghfin Sponge Beds. Due to the rarity of ammonites, the Cretaceous sediments have been dated using echinoids and belemnites. Overlying the Senonian Greensands is the White Limestone, consisting of chalk with flint, with glauconitic beds at the base.

Thin outliers of marine Upper Cretaceous sediments occur throughout western Scotland, representing mere remnants of an originally much more widespread Mesozoic cover, now largely removed by Tertiary and Quaternary erosion (Hallam 1983). The Cretaceous beds rest on an eroded surface of Jurassic and Triassic rocks; occasional glauconitic sediments are preserved. In Mull and Morvern, around 13m of Cenomanian glauconitic sandstone is present.

It is overlain by the pure White Sandstone, a few cm of clay, and a thin bed of Senonian silicified chalk. In addition, small patches of Upper Cretaceous sandstone and sandy limestone, of probable Cenomanian age, are found in Skye, Raasay, and Eigg. On Eigg, the Laig Gorge Beds (5.1m in thickness; Upper Cretaceous) (Hudson 1960) consist of coarse calcareous sandstone resting on the Middle Jurassic Great Estuarine Series. A basal conglomerate is developed, containing phosphatic pebbles, glauconite, and vein quartz), nodular calcareous sandstone, and fine-grained bioclastic limestone (the Laig Gorge Sandstone). At Clach Alastair, the Glauconitic Sandstone, probably of Cenomanian age, rests on Oxfordian shales.

Cretaceous glauconitic sediments have also been recorded from the Faroe Basin to the north-west of the Shetland Islands, in a series of offshore wells (Mudge & Rashid 1987; Meadows *et al.* 1987). In a number of wells, an arenaceous unit of Cenomanian-Turonian age rests on Albian beds, and consists of basal limestones with occasional thin glauconitic sandstones, which pass up into calcareous sandstones.

In the Solan Basin, south-west of the Shetlands, early Cretaceous intervals are typified by argillaceous lime mudstones containing abundant siliceous sponge spicules, planktonic foraminifera and disarticulated bivalve fragments. The sediments contain siderite, phosphate, and glauconite, also early diagenetic calcareous and siliceous nodules. Evidence for storm influence is shown by occasional thin interbedded sandstones with bioturbated tops. This lime mudstone facies appears to have been dominant throughout the Solan Basin during the early Cretaceous (Meadows *et al.* 1987).

6.2.5 Paris Basin

In the Paris Basin, glauconitic sediments of Upper Aptian age are widely developed (Mégnien 1980). In the Boulonnais, northern France, the Formation du Cat Cornu (upper Lower Aptian) consists of 11m of glauconitic sandstones, passing laterally into a thin phosphatic layer. They contain a fossil assemblage of ammonites, bivalves, brachiopods and echinoids. These sediments are the oldest representative of the Cretaceous transgression in the Boulonnais, resting on Wealden strata. The Formation de Verlincthun (Upper Aptian) (0.12-8m) consists of green

glauconitic sands, passing up into white sands towards the top. Various laterally-equivalent muddy greensands and ferruginous gravels are rich in oysters. The Formation de Wissant (Upper Aptian) (up to 3m) consists of muddy glauconitic sands with small black phosphatic nodules; these sediments represent the deposits of a third Cretaceous transgression across the area; they contain a fauna of ammonites, bivalves, brachiopods, and echinoids.

Upper Aptian glauconitic sediments are also developed in Normandy. The Sables Ferrugineux (Upper Aptian) (10-25m) consist of dark-grey sands weathering to a yellowish colour; they are argillaceous and glauconitic, with several coarse, gravel interbeds. The formation rests unconformably on Kimmeridgian strata.. The (Minerai de) Bois des Loges (Upper Aptian) are developed in the Ardennes (Belgium), and consists of 1-3m of interbedded muddy, glauconitic sand and green sandy muds. The unit contains an abundant macrofauna. The Sables et grès jaunâtres (Upper Aptian) (5-20m) are developed in the Haute-Marne area. Overlying a basal erosion surface cut into the top of the Argiles à plicatules du Bèdoulien is a lag deposit containing phosphate nodules in a glauconitic (up to c.30%), muddy sand matrix with abundant pyrite. These pass up into soft, white or yellowish sands and white or greyish sands, very rich in glauconite, with several lenses of carbonate-cemented sandstone rich in organic matter.

Upper Albian glauconitic sediments are developed in northern France in the Normandy area, with facies types similar to those in southern England (Chapter 2). The Gaize (Inférieur and Supérieur) contains glauconitic lithologies, and the Glauconie de base represents a thin glauconitic sequence developed on the eastern edge of the Armorican Massif. Regions of glauconite deposition in the overlying Upper Cretaceous chalks have been shown on the facies maps of Mégnien (1980), developing over submarine highs and on the northeastern margin of the basin. In the areas of Perche and Maine on the western side of the basin, Cenomanian glauconitic sands and glauconitic chalks and marls also developed, and glauconitic sands are found in the southern parts of the basin in the Cher region (Berry-Sancerrois).

6.2.6 West Netherlands Basin

A Cretaceous glauconitic facies is developed in the Rijswijk Oil Province of the West Netherlands Basin. This depocentre developed between the London-Brabant massif to the south, and the narrow Zandvoort Ridge to the north (Bodenhausen & Ott 1981). The Holland Greensand and the Upper Holland Marls were deposited during the Aptian-Albian transgression. The Texel Greensand developed during the lowermost Cenomanian. The basin margins were progressively onlapped by transgressions during the Cretaceous; the Zandvoort Ridge was eventually submerged in Cenomanian times. Late Cenomanian to Danian strata consist of chalk/marl facies.

6.2.7 Germany

In western Germany, Cretaceous glauconitic sediments are developed on the southern side of the Lower Saxony/Münster Basin and on the northern side of and transgressive over parts of the Rhenish/Rhenian Massif (Kemper 1972; Kemper & Zimmerle 1983). Glauconite is absent or rare in the Berriasian-Barremian sediments, but a glauconite-siderite-phosphate facies is an important element of the Aptian and Albian sediments on the southern side of the basin, and a sponge-glauconite facies is developed throughout almost the whole of the Albian. Pale marls, characterised by rich benthic faunas, were deposited in the central parts of the basin, in the shallow areas of the northern part of the basin, and on the progressively-submerging Pomeckj's Swell. Also, dark sediments are developed, with either no benthic fauna or an impoverished fauna. Kemper & Zimmerle (1983) subdivided the Aptian and Albian sediments of the Lower Saxony Basin into 3 facies belts: Belt 1: a southern belt marginal to the source area, the Rhenish Massif, Belt 2: a middle belt to the north, and Belt 3: a northern belt in the deeper parts of the basin.

In the Aptian, Belt 1 is characterised by dark-coloured clays and muddy silts, with interbedded muddy glauconitic sandstones/greensands. Phosphorite concretions are found at several horizons, and in the west, siderite-cemented beds occur. Microfaunas are diverse, and include radiolarians. Belt 2 is mainly characterised by dark-coloured clays, with slightly higher

orgC contents than in Belt 1. The microfauna is of low diversity and includes siliceous diatoms and radiolarians. Belt 3 contains lower Upper Aptian light-coloured marls, and upper Upper Aptian dark-coloured clays with moderate orgC contents and numerous phosphate and siderite-phosphate concretions; glauconite is rare.

In the Albian, Belt 1 is again characterised by greensands and glauconitic clays, with siliceous sponge spicules and radiolarians. Belt 2 consists of marls and the Flammenmergel (see below). Siliceous sponge spicules are commonly associated with radiolarians and diatoms. These contain low-diversity benthic communities, but abundant siliceous sponge remains suggest only minor oxygen depletion. Belt 3 comprises bioturbated, light grey marls with common phosphate nodules. The microfaunas are rich and diverse. Muddy glauconitic sediments, with incomplete and partly-condensed sequences (highest Lower Albian-Middle Albian age) are typical of the transgressive Middle Albian, and cover the northern part of the Rhenish Massif.

The benthic fauna of the dark mudstones of the highest Upper Aptian consist predominantly of arenaceous foraminifera adapted to a poorly-oxygenated environment; the ostracod fauna also supports this interpretation. In the Lower Albian, dark sediments were deposited over large areas of the basin, with various sandy and glauconitic sediments being deposited along the southern margin. Middle Albian sediments generally have higher carbonate contents and a much richer benthic fauna than the Lower Albian sediments. Upper Albian sediments of the south and south-east were deposited in an open-marine environment (Flammenmergel).

Aptian and Albian glauconitic sediments include the: Hils Sandstone (glauconitic, with sponge spicules) (Upper Aptian-Lower Albian); Rothenberg Sandstone (glauconitic-sideritic) (Upper Aptian-Lower Albian); Dörenther Sandstone (Aptian-Lower Albian); Osning Sandstone (Aptian to Lower Albian); Osning Greensand (alternating muddy greensands and glauconitic sandy shales and mudstones) (Middle Albian) (developed in the south-west, in the Alstätte Embayment); Altenbecken Greensand (Upper Albian) (Rhenish Massif); Rüthen Greensand (Upper Albian) (Rhenish Massif); Minimum Greensand (Albian); Hils Clay (glauconitic clay) (Albian); Flammenmergel (a strongly-bioturbated, glauconitic, pyritic, siliceous marl) (uppermost

Middle Albian-lower Upper Albian). The thickness of Aptian strata varies from a few metres at the margins of the basin, to 200-300m in the central parts of the basin and in troughs in front of the Rhenish Massif. The thickness of the Lower Albian is up to 200m, the Middle Albian is thin, generally less than 50m, and the Upper Albian up to 300m. The thicknesses are lower at the margins of the basin.

Kemper & Zimmerle (1983) have interpreted this particular Aptian and Albian facies association as the product of a boreal upwelling system, directed from north to south, which was associated with a late Aptian cooling, causing the influx of cooler Arctic waters from the north.

Around Essen in western Germany, the basal Cretaceous is prominently transgressive, and consists of pockets of sediment resting in hollows about 0.5m deep in the underlying Carboniferous. These have been named "Klippenfacies"; Hancock *et al.* (1972) have described ammonites from the basal part of the succession at the Rauen quarry, Mülheim-Broich, near Essen. At this locality, the Klippenfacies consists of a conglomeratic sandy limestone, overlain by 0.15-3m of chalky marl of basal Cenomanian age. The Middle and Upper Cenomanian are missing, as may be the case over most of the region; on the western side of the quarry, the Turonian Bochumer Greensand rests directly on Carboniferous. In the Becker Quarry, 0.5km to the west, the Klippenfacies is not developed, but beneath the glauconitic marl is the "Glauconitische Schammergel", a greensand composed of glauconite in a clay matrix, which has often been called the Essen Greensand (Hancock *et al.* 1972).

In eastern Germany, a glauconitic facies marks the basal deposits of the Albian transgression onto older basement, with the development of a basal conglomerate with phosphorite concretions and greensands; this passes up into clays and marls. Similarly, where the Cenomanian transgresses directly onto older basement, a basal conglomerate with phosphorite concretions, passing up into greensands is developed; these are overlain by marls, marly limestones and limestones (Tröger 1981).

6.2.8 Denmark and southern Sweden

Glauconitic sediments are developed in the Cretaceous succession of Bornholm, Denmark and of southern Sweden. During the Mesozoic, these areas formed part of the stable Fennoscandian shield area (in the north), the subsiding Danish Basin (in the south; Malmö area), and the block-faulted, north-west - south-east -trending Fennoscandian border zone (a transition zone between the two). Over the shield area, the sediments are composed of calcarenites and quartz sands (<200m); in the border zone, glauconitic sandstones and siltstones are predominant (around 800m); and in the Danish Basin, limestones (including chalk), with localised glauconitic sandstones and siltstones are the dominant sediments (about 1600-1700m). This summary is based principally on the work of Bromley (1979), Kennedy *et al.* (1981) and Christensen (1984).

The island of Bornholm represents a horst in the Fennoscandian Border Zone. The Cretaceous formations comprise the Arnager Greensand, the Arnager Limestone, and the Bavnødde Greensand. The Arnager Greensand is a poorly-sorted and richly-glauconitic quartz sand around 85m in thickness, which rests with slight unconformity on the lagoonal-lacustrine Jydegaard Formation (Berriasian-Valanginian). The contact is marked by *Thalassinoides* burrowing, with resultant sediment mixing, and introduction of greensand for over one metre into the underlying sediment. The basal bed of the formation is a 30cm-thick glauconitic quartz sand, rich in shark teeth, and is succeeded by a conglomerate horizon (0.18-0.55m thick), consisting of complexly-phosphatised pebbles and cobbles (hiatus concretions), with Lower Cambrian sandstone and quartzite and Jurassic or early Cretaceous lignite also reported. Two generations of phosphate nodules have been recognised: primary nodules consisting mainly of glauconitized sandstone, and secondary nodules built up of primary nodules cemented together by phosphatised glauconitic sand. The nodules often bear an encrusting fauna. The greensand above the conglomerate is unconsolidated, except for a few thin horizons in the lower part; it is strongly-bioturbated and contains scattered phosphatised pebbles. The phosphatic conglomerate represents three time intervals: primary nodules yield Lower Albian ammonites; secondary nodules yield Lower Cenomanian ammonites; and the greensand itself, *sensu stricto*, is of low

Middle Cenomanian age), based on ammonites and planktonic foraminifera (Kennedy *et al.* 1981; M. B. Hart 1979). M. B. Hart (1979) considers that the benthic foraminifera in the basal 5m of the greensand are of early Cenomanian age, while the main thickness is of early Middle Cenomanian age. There is a major hiatus between the Arnager Greensand and the Arnager Limestone coinciding with a major Turonian regression.

The Arnager Limestone (12-20m thick) overlies the Arnager Greensand. The junction with the underlying formation is complex, with compound phosphatised hiatus concretions which have undergone repeated episodes of sedimentation, cementation, erosion, and phosphatisation (Bromley 1979). The limestone consists of a white calcilutite, containing both clay and fine-grained sand. Its fauna is dominated by siliceous sponges, with common bivalves. Both unlined *Thalassinoides* burrows and spicule-lined burrows are present. The age of the limestone has been disputed, but Christensen (1984) considers it to be of Coniacian age.

The Bavnødde Greensand (Upper Coniacian-Lower/Middle Santonian) rests upon the Arnager Limestone, without any phosphatic nodule or conglomerate development. It consists of a glauconitic, fine-grained, poorly-sorted, silty sand (around 180m thick), strongly-bioturbated, with *Thalassinoides* burrows. The greensand is mostly poorly-cemented, but contains several thin horizons with phosphatic clasts, which are irregularly-cemented by both calcite and quartz, and apparently concordant with bedding (Bromley 1979).

In southern Sweden, Cretaceous glauconitic sediments have also been recorded; their distribution and age have been summarised by Christensen (1984). The Kristianstad Basin contains around 200m of Cretaceous marine sediments; these are bounded to the south-west by prominent horst structures, and limited to the north and west by thinning and Tertiary/Quaternary erosion. The sediments consist predominantly of carbonates (skeletal calcirudites, calcarenites and calcisiltites), with sporadic glauconitic sands. Calcareous glauconitic sands of Barremian, Aptian-Albian and Cenomanian age have been recorded from the Härlöv (Kristianstad U1B) borehole. In the Åhus borehole, 25m of Santonian age glauconitic sand were recorded (Bergström *et al.* 1973). The Båstad Basin also contains Cretaceous sediments, limited to the south-west by a horst, and to the east by thinning and later erosion. Albian-Cenomanian

glauconitic sand and limestone have been recorded. In the Vomb Trough, a long, narrow Mesozoic graben within the Fennoscandian border zone, Cretaceous sediments are known from several outcrops and five deep boreholes (785m thick). The sediments recorded in the borings consist of glauconitic, calcareous and clayey siltstones. Calcareous sandstones and conglomerates are present at outcrop. In the Malmö area of the Danish Basin, the Cretaceous sediments consist predominantly of limestones, including chalk and marly chalk; these are about 1640m in thickness. In the Höllviken borings, about 60m of Albian-Cenomanian glauconitic calcareous sandstone has been recorded; these rest on Aptian shales, and are overlain by Turonian-Maastrichtian limestone and Upper Maastrichtian chalk. Near to the Romeleåsen Fault, borings have penetrated Albian-Cenomanian glauconitic sandstones, Coniacian-early Santonian glauconitic clayey siltstones (Eriksdal Marl), and Santonian-Campanian glauconitic sandstones (Lund Sandstone).

6.2.9 Polish Lowlands

A widespread Cretaceous glauconitic facies is developed in Poland (Marek & Raczyńska 1972). In the Polish Lowlands, Berriasian brackish-marine deposits with minor occurrences of glauconite are succeeded by fully marine Upper Hauterivian glauconitic sandstones and clays. Above this is a (?Barremian-?Middle Albian) conglomeratic-based sandy glauconitic series marking a further transgressive cycle.

Higher up in the sequence, marine transgression, with a transition from fluvial-lacustrine to marine sedimentation, occurred in the Middle Albian. The marine Middle Albian consists of glauconitic sands with basal conglomerates. In the upper part of the Middle Albian, phosphorites formed in many regions; these are especially well-developed in the northern Holy Cross Mountains. In the Upper Albian, deepening resulted in marly sedimentation in the central parts of the basin, with typical "gaize" facies and "spongolites" developed in the Holy Cross Mountains area. Transgression reached maximum during the early Upper Albian; above this, relative regression resulted in a facies change from carbonates to sandstones. Renewed transgression in the Cenomanian resulted in predominantly marly facies, with nearshore

glauconitic sands, conglomerates and clays passing into offshore glauconitic marls developed in the Miechów synclinorium and Pomerania regions, interpreted as deltaic facies in the latter area. The Albian and Cenomanian succession ranges from a few metres to over 350m in thickness.

6.2.10 Russian Platform

During the mid-Cretaceous, transgression resulted in submergence of the southern parts of the Russian platform; glauconitic sediments of Aptian-Cenomanian age developed widely across this area. In the Bol'shoi Balkhan area, 200-300m of Aptian greenish glauconitic sandstones with beds of clay and marls are developed; these are overlain by 300-450m of Albian sandstones, which are sometimes glauconitic, with occasional beds of clay (Nalivikin 1973). In the Baltic region of the Russian platform, transgression occurred in the Upper Albian. A borehole at Sovyelsk, Lithuania, in the Polish-Lithuanian depression, penetrated 18m of Albian glauconitic sandstones with a basal bed of phosphatic pebbles and black shale beds. Overlying these, 16m of Cenomanian glauconitic sandstones with clay laminae and a phosphatic horizon are developed. Across the platform, the Cenomanian is marked by the development of a vast distribution of sandy facies, including quartz sands with glauconite and phosphorites (Nalivikin 1973). Around 4-48m of Cenomanian glauconitic sands have been reported from locations around the Ukraine (Chernigov, Smeloye, Romny, Kupyansk). Albian and Cenomanian glauconitic sands with beds of phosphorite and clays are also developed to the south of the region, around Kaliningrad, Polessk, Lidsbark and Lublin. Upper Albian or Cenomanian quartz-glauconitic sandstones have been recorded from the Pripet depression (to the north of the Ukraine) (Nalivikin 1973). Upper Aptian, Lower Albian and Cenomanian glauconitic sediments have been recorded from the Kislovodsk and Daghestan regions of the northern Caucasus (Nalivikin 1973; Naidin 1981). The Upper Aptian consists of 12-160m of calcareous glauconitic sandstones with occasional beds of black clay and the Lower Albian is represented by 30-235m of glauconitic sandstones, becoming a coarser cross-bedded facies in the upper part. The Cenomanian of Daghestan comprises 1.5-100m of glauconitic sandy limestones and limestones

and marls. Lower Cenomanian sandy marls and limestones of the Crimea commonly have a basal quartz glauconitic sandstone, which transgressively overlies Middle Jurassic to Albian beds. In the Tuar-Kyr range (east of the Caspian Sea), 50-100m of greenish, glauconitic sandstones with phosphorites are developed (Nalivikin 1973). In the Kopet-Dag range (south-east of the Caspian), Aptian-Cenomanian glauconitic facies are developed; these comprise 500-900m of Aptian greenish-grey glauconite-quartz sandstones, 600-100m of Albian glauconite-quartz sandstones, sandy clays and clays, and 170-350m of Cenomanian glauconitic sandstones and siltstones overlying black clays with beds of sandstone and limestone (Nalivikin 1973).

The Turonian and Coniacian deposits of the Russian Platform are characterised by deposition of chalk, chalky limestones, and marls (Naidin 1981). In the Santonian, widespread glauconitic sands and gaizes (60-90m thick) developed on the western slopes of the Arctic Urals, Usa Basin. These represent the deposits of a major transgression which advanced from the south (Nalivikin 1973).

In the Campanian, glauconitic sediments have been recorded from a borehole at Sovyelsk, Lithuania, in the Polish-Lithuanian depression; this penetrated 22m of glauconitic sandstones with beds of marl. Campanian glauconitic sandstones, gaizes and black clays with belemnites are also developed in the Kamyshin area of the Russian Platform (north-west of the Caspian) (Nalivikin 1973).

6.2.11 Bohemian Massif

The Bohemian Massif occupies the western half of Czechoslovakia and adjacent parts of Austria, Poland and Germany. The Bohemian Cretaceous Basin covers a considerable part of the area; Lower Cretaceous deposits are absent, whereas the Upper Cretaceous sediments are transgressive across the Massif (Svoboda *et al.* 1966). In the Upper Cenomanian, transgression of the north Bohemian sea occurred, perhaps related to subsidence associated with the Alpine-Carpathian orogenic phase. The sea transgressed from the north-east, probably through the Intra-Sudetic depression and the present-day Orlické hory Mountains region, to produce a 300km long and 100km wide, elongate (north-west - south-east) basin. In parts of the basin,

Cenomanian lacustrine sediments pass up into marine deposits; in others, marine sediments rest unconformably on older rocks.

The Upper Cretaceous deposits reach up 600-700m in thickness; they consist of Cenomanian-Lower Santonian shallow water sandstones, marls, sandy marls and marly clays. The Lower-Middle Cenomanian deposits represent a fluvio-lacustrine fresh-water facies. The Upper Cenomanian is brackish and marine, and consists mainly of sandstones, with some shallow-water pebbly conglomerates and sandy limestones. Two units can usually be distinguished: a basal division of sandstones of varying grain size, with or without glauconite, and an upper division of fine to medium-grained sandstones, often with considerable amounts of glauconite. The sandy conglomerates, calcareous sandstones, and sandy limestones developed as a near-shore facies, adjacent to islands and on shallow banks; *Exogyra*, pachydonts, gastropods and corals have been recorded from the limestones. The thickness of the marine Cenomanian deposits is commonly around 20-30m, occasionally reaching up to 70-80m. The Lower Turonian sediments (40-70m thick) consist of quartz sandstones, a marly facies in the central part of the basin, and spongolitic deposits; these are generally glauconitic. The transitional Cenomanian-Lower Turonian succession at the base of the unit is usually developed in the marly facies. Middle Turonian sediments (60-300m) are represented by various lithologies. In the north, up to 250m of quartz sandstones, with marly and glauconitic sandstone at the base, are developed; to the south, there are sandstones with intercalated marly sands. Further south, there are Middle Turonian silty marls and occasional marly sandstones. In the Orlice region, glauconitic and spongolitic fine-grained calcareous sandstones are developed. The basal Upper Turonian is marked by abundant glauconite and phosphates, or by clayey sands above Middle Turonian sandstones. Upper Turonian sediments consist of a marly facies throughout the Cretaceous basin, apart from a small area of sandstone. These sediments continue into the Coniacian. Regression, resulting in basin emergence, occurred during the Upper Coniacian and Lower Santonian.

Cretaceous strata of the Central Sudetes of Poland were deposited in a marginal zone of the Bohemian Cretaceous basin. Glauconitic sandstones of ?Middle-Upper Cenomanian age

occur at the base of the succession in the north-east of the Table Mountains, resting on Permian conglomerates. The Zlotno Sandstone (150m; middle Middle Turonian) and the Skalniak Sandstone (150m; Upper Turonian) both contain glauconitic sediments, within an assemblage of homogeneous bioturbated sandstones and large-scale cross-bedded sandstones, interpreted as prograding sediment bodies over a scarp-like basin floor (Wojewoda 1986).

6.2.12 Hungary

The Lower Cretaceous Bakony unit of the north-west Pannonian Basin, Hungary, has been described by Kázmér (1988). The Tata Limestone (Aptian) consists of a crinoidal limestone with siliceous sponge spicules, rare chert nodules, glauconite, and sandy intercalations. Brachiopod and ammonite faunas occur at the base, and benthic and planktonic foraminifera above. Carbonate intraclasts are common. Glauconite-rich lenses are developed in the lower part (Haas *et al.* 1985). In the Gerecse Mountains (Transdanubian Central Range), Albian limestones named the Zirc Limestone Formation are developed (Czászár & Haas 1984). The upper member of the formation (Upper Albian) consists of pale brown to grey bioclastic limestone, composed mainly of echinoderm debris; the limestone is bedded on a 15-40cm scale. There is a marked enrichment of glauconite in the upper part, associated with plant fragments, and in the basal part of the overlying Pénzeskút Marl. In the Transdanubian Midmountains, overlying the Tata Limestone and the Zirc Limestone is a mid-Cretaceous cycle, including the Pénzeskút Marl (up to 476m in thickness) (upper Upper Albian-Lower Cenomanian) (Bodrogi 1988). The Marl occupies a narrow zone along the axis of the Midmountains syncline, about 60km in length, and 3-10km wide. The basal part of the formation is glauconitic, consisting of 0.5-1.0m of glauconitic marl; this passes up into dark grey dolomitic marl and interbedded dolomitic silty marl, siltstone, and sandstone.

6.2.13 North Tethyan margin (Spain, France, Switzerland, Austria, Czechoslovakia, Poland)

Condensed glauconitic and phosphatic sediments of mid-Cretaceous age (Lower Aptian-Lower Cenomanian) represent a widespread facies association along the northern Tethyan margin. Such

condensed deposits occur in numerous parts of the Alpine fold belt and their distribution has been reviewed by Delamette (1988), including development in the Betic cordillera of Spain, the eastern coastal area of Sardinia, the Helvetics of France, the Briançonnais domain, the north Provençal domain, Switzerland and Austria, the western Carpathians, the Polish Jura, and central Polish uplands. Typical condensed sequences formed following drowning of the Urgonian carbonate platforms, and are themselves overlain by deeper-water pelagic deposits.

A carbonate-glauconite-phosphate association of Albian age has been documented from the Sierra de Espuña, Betic Cordilleras, Malaga nappe, Spain (Debrabant & Paquet 1975); this represents a shelf-edge setting or submarine high, with negligible detrital input. The phosphate and carbonate supplies have been attributed to the upwelling of deep waters.

In the southern Helvetics of the French Alps, Upper Aptian and Albian deposits comprise thin condensed glauconitic and phosphatic sediments, including glauconitic sponge limestones, muddy fine sandstones, phosphate beds, and glauconitic calcarenaceous sandstones rich in bryozoans. The condensed Albian deposits of the Helvetics comprise <10m of sediments, with generally unfossiliferous glauconitic sandy sediments, and richly fossiliferous condensed phosphatic deposits. The condensed deposits developed in outer shelf settings along the north Tethyan margin, with inner shelf sandy bedforms indicating unidirectional currents; these associations have been interpreted as the result of an oceanic current-dominated regime (Delamette 1988). Complex condensation in Albian glauconitic sediments from Clars, south-east France, has been interpreted as the result of storm winnowing and resedimentation (Gebhard 1982). Glauconitic beds are also developed in association with black shales in the mid-Cretaceous of the Vocontian Basin, southeastern France (Bréhéret & Delamette 1989).

The Garschella Formation ("Gault") (Upper Aptian-Albian) of the western Austrian and central Swiss Helvetics has a very complex stratigraphy, comprising a variety of lithologies including glauconitic sandstones and sandy shales, echinoderm limestones, glauconitic, nodular limestones, and several glauconitic, phosphoritic, condensed horizons (Funk & Herb 1987). The Seewen Limestone (Cenomanian-Coniacian) consists of thinly-bedded, pelagic biomicrites. At the base is a thin, distinct glauconitic horizon, the Ueberturriliten bed, which contains

Cenomanian planktonic and benthic foraminifera and calcispheres. The mid-Cretaceous "triad" of shallow-water platform carbonates, condensed phosphatic and glauconitic sediments, and pelagic carbonates has been described in detail from western Austria by Föllmi (1989; 1990). In this region, phosphogenesis took place from the earliest Aptian to early Cenomanian, with a short decline during the middle late Aptian. Phosphogenesis occurred in a zone of very low accumulation rates, induced by a north Tethyan westward-directed geostrophic current system; such phosphogenesis was apparently coincident with the upper boundary of an oxygen minimum zone; phosphatised microbial mats are a major constituent of many phosphate beds. Glauconitic sediments are widespread in the inner shelf zone of moderate to high detrital input and moderate sediment winnowing, with oxygenated bottom waters, and net sedimentation rates of 10-30mm/100yrs.

In the western Carpathians of Czechoslovakia, Cretaceous glauconitic sediments have been reported by Mahel', Buday *et al.* (1968). In the Manín Unit of the Strážovská Hornatina Mountains, Albian and Cenomanian marlstones and sandstone facies are developed. The basal part of the sandstone facies with conglomerates and subordinate marlstones is Upper Albian in age; the sandstones are often glauconitic. In places, lenses of dark grey, fine-grained, glauconitic limestone have been recorded. In the Pavlov-Waschberg area of the western part of the west Carpathian flysch belt, the Upper Turonian and Lower Senonian are represented by the Klement Formation, up to 20m of greenish-grey, sandy, calcareous clay with thin, lenticular beds of clayey, calcareous, glauconitic sandstone. In the Silesian Nappe, western part of the west Carpathian flysch belt, the Baška Formation (upper Middle Albian to Lower Cenomanian) consists mainly of sandstones (500m); these are fine- to medium-grained, feldspathic, calcareous, often siliceous (cherty), and pass up into limestones composed of fragments of bryozoans, sponge spicules, echinoderms, bivalves and foraminifera. In places, the sandstones are glauconitic. The Godula Variegated Formation, Godula Group (100-350m) consists of alternating claystones (up to few metres in thickness) and fine-grained, glauconitic sandstones. This is a flysch deposit of Cenomanian age. Lenticular beds occur, several tens of metres thick, these are composed mainly of glauconitic sandstone, the Ostravice Sandstone. The sandstone is pale-

coloured, glauconitic, non- or only weakly-calcareous, and contains abundant layers of oligomictic breccia and conglomerate with limestone lithoclasts. The overlying Godula Formation (60-3,000m thick) (latest Cenomanian to Lower Senonian) is a typical flysch deposit, consisting of interbedded grey, generally non-calcareous claystones (up to several metres thick) and fine-to medium-grained (locally coarser) quartzose or feldspathic glauconitic sandstones (up to 4.5m thick). Grey calcareous claystones, with sporadic beds of marly limestone and fine-grained sandstone with glauconitic laminae form the Hluk Formation (Barremian and Albian) in the outer part of the Klippen Belt. Albian glauconitic sediments are also developed in the High Tatric Series of the Tatra Mountains, western Carpathians (north-east Czechoslovakia) (Mahel', Buday *et al.* 1968; Krajewski 1984). The Glauconitic Limestone (Lower-Upper Albian) consists of a thin, condensed horizon, generally <1m thick, covering an Urgonian carbonate platform complex of Barremian to Lower Aptian age; it is overlain by basinal marly mudstone of the latest Albian to Lower Turonian. This condensed limestone consists of pelletal echinoderm grainstones, with an upper hardground surface, and foraminiferal glauconitic wackestones. The early diagenetic phosphate cements have been related to rapid sea-level rise, with a resulting increased influence of nutrient-rich Tethyan waters (Krajewski 1984).

In a variety of the Niedzica Succession in the Pieniny Klippen Belt of the Polish Carpathians, a condensed glauconitic facies has been recognised at the junction between the Pieniny Limestone and Kapuśnica Formations (Obermajer 1987). Overlying a hardground (with ferro-manganese crusts) developed in the uppermost part of the cherty Pieniny Limestone, is a very thin foraminiferal limestone, containing fish teeth, phosphatic pellets, glauconite, quartz grains, and lithoclasts of the underlying formation. The age of this horizon is ?Upper Aptian-Albian. The foraminiferal limestone is overlain by green and black marls and shales of the Kapuśnica Formation (Albian).

6.2.14 India and Pakistan

In India, glauconitic sediments have been recorded from the Garhwal-Kumaun region of the Himalayas. The Spiti Shales grade up into massive, thickly-bedded glauconitic sandstone and

glauconitic siliceous sandy shale, the lower Giumal Sandstone. This is probably of Hauterivian-Lower Albian age, and the total thickness of the Giumal sandstones is around 500m (Ganser 1964; Bhalla, 1978; Sinha 1981). Campanian glauconitic sediments have been reported from the Assam shelf in northeastern India; the Mahedo Formation consists of massive sandstones with glauconite and a rich fossil fauna (Bhalla 1978).

A glauconitic facies has been reported from the Lower Indus Basin of Pakistan, the Belemnites Shale Formation, Parh Group. This ranges from Necomian to Albian, and comprises up to 1220m of green to brown glauconitic shale, rich in belemnites, with interbedded marls and limestones (Kureshi 1978).

6.2.15 Southeastern Africa

In southeastern Africa, the glauconitic facies is well-developed in the South Mozambique - Zululand-Natal coastal basin, which extends over a distance of approximately 1200km and occupies the coastal areas and adjacent continental shelf of southern Mozambique and the Zululand and Natal provinces of South Africa. The basin is at its widest (400km) in southern Mozambique (Förster 1975). Glauconitic sediments accumulated during the Barremian-Cenomanian and Coniacian-Maastrichtian stages. In southern Mozambique, the major part of the marine succession consists of fine-grained glauconitic sandstones and siltstones; limestones are occasionally present as thin layers of bioclastic grainstone and coquina in the marginal parts of the basin, and as glauconitic, quartzose, concretionary horizons (Förster 1981). Small-scale cycles with shelly concretionary layers are developed in the Albian part of the Maputo Formation; these vary from 1-2m to 10m in thickness, and the small-scale cycles show fining-upwards sequences, with a coarser basal sandstone being intensely bioturbated and enriched in glauconite. The bioturbated, fine-grained glauconitic sands and silts of the Cenomanian contain several concretionary and shelly horizons, and hardgrounds, one with hiatus concretions (Förster 1981). In southern Mozambique, following renewed transgression, Santonian and Campanian sedimentation continued in the same facies, glauconitic sandstones of littoral character; these form over ten successive sand bodies, intercalated with marls, and are classed as the Grudja

Formation. Sedimentation continued without a break until the Palaeocene (Förster 1981). The bulk of the uniform glauconitic sequences of the Barremian to Aptian yield few fossils, the majority occurring in early diagenetic concretions, in shelly concretionary layers and in hardgrounds. The Upper Albian, however, is apparently rich in fossils, with the shelly concretionary layers yielding abundant fragments of heteromorph ammonites. The Cenomanian contains abundant echinoids, local clusters of drifted shells, also *Thalassinoides* and *Chondrites* burrows. The Cenomanian sedimentary and biostratonomic evidence suggests near-shore deposition. Overall, bivalves and gastropods are the most common invertebrates; echinoderms and brachiopods are less important.

The Cretaceous succession in Natal and Zululand consists of three transgressive formations, which thicken eastwards and northwards, and progressively onlap to the south-west. This summary is based on work by Kennedy & Klinger (1971; 1972; 1975), Dingle (1978), and Tankard *et al.* (1982). The earliest deposits comprise Upper Barremian conglomerates, sandstones, and siltstones, attributed to progradation of braided, fluvial deposits into a shallow sea (Tankard *et al.* 1982). The earliest marine sediments are of late Barremian age (Makatini Formation) and are overlain by Barremian and Aptian glauconitic sands and silts (Dingle 1978). The overlying Mzinene (Lower Albian-Upper Cenomanian) and St. Lucia (Lower Coniacian-Maastrichtian) Formations consist of sediments similar to those of southern Mozambique, composed mainly of silt to sand-grade clastics; pure clays are rare, and conglomerates are also infrequent, confined to the basal part of the sequence, or associated with breaks in the succession. At the junction between the Makitini and overlying Mzinene Formations is a hardground disconformity of bored and rolled fossils overlain by a Lower Albian conglomerate. The glauconitic sediments are intensely bioturbated, large arthropod burrows being abundant, and small-scale sedimentary structures are usually absent. Small-scale sedimentary cycles are, however, conspicuous; these frequently consist of alternations of shell beds (the shells showing current alignment), and silts with an *in situ* fauna, or sequences in which the sediment fines upwards. The base of each sequence is crowded with pelletal glauconite and rests on a sharp sedimentary discontinuity with early diagenetic concretions at

some horizons; some were disinterred by high energy events and then bored and encrusted (Kennedy & Klinger 1972). The asymmetric cycles have been attributed to fluctuations in the rate of sediment influx into a continuously subsiding basin, and the thin basal disconformities with bored concretions to westward transgression during periods of extremely low sediment influx, accompanied by erosional shoreface retreat. The dominant, fine-grained part of each cycle then resulted from renewed shoreline progradation (Tankard *et al.* 1982). A borehole 24km to the east of the Natal coast has shown that the glauconitic sediments pass offshore into non-glauconitic claystones with subordinate siltstones and very fine-grained sandstones (Du Toit & Leith 1974). The glauconitic fine sands and silts of the Zululand Group are richly fossiliferous, the fauna including infaunal and epifaunal bivalves, gastropods, ammonites, nautiloids and echinoids, with driftwood and plant debris. The succession beneath Durban also contains a diverse fauna of molluscs, serpulids, corals, echinoderms, foraminifera, and plants.

A major regressive phase occurred in late Cenomanian times, extending into the Turonian. Thus, marine Turonian is only known from the deeper parts of the basin to the east, where uniform sedimentation of fine-grained sediments continued into the Upper Cretaceous. These are classed as the Domo Formation, described by Flores (1973). The contact between the Domo and the underlying Maputo Formation is gradational, and the formation consists of dark grey to black, thin-bedded marly shales, with rare sand streaks. It ranges from Aptian/Albian to Turonian in age. The environment is interpreted as characteristically euxinic throughout most of the formation, with occasional minor influxes of plankton from open waters, particularly in the northern and southern wells drilled. North of the Zambezi delta, the Domo shales are replaced by a more open marine facies. The shales contain dwarfed mollusca in the lower part of the formation (Flores 1973).

Cretaceous sediments are also exposed on the eastern side of the Mozambique Basin, occupying a narrow strip along the western seaboard of Madagascar. A glauconitic facies has been reported from the Manosoa-Onilahy district (Cooper 1977); it consists of green, glauconitic sandstones of Coniacian age, overlying late Turonian sandstones with interbedded gypsum.

6.2.16 Northwestern Australia

The Jurassic and Cretaceous sediments of the Canning Basin form a unit up to about 760m in thickness, covering an area of approximately 260,000 Km^2 . The Jurassic and Cretaceous rocks have been considered to represent the deposits of a single transgressive-regressive episode which began in the Middle Jurassic, and ended towards the end of the Lower Cretaceous. There is a well-developed glauconitic facies, and both Jurassic and Cretaceous (Neocomian-Aptian/Albian) glauconitic sediments are present. This account is based on Veevers & Wells (1961).

The Jurassic and Cretaceous sediments comprise nearshore conglomerates and coarse to conglomeratic plant-bearing sandstones and siltstone, passing offshore into deeper-water clays and pyritic, glauconitic siltstone. Sedimentation occurred with only minor breaks from the Middle Jurassic to the end of the Lower Cretaceous, at slow depositional rates. In fairly complete sections of the succession, conglomerate or coarse conglomeratic sandstone is developed at the base, overlain by siltstones or claystones, with conglomerate or coarse conglomeratic sandstone at the top.

The first glauconitic sediments in the "on-shore" basin are of transgressive Oxfordian glauconitic sandstone, though this facies probably previously developed further westwards, in the area of the present-day Rowley Shelf. Oxfordian-Kimmeridgian and uppermost Tithonian glauconitic siltstones are developed in the Langley Crossing - Yeeda area. During the Kimmeridgian, there was a southern shift of the glauconite-producing area, accompanying southwards transgression in the north-west part of the basin. Glauconitic sediments of Kimmeridgian age are known in the Broome area. The sea transgressed further eastwards probably having its widest extent at the beginning of the Neocomian, and the southern part of the basin became the main area of deposition of fine-grained sediments. Glauconitic sediments of Neocomian age are known at Samphire Marsh. Deposition of fine-grained glauconitic sediments (Anketell and Parda Formations) continued from the Neocomian to Aptian/Albian; in the Aptian, siliceous, radiolarian claystones and shales were deposited, and are of a similar age to radiolarian sediments in the Carnarvon, Eucla, and Great Artesian Basins. Coarse-grained

Aptian and Albian sediments also occur at the top of the succession, associated with the widespread Lower Cretaceous regression from the Canning Basin.

The Jowlaenga Formation (?Upper Tithonian-Neocomian) consists of medium to fine-grained glauconitic and pyritic marine sandstone up to 76m in thickness, with sandy siltstone silty, sparsely glauconitic sandstone, and thin beds of clay and of siltstone. The sediments contain radiolaria and foraminifera, belemnites, bivalves, ammonites, and spores, indicating a Neocomian age, perhaps also uppermost Jurassic. The Parda Formation (Neocomian-Aptian/Albian) consists of siltstone interbedded with fine-grained sandstones; this passes laterally into shale, claystone, siltstone, and sandstone with several thin beds of conglomerate, of the Ankatell Formation; it is characterised by an alternation of the finer-grained sediments with sandstone.

6.2.17 Western Australia

A well-developed glauconitic facies of Cretaceous age is found throughout the Carnarvon and Perth Basins of Western Australia, continuing into the Tertiary (Palaeocene-Eocene). The facies is developed as glauconite-rich greensand beds throughout the succession.

Cretaceous sediments of the Carnarvon Basin has been classified as the Winning Group. The Grierson Member, Birdrong Formation (Aptian) is a 29m-thick unit of carbonaceous siltstone and glauconitic sandstone (McWhae *et al.* 1958). It occurs at the base of the formation, which is transgressive over Devonian dolomite. With the exception of fossil wood, fossils are apparently rare; only a few poorly-preserved bivalves have been documented. The overlying Muderong Greensand Member, Muderong Shale (Aptian) marks the base of the Aptian transgression, and is found in the Barrow and Dampier sub-basins, in the north of the Carnarvon Basin (Ludbrook 1978, Table 1). It passes up into a sequence of clay and siltstone. Evidence for high seawater productivity within this interval is indicated by the association with radiolarian sediments; the Windalia Radiolarite (Aptian-Lower Albian) rests conformably on the Muderong Shale, consisting of 35-90m of light-grey to dark-grey radiolarian claystone and radiolarite, which in some areas is associated with thin beds of limestone, greensand and black

chert. The fauna consists of radiolaria, sponge spicules, foraminifera, ostracods, ammonites and bivalves (Brunnschweiler 1959). The Peepingee Greensand is a 10m-thick sequence of glauconitic, feldspathic, fine to medium-grained sandstone, disconformably overlying the Windalia Radiolarite (McWhae *et al.* 1958). No fossils have been recorded from the greensand, which may be of Albian, Cenomanian or Turonian age (McWhae *et al.* 1958). The Alinga Formation (Alinga Greensand) comprises a sequence of glauconitic siltstone and greensand containing radiolaria, fish remains and belemnites (McWhae *et al.* 1958). The Miria Marl (Maastrichtian) (Brunnschweiler 1966; Henderson & McNamara 1985) is a condensed glauconitic, phosphatic, cream-coloured calcarenite, (though not a greensand), only 0.60-2.15m in thickness. It is disconformably overlain by the Boongeroonda Greensand, of Tertiary age.

Glauconitic sediments are also developed in the Perth Basin to the south of the Carnarvon Basin, but are very poorly dated. The Osborne Formation (?Middle Albian-Turonian) comprises up to 115m of glauconitic sandstone and shale, with abundant microfossils (Brown *et al.* 1968; Cookson & Einsack 1962a; 1962b; Ludbrook 1978, Table I). The Molecap Greensand (?Middle Turonian to Lower Coniacian: Deflandre & Cookson 1955; McWhae *et al.* 1958); Brown *et al.* 1968; Ludbrook 1978) consists of a 10m-thick sequence of greensand and glauconitic sandstone, lying conformably on the Dandaragan Sandstone, or unconformably on the Strathalbyn Sandstone. Well-developed 0.6m-thick phosphate beds, with phosphatised wood, are present at both the top and the bottom of the formation in the Dandaragan area. *Ichthyosaurus* and *Plesiosaurus* bones, belemnites, and a single specimen of *Pecten* have been recorded. Overlying the Molecap Greensand is the richly fossiliferous Gingin Chalk. This contains a rich Santonian fossil assemblage. The Poison Hill Greensand (probably Campanian) consists of over 30m of unfossiliferous greensand and glauconitic sandstone with thin shaly bands; thin phosphate beds are developed in the basal part (McWhae *et al.* 1958; Brown *et al.* 1968; Ludbrook 1978).

6.2.18 Southern Australia

Cretaceous sediments are present in the Eucla Basin, where they rest on the Precambrian, but

are only known from the sub-surface, below a Tertiary cover. The glauconitic facies is apparently well-developed; this is deduced from borehole records. The Madura Formation (Madura Shale), is a sequence of shale, sandstone and greensand overlying the Loongana Conglomerate, and underlying Tertiary limestones. The lowest strata are mudstones and glauconitic, carbonaceous and pyritic siltstones which are lithologically and faunally similar to those of the Great Artesian Basin (Ludbrook 1978). Overlying these are highly glauconitic mudstone and siltstone, generally devoid of foraminifera, but with radiolaria in varying abundance. Lowry (1970) notes that the formation is mostly carbonaceous and glauconitic, glauconite being abundant in some beds, particularly near the top of the formation. For example, glauconite forms about 90% of the grains in the Madura Bore core, from 310-334m. The thickness of the formation is typically around 195-360m (Loongana and Madura boreholes respectively), increasing in thickness over the continental shelf to over 600m. Lowry (1970) suggests that the poor sorting suggests weak bottom currents, and that the abundance of pyrite, glauconite, and carbonaceous material indicates that during deposition, there was a reducing environment in the sediment, and probably also at times in the overlying water. The age of the formation is Aptian to Santonian (Brown *et al.* 1968; Lowry 1970; Ludbrook 1978. The late Cretaceous sediments are known only from the western part of the Eucla Basin.

Glauconitic sediments of Cretaceous age are also found in the Otway Basin of southern Australia. Previous confusion between glauconite and chlorite has been addressed by Hawkins & Dellenbach (1971). The Belfast Mudstone Member (Cenomanian-Santonian) (184m thick at the type section; Glenie 1971) is a massive, dark grey marine mudstone with abundant glauconite, fine disseminated pyrite, and some organic matter. Minor sandy and silty beds occur within the sequence. A major regression in the upper part of the member is represented by three minor sub-cycles, each showing a rapid change upwards from paralic sandy deposits to marine shales (Bock & Glenie 1965). Hawkins & Dellenbach (1971) consider that the member represents sedimentation in a restricted basinal setting, in calm, slightly alkaline waters, reducing conditions resulting in the formation of glauconite and sulphides. The palaeontology and palaeoecology of the unit have been described by Taylor (1964). Foraminifera are the most

widespread and diverse element of the fauna; macrofossils appear to be sparse throughout much of the sequence, with the exception of *Inoceramus* (which is most abundant in the lower part and concentrated at certain horizons near the top of the member. Near the top, however, the macrofauna is diverse, with bivalves, scaphopods, belemnites, ammonites, rotularid worm tubes, echinoid plates and fish teeth and scales; in addition, there are ostracods, radiolaria, and arenaceous and planktonic foraminifera. The foraminiferal palaeocology has been documented by Taylor (1964). Arenaceous foraminifera are dominant; calcareous foraminifera are restricted in their distribution, and never comprise >30% of the fauna in any one sample. The planktonic foraminifera fauna is neither rich, nor uniform throughout. The member contains alternations of arenaceous species with assemblages of associated calcareous and arenaceous species. Taylor considers that this is not due to temperature fluctuations, but that the Turonian fine-grained, dark mudstones contain faunas inhibited by anaerobic conditions (possibly due to restriction of water circulation under "barred basin" conditions). The highest dark mudstones contain planktonic faunas and uninhibited benthonic faunas, suggesting that water circulation was not restricted. The Belfast Mudstone Member has been thus subdivided into three units based on the foraminiferal assemblages and the palaoecological interpretation of the depositional environment: 1) a lower arenaceous-calcareous assemblage, signifying a neritic, clear-water environment, with good sea-floor water circulation, but isolation from open-marine conditions (no planktonic foraminifera); 2) a middle arenaceous assemblage, signifying deep, clear water, with apparently anaerobic benthonic conditions, due to restricted water circulation, and 3) an upper arenaceous-calcareous assemblage, which signifies deep, clear benthonic conditions, with good water circulation both at the sea floor and near the surface, with ocean currents introducing a planktonic foraminiferal fauna. Drilling offshore has revealed more open marine conditions, without alternations of arenaceous and arenaceous/calcareous assemblages (Douglas & Ferguson 1976). These authors regard the near-shore part of the member as a delta front or salt-marsh deposit, passing offshore into fairly shallow water. The member passes landwards into a chloritic sandstone, the Nullawarre Greensand Member (Hawkins & Dellenbach 1971).

6.2.19 Northern and northeastern Australia

A glauconitic facies has been reported from northern central Australia by Ludbrook (1978), comprising glauconitic and carbonaceous clays, silts and fine sands developed over a wide area during the stable basin conditions of the Aptian-Albian. The Aptian/Albian marine sequence in the Great Artesian Basin comprises the Roma Formation (<100m; spanning most of the Aptian), and the Tambo Formation (180m; Upper Albian) (Brunnschweiler 1959). Lithologically, the two formations are very similar, consisting largely of soft micaceous and glauconitic mudstone, sandy siltstone and shale. A few thin, commonly lensoid beds of fine-grained sandstone and marly limestone are developed. Throughout the series, pyrite and gypsum (mostly selenite, present as thin concordant layers or discordant veins) are common. The Roma Formation contains bivalves and belemnites; the Tambo Formation contains an entirely different fauna, with very abundant *Aucellina* bivalves, and common inoceramids in the basal 45m. Between the latest Aptian and earliest Upper Albian, there is a highly glauconitic sequence, around 15m thick, with brachiopods, but no mollusca. The sediment is cross-bedded where sandy, and more horizontally-bedded where shaly or calcareous. Brunnschweiler (1959) notes that not only in Western and north-western Australia, but also in the Darwin area of northern Australia, and in the Great Artesian Basin of eastern Australia, there are varicoloured radiolarites and siltstones making up considerable portions of the Aptian and Albian sequence. In some areas, the sediment can consist of as much as 95% silica, grading vertically and laterally into nearly pure kaolinites over large distances. Regression of the epicontinental sea from the basin began in the Albian, but in the southern part, marine conditions may have continued to the Cenomanian (Ludbrook 1978).

In the Laura Basin of northeastern Australia, Brown *et al.* (1968) have documented locally-glauconitic quartzose and shaly sandstones of the Battle Camp Formation (>300m; broadly assigned to the Neocomian). The upper part of the formation is mainly shale, and contains Aptian marine fossils, principally bivalves. The formation is overlain by about Albian calcareous claystones.

6.2.20 New Zealand

There is a well-developed glauconitic facies of late Cretaceous and early Tertiary age developed in the eastern coastal area of New Zealand. Cretaceous marine sediments are developed primarily in five regions: Otago, Marlborough, south-east Wellington (Wairarapa), the Raukumara Peninsula, and Northland (Stevens & Speden 1978). A notable feature of the late Cretaceous in many areas is the latest Cretaceous-early Tertiary peneplanation and complementary transgression; volcanic activity during this interval is evidenced by the presence of bentonitic mudstones (Suggate *et al.* 1978). It has been deduced from such features as unconformities and grain-size variations that much of the Cretaceous sediment was derived from a land mass to the west, though in Marlborough, sources to the east and south are suggested locally (Speden 1975; Lensen in Suggate *et al.* 1978). The palaeogeographic reconstructions of Suggate *et al.* 1978) suggests a complex double-sided basin of deposition within the east coast fold and fault belt. Datings are often unsure; the correlation of the boundaries of the twelve New Zealand Cretaceous stages with those of the international stages is uncertain (Stevens & Speden 1978).

From the east coast of Otago, South Island, latest Maastrichtian-Palaeocene glauconitic sediments have been recorded (Suggate *et al.* 1978). The Abbotsford Mudstone comprises sulphurous, black glauconitic siltstone or fine sandstone, passing into littoral sandstones and conglomerates of the Wangaloa Formation. The littoral beds are rich in macrofossils, but both the littoral and offshore sediments are relatively poor in microfossils, due to reducing conditions during deposition; this has hindered attempts to date the formation accurately.

In Marlborough, South Island, the Iwitahi Group (Cenomanian-Maastrichtian) consists of intertonguing formations of sandstone, greensand, siltstone (massive and bedded), and alternating sandstone and siltstone. These were deposited in shallow water, marginal to a landmass sited to the west and an impersistent land area to the south-east (Stevens & Speden 1978; Suggate *et al.* 1978). To the south-west, the lowest beds are non-marine, with thick volcanics present. The Nidd Formation (150m; Middle Cenomanian-Upper Santonian) is the lowest formation of the Iwitahi Group; it consists of a glauconitic, muddy sandstone, containing

fossiliferous concretionary horizons. This thins and becomes coarser-grained both to the north-east and the south-east, where shell beds are present. The Paton Formation (uppermost Santonian-Campanian) consists of 10m of greensand, overlain by 15m of alternating glauconitic sandstone and sandy siltstone; it contains inoceramids (Suggate *et al.* 1978). The formation passes laterally into the Ess Creek Formation (>30m), a bentonitic mudstone with a few slightly glauconitic silty sandstone beds. The Herring Formation (Lower Maastrichtian) (Suggate *et al.* 1978) consists of 60m of well-bedded fine sandstone with thin bands of dark sulphurous siltstone, overlain by 73m of greensand and dark micaceous siltstone with concretionary bands in the upper part. The formation reaches 335m in thickness; it passes laterally into siliceous muddy siltstones of the Woolshed and Mizra Formations, and the Butt Formation (Upper Maastrichtian) which overlies the Mizra in coastal areas. Between the Mizra and Butt is a transition zone, 9m in thickness, containing greensand bands. The Butt Formation itself consists of up to 290m of sandstone and siltstone with chert lenses (Suggate *et al.* 1978). In the Haumuri Bluff district of South Marlborough, the Claverley Sandstone (32m; Upper Maastrichtian-Lower Palaeocene) consists of glauconitic and locally-calcareous sandstone (Warren & Speeden 1977). The sandstone is generally fine-grained, the glauconite content is mostly 5-10%, locally reaching 30%, and there are scattered small phosphate nodules; the sediment is strongly-bioturbated. The Mead Hill Flint (up to around 300m; Upper Maastrichtian-Upper Palaeocene) consists of bedded chert, with greensand partings in the Upper Maastrichtian lower part, and thin limestone partings in the Palaeocene upper part (Suggate *et al.* 1978).

Glauconitic sediments are also known locally from south Westland, on the western coast of South Island. At Bruce Bay-Bullock Creek, highly glauconitic, massive, brown, quartzose, marine sandstone and siltstone of late Cretaceous age are developed overlying coal measures. These are overlain by the Arnott Volcanics (Suggate *et al.* 1978).

Glauconitic sediments are developed in North Island. In south-east Wellington, conglomerates associated with quartz sands are developed, which are commonly glauconitic, and contain greensand bands; these pass offshore into sandy mudstones (Suggate *et al.* 1978).

In the Raukumara Peninsula, Campanian marine sandstones, locally with non-marine

beds, are disconformably overlain by Maastrichtian (Haumurian) dark grey, micaceous Whangai facies siltstone. South-west of Motu, a bedded quartzose and glauconitic sandstone basal phase, the Tahora Sandstone (20m; basal Maastrichtian) is generally present. The westernmost Maastrichtian outcrops consist dominantly of sandstone lithologically similar to the Tahora Sandstone, up to several hundred metres thick (Speden 1973). In the Koranga area, Speden (1975) has described fine, muddy glauconitic sandstones of the Raukumara Formation. Rapid lateral changes in the basal sandstone phase suggest that it may not be a continuous unit. North of the Mangaotane Valley, and in the south-west, the sequence is dominated by siltstone; elsewhere, the Senonian-Maastrichtian consists mostly of plant-rich, nearshore alternating quartzose and glauconitic sandstone and siltstone, similar to the Raukaumara Series sequences. The predominantly Maastrichtian Whangai Formation siltstones locally extend into the basal part of the Tertiary.

6.2.21 Venezuela

A widespread glauconitic facies is developed in Venezuela. In the Serranía del Interior of northeastern Venezuela, Upper Aptian shales, quartz sands and carbonates characterised by an abundance of glauconite are developed in the lower part of the Valle Grande Formation (Renz 1982). The Chimana Formation (up to 800m; Lower-lower Middle Albian) of the Serranía del Interior, eastern Venezuela is also characterised by high glauconite concentrations and is developed above a sequence of massively-bedded limestones; it consists of dark shales irregularly interbedded with massive limestones and glauconitic sands. The shale intercalations contain rich benthonic and planktonic foraminiferal associations and ammonites (Renz 1982). In the eastern interior ranges, reefal limestones, glauconitic sandstones and deeper-water shales of the Aptian-Cenomanian El Cantil, Chimaná and Barracha Formations, upper Sucre Group, are developed. Upper Cretaceous glauconitic sandstones and mudstones of the Tigre Formation, upper Tremblador Group (600m; Turonian) are known from the subsurface in the Orinoco region (Maresch 1978). Upper Aptian to Albian glauconitic sediments are also developed in western Venezuela and Colombia, comprising 55-180m of glauconitic sandstone, sandy

glauconitic marls and sandy glauconitic limestone of the Lisure and Aguardiente Formations. These have been interpreted as transgressive deposits across a peneplaned Palaeozoic-Triassic-Jurassic terrace in the eastern Andean region (Maresch 1978; Renz 1982).

Deposition of the thick organic-rich source rocks of the region, the La Luna Formation commenced in the late Albian, and progressively spread over the Maracaibo platform during the Turonian, and further northwards over the Goarjira peninsula during the Coniacian. The La Luna sediments comprise predominantly bituminous thinly-bedded black micritic limestones; the Sebaruco Member is an interval of massive grey limestones and glauconitic sandstones, developed within La Luna Formation (Renz 1981). La Luna deposition has been related to sedimentation within a shallow stratified water column, perhaps with coastal upwelling (Tribovillard 1991).

A thin condensed bed, the Tres Equinas Member (Santonian-Campanian) is developed in the Venezuelan Andes at the junction between La Luna and the overlying Colon Formation (Renx 1981; Ghosh 1984). This bed consists of a glauconitic and phosphatic foraminiferal sandy packstone, 1-3m in thickness, also with dolomite, pyrite and silica. It has been related to deposition in a depositional setting of low detrital input, with mineralisation the result of upwelling and an expanded oxygen minimum layer (Ghosh 1984).

6.2.22 Eastern coastal plain, U.S.A.

A glauconitic facies developed along the Atlantic coastal plain of North America during the Campanian-Maastrichtian (Owens & Sohl 1973; Owens 1978). In this region, the Upper Cretaceous rocks form a thin sheet over older sequences; glauconite is more abundant in the northern costal plain than in the southern parts, though it may be locally-common in the southern region. The Campanian beds represent an extensive transgression of the continental margin, and reflect a wide variety of marginal marine to normal marine environments. Between New Jersey and Georgia, the Merchantville and Marshalltown Formations (Campanian) show characteristic cyclicity, with glauconitic sand forming the basal transgressive unit of each cycle, and quartz sand developed in the upper part. At least two cycles are developed in the

Campanian of New Jersey. At outcrop, the glauconitic sediments are associated with carbonaceous black silts or clays; they are associated offshore with calcareous shales (in the north) and carbonate banks (in the south). Maastrichtian to Palaeocene glauconitic sediments are also developed in the northern coastal plain of New Jersey, including the Navesink Formation (uppermost Campanian-mid Maastrichtian) (clayey glauconitic sand to sandy clay with sandy layers); the Redbank Formation (late Maastrichtian) (glauconitic sand and sandy clay); the Tinton Formation (late Maastrichtian) (muddy, medium to coarse, glauconitic quartz sandstone, with lenses of sideritic mudstone) (Olsson 1963; Montag & Seidemann 1981).

6.2.23 Western Interior Seaway of North America, Canada

Albian glauconitic sediments have been reported from many parts of the southern interior plains of Canada, in the southern Alberta-southern Saskatchewan-southwestern Manitoba areas, and in the Liard River area of British Columbia. Glauconite occurs in the Cantaur and Pense Formations, Manville Group (Albian) (southwestern Saskatchewan) (Christopher 1975; Christopher 1984). In the Cantaur Formation, a glauconitic foraminiferal marine shale marks the basal part of the Clearwater facies, and in the Pense Formation, glauconite occurs within well-sorted quartzose, fine-grained sandstones with planar and trough cross-bedding; these have been interpreted as the deposits of a marine bar. The Fort St. John Group of the southern interior plains has been described by Caldwell (1984): The Buckinghorse (?Upper Aptian-lower Upper Albian) and Garbutt (?Upper Aptian-upper Lower Albian) Formations, developed in the British Columbia-North-West Territories region comprise basal sandy or silty sediments which grade up through glauconitic mudstones into shales. The Bluesky Formation (middle lower Albian) (Alberta) comprises well-sorted fine-grained glauconitic sands. The lower part of the Moosebar Formation (upper Lower Albian) (northern Alberta-British Columbia) comprises lenses of lag conglomerate associated with glauconitic mudstone. The Bulwell Member (upper Lower Albian) (northern British Columbia-southern North-West Territories) comprises ripple cross-laminated fine-grained sandstones with glauconite and a rich ichnofauna. The Scatter Formation, Fort St. John Group (late Middle Albian) (north-east British Columbia) comprises about 350m of fine-

grained highly glauconitic sandstone and siltstone, and silty marine shales (Stott 1975). The Spinney Hill Sandstone, Joli Fou Formation (upper Middle Albian) (Sasketchewan) comprises fine-grained muddy glauconitic sandstones with up to 20% glauconite; these are the deposits of an estuarine delta and pass into offshore mudstones (Simpson 1975). The upper part of the Swan River Formation (late Middle Albian-early late Albian) (Sasketchewan-Manitoba escarpment) comprises richly-glauconitic, well-sorted, fine-grained sands with black clay interbeds (McNeill 1984). The Skull Creek Member, Ashville Formation (Ashville Sand) (Colorado Group) (lower Upper Albian) (Sasketchewan-Manitoba escarpment) comprises a sheet of interbedded glauconitic fine-grained sandstones and siltstones, and mudstones. The unit is typically around 7m in thickness; in places, the sandstones contain up to 25% glauconite (Simpson 1975; Caldwell 1984). The Flotten Lake Sand, Colorado Group (lower Upper Albian) (Sasketchewan) comprises a blanket deposit of glauconitic sandstones and siltstones (Simpson 1975).

Further north, the Martin House and basal Arctic Red Formations of the Peel Trough, McKenzie area of the North-West Territories (Aptian and Lower Albian respectively) contain a basal coarse glauconitic sandstone overlying a thick fossiliferous mudstone sequence (Yorath & Cook 1984).

6.3 Interpretation of temporal and spatial patterns of Cretaceous glauconite enrichment

6.3.1 Palaeogeographic reconstructions

The distribution of glauconitic facies for each Cretaceous stage is plotted on a series of palaeogeographic reconstructions (taken from Funnel 1990) (Figs.124-135). The maps show that the development of Cretaceous glauconitic facies tended to be concentrated in specific provinces. Such sediments are an important component of the Cretaceous successions in stable epicontinental settings across a wide area of northern Europe (Britain, France, Netherlands, Denmark, Germany, Poland, Russia), on the north Tethyan continental margin (Spain, France,

Switzerland, Austria, Czechoslovakia, Poland), on the continental shelf off southeastern Africa, in the interior seaway of the Canning Basin, northwestern Australia, on the continental shelf of Western Australia, in restricted sedimentary basins (Eucla and Otway Basins) of southern Australia, in the epicontinental seaway of northeastern-central Australia, in the complex fold belt (with associated volcanics) of New Zealand, on the continental platform of northern Venezuela, on the eastern continental margin of North America, and in the northern part of the epicontinental seaway of North America.

As discussed in Chapter 2, the presence of glauconite in the Upper Albian of the Anglo-Paris Basin reflects slow sedimentation rates during which authigenic growth of glauconitic minerals occurred. High glauconite concentrations have been interpreted as intervals during which the supply of clastic or carbonate dilutants significantly slowed or halted; this appears to be controlled by small-scale relative sea-level change. In the world-wide review of glauconitic facies, greensands often mark transgressive intervals of reduced sediment supply. The global sea-level highstand which occurred during the middle and Upper Cretaceous resulted in significantly increased shelf area across which potential sediment starvation could occur. Glauconite enrichments are generally associated with fine sands, silts, marls and limestones (usually chalks); glauconitic clays are more rare. Iron limitation does not appear to prevent glauconite concentrations in carbonate facies, this is probably due in part to supply of faecal pellets which represent ready substrates for glauconitization. Greensands are commonly associated with authigenic phosphate; siderite is rare, but has been documented from examples in Germany and in Egypt (see later). Only very rarely do greensands appear to show marked pyrite enrichment (southern Australian occurrences). Several simple models are presented, to demonstrate the settings and associations of Cretaceous glauconitic facies.

6.3.2 Depositional settings of Cretaceous glauconitic sediments

1) Directly overlying unconformities. Thin transgressive greensands commonly form the basal deposits of sequences onlapping onto older strata. e.g. the thin Ryazanian phosphorites and greensands of eastern England, which mark a transgression across Kimmeridgian clays on the northern margin of the London Platform. e.g. the Glauconie de base, which marks the Albian transgression onto the eastern edge of the Armorican Massif. e.g. the phosphatic conglomerates and greensands which mark the base of the Albian and Cenomanian transgressions onto older basement in eastern Germany. e.g. Cenomanian and Upper Coniacian-Santonian greensands of Northern Ireland, each of which are marked by prominent onlap onto pre-Liassic formations, and onto Dalradian basement respectively. Greensands in these settings represent intervals of starvation during transgression, during which sediment was being held in nearshore areas. As the rate of relative sea-level rise slowed, increased sediment supply reached the areas of glauconite concentration, progressively diluting and buring the interval.

2) Wide epicontinental shelf areas. Thicker glauconitic sandstone, siltstone and limestone sequences, often associated with phosphoritic beds developed across wide epicontinental shelf sea areas created by the sea-level high-stand of the middle and Upper Cretaceous. e.g. the Upper Greensand of southern England; the Cenomanian glauconitic sands of the Russian platform; the glauconitic sandstones of the Maracaibo platform, Venezuela; the lowermost Cretaceous glauconitic sediments of the Canning Basin, Australia. The environmental inrepretation of glauconitic facies developed in the southern Canada region of the western Interior Seaway is unsure, but the glauconite concentrations do not appear to be high. Within these sequences, more glauconite-rich beds appear to reflect starvation surfaces caused by higher frequency relative sea-level change e.g. those described from the Upper Albian of the Anglo-Paris Basin.

3) Stable passive continental margins. Glauconitic sandstones and siltstones developed on

passive continental margins off southeastern Africa and eastern North America during the Cretaceous. In southern Mozambique and eastern South Africa, a cyclicity is developed, comprising small fining-up sequences, the basal parts of which are glauconite-rich; these may record small-scale transgressive sequences resulting in periods of sediment starvation. The presence of glauconite in the Barremian-Cenomanian and Coniacian-Maastrichtian sediments suggests relatively stable shelf conditions with low rates of detrital input throughout much of the Cretaceous. Similarly, glauconitic cycles in the passive margin setting of the Atlantic coastal plain of the U.S.A. infer a transgression/sediment supply control mechanism on glauconite enrichment. Campanian sediments mark an extensive transgresssion of the continental margin, and glauconitic sands form the basal transgressive units of cycles in the Campanian-Maastrichtian strata; in each cycle, these pass up into quartz sands. A recent analysis of the stratigraphy of the area has confirmed that the glauconitic formations represent transgressive periods with increasing palaeobathymetry (Olsson 1988).

4) Starved continental margins with geostrophic currents. Thin glauconite and phosphate-rich sediments mark a zone of very low sedimentation rates along the north Tethyan margin, extending from Spain in the west to Poland in the east. These condensed sequences are developed above drowned Cretaceous carbonate platforms and are themselves overlain by pelagic sediments. Detailed studies have led to a model of glauconitic sediment development in inner shelf settings, with oxygenated bottom waters and moderate sediment winnowing and transport due to a westerly-directed geostrophic current along northern Tethys. Phosphogenesis occurred in outer shelf settings, conicident with the upper edge of an oxygen minimum zone.

5) Restricted sedimentary basins. Glauconite enrichments occur in certain restricted sedimentary basins, associated with pyrite and some organic matter enrichment. e.g. the Madura Formation of the Eucla Basin and the Belfast Mudstone Member of the Otway Basin, southern Australia. These sediments comprise glauconitic pyritic mudstones and siltstones. The Madura Formation is generally devoid of foraminifera, and while foraminifera are present in the Belfast Mudstone

Member, their distribution shows fluctuations interpreted as due to restriction of water circulation; macrofaunanal elements are rare. In these examples, low bottom-water oxygenation may have played an important role in glauconite authigenesis by promoting the development of redox interfaces within the sediment (see Chapter 5). The Upper Aptian-Lower Albian glauconitic sediments of western Germany are associated with dark mudstones with moderate organic carbon contents and foraminifera adapted to low water oxygenation. This has been interpreted as an assemblage of facies resulting from a boreal upwelling system, but may simply reflect very restricted basinal circulation. Greensand deposition continued into the better-oxygenated facies of the Middle and Upper Albian, and appears to be controlled by low detrital inputs and transgression over the basin margins (e.g. the Rhenish Massif).

6) Submarine highs. Glauconitic facies in Bornholm, Denmark mark the presence of a submarine horst within the Fennoscandian border zone. Thick, glauconitic, muddy fine sands developed during the Middle Cenomanian and Upper Conicacian to Lower/Middle Santonian. The Middle Cenomanian example (Arnager Greensand) overlies lacustrine sediments of Berriasian-Valanginian age and is thus demonstrably transgressive.

7) Transgression within a complex active fold belt. Glauconitic facies developed in the complex double-sided basin within the east coast fold belt of New Zealand. Greensands mark a late Cretaceous and early Tertiary peneplanation and complementary transgression. Bentonitic clays derived from volcanic activity are a feature of this interval.

8) Zones of upwelling. Glauconitic facies are often associated with upwelling facies. An example of a Campanian upwelling system from Egypt has recently been documented (Glenn 1990; Glenn & Arthur 1990), where glauconitic sandstones are associated with phosphorites, black shales, porcellanites, chert, and shallow-water reef limestones. Glauconitization has been related to high iron inputs and to thicker zones of iron reduction in reducing sediments; the glauconite grains were later reworked as a lowstand progradational wedge. Indications of high

productivity are shown by certain Cretaceous facies associations in Australia. Greensands, shales and radiolarites are developed in the Carnarvon Basin, and glauconitic sediments and chalks are also present in the Perth Basin to the south; thin greensand beds appear to mark transgressions within the succession. Aptian and Albian radiolarian siltsones are also developed in the Great Artesian Basin of eastern Australia, and glauconitic beds are occasionally developed. The organic-rich sediments of Venezuela are preceded by deposition of glauconitic sediments along the basin margins, but the two facies types are not commonly developed in close spatial association.

6.3.3 Role of smectitic clays

An additional factor which must be considered is why greensands are **not** developed at certain unconformities and are not the expressions of all transgressions. The presence/absence of a suitable sediment substrate for glauconitization is probably the controlling prerequesite. Jeans *et al.* (1982) stressed the important role of smectitic clays in glauconitization processes in the Cretaceous greensands from southern England and Northern Ireland, and also noted the occurrence of a possible bentonite in the Upper Cretaceous sediments of New Jersey, where a well-developed glauconitic facies occurs. Smectitic clays are an important element of the mid-Cretaceous sediments of the Vocontian Basin (Bréhéret & Delamette 1989). Bentonites are also developed in the Upper Cretaceous and Tertiary sediments of New Zealand, where a glauconitic facies is associated with Upper Cretaceous transgression. Similarly, volcanic activity characterised the eastern margin of Australia during the Jurassic and Cretaceous. Andesitic volcanic material is developed at various levels in the sedimentary succession of the Great Artesian Basin, with a conspicuous and extensive occurrence in marine sediments of Albian age (Veevers & Evans 1973). Other glauconitic facies may similarly be associated with smectitic or bentonitic clay minerals; evaluation of this awaits the compilation of further data. A widespread glauconite-rich facies is, however, not developed in the western interior of North America, where bentonites are common (Kauffman 1984); the reasons for this are uncertain.

6.3.4 Calculation of Cretaceous glauconite-production rates

The data set listed above was used to calculate estimates of the glauconite-production rates for each Cretaceous substage. Such calculations are only semi-quantitative, and have a number of uncertainties, of which the most important is the imprecise dating of many formations. They are nonetheless useful and once established, can be updated as more precise ages become available.

For each formation, an estimate of the areal extent of the glauconitic sediments was estimated by plotting the occurrence on the palaeocontinental reconstructions of Funnel (1990), followed by a simple counting squares method (where one whole square represents an area of 62500km^2). The average thickness of the deposit across this area was then estimated from the published data; where such data were not available, an arbitrary thickness of 25m was assigned. The average glauconite concentration was then used to complete the volumetric calculation. For many of the formations this was unknown, and a value of 5% was assigned; in occasional clear cases of very strong glauconite enrichment, however, values from 10-25% were designated. Thus for each occurrence, a volume of glauconite (km^3) was calculated.

The lengths of the Cretaceous stages and substages vary widely (e.g. the Albian stage has large numbers of reported glauconitic formations, but is also the longest stage); thus, to consider possible controls on the development of the facies, the rates of glauconite production were considered. Resolution of the formation ages down to substage level proved possible for many examples, and this was used as the fundamental unit for which the production rates were calculated. The Cretaceous time scale and relative stage and substage lengths complied by Haq *et al.* (1988) was used in the calculations. A final assumption is that where a glauconitic formation spans more than one substage, the thickness of sediment for each substage is calculated by a division of the total value assuming a constant sedimentation rate throughout.

The calculated glauconite production rates are shown graphically in Figure 136. The graph shows a major increase in the glauconite production rates (GPR) in the middle and Upper Cretaceous, commencing in the Aptian, with a 4-5 -fold increase. Three GPR peaks are developed:

3) a Lower Coniacian-Upper Santonian: broad peak.

2) an Upper Albian-Upper Cenomanian: major peak, with a large Middle Cenomanian subpeak.

1) a Lower Aptian-Lower Albian: major peak centred on the Upper Aptian.

6.3.5 Links with sea-level change and anoxia

These high GPR rates are linked to global transgressive episodes which resulted in sediment-starved areas of shelf seas. The correlation between global sea-level change (best current compliation is the cycle chart of Haq *et al.* 1988), peak glauconite production rates, and Cretaceous Oceanic Anoxic Events (proposed by Jenkyns 1980; Schlanger *et al.* 1987; Arthur *et al.* 1990; Jenkyns 1991) is given in Figure 137. It can be seen that the broad time envelope of high glauconite production rates correlates well with middle and Upper Cretaceous rising sea-levels and sea-level highstand. During this time period, world-wide burial of organic carbon (Oceanic Anoxic Events) occurred. In detail, the Aptian-Albian anoxic subevents fall within periods of high GPR values (Note that the GPRs do not have as fine a stratigraphic resolution as the OAEs). The Cenomanian-Turonian boundary OAE shows no associated glauconite production peak, however; a GPR peak is developed earlier in the Middle Cenomanian. The Upper Coniacian OAE (Jenkyns 1991) falls within the broad Coniacian-Santonian GPR peak. In only few instances, however, does there appear to be a direct link between low water-oxygenation or high organic-carbon contents in the sediment, and enhanced glauconitization processes. Exceptions include the Madura Formation and Belfast Mudstone Members of South Australia, a Campanian upwelling system in Egypt (Duwi Formation) (Glenn & Arthur 1990) and the Marnes Bleues of the Vocontian Trough (Bréhéret & Delamette 1989). In modern environments, glauconite may form along the upper edge of an oxygen-mimimum zone on the outer shelf, for example, off Central California (Vercoutere *et al.* 1987) and on the outer shelf of the east Australian continental margin, where a glauconite-phosphate association has developed at a transition zone between organic matter-poor outer shelf sediments and deeper-water organic matter-rich sediments (O'Brien *et al.* 1990). Few Cretaceous examples occur in

analogous depositional settings, the north Tethyan examples being an exception. In many facies, there is little or no evidence for reduced water-oxygenation (though this may be difficult to discern unless oxygen depletion is very strong), and gross sedimentation rate fluctuations appear to have been a dominant control. As noted by Odin & Fullagar (1988), glauconite is not depth-specific, but occurs mostly at depths between 60 and 550m in present-day environments.

6.4 Conclusions

In summary, a thorough review of published data on middle and Upper Cretaceous glauconitic facies indicates a wide range of depositional settings and facies associations. These include greensands directly overlying unconformities, over wide epicontinental shelf areas, on submarine highs within broad shelf areas, on stable passive continental margins, on starved continental margins with geostrophic currents, in restricted sedimentary basins, marking transgression within a complex active fold belt, and in zones of upwelling of nutrient-rich waters. Many greensands appear to be associated with smectitic clays of probable volcanogenic origin. Volumetric calculations of Cretaceous glauconite production rates has shown that this facies was most most common during a specific interval from Aptian to Santonian times; peaks within this interval appear to be linked to widespread transgressions and sediment starvation across the extensive broad shelf seas which developed during this time of global rising sea-level and sea-level highstand. World-wide correlation of many individual greensand beds, however, awaits more detailed stratigraphic work and more precise dating, to zonal and subzonal levels.

REFERENCES

ADATTE, T. & RUMLEY, G. 1987. Cretaceous of the Jura Mountains, Part 3. *In*: Field Guide A - Central Switzerland, *3rd International Cretaceous Symposium*, Tübingen, 26.8 - 8.9.1987, 69-91.

AIGNER, T. 1982. Calcareous Tempestites : Storm-dominated Stratification in Upper Muschelkalk Limestones (Middle Trias, SW-Germany). *In* EINSELE, G. & SEILACHER, A. (eds.) *Cyclic and Event Stratification*, Heidelberg, Springer-Verlag, 180-198.

AIGNER, T. 1985. Storm Depositional Systems. Dynamic Stratigraphy in Modern and Ancient Shallow-Marine Sequences. *In*: FRIEDMAN, G. M., NEUGEBAUER, H. J. & SEILACHER, A. (eds.) *Lecture Notes in Earth Sciences*, **3**, Springer-Verlag, Berlin, 1-174.

AINSWORTH, N. R., O'NEILL, M., RUTHERFORD, M. M., CLAYTON, G., HORTON, N. F. & PENNEY, R.A. 1987. Biostratigraphy of the Lower Cretaceous, Jurassic and uppermost Triassic of the North Celtic Sea and Fastnet Basins. *In*: BROOKS, J. & GLENNIE, K. (eds.) *Petroleum Geology of North West Europe*, vol.2, 611-622.

ALI, M. T. 1974. Environmental Implications of Infillings in the Upper Greensand of the Beer District, South Devon. *Proceedings of the Geologists' Association, London*, **85**, 519-531.

ALI, M. T. 1976. The significance of a mid-Cretaceous cobble conglomerate, Beer District, south Devon. *Geological Magazine*, **113**, 151-158.

ALLEN, J. R. L. 1984. Experiments on the settling, overturning and entrainment of bivalve shells and related models. *Sedimentology*, **31**, 227-250.

ALLEN, P. A. & UNDERHILL, J. R. 1989. Swaley cross-stratification produced by unidirectional flows, Bencliff Grit (Upper Jurassic), Dorset, U.K.. *Journal of the Geological Society, London*, **146**, 241-252.

ANDERTON, R., BRIDGES, P. H., LEEDER, M. R. & SELLWOOD, B. W. 1983. *A Dynamic Stratigraphy of the British Isles*. A Study in Crustal Evolution., 3rd edn., 1-301.

ARKELL, W. J. 1947. *The Geology of the Country around Weymouth, Swanage, Corfe and Lulworth*. Memoirs of the Geological Survey of Great Britain, Explanation of sheets 341, 342 & 343. (Contributions by C. W. Wright & H. J. Osbourne White).

ARNAUD-VANNEAU, A., ARNAUD, H., ADDATTE, T., ARGOT, M., RUMBEY, G. & THIENLOY, J. P. 1987. The Lower Cretaceous from the Jura Platform to the Vocontian Basin (Swiss Jura, France). Field Guide Excursion D, Grenoble, France, *3rd International Cretaceous Symposium, Tübingen.*

ARTHUR, M. A., ANDERSON, T. F., KAPLAN, I. R., VEIZER, J. & LAND, L. S. 1983. *Stable isotopes in Sedimentary Geology*. Society of Economic Paleontologists and Economic Mineralogists, Short Course, **10**.

ARTHUR, M. A. & PREMOLI SILVA, I. 1982. Development of Widespread Organic Carbon-Rich Strata in the Mediterranean Tethys. *In*: SCHLANGER, S. O. & CITA, M. B. (eds.) *Nature and Origin of Cretaceous Carbon-rich Facies*, Academic Press, 7-54.

ARTHUR, M. A., SCHLANGER, S. O. & JENKYNS, H. C. 1987. The Cenomanian-Turonian Oceanic Anoxic Event, II. Palaeoceanographic controls on organic-matter production and preservation. *In*: BROOKS, J. & FLEET, A. J. (eds) *Marine Petroleum Source Rocks*, Geological Society, London, Special Publication, **26**, 401-420.

ARTHUR, M. A., BRUMSACK, H.-J., JENKYNS, H. C. & SCHLANGER, S. O. 1990. Stratigraphy, geochemistry, and paleoceanography of organic carbon-rich Cretaceous sequences. *In*: GINSBURG, R. N. & BEAUDOIN, B. (eds) *Cretaceous Resources, Events and Rhythms*. NATO ASI Series C, **304**, 75-119.

BENTNOR, Y. K. & KASTNER, M. 1965. Notes on the mineralogy and origin of glauconite. *Journal of Sedimentary Petrology*, **35**, 155-166.

BERG-MADSEN, V. 1983. High-Alumina glaucony from the Middle Cambrian of Öland and Bornholm, southern Baltoscandia. *Journal of Sedimentary Petrology*, **53**, 875-893.

BERGER, A. 1988. Milankovitch theory and climate. *Reviews of Geophysics*, **26**, 624-657.

BERGSTRÖM, J., CHRISTENSEN, W. K., JOHANSSON, C., & NORLING, E. 1973. An extension of Upper Cretaceous rocks to the Swedish west coast at Särdal. *Bulletin of the Geological Society of Denmark*, **22**, 83-154.

BERNER, R. A. 1984. Sedimentary pyrite formation: An update. *Geochimica et Cosmochimica Acta*, **48**, 605-615.

BESNOSOV, N. V., GORBATCHNIK, T. N., MIKHAILOVA, I. A. & PERGAMENT, M. A. 1978. Soviet Union. *In*: MOULLADE, M. & NAIRN, A. E. M. (eds.) *Phanerozoic Geology of the World*, II, The Mesozoic, A, Elsevier, 5-53.

BHALLA, S. N. 1978. India. *In*: MOULLADE, M. & NAIRN, A. E. M. (eds.) *Phanerozoic Geology of the World*, II, The Mesozoic, B, Elsevier, 305-351.

BIRKENMAJER, K. & JEDNOROWSKA, A. 1987. Late Cretaceous foraminiferal biostratigraphy of the Pieniny Klippen Belt, Carpathians (Poland). *Studia Geologica Polonica*, **92**: BIRKENMAJER, K. (ed.) Geology of the Pieniny Klippen Belt, Carpathians, Poland, Part 7, 7-28.

BISMUTH, H., BOTTENHAGEN, C., DONZE, P., LEFEVRE, J. & SAINT-MARC, P. 1982. Etude Sédimentologique et Biostratigraphique du Crétacé Moyen et Supérieure du Djebel Semmama (Tunisie du Centre Nord). *Cretaceous Research*, **3**, 171-185.

BJERKLI, K. & ÖSTMO-SAETER, J. S. 1973. Formation of glauconie in foraminiferal shells on the continental shelf off Norway. *Marine Geology*, **14**, 169-178.

BOCK, P. E. & GLENIE, R. C. 1965. Late Cretaceous and Tertiary Depositional Cycles in south-western Victoria. *Proceedings of the Royal Society of Victoria*, **79**, 153-163.

BODENHAUSEN, J. W. A. & OTT, W. F. 1981. Habitat of the Rijswijk Oil Province, Onshore, The Netherlands. *In*: ILLING, L. V. & HOBSON, G. D. (eds.) *Petroleum Geology of the Continental Shelf of North-West Europe*, 301-309.

BODROGI, I. 1988. Planktonic foraminifera of the Pénzeskút Marl Formation (Albian-Cenomanian), Transdanubian Midmountains, Hungary. Part I : The Jásd J-42 stratotype profile. *Annales Universitatis Scientiarium Budapestinensis de Rolando Eötvös Nominatae, Sectico Geologica*, **28**, 177-207.

BORNHOLD, B. D. & GIRESSE, P. 1985. Glauconitic sediments on the continental shelf off Vancouver Island, British Columbia, Canada. *Journal of Sedimentary Petrology*, **55**, 653-664.

BRALOWER, T. J. & THIERSTEIN, H. R. 1984. Low productivity and slow deep-water circulation in mid-Cretaceous oceans. *Geology*, **12**, 614-618.

BRANDT, D. S. 1986. Preservation of Event Beds through Time. *Palaios*, **1**, 92-96.

BRÉHÉRET, J.-G. 1988. Episodes de sédimentation riche en matière organique dans les marnes bleues d'âge aptien et albien de la partie pélagique du bassin vocontien. *Bulletin de la Société Géologique de France*, sér.8, **4**, 349-356.

BRÉHÉRET, J.-G. & DELAMETTE, M. 1989. Correlations between Mid-Cretaceous Black Shales and Helvetic Phosphorites in the Western External Alps. *In*: WIEDMANN, J. (ed.) *Cretaceous of the Western Tethys*, Proceedings of the 3rd International Cretaceous Symposium, Tübingen, 637-655.

BRENCHLEY, P. J. & NEWALL, G. 1970. Flume Experiments on the Orientation and Transport of Models and Shell Valves. *Palaeogeography, Palaeoclimatology, Palaeoecology*, **7**, 185-220.

BRENCHLEY, P. J., NEWALL, G. & STANISTREET, I. G. 1979. A storm surge origin for sandstone beds in an epicontinental platform sequence, Ordovician, Norway. *Sedimentary Geology*, **22**, 185-217.

BRENNER, R. L. & DAVIES, D. K. 1973. Storm-Generated Coquinoid Sandstone : Genesis of High-Energy Marine Sediments from the Upper Ordovician of Wyoming and Montana. *Bulletin of the Geological Society of America*, **84**, 1685-1689.

BRETT, C. E., LIDDELl, W. D. & DERSTLER, K. L. 1983. Late Cambrian hard substrate communities from Montana/Wyoming: the oldest known hardground encrusters. *Lethaia*, **16**, 281-289.

BROMLEY, R. G. 1967. Some observations on burrows of thalassinidean Crustacea in chalk hardgrounds. *Quarterly Journal of the Geological Society, London*, **123**, 157-182.

BROMLEY, R. G. 1975. Trace Fossils at Omission Surfaces. *In*: FREY, R. (ed.) *The Study of Trace Fossils*, Springer-Verlag, 399-428.

BROMLEY, R. G. 1979. Field Meeting in southern Scandinavia 18 - 28 September 1975. Report by the Director. *Proceedings of the Geologists' Association, London*, **90**, 181-191.

BROWN, D. A., CAMPBELL, K. S. W. & CROOK, K. A. W. 1968. *The Geological Evolution of Australia and New Zealand*. Pergamon. 1-409.

BRUNNSCHWEILER, R. O. 1959. New Aconeceratinae (Ammonoidea) from the Albian and Aptian of Australia. *Bulletin of the Bureau of Mineral Resources, Geology and Geophysics of Australia*, **54**, 1-19.

BRUNNSCHWEILER, R. O. 1966. Upper Cretaceous Ammonites from the Carnarvon Basin of Western Australia I: The Heteromorph Lytoceratina. *Bulletin of the Bureau of Mineral Resources, Geology and Geophysics of Australia*, **58**, 1-58.

BURST, J. F. 1958a. "Glauconite" pellets: their mineral nature and applications to stratigraphic interpretations. *Bulletin of the American Association of Petroleum Geologists*, **42**, 310-327.

BURST, J. F. 1958b. Mineral heterogeneity in glauconite pellets. *American Mineralogist*, **43**, 481-497.

BYERS, C. W. & LARSON, D. W. 1979. Paleoenvironments of Mowry Shale (Lower Cretaceous), Western and Central Wyoming. *Bulletin of the American Association of Petroleum Geologists*, **63**, 354-375.

CALDWELL, W. G. E. 1984. Early Cretaceous Transgressions and Regressions in the Southern Interior Plains. *In*: STOTT, D. T. & GLASS, D. J. (eds.) *The Mesozoic of Middle North America*, Canadian Society of Petroleum Geologists Memoir, **9**, 173-203.

CARTER, D. J. & HART, M. B. 1977. Aspects of mid-Cretaceous stratigraphical micropalaeontology. *Bulletin of the British Museum (Natural History) Geology*, **29**, 1-135.

CASEY, R. 1959. Field Meeting at Wrotham and the Maidstone By-Pass. *Proceedings of the Geologists' Association, London*, **70**, 206-209.

CASEY, R. 1972. The ammonite succession at the Jurassic - Cretaceous boundary in eastern England. *In*: CASEY, R. & RAWSON, P. F. (eds.) *The Boreal Lower Cretaceous*, Geological Journal Special Issue, **5**, 193-266.

CAVON, M. & SCHWIZER, B. 1987. Cretaceous of the Prealpine Nappes of the Fribourg Alps, Part 2. *In*: Field Guide A - Central Switzerland, *3rd International Cretaceous Symposium*, Tübingen, 26.8 - 8.9.1987, 28-68.

CHARRIER, R. & LAHSEN, A. 1969. Stratigraphy of Late Cretaceous-Early Eocene, Seno Skyring-Strait of Magellan area, Magellanes Province, Chile. *Bulletin of the American Association of Petroleum Geologists*, **53**, 568-590.

CHAVE, K. E. 1964. Skeletal Durability and Preservation. *In*: IMBRIE, J. & NEWELL, N. (eds.) *Approaches to Paleoecology*, J. Wiley & Sons, 377-387.

CHRISTENSEN, W. K. 1984. The Albian to Maestrichtian of Southern Sweden and Bornholm, Denmark : a Review. *Cretaceous Research*, **5**, 313-327.

CHRISTOPHER, J. E. 1975. The Depositional Setting of the Mannville Group (lower Cretaceous) in southwestern Saskatchewan. *In*: CALDWELL, W. G. E. (ed.) *The Cretaceous System in the Western Interior of North America*, Special Paper of the Geological Association of Canada, **13**, 523-552.

CHRISTOPHER, J. E. 1984. The Lower Cretaceous Manville Group, Northern Williston Basin Region, Canada. *In*: STOTT, D. F. & GLASS, D. J. (eds.) *The Mesozoic of Middle North America*, Canadian Society of Petroleum Geologists Memoir, **9**, 109-126.

CLAYTON, C. J. 1986. The chemical environment of flint formation in Upper Cretaceous chalks. *In*: SIEVIKING, G. DE G. & HART, M. B. (eds). *The scientific study of flint and chert.* Proceedings of the fourth international flint symposium, Brighton, 1983, 43-54.

CLIFTON, H. E. 1971. Orientation of empty pelecypod shells and shell fragments in quiet water. *Journal of Sedimentary Petrology*, **41**, 671-682.

CLIFTON, H. E. & BOGGS, S. 1970. Concave-up pelecypod (*Psephida*) shells in shallow marine sand, Elk River Beds, southwestern Oregon. *Journal of Sedimentary Petrology*, **40**, 888-897.

COLEMAN, J. M. & GAGLIANO, S. M. 1965. Sedimentary Structures : Mississippi River Deltaic Plain. *In*: MIDDLETON, G. V. (ed.) *Primary Sedimentary Structures and their Hydrodynamic Interpretation*, Society of Economic Mineralogists and Palaeontologists, Special Publication, **12**, 133-148.

COLLEY, M. G., MCWILLIAMS, A. S. F. & MYERS, R. C. 1981. Geology of the Kinsdale Head Gas Field, Celtic Sea, Ireland. *In* ILLING, L. V. & HOBSON, G.D. (eds.) *Petroleum Geology of the Continental Shelf of North West Europe*, 504-510.

COOKSON, I. C. & EINSACK, A. 1962a. Additional microplankton from Australian Cretaceous sediments. *Micropalaeontology*, **8**, 485-507.

COOKSON, I. C. & EINSACK, A. 1962b. Microplankton from Australian and New Guinea Upper Mesozoic Sediments. *Proceedings of the Royal Society of Victoria*, **70**, 19-79.

COOPER, M. R. 1977. Eustacy during the Cretaceous; its inplications and importance. *Palaeogeography, Palaeoclimatology, Palaeoecology*, **22**, 1-60.

COOPER, M. R. & KENNEDY, W. J. 1977. A revision of the Baculitidae of the Cambridge Greensand. *Neues Jahrbuch für Geologie und Paläontologie*, **11**, 641-658.

CROKER, P. F. & SHANNON, P. M. 1987. The evolution and hydrocarbon prospectivity of the Porcupine Basin, Offshore Ireland. *In*: BROOKS, J. & GLENNIE, K. (eds.) *Petroleum Geology of North West Europe*, vol.2, 633-642.

CUNNINGHAM, R. & GILBERT, D. 1985. Organic facies of Cenozoic and Cretaceous sediments from Deep Sea Drilling Project Sites 548-551, northern North Atlantic. *In*: GRACIANSKY, P. C. DE, POAG, C. W. *et al. Initial Reports of the Deep Dea Drilling Project*, **80**, 969-981.

CZÁSZÁR, G. & HAAS, J. 1984. *Hungary Excursion 104 guidebook*, International Geological Congress, XXVIIth Session, Budapest, 1984.

DAVIS, J. C. 1970. Petrology of Cretaceous Mowry Shale of Wyoming. *Bulletin of the American Association of Petroleum Geologists*, **54**, 487-502.

DEAN, W. E., CLAYPOOL, G. E. & THIEDE, J. 1978. Origin of organic-carbon-rich mid-Cretaceous limestones, mid-Pacific mountains and southern Hess Rise. *In*: Thiede, J., Vallier, T. L. *et al. Initial Reports of the Deep Dea Drilling Project*, **62**, 877-890.

DEAN, W. E., CLAYPOOL, G. E. & THIEDE, J. 1984. Accumulation of organic matter in Cretaceous oxygen-deficient depositional environments in the Central Pacific Ocean. *Organic Geochemistry*, **7**, 39-51.

DEBRABANT, P. & PAQUET, J. 1975. L'association glauconites-phosphates-carbonates (Albien de la Sierra de Espuña, Espagne méridionale), *Chemical Geology*, **15**, 61-75.

DEFLANDRE, G. & COOKSON, F. C. 1955. Fossil Microplankton from Australian Late Mesozoic and Tertiary Sediments. *Australian Journal of Marine and Freshwater Research*, **6**, 242-313.

DELALOYE, M. F. & ODIN, G. S. 1988. Chamosite, the green marine clay from Chamoson; A study of Swiss oolitic ironstones. *In*: ODIN, G. S. (ed.) *Green Marine Clays*, Developments in Sedimentology, Elsevier, **45**, 7-28.

DELAMETTE, M. 1988. Relation between the condensed Albian deposits of the Helvetic domain and the oceanic current-influenced continental margin of the northern Tethys. *Bulletin de la Societé Géologique de France*, **8**, 739-745.

DESTOMBES, P., GAMBLE, H. J., JUIGNET, P. & OWEN, H. G. 1977. Cretaceous and lower Tertiary of Seine-Maritime, France: a guide to key localities. *Proceedings of the Geologists' Association, London*, **88**, 15-38.

DINGLE, R. V. 1978. South Africa. *In*: MOULLADE, M. & NAIRN, A. E. M. (eds.) *The Phanerozoic Geology of the World II. The Mesozoic, A*, Elsevier, 401-434.

DINGLE, R. V. & KLINGER, H. C. 1972. The stratigraphy and ostracod faunas of the Upper Jurassic sediments from Brenton, in the Knysna outlier, Cape Province. *Transactions of the Royal Society of South Africa*, **40**, 279-298.

DOUGLAS, J. G. & FERGUSON, J. A. (eds.) 1976. Geology of Victoria. *Special Publication of the Geological Society of Australia*, **5**, 1-528.

DOWNES, W. 1882. The Zones of the Blackdown Beds, and their Correlation with those at Haldon, with a List of the Fossils. *Quarterly Journal of the Geological Society, London*, **38**, 75-92.

DRISCOLL, E. G. 1970. Selective Bivalve Shell Destruction in Marine Environments, a Field Study. *Journal of Sedimentary Petrology*, **40**, 898-905.

DRUMMOND, P. V. O. 1970. The Mid-Dorset Swell. Evidence of Albian-Cenomanian Movements in Wessex. *Proceeding of the Geologists' Association, London*, **81**, 679-714.

DUKE, W. L. 1985. Hummocky cross-stratification, tropical hurricanes, and intense winter storms. *Sedimentology*, **32**, 167-194.

DUKE, W. L. 1987. Reply to Discussion : Hummocky cross-stratification, tropical hurricanes, and intense winter storms. *Sedimentology*, **34**, 344-359.

DURRANCE, E. M. & HAMBLIN, R. J. O. 1969. The Cretaceous structure of Great Haldon, Devon. *Bulletin of the Geological survey of Great Britain*, **30**, 71-88.

DU TOIT, S. R. & LEITH, M. J. 1974. The J(C)-1 bore-hole on the continental shelf near Stanger, Natal. *Transactions of the Geological Society of South Africa*, **77**, 247-252.

EKDALE, A. A., BROMLEY, R. G. & PEMBERTON, S. G. 1984. Ichnology. The Use of Trace Fossils in Sedimentology and Stratigraphy. *Society of Economic Palaeontologists and Mineralogists Short Course*, **15**, 1-317.

EL-SHARKAWI, M. A. & AL-AWADI, S. A. 1982. Alteration Products of Glauconite in Burgan Oil-Field, Kuwait. *Journal of Sedimentary Petrology*, **52**, 999-1002.

ELLIOTT, T. 1986. Siliciclastic Shorelines. *In*: READING, H. G. (ed.). *Sedimentary Environments and Facies*, 2nd edn., Blackwell, 155-188.

EMERY, K. O. 1968. Positions of Empty Pelecypod Valves of the Continental Shelf. *Journal of Sedimentary Petrology*, **38**, 264-269.

ENSOM, P. C. 1985. Hiatus concretions with a cemented, pedically and bysally attached fauna from the Eype Nodule Bed, Middle Lias, Dorset. *Proceedings of the Dorset Natural History and Archaeological Society.*, **106**, Geology Report, 164.

ERBA, E., LOTTAROLI, F., PREMOLI SILVA, I. & TORNAGHI, M. E. 1991. Aptian-Albian Anoxic events from the Italian sequences. Abstract. *Terra Abstracts*, **3**(1), 293.

FAUCONNIER, D. & SLANSKY, M. 1979. The Possible Role of Dinoflagellates in Phosphate Sedimentation. *In*: COOK, P. J. & SHERGOLD, J. H. (eds.) *Proterozoic-Cambrian Phosphorites*, IGCP Project of UNESCO-IUGS, **156**, 93-101.

FLEXER, A. 1971. Late Cretaceous Palaeogeography of Northern Israel and its Significance for the Levant Geology. *Palaeogeography, Palaeoclimatology, Palaeoecology*, **10**, 293-316.

FLORES, G. 1973. The Cretaceous and Tertiary sedimentary basins of Mozambique and Zululand. *In*: BLANT, G. (ed.) *Bassins Sedimentaires du Littoral Africain*, 2eme partie: Littoral austral et oriental, Association des Services Geologiques Africains, Paris, 81-111.

FÖLLMI, K. B. 1989. Evolution of the Mid-Cretaceous Triad, *Lecture Notes in Earth Sciences*, **23**, Springer-Verlag, 1-153.

FÖLLMI, K. B. 1990. Condensation and phosphogenesis: example of the Helvetic mid-Cretaceous (northern Tethyan margin). *In*: NOTHOLT, A. J. G. & JARVIS, I. (eds.) *Phosphorite Research and Development*, Geological Society, London, Special Publication, **52**, 237-252..

FÖRSTER, R. 1975. The Geological History of the Sedimentary Basin of Southern Mozambique, and some aspects of the origin of the Mozambique Channel. *Palaeogeography, Palaeoclimatology, Palaeoecology*, **17**, 267-287.

FÖRSTER, R. 1981. Mozambique. *In*: REYMENT, R. A. & BENGTSON, P. (eds.) *Aspects of Mid-Cretaceous Regional Geology*, Academic Press, 161-174.

FRANKS, P. C. 1975. The Transgressive sequence of the Cretaceous Cheyenne, Kiowa and Dakota Formations of Kansas. *In*: *The Cretaceous System in the Western Interior of North America*, Special Paper of the Geological Association of Canada, **13**, 469-521.

FREY, R. W. & SEILACHER, A. 1980. Uniformity in marine invertebrate ichnology. *Leithaia*, **13**, 183-207.

FUNK, H. P. & HERB, R. 1987. Cretaceous in the Helvetic Zone of Central Switzerland, Part 1. *In*: Field Guide A - Central Switzerland, *3rd International Cretaceous Symposium*, Tüblingen, 26.8. - 8.9.1987, 1-28.

FUNNEL, B. M. 1990. Global and European Cretaceous Shorelines, Stage by Stage. *In*: GINSBURG, R. N. & BEAUDOIN, B. (eds.) *Cretaceous Resources, Events and Rhythms*, Nato ASI Series C, **304**, 221-235.

FÜRSICH, F. T. & FLESSA, K. W. 1987. Taphonomy of Tidal Flat Molluscs in the Northern Gulf of California: Paleoenvironmental Analysis Despite the Perils of Preservation. *Palaios*, **2**, 543-559.

FÜRSICH, F. T. & OSCHMANN, W. 1986. Storm shell beds of *Nanogyra virgula* in the upper Jurassic of France. *Neues Jahrbuch für Geologie und Paläontologie Abh.*, **172**, 141-146.

FUTTERER, E. 1978. Studien, über die Einregelung, Anlagerung und Einbettung biogeres Hartteile im Strömungskanal. (Flume studies on the orientation, accumulation and burial of biogenic particles). *Neues Jahrbuch für Geologie und Paläontologie Abh.*, **156**, 87-131.

GALLOIS, R. W. & MORTER, A. A. 1982. The stratigraphy of the Gault of East Anglia. *Proceedings of the Geologists' Association, London*, **93**, 351-368.

GANNSER, A. 1964. *A Geology of the Himalayas*, John Wiley, 1-289.

GARRISON, R. E., KENNEDY, W. J., & PALMER, T. J. 1987. Early Lithification and Hardgrounds in Upper Albian and Cenomanian Calcarenites, Southwest England. *Cretaceous Research*, **8**, 1-38.

GEBHARD, G. 1982. Glauconitic Condensation Through High-Energy Events in the Albian Near Clars (Escragnolles, Var, SE-France). *In*: EINSELE, G.& SEILACHER, A. (eds.) *Cyclic and Event Stratification*, Heidelberg, Springer-Verlag, 286-298.

GHOSH, S. K. 1984. Late Cretaceous Condensed Sequences, Venezuelan Andes. *Geological Society of America Memoir*, **162**, 317-324.

GLENIE, R. C. 1971. Upper Cretaceous and Tertiary rock-stratigraphic units in the Central Otway Basin. *In*: WOPFNER, H. & DOUGLAS, J. G. (eds.) *The Otway Basin of south-eastern Australia*. Special Bulletin of the Geological Surveys of South Australia & Victoria, 193-215.

GLENN, C. G. 1990. Depositional sequences of the Duwi, Sibäîya and Phosphate Formations, Egypt: phosphogenesis and glauconitization in a Late Cretaceous eperic sea. *In*: NOTHOLT, A. J. G. & JARVIS, I. (eds.) *Phosphorite Research and Development*, Geological Society, London, Special Publication, **52**, 205-222.

GLENN, C. R. & ARTHUR, M. A. 1990. Anatomy and origin of a Cretaceous phosphorite-greensand giant, Egypt. *Sedimentology*, **37**, 123-154.

GOVINDAN, A. 1982. Imprint of global "Cretaceous Anoxic Events" in East coast basins of India and their implications. *Bulletin O.N.G.C.*, **19**, 256-270.

HAAS, J., J. EDELENYI, E., GIDAI, L., KAISER, M., KRETZOI, M. & ORAVECZ, J. 1985. Geology of the Sümeg area. *Geologica Hungarica, ser. Geol.*, **20**, 1-365.

HALL, W. D. M. & GOODE, A. D. T. 1978. The Early Proterozoic Nabberu Basin and Associated Iron Formations of Western Australia. *Precambrian Research*, **7**, 129-184.

HALLAM, A. 1983. Jurassic, Cretaceous and Tertiary Sediments. *In*: CRAIG, G. Y. (ed.) *Geology of Scotland*, 2nd edn., 343-356.

HAMBLIN, R. J. O. & WOOD, C. J. 1976. The Cretaceous (Albian-Cenomanian) stratigraphy of the Haldon Hills, south Devon, England. *Newsletters on Stratigraphy*, **4**, 135-149.

HANCOCK, J. M. 1961. The Cretaceous System in Northern Ireland. *Quarterly Journal of the Geological Society, London*, **117**, 11-36.

HANCOCK, J. M. 1969. Transgression of the Cretaceous Sea in South-West England. *Proceedings of the Ussher Society*, **2**, 61-83.

HANCOCK, J. M. 1975. The petrology of the Chalk. *Proceedings of the Geologists' Association, London*, **86**, 499-535.

HANCOCK, J. M. 1989. Sea-level changes in the British Region during the Late Cretaceous. *Proceedings of the Geologists' Association, London*, **100**, 565-594.

HANCOCK, J. M., KENNEDY, W. J. & KLAUMANN, H. 1972. Ammonites from the transgressive Cretaceous on the Rhenish Massif, Germany. *Palaeontology*, **15**, 445-449.

HARMS, J. C., SOUTHARD, J. B., SPEARING, D. R. & WALKER, R. G. 1975. Depositional Environments as Interpreted from Primary Sedimentary Structures and Stratification Sequences. *Society of Economic Palaeontologists and Mineralogists Short Course*, **2**, 1-161.

HAQ, B. U., HARDENBOL, J. & VAIL, P. R. 1988. Mesozoic and Cenozoic chronostratigraphy and cycles of sea-level change. *In*: WILGUS, C. K., HASTINGS, B. S., KENDALL, C, G. ST. C., POSAMENTIER, H. W., ROSS, C. A. & VAN WAGONER, J. C. *Sea-Level Changes: An Integrated Approach*, Society of Economic Palaeontologists and Mineralogists Special Publication, **42**, 71-108.

HARDER, H. 1978. Synthesis of Iron Layer Silicate Minerals under natural conditions. *Clays and Clay Minerals*, **26**, 65-72.

HARDER, H. 1980. Synthesis of Glauconite at Surface Temperatures. *Clays and Clay Minerals*, **28**, 217-222.

HART, M. B. 1971. Micropalaeontological evidence of mid-Cenomanian flexuring in South West England. *Proceedings of the Ussher Society*, **2**, 315-325.

HART, M. B. 1973a. A correlation of the macrofaunal and microfaunal zonations of the Gault Clay in southeast England. *In*: CASEY, R. & RAWSON P. F. (eds) *The Boreal Lower Cretaceous*. Geological Journal Special Issue, **5**, 267-288.

HART, M. B. 1973b. Foraminiferal Evidence for the Age of the Cambridge Greensand. *Proceedings of the Geologists' Association, London*, **84**, 65-82.

HART, M. B. 1973c. Some observations on the Chert Beds (Upper Greensand) of South West England. *Proceedings of the Ussher Society*, **4**, 599-608.

HART, M. B. 1979. Biostratigraphy and palaeozoogeography of planktonic Foraminiferida from the Cenomanian of Bornholm, Denmark. *Newsletters on Stratigraphy*, **8**, 83-96.

HART, M. B., MANLEY, E. .C & WEAVER, P. P. E. 1979a. A Biometric analysis of an Orbitolina fauna from the Cretaceous succession at Wolborough, S.Devon. *Proceedings of the Ussher Society*, **4**, 317-326.

HART, M. B., WEAVER, P. P. E. & HARRIS, C. S. 1979b. Microfaunal investigation of Shapwick Grange Quarry, East Devon. *Proceedings of the Ussher Society*, **4**, 312-316.

HART, M. B. & WILLIAMS, C. L. 1990. The Upper Greensand in East Devon: new data but old problems. *Proceedings of the Ussher Society*, **7**, 273-278.

HARWOOD, G. 1988. Microscopic techniques: II. Principles of sedimentary petrography. *In*: TUCKER, M. (ed.) *Techniques in Sedimentology*, Blackwell, 108-173.

HAWKINS, P. J. & DELLENBACH, J. 1971. Stratigraphy. *In*: A Review of the Otway Basin, *Bulletin of the Bureau of Mineral Resources, Geology and Geophysics of Australia*, **134**, 7-29.

HAYES, M. O. 1967. Hurricanes as geological agents : case studies of Hurricane Carla, 1961, and Cindy, 1963. *Rep. Invest. Bur. econ. Geol., Austin Texas*, **61**, 1-54.

HENDERSON, R. A. & MCNAMARA, K. J. 1985. Maastrichtian non-heteromorph ammonites from the Miria Formation, Western Australia. *Palaeontology*, **28**, 35-88.

HESSELBO, S. P., COE, A. L. & JENKYNS, H. C. 1990. Recognition and documentation of depositional sequences from outcrop: an example from the Aptian and Albian on the eastern margin of the Wessex Basin. *Journal of the Geological Society, London*, **147**, 549-559.

HIRANO, H., MATSUMOTO, T. & TANABE, T. 1976. Mid-Cretaceous stratigraphy of the Oybari Area, Central Hokkaido. *In*: Mid Cretaceous Events - Hokkaido Symposium, 1976. *Palaeontological Society of Japan Special Paper*, **21**, 1-10.

HOLDAWAY, H. K. & CLAYTON, C. J. 1982. Preservation of shell microstructure in silicified brachiopods from the Upper Cretaceous Wilmington Sands of Devon. *Geological Magazine*, **119**, 371-382.

HUDSON, J. D. 1960. The Laig Gorge Beds, Isle of Eigg. *Geological Magazine*, **97**, 313-322.

HUGHES, A. D. & WHITEHEAD, D. 1987. Glauconitization of detrital silica substrates in the Barton Formation (upper Eocene) of the Hampshire Basin, southern England. *Sedimentology*, **34**, 825-835.

IRELAND, B. J., CURTIS, C. D. & WHITEMAN, J. A. 1983. Compositional variation within some glauconites and illites and implications for their stability and origin. *Sedimentology*, **30**, 769-786.

JARVIS, I. & WOODROOF, P. B. 1984. Stratigraphy of the Cenomanian and basal Turonian (Upper Cretaceous) between Branscombe and Seaton, SE Devon, England. *Proceedings of the Geologists' Association, London*, **95**, 193-215.

JARVIS, I., CARSON, G., HART, M., LEARY, P. & TOCHER, B. 1988. The Cenomanian-Turonian (late Cretaceous) anoxic event in SW England: evidence from Hooken Cliffs near Beer, SE Devon. *Newsletters on Stratigraphy*, **18**, 147-164.

JEANS, C. V. 1978. Silicifications and associated clay assemblages in the Cretaceous marine sediments of southern England. *Clay Minerals*, **13**, 101-126.

JEANS, C. V., MERRIMAN, R. J., MITCHELL, J. G. & BLAND, D. J. 1982. Volcanic clays in the Cretaceous of southern England and Northern Ireland. *Clay Minerals*, **17**, 105-156.

JENKYNS, H. C. 1980. Cretaceous anoxic events: from continents to oceans. *Journal of the Geological Society, London*, **137**, 171-188.

JENKYNS, H. C. (in press). Impact of Cretaceous sea-level rise and anoxic events on the Mesozoic carbonate platform of Yugoslavia. *Bulletin of the American Association of Petroleum Geologists*, **75**.

JUIGNET, P. 1974. *La transgression crétacée sur la bordure orientale du Massif armoricain*. Thèse de Doctorat d'Etat, Université de Caen.

JUIGNET, P. 1980. Transgressions-Régressions, Variations Eustatiques et Influences Tectoniques de l'Aptien au Maastrichtien dans le Bassin de Paris Occidental et sur la Bordure du Massif Armoricain. *Cretaceous Research*, **1**, 341-357.

JUIGNET, P. & KENNEDY, W. J. 1976. Faunes d'Ammonites et biostratigraphie comparée du Cenomanian du nord-ouest de la France (Normandie) et du sud de l'Angleterre. *Bulletin Trimestriel de la Société Géologique de Normandie et des Amis du Muséum du Havre*, **63**, 1-192.

JUKES-BROWNE, A. J. 1877. Notes on the correlation of the beds constituting the Upper Greensand and Chloritic Marl. *Geological Magazine*, **4**, 350-364.

JUKES-BROWNE, A. J. 1879. Correspondence, Chloritic Marl and Upper Greensand. *Geological Magazine*, **6**, 47-48.

JUKES-BROWNE, A. J. & HILL, W. 1900. *The Gault and Upper Greensand of England*. Memoirs of the Geological Survey of the United Kingdom, **1**, 1-499.

JUKES-BROWNE, A. J. & SCANES, J. 1901. On the Upper Greensand and Chloritic Marl of Maiden Bradley in Wiltshire. *Quarterly Journal of the Geological Society, London*, **57**, 96-125.

KADDOWVI, N. 1982. Tel Hajar: A New Cenomanian-Lower Turonian Stratigraphic Unit from North-west Iraq. *Cretaceous Research*, **3**, 391-395.

KAUFFMAN, E. G. 1984. Paleobiogeography and evolutionary response dynamics in the Cretaceous Western Interior Seaway of North America. *In*: WESTERMANN, G. E. G. (ed.) *Jurassic-Cretaceous Biochronology and Paleogeography of North America*. Geological Association of Canada, Special Paper, **27**, 273-306.

KÁZMÉR, M. 1988. Lower Cretaceous facies zones in the Bakony unit of Hungary. *Annales Universitatis Scientiarium Budapestinensis de Rolando Eötvös Nominatae, Sectio Geologica*, **28**, 161-168.

KELLY, S. R. A. 1971. A New Section in the Upper Greensand, near Edington, Wiltshire. *Proceedings of the Geologists' Association, London*, **82**, 446-448.

KEMPER, E. 1972. The Aptian and Albian stages in northwest Germany. *In*: CASEY, R. & RAWSON, P. F. (eds.) *The Boreal Lower Cretaceous*, Geological Journal Special Issue, **5**, 345-360.

KEMPER, E. & ZIMMERLE, W. 1983. Facies patterns of a Cretaceous/Tertiary Subtropical Upwelling System (Great Syrian Desert) and an Aptian/Albian Boreal Upwelling System (NW Germany). *In*: THEIDE, J. & SUESS, E. (eds.) *Coastal Upwelling. Its Sediment Record*. Part B: Sedimentary Records of Ancient Coastal Upwelling. Nato Conference Series, IV: Marine Sciences, **10b**, 501-533.

KENNEDY, W. J. 1967. Field Meeting at Eastbourne, Sussex. Lower Chalk Sedimentation. *Proceedings of the Geologists' Association, London*, **77**, 365-370.

KENNEDY, W. J. 1969. The Correlation of the Lower Chalk of South-East England. *Proceedings of the Geologists' Association, London*, **80**, 459-551.

KENNEDY, W. J. 1970. A Correlation of the Uppermost Albian and Lower Cenomanian of South-West England. *Proceedings of the Geologists' Association, London*, **81**, 613-677.

KENNEDY, W. J., CHAHIDA, M. R. & DJAFARIAN, M. A. 1979. Cenomanian Cephalopods from the Glauconitic Limestone Southeast of Esfahan, Iran. *Acta Palaeontologica Polonica*, **24**, 3-50

KENNEDY, W. J. & GARRISON, R. E. 1975a. Morphology and genesis of nodular chalks and hardgrounds in the Upper Cretaceous of southern England. *Sedimentology*, **22**, 311-386.

KENNEDY, W. J. & GARRISON, R. E. 1975b. Morphology and genesis of nodular phosphates in the Cenomanian Glauconitic Marl of south-east England. *Lethaia*, **8**, 339-360.

KENNEDY, W. J. & KLINGER, H. K. 1971. A major intra-Cretaceous unconformity in eastern South Africa. *Journal of the Geological Society, London*, **127**, 183-186.

KENNEDY, W. J. & KLINGER, H. K. 1972. Hiatus Concretions and Hardground Horizons in the Cretaceous of Zululand, (S.Africa). *Palaeontology*, **15**, 538-549.

KENNEDY, W. J. & KLINGER, H. K. 1975. Cretaceous Faunas from Zululand and Natal, South Africa. Introduction, Stratigraphy. *Bulletin of the British Museum of Natural History (Geology)*, **25**, 263-315.

KENNEDY, W. J. & ODIN, G. S. 1982. The Jurassic and Cretaceous time scale in 1981. *In*: ODIN, G. S. (ed.) *Numerical Dating in Stratigraphy*, John Wiley & Sons, 557-592.

KENNEDY, W. J., HANCOCK, J. M. & CHRISTENSEN, W. K. 1981. Albian and Cenomanian ammonites from the island of Bornholm (Denmark). *Bulletin of the Geological Society of Denmark*, **29**, 203-244.

KIDWELL, S. M. & JABLONSKI, D. 1983. Taphonomic feedback : ecological consequences of shell accumulation. *In*: TEVESZ, M. J. S. & MCCALL, P. L. (eds.) *Biotic Interactions in Recent and Fossil Benthic Communities*, Plenum Press, 195-248.

KIDWELL, S. M., FÜRSICH, F. T. & AIGNER, T. 1986. Conceptual Framework for the Analysis and Classification of Fossil Concentrations. *Palaios*, **1**, 228-238.

KOHLER, E. E. & KÖSTER, H. M. 1976. Zur mineralogie, kristallchemie und geochemie kretazischer glaukonite. *Clay Minerals*, **11**, 273-302.

KRAJEWSKI, K. P. 1984. Early diagenetic phosphate cements in the Albian glauconitic limestone of the Tatra Mountains, Western Carpathians. *Sedimentology*, **31**, 443-470.

KREISA, R. D. 1981. Storm-Generated Sedimentary Structures in Subtidal Marine Facies with examples from the Middle and Upper Ordovician of Southwestern Virginia. *Journal of Sedimentary Petrology*, **51**, 823-848.

KREISA, R. D. & BAMBACH, R. K. 1982. The Role of Storm Processes in Generating Shell Beds in Paleozoic Shelf Environments. *In*: EINSELE, G. & SEILACHER, A. (eds.). *Cyclic and Event Stratification*, Heidelberg, Springer-Verlag, 200-207.

KUMAR, N. & SANDERS, J. E. 1976. Characteristics of Shoreface Storm Deposits : Modern and Ancient Examples. *Journal of Sedimentary Petrology*, **46**, 145-162.

KURESHI, A. A. 1978. Pakistan. *In*: MOULLADE, M. & NAIRN, A. E. M. (eds.) *The Phanerozoic Geology of the World II*. The Mesozoic, B, Elsevier, 353-374.

LANG, W. D. 1914. The Geology of the Charmouth cliffs, beach and fore-shore. *Proceedings of the Geologists' Association, London*, **25**, 293-360.

LLOYD, C. R. 1982. The Mid-Cretaceous Earth. Paleogeography ; Ocean Circulation and Temperature ; Atmospheric Circulation. *Journal of Geology*, **90**, 393-413.

LOUTIT, T. S., HARDENBOL, J. & VAIL, P. R. 1988. Condensed sections: the key to age determination and correlation of continental margin sequences. *In*: WILGUS, C. K., HASTINGS, B. S., KENDALL, C. G. ST. C., POSAMENTIER, H. W., ROSS, C. A. & VAN WAGONER, J. C. *Sea-Level Changes: An Integrated Approach*, Society of Economic Palaeontologists and Mineralogists Special Publication, **42**, 183-213.

LOWRY, D. C. 1970. Geology of the Western Australian part of the Eucla Basin. *Bulletin of the Geological Survey of Western Australia*, 122, 122-199.

LUDBROOK, N. H. 1978. Australia. *In*: MOULLADE, M. & NAIRN, A. E. M. (eds.) *The Phanerozoic Geology of the World II*. The Mesozoic, A, Elsevier, 209-249.

MACDONALD, H., ALLAN P. M. & LOVELL, J. P. B. 1987. Geology of oil accumulation in Block 26/28, Porcupine Basin, Offshore Ireland. *In*: BROOKS, J. & GLENNIE (eds.) *Petroleum Geology of North West Europe*, vol.2, 643-651.

MAHEL', M., BUDAY, T. *et al.* 1968. *Regional Geology of Czechoslovakia*. Part II, The West Carpathians. Geological Survey of Czechoslovakia, 1-723.

MALIVA, R. G. & SIEVER, R. 1988. Mechanism and controls of silicification of fossils in limestones. *Journal of Geology*, **96**, 387-398.

MALIVA, R. G. & SIEVER, R. 1989. Chertification histories of some Late Mesozoic and Middle Palaeozoic platform carbonates. *Sedimentology*, **36**, 907-926.

MAREK, S. & RACZYŃSKA, A. 1972. The stratigraphy and palaeogeography of the Lower Cretaceous deposits of the Polish Lowland area. *In*: CASEY, R. & RAWSON, P. F. (ed.) *The Boreal Lower Cretaceous*, Geological Journal Special Issue, **5**, 369-386.

MARESCH, W. V. 1978. The Northern Andes. *In*: MOULLADE, M. & NAIRN, A. E. M. (eds.) *The Phanerozoic Geology of the World, II*, The Mesozoic, B, Elsevier, 121-149.

MARSAGLIA, K. M. & KLEIN, G. D. 1983. The Paleogeography of Paleozoic and Mesozoic Storm Depositional Systems. *Journal of Geology*, **91**, 117-142.

MCCAVE, I. N. 1971. Sand waves in the North Sea off the coast of Holland. *Marine Geology*, **10**, 199-225.

MCCONCHIE, D. M. & LEWIS, D. W. 1980. Varieties of glauconite in late Cretaceous and early Tertiary rocks of the South Island of New Zealand, and new proposals for classification. *New Zealand Journal of Geology and Geophysics*, **23**, 413-437.

MCLACHLAN, I. R., BRENNER, P. W. & MCMILLAN, I. K. 1976. The stratigraphy and micro-palaeontology of the Cretaceous Brenton Formation and the PB-A/1 well, near Knysna, Cape Province. *Transactions of the Geological Society of South Africa*, **79**, 341-370.

MCNEILL, D. H. 1984. The Eastern Facies of the Cretaceous System in the Canadian Western Interior. *In*: STOTT, D. F. & GLASS, D. J. (eds.) *The Mesozoic of Middle North America*, Canadian Society of Petroleum Geologists Memoir, **9**, 145-171.

MCRAE, S. G. 1972. Glauconite. *Earth Science Reviews*, **8**, 397-440.

MCWHAE, J. R. H., PLAYFORD, P. E., LINDNER, A. W., GLENISTER, B. F., & BALME, B. E. 1958. The Stratigraphy of Western Australia. *Journal of the Geological Society of Australia*, **4**, 1-161.

MEADOWS, N. S., MACCHI, L., CUBITT, J. M. & JOHNSON, B. 1987. Sedimentology and reservoir potential in the west of Shetland, UK, exploration area. *In*: BROOKS, J. & GLENNIE, K. (eds.) *Petroleum Geology of North West Europe*, vol.2, 723-736.

MÉGNIEN, C. (ed.) 1980. Synthèse Géologique de Bassin de Paris. *Memoire BRGM*, **11**, 3 vols.

MEYER, C. J. A. 1874. On the Cretaceous rocks of Beer Head and the adjacent cliff-sections, and on the relative horizons therein of the Warminster and Blackdown fossiliferous deposits. *Quarterly Journal of the Geological Society, London*, **30**, 369-393.

MEYER, C. J. A. 1878. Notes respecting Chloritic Marl and Upper Greensand. *Geological Magazine*, **5**, 547-551.

MILBOURNE, R. A. 1963. The Gault at Ford Place, Wrotham, Kent. *Proceedings of the Geologists' Association, London*, **74**, 55-79.

MILLER, K. B., BRETT, C. E. & PARSONS, K. M. 1988. The Paleoecologic Significance of Storm Generated Disturbance within a Middle Devonian Muddy Epeiric Sea. *Palaios*, **3**, 35-52.

MOLLAN, R. G., CRAIG, R. W. & LOFTING, M. J. W. 1970. Geologic Framework of continental Shelf off Northwest Australia. *Bulletin of the American Association of Petroleum Geologists*, **54**, 583-600.

MONTAG, R. L. & SEIDEMANN, D. E. 1981. A test of the reliabilty of Rb-Sr dates for selected glauconite morphologies of the Upper Cretaceous (Navesink Formation) of New Jersey. *Earth and Planetary Science Letters*, **52**, 285-290.

MORTIMORE, R. N. 1986. Controls on Upper Cretaceous sedimentation in the South Downs, with particular reference to flint distribution. *In*: SIEVIKING, G. DE G. & HART, M. B. (eds.) *The scientific study of flint and chert*, Cambridge University Press. 21-42.

MORTIMORE, R. N. & POMEROL, B. 1991. Upper Cretaceous tectonic disruptions in a placid Chalk sequence in the Anglo-Paris Basin. *Journal of the Geological Society, London*, **148**, 391-404.

MORTON, R. A. 1981. Formation of storm deposits by wind-forced currents in the Gulf of Mexico and the North Sea. *In*: NIO, S.-D., SHÜTTENHELM, R. T. E. & VAN WEERING Tj. C. E. (eds.) *Holocene Marine Sedimentation in the North Sea Basin*, International Association of Sedimentologists Special Publication, **5**, 385-396.

MUDGE, D. C. & RASHID, B. 1987. The geology of the Faeroe Basin area. *In*: BROOKS, J. & GLENNIE, K. (eds.) *Petroleum Geology of North West Europe*, vol.2, 751-763.

NAGLE, J. S. 1967. Wave and Current Orientation of Shells. *Journal of Sedimentary Petrology*, **37**, 1124-1138.

NAIDIN, D. P. 1981. The Russian Platform and the Crimea. *In*: REYMENT, R. A. & BENGTSON, P. (eds.) *Aspects of Mid Cretaceous Regional Geology*, Academic Press, 29-68.

NALIVIKIN, D. V. 1973. *Geology of the U.S.S.R.*. ed. RAST, N. & WESTOLL, T. S., 1-855.

NELSON, C. H. 1982. Modern shallow-water graded sand layers from storm surges, Bering shelf: a mimic of Bouma sequences and turbidite systems. *Journal of Sedimentary Petrology*, **52**, 537-545.

NICHOLS, J. A., ROWE, G. T., CLIFFORD, C. H. & YOUNG, R. A. 1978. In Situ Experiments on the Burial of Marine Invertebrates. *Journal of Sedimentary Petrology*, **48**, 419-425.

NIXON, R. P. 1973. Oil Source Beds in Cretaceous Mowry Shale of Northwestern Interior United States. *Bulletin of the American Association of Petroleum Geologists*, **57**, 136-161.

OBATA, I. & FUTOKOMI, M. 1976. The Cretaceous sequence of the Manji Dome, Hokkaido. *In*: Mid Cretaceous Events - Hokkaido Symposium, 1976. *Palaeontological Society of Japan Special Paper*, **21**, 23-30.

O'BRIEN, G. W., MILNES, A. R., VEEH, H. H., HEGGIE, D. T., RIGGS, S. R., CULLEN, D. J., MARSHALL, J. F. & COOK, P. J. 1990. Sedimentation dynamics and redox iron-cycling: controlling factors for the apatite-glauconite association on the East Australian continental margin. *In*: NOTHOLT, A. J. G. & JARVIS, I. (eds.) *Phosphorite Research and Development*, Geological Society, London, Special Publication, **52**, 61-86.

OBERMAJER, M. 1987. Lower Cretaceous sedimentary break in the Niedzica Succession near Niedzica, Pieniny Klippen Belt, Carpathians (Poland). *Studia Geologica Polonica*, **92**, Geology of the Pieniny Klippen Belt, Carpathians, Poland, ed. K. Birkenmajer, Part 7, 55-68 (In Polish, with English summary).

ODIN, G. S. & FULLAGAR, P. D. 1988. Geological significance of the glaucony facies. *In*: ODIN, G. S. (ed.) *Green Marine Clays*, Developments in Sedimentology, Elsevier, **45**,295- 332.

ODIN, G. S. & MATTER, A. 1981. De glauconarium origine. *Sedimentology*, **28**, 611-641.

ODOM, I. E. 1985. Glauconite and Celadonite minerals. *In*: BAILEY, S. W. (ed.) *Micas*, Reviews in Mineralogy, **13**, 545-572.

OLSSON, R. K. 1963. Latest Cretaceous and Early Tertiary Stratigraphy of the New Jersey Coastal Plain. *Bulletin of the American Association of Petroleum Geologists*, **47**, 643-685.

OLSSON, R. K. 1988. Foraminiferal modeling of sea-level change in the late Cretaceous of New Jersey. *In*: WILGUS, C. K., HASTINGS, B. S., KENDALL, C, G. ST. C., POSAMENTIER, H. W., ROSS, C. A. & VAN WAGONER, J. C. *Sea-Level Changes: An Integrated Approach*, Society of Economic Palaeontologists and Mineralogists Special Publication, **42**, 289-297.

OWEN, H. G. 1971a. Middle Albian Stratigraphy in the Anglo-Paris Basin. *Bulletin of the British Museum (Natural History) Geology*, **8**, 1-164.

OWEN, H. H. 1971b. The Stratigraphy of the Gault in the Thames Estuary and its bearing on the Mesozoic Tectonic History of the Area. *Proceedings of the Geologists' Association, London*, **82**, 187-207.

OWEN, H. G. 1972. The Gault and its junction with the Woburn Sands in the Leighton Buzzard area, Bedfordshire and Buckinghamshire. *Proceedings of the Geologists' Association, London*, **83**, 287-312.

OWEN, H. G. 1976. The stratigraphy of the Gault and Upper Greensand of the Weald. *Proceedings of the Geologists' Association, London*, **86** (for 1975), 475-498.

OWEN, H. G. 1984. The Albian Stage : European Province Chronology and Ammonite Zonation. *Cretaceous Research*, **5**, 329-344.

OWENS, J. P. 1978. The northwestern Atlantic ocean margin. *In*: MOULLADE, M. & NAIRN, A. E. M. (eds.) *The Phanerozoic Geology of the World II. The Mesozoic, A*, 33-60.

OWENS, J. P. & SOHL, N. F. 1973. Glauconites from New Jersey - Maryland Coastal Plain: Their K-Ar ages and Application in Stratigraphic Studies. *Bulletin of the Geological Society of America*, **84**, 2811-2838.

PARRISH, J. T. & CURTIS, R. L. 1982. Atmospheric circulation, upwelling and organic-rich rocks in the Mesozoic and Cenozoic eras. *Palaeogeography, Palaeoclimatology, Paleoecology*, **40**, 31-66.

PEDERSEN, T. F. & CALVERT, S. E. 1990. Anoxia vs. Productivity: What Controls the Formation of Organic-Carbon-Rich Sediments and Sedimentary Rocks? *Bulletin of the American Association of Petroleum Geologists*, **74**, 454-466.

PEMBERTON, S. G. & FREY, R. W. 1984. Ichnology of Storm-Influenced Shallow Marine Sequence : Cardium Formation (Upper Cretaceous) at Seebe, Alberta. *In*: STOTT, D. F. & GLASS, D. J. (eds.) *The Mesozoic of Middle North America*, Canadian Society of Petroleum Geologists Memoir, **9**, 281-304.

PORRENGA, C. H. 1967. Glauconite and chamosite as depth indicators in the marine environment. *Marine Geology*, **5**, 495-501.

POSAMENTIER, H. W., JERVEY, M. T. & VAIL, P. R. 1988. Eustatic controls on clastic deposition I - conceptual framework. *In*: WILGUS, C. K., HASTINGS, B. S., KENDALL, C. G. ST. C., POSAMENTIER, H. W., ROSS, C. A. & VAN WAGONER, J. C. *Sea-Level Changes: An Integrated Approach*, Society of Economic Palaeontologists and Mineralogists Special Publication, **42**, 109-124.

POSAMENTIER, H. W. & VAIL, P. R. 1988. Eustatic controls on deposition II - sequence and systems tract models. *In*: WILGUS, C. K., HASTINGS, B. S., KENDALL, C. G. ST. C., POSAMENTIER, H. W., ROSS, C. A. & VAN WAGONER, J. C. *Sea-Level Changes: An Integrated Approach*, Society of Economic Palaeontologists and Mineralogists Special Publication, **42**, 125-154.

POWELL, J. D. (ed.) 1970. Field Trip Guidebook, *First Interamerican Micropalaeontological Colloqium*, July 19-30, 1970, University of Texas, Arlington.

PRICE, R. J. 1976. Palaeoenvironmental interpretations in the Albian of western and southern Europe, as shown by the distribution of selected foraminifera. *In*: SCHAFER, C. T. & PELLETIER, B. R. (eds.) *First International Symposium on Benthonic Foraminifera of Continental Margins*, Part B : Paleoecology and Biostratigraphy. Special Publication of Maritime Sediments, **1**, 625-648.

PRICE, R. J. 1977a. The stratigraphical zonation of the Albian sediments of north-west Europe, as based on foraminifera. *Proceedings of the Geologists' Association, London*, **88**, 65-91.

PRICE, R. J. 1977b. The evolutionary interpretation of the foraminiferida *Arenobulimina*, *Gavelinella*, and *Hedbergella*, in the Albian of North-West Europe. *Palaeontology*, **20**, 503-527.

RAGOT, J. 1989. La sedimentation cretacée aux abords de l'accident Fecamp-Lillebonne-Villequier (Seine-Maritime, France). Biostratigraphie et controle structural. *Bulletin Trimestriel de la Societé Géologique de Normandie et des Amis du Muséum du Havre*, **76**, 1-139.

RAISWELL, R. & BERNER, R. A. 1985. Pyrite formation in euxinic and semi-euxinic sediments. *American Journal of Science*, **285**, 710-724.

RAMSDEN, A. R. 1983. Microscopic petrography of oil shales at Julia Creek, northwestern Queensland. *Journal of the Geological Society of Australia*, **30**, 17-23.

RAMSDEN, A. R., DICKSON, B. L. & MEAKINS, R. L. 1982. Origin and significance of the Toolebuc gamma-ray anomaly in parts of the Erromanga Basin. *Journal of the Geological Society of Australia*, **29**, 285-296.

REINECK, H. -E. & SINGH, I. B. 1972. Genesis of laminated sand and graded rhythmites in storm sand layers of shelf mud. *Sedimentology*, **18**, 123-128.

REINECK, H. -E. & SINGH, I. B. 1973. *Depositional Sedimentary Environments*, Springer-Verlag, 1-439.

RENZ, O. 1981. Venezuela. *In*: REYMENT, R. A. & BENGTSON, P. (eds.) *Aspects of Mid-Cretaceous Regional Geology*, Academic Press, 197-220.

RENZ, O. 1982. *The Cretaceous Ammonites of Venezuela*, ed. Maraven, Petroleos de Venezuela, S.A..

RINALDI, C. A. 1982. The Upper Cretaceous in the James Ross Island Group. *In*: CRADDOCK, C. (ed.), *Antarctic Geoscience*, 281-286.

ROBASZYNSKI, F., AMEDRO, F., FOUCHER, J. C., GASPARD, D., MAGNIEZ-JANNIN, F., MANIVIT, H. & SORNAY, J. 1980. Synthèse biostratigraphique de l'Aptien au Santonien du Boulonnais à partir de sept groupes paléontologiques : foraminifères, nannoplancton, dinoflagellés et macrofaunes. *Revue de micropaléontologie*, **22**, 195-321.

SALAZAR-JIMÉNEZ, A., FREY, R. W. & HOWARD, J. B. 1982. Concavity Orientations of Bivalve Shells in Estuarine and Nearshore Shelf Sediments, Georgia. *Journal of Sedimentary Petrology*, **52**, 565-586.

SARG, J. F. 1988. Carbonate Sequence stratigraphy. *In*: WILGUS, C. K., HASTINGS, B. S., KENDALL, C. G. ST. C., POSAMENTIER, H. W., ROSS, C. A. & VAN WAGONER, J. C. *Sea-Level Changes: An Integrated Approach*, Society of Economic Palaeontologists and Mineralogists Special Publication, **42**, 155-181.

SCHLAGER, W. 1981. The paradox of drowned reefs and platforms. *Bulletin of the Geological Society of America*, **92**, 197-211.

SCHLANGER, S. O., ARTHUR, M. A., JENKYNS, H. C. & SCHOLLE, P. A. 1987. The Cenomanian-Turonian Oceanic Event, I. Stratigraphy and distribution of organic carbon-rich beds and the marine $\delta^{13}C$ excursion. *In*: BROOKS, J. & FLEET, A. J. (eds.) *Marine Petroleum Source Rocks*. Geological Society, London, Special Publication, **26**, 371-399.

SCHLANGER, S. O. & JENKYNS, H. C. 1976. Cretaceous oceanic anoxic events: causes and consequences. *Geologie en Mijnbouw*, 55, 179-184.

SCHOLLE, P. A. & ARTHUR, M. A. 1980. Carbon Isotope Fluctuations in Cretaceous Pelagic Limestones: Potential Stratigraphic and Petroleum Exploration Tool. *Bulletin of the American Association of Petroleum Geologists*, **64**, 67-87.

SCHROEDER, R., SIMMONS, M. D., HART, M. B. & WILLIAMS, C. L. 1986. A Note on the Occurrence of *Orbitolina (Orbitolina) sefini* Henson, 1948 (Foraminiferida) in the Upper Greensand of S.W. England. Short Communication, *Cretaceous Research*, **7**, 381-387.

SCRUTTON, R. A. & DINGLE, R. V. 1976. Observations on the processes of sedimentary basin formation at the margins of southern Africa. *Tectonophysics*, **36**, 143-156.

SEILACHER, A. 1982. Distinctive Features of Sandy Tempestites. *In*: EINSELE, G. & SEILACHER, A. (eds.) *Cyclic and Event Stratification*, Heidelberg, Springer-Verlag, 333-349.

SEILACHER, A. 1984. Constructional Morphology of Bivalves : Evolutionary Pathways in Primary Versus Secondary Soft-Bottom Dwellers. *Palaeontology*, **27**, 207-237.

SEILACHER, A., MATYJA, B. A. & WIERBOWSKI, A. 1985. Oyster Beds : Morphologic Response to Changing Substrate Conditions. *In*: BAYER, U. & SEILACHER, A. (eds.) *Sedimentary and Evolutionary Cycles*, Lecture Notes in Earth Sciences, **1**, Springer-Verlag, 1-465.

SELWOOD, E. B. and others 1984. Geology of the country around Newton Abbot. *Memoir of the British Geological Survey*, Sheet 339. 1-212.

SEPKOSKI, J. J. 1982. Flat-Pebble Conglomerates, Storm Deposits, and the Cambrian Bottom Fauna. *In*: EINSELE, G. & SEILACHER, A. (eds.) *Cyclic and Event Stratification*, Heidelberg, Springer-Verlag, 371-385.

SIMPSON, F. 1975. Marine Lithofacies and Biofacies of the Colorado Group (Middle Albian to Santonian) in Saskatchewan. *In*: CALDWELL, W. G. E. (ed.) *The Cretaceous System in the Western Interior of North America*, Special Paper of the Geological Association of Canada, **13**, 553-587.

SINHA, A. K. 1981. Geology and Tectonics of The Himalayan Region of Ladakh, Himachal, Garwhal-Kumaun and Arunachal Pradesh : A Review. *In*: GUPTA, H. K. & DEWEY, F. M. (eds.) *Zagros. Hindu Kush. Himalaya Geodynamic Evolution*, Geodynamics Series, **3**, 122-148.

SMITH, A. B., PAUL, C. R. C., GALE, A. S. & DONOVAN, S. K. 1988. Cenomanian and Lower Turonian echinoderms from Wilmington, south-east Devon, England. *Bulletin of the British Museum (Natural History) Geology*, **42**, 1-245.

SMITH, W. E. 1957. The Cenomanian Limestone of the Beer District, South Devon. *Proceedings of the Geologists' Association, London*, **68**, 115-133.

SMITH, W. E. 1961. The Detrital Mineralogy of the Cretaceous Rocks of South-East Devon, with Particular Reference to the Cenomanian. *Proceedings of the Geologists' Association, London*, **72**, 303-332.

SOLIMAN, S. M. & EL BADRY, O. 1970. Nature of Cretaceous Sedimentation in Western Desert, Egypt. *Bulletin of the American Association of Petroleum Geologists*, **54**, 2349-2370.

SPATH, L. F. 1923-1943. A Monograph of the Ammonoidea of the Gault. *Palaeontographical Society, London*, 2 vols., 1-787.

SPECHT, R. W. & BRENNER, R. L. 1979. Storm Wave Genesis of Bioclastic Carbonates in Upper Jurassic Epicontinental Mudstones, East-Central Wyoming. *Journal of Sedimentary Petrology*, **49**, 1307-1332.

SPEDEN, I. G. 1973. Distribution, stratigraphy and stratigraphic relations of Cretaceous sediments, western Raukumara Peninsula, New Zealand. *New Zealand Journal of Geology and Geophysics*, **16**, 243-268.

SPEDEN, I. G. 1975. Cretaceous stratigraphy of Raukumara Peninsula. *Bulletin of the New Zealand Geological Survey*, **91**, 1-70.

STAPLETON, R. P. & BEER, E. M. 1977. Micropalaeontological age determination for the Brenton beds. *Bulletin of the South African Geological Survey*, **60**, 1-9.

STEIN, R., RULLKÖTTER, J & WELTE, D. H. 1989. Changes in paleoenvironments in the Atlantic Ocean during Cretaceous times : results from black shales studies. *Geologische Rundschau*, **78**, 883-901.

STEVENS, G. R. & SPEDEN, I. G. 1978. New Zealand. *In*: MOULLADE, M. & NAIRN, A. E. M. (eds.) *The Phanerozoic Geology of the World II. The Mesozoic, A*, Elsevier, 251-328.

STOTT, D. F. 1975. The Cretaceous System in Northeastern British Columbia. *In*: CALDWELL, W. G. E. (ed.) *The Cretaceous System in the Western Interior of North America*, Geological Association of Canada Special Paper, **13**, 441-467.

SUGGATE, R. P., STEVENS, G. R. & TE PUNGA, M. T. 1978. *The Geology of New Zealand*, Volume II. New Zealand Geological Survey, Department of Scientific Research, Wellington.

SUMMERHAYES, C. P. 1981. Organic Facies of Middle Cretaceous Black Shales in Deep North Atlantic. *Bulletin of the American Association of Petroleum Geologists*, **65**, 2364-2480.

SVOBODA, J. *et al.* 1966. *Regional Geology of Czechoslovakia.* Part I. The Bohemian Massif. Geological Survey of Czechoslovakia, 1-668.

SWIFT, D. J. P., FIGUEIREDO, A. G., FREELAND, G. L. & OERTEL, G. F. 1983. Hummocky Cross-Stratification and Megaripples : A Geological Double Standard ? *Journal of Sedimentary Petrology*, **53**, 1295-1317.

SWIFT, D. J. P., HUDELSON, P. M., BRENNER, R. L. & THOMPSON, P. 1987. Shelf construction in a foreland basin : storm beds, shelf sandbodies, and shelf-slope depositional sequences in the Upper Cretaceous Mesaverde Group, Book Cliffs, Utah. *Sedimentology*, **34**, 423-457.

TANKARD, A. J., JACKSON, M. P. A, ERIKSON, K. A, HOBDAY, D. K., HUNTER, D. R., & MINTER, W. E. L. 1982. *Crustal Evolution of Southern Africa. 3.8 Billion Years of Earth History*. Springer-Verlag. 1-523.

TAYLOR, J. D. 1964. Foraminifera and the Stratigraphy of the Western Victoria Cretaceous Sediments. *Proceedings of the Royal Society of Victoria*, **77**, 535-603.

TAYLOR, J. D., CLEEVELY, R. J. & MORRIS, N. J. 1983. Predatory gastropods and their activities in the Blackdown Greensand (Albian) of England. *Palaeontology*, **26**, 521-553.

THIEDE, J., DEAN, W. E. & CLAYPOOL, G. E. 1982. Oxygen-deficient Depositional Paleoenvironments in the Mid-Cretaceous Tropical and Subtropical Central Pacific Ocean. *In*: SCHLANGER, S. O. & CITA, M. B. (eds.) *Nature and Origin of Cretaceous Carbon-rich Facies*, Academic Press, 79-100.

THOMPSON, G. R. & HOWER, J. 1978. The mineralogy of glauconite. *Clays and Clay Minerals*, **23**, 289-300.

TISSOT, B., DEMAISON, G., MASSON, P., DELTEIL, J. R. & COMBAZ, A. 1980. Paleoenvironment and Petroleum Potential of Middle Cretaceous Black Shales in Atlantic Basins. *Bulletin of the American Association of Petroleum Geologists*, **64**, 2051-2063.

TOSHIMITSU, S. 1988. Biostratigraphy of the Upper Cretaceous Santonian Stage in Northwestern Hokkaido. *Memoirs of the Faculty of Science, Kyushu University*, Series D, Geology, **36**, 125-192.

TRESISE, G. R. 1960. Aspects of the Lithology of the Wessex Upper Greensand. *Proceedings of the Geologists' Association, London*, **71**, 316-339.

TRESISE, G. R. 1961. The Nature and Origin of Chert in the Upper Greensand of Wessex. *Proceedings of the Geologists' Association, London*, **72**, 333-354.

TRIBOVILLARD, N.-P., STEPHAN, J.-F., MANIVIT, H., REYRE, Y., COTILLON, P. & JAUTEÉ, E. 1991. Cretaceous black shales of Venezuelan Andes: preliminary results on stratigraphy and paleoenvironment interpretations. *Palaeogeography, Palaeoclimatology, Palaeoecology*, **81**, 313-332.

TRIPLEHORN, D. M. 1966. Morphology, internal structure, and origin of glauconite pellets. *Sedimentology*, **6**, 247-266.

TRÖGER, K.-A. 1981. German Democratic Republic. *In*: REYMENT, R. A. & BENGTSON, P. (eds.) *Aspects of Mid-Cretaceous Regional Geology*, Academic Press, 1-28.

TYSON, R. V. & FUNNEL, B. M. 1990. European Cretaceous Shorelines, Stage by Stage. *In*: GINSBURG, R. N. & BEAUDOIN, B. (eds.) *Cretaceous Resources, Events and Rhythms*, Nato ASI Series C, **304**, 237-272.

VALETON, I., ABDUL-RAZZAK, A. & KLUSSMAN, D. 1982. Mineralogy and Geochemistry of Glauconite Pellets from Cretaceous sediments in Northwest Germany. *Geologisches Jahrbuch*, Reihe D, **52**, 5-87.

VAN HINTE, J. E., ADAMS, J. A. S. & PERRY, D. 1975. K/Ar Age of Lower-Upper Cretaceous Boundary at Orphan Knoll (Labrador Sea). *Canadian Journal of Earth Science*, **12**, 1484-1491.

VAN HOUTEN, F. B. & PURUCKER, M. E. 1984. Glauconitic Peloids and Chamositic Ooids - Favorable Factors, Constraints, and Problems. *Earth Science Reviews*, **20**, 211-243.

VAN HOUTEN, F. F. N. & SMITH, S. R. 1984. The Lower Cretaceous Sparky Formation, Lloydminster area: Stratigraphy and Palaeoenvironment. *In*: *The Mesozoic of Middle North America*, Canadian Society of Petroleum Geologists Memoir, **9**, 431-440.

VEEVERS, J. J & EVANS, A. T. 1973. Sedimentary and magnetic events in Australia and the Mechanism of World-wide Cretaceous Transgression. *Nature*, **245**(142), 33-36.

VEEVERS, J. J. & WELLS A. T. 1961. The Geology of the Canning Basin, Western Australia. *Bulletin of the Bureau of Mineral Resources, Geology and Geophysics of Australia*, **60**, 1-323.

VERCOUTERE, T.L., MULLINS, H. T., MCDOUGAL, K. & THOMPSON, J. B. 1987. Sedimentation across the central California Oxygen Minimum Zone: an alternative coastal upwelling sequence. *Journal of Sedimentary Petrology*, **57**, 709-722.

WALKER, R. G. 1984. Shelf and Shallow Marine Sands. *In*: WALKER, R. G. (ed.) *Facies Models*, 2nd. edn., Geoscience Canada Reprint Series, **1**, 141-170.

WARREN, G. & SPEDEN, I. 1977. The Piripauan and Haumurian stratotypes (Mata Series, Upper Cretaceous) and correlative sequences in the Haumuri Bluff district, South Marlborough (S56). *Bulletin of the Geological Survey of New Zealand*, **92**, 1-60.

WEBB, P. N. 1971. New Zealand Late Cretaceous (Haumurian) Foraminifera and stratigraphy: a summary. *New Zealand Journal of Geology and Geophysics*, **14**, 795-828.

WEBER, J. N. & RAUP, D. M. 1966a. Fractionation of the stable isotopes of carbon and oxygen in marine calcareous organisms - the Echinoidea. Part I. Variation of C^{13} and O^{18} content within individuals. *Geochimica et Cosmochimica Acta*, **30**, 681-703.

WEBER, J. N. & RAUP, D. M. 1966b. Fractionation of the stable isotopes of carbon and oxygen in marine calcareous organisms - the Echinoidea. Part II. Environmental and genetic factors. *Geochimica et Cosmochimica Acta*, **30**, 705-736.

WEBER, J. N. & RAUP, D. M. 1968. Comparison of C^{13}/C^{12} and O^{18}/O^{16} in the skeletal calcite of recent and fossil echinoids. *Journal of Palaeontology*, **42**, 37-50.

WHITAKER, J. H. MC D. 1973. "Gutter casts", a new name for scour-and-fill structures: with examples from the Llandoverian of Ringerike and Malmöya, southern Norway. *Norsk Geologisk Tidsskrift*, **53**, 403-417.

WIGNALL, P. B. & RUFFELL, A. H. 1990. The influence of a sudden climatic change on marine deposition in the Kimmeridgian of northwest Europe. *Journal of the Geological Society, London*, **147**, 365-371.

WILLIAMS, C. L. 1986. The cherts of the Upper Greensand (Cretaceous) of south-east Devon. *In*: SIEVEKING, G. DE G. & HART, M. B. (eds.) *The scientific study of flint and chert*, Cambridge University Press, 63-70.

WILLIAMS, C.L., HART, M. B. & LEARY, P. 1988. Foraminifera and correlation of the Upper Greensand, Branscombe, south-east Devon. *Proceedings of the Ussher Society*, **7**, 97-99.

WILSON, H. E. 1981. Permian and Mesozoic. *In*: HOLLAND, C. H. (ed.) *A Geology of Ireland*, Chapter 12, 207-212.

WILSON, V., WELCH, F. B. A., ROBBIE, J. A. & GREEN, G. W. 1958. Geology and the Country around Bridport and Yeovil. *Memoir of the Geological Survey of Great Britain*, Explanation of One-inch Geological Sheets 327 & 312, New Series, 1-239.

WINTERER, H. DE LA R. 1973. Geology of the Algoa Basin South Africa. *In*: BLANT, G. (ed.) *Bassins Sedimentaires du Littoral Africain*, 2eme partie: Littoral austral et oriental, Association des Services Geologiques Africains, Paris, 17-48.

WOJEWODA, J. 1986. Fault-Scarp Induced Shelf Sand Bodies: Turonian of the Intrasudetic Basin. *In*: TEISSEYRE, A. K. (ed.) *Excursion Guidebook, Kraków-Poland*, 7th IAS European Regional Meeting. 31-52.

WRIGHT, C. W. & KENNEDY, W. J. 1984. The Ammonoidea of the Lower Chalk. *Monograph of the Palaeontographical Society, London*, **1**, 1-126.

WRIGHT, C. W. & WRIGHT, E. V. 1942. New Records of Cretaceous Fossils from the Isle of Wight. *Proceedings of the Isle of Wight Natural History and Archaeological Society*, **3**, 283-287.

YORATH, C. J. & COOK, D. G. 1984. Mesozoic and Cenozoic Depositional History of the Northern Interior Plains of Canada. *In*: STOTT, D. F. & GLASS, D. J. (eds.) *The Mesozoic of Middle North America*, Canadian Society of Petroleum Geologists Memoir, **9**, 69-83.

YOUNG, B. 1978. The Upper Greensand of Eastbourne, Sussex. *In*: Guide to South East England Excursion, *Sixth International Clay Conference, Oxford*, 48-52.

ZUMPE, H. H. 1971. Microstructures in Cenomanian glauconite from the Isle of Wight, England. *Mineralogical Magazine*, **38**, 215-224.